



Fisheries and Oceans
Canada

Pêches et Océans
Canada

Ecosystems and
Oceans Science

Sciences des écosystèmes
et des océans

Canadian Science Advisory Secretariat (CSAS)

Research Document 2022/049

Quebec Region

Review of the assessment framework for Atlantic cod in NAFO 3Pn4RS: Fishery independent surveys

Hugues P. Benoît¹, Jordan Ouellette-Plante¹, Yihao Yin² and Claude Brassard¹

¹Fisheries and Oceans Canada
Maurice Lamontagne Institute
Mont Joli, QC G5H 3Z4

²Fisheries and Oceans Canada
Bedford Institute of Oceanography
Dartmouth, NS B2Y 4A2

Foreword

This series documents the scientific basis for the evaluation of aquatic resources and ecosystems in Canada. As such, it addresses the issues of the day in the time frames required and the documents it contains are not intended as definitive statements on the subjects addressed but rather as progress reports on ongoing investigations.

Published by:

Fisheries and Oceans Canada
Canadian Science Advisory Secretariat
200 Kent Street
Ottawa ON K1A 0E6

[http://www.dfo-mpo.gc.ca/csas-sccs/
csas-sccs@dfo-mpo.gc.ca](http://www.dfo-mpo.gc.ca/csas-sccs/csas-sccs@dfo-mpo.gc.ca)



© His Majesty the King in Right of Canada, as represented by the Minister of the
Department of Fisheries and Oceans, 2022

ISSN 1919-5044

ISBN 978-0-660-45213-5 Cat. No. Fs70-5/2022-049E-PDF

Correct citation for this publication:

Benoît, H.P., Ouellette-Plante, J., Yin, Y, and Brassard, C. 2022. Review of the assessment framework for Atlantic cod in NAFO 3Pn4RS: Fishery independent surveys. DFO Can. Sci. Advis. Sec. Res. Doc. 2022/049. xiii + 130 p.

Aussi disponible en français :

Benoît, H.P., Ouellette-Plante, J., Yin, Y, et Brassard, C. 2022. Revue du cadre d'évaluation de la morue franche de la zone OPANO 3Pn4RS : relevés indépendants de la pêche. Secr. can. des avis sci. du MPO. Doc. de rech. 2022/049. xv + 135 p.

TABLE OF CONTENTS

ABSTRACT.....	xiii
1. INTRODUCTION	1
2. SUMMER RESEARCH VESSEL SURVEYS.....	1
2.1. METHODS	2
2.1.1. General	2
2.1.2. Comparative fishing	2
2.1.3. Comparative fishing data analysis	2
2.1.4. Survey data analysis	6
2.2. RESULTS.....	7
2.2.1. Comparative fishing data analysis	7
2.2.2. RV survey indices	8
3. JANUARY RESEARCH VESSEL SURVEYS	10
4. HISTORICAL RESEARCH SURVEYS	11
5. SENTINEL MOBILE GEAR SURVEYS	11
5.1. METHODS	12
5.2. RESULTS.....	12
6. SENTINEL FIXED GEAR SURVEYS	12
6.1. LONGLINE SENTINEL.....	14
6.1.1. Methods	14
6.1.2. Results - Sentinel longline indices	18
6.2. GILLNET SENTINEL.....	18
6.2.1. Gear saturation	19
6.2.2. Strata for the abundance indices	19
6.2.3. Results – Sentinel gillnet indices.....	20
7. COMPARISON OF TOTAL MORTALITY TRENDS.....	20
8. SUMMARY AND CONCLUSIONS.....	21
9. ACKNOWLEDGEMENTS	22
10. REFERENCES CITED.....	23
11. TABLES	26
12. FIGURES	32
13. APPENDIX I.....	101
13.1. SUPPLEMENT FIGURES	101
14. APPENDIX II.....	129
14.1. CATCH AT AGE FOR FIXED SENTINEL FISHERY DATA	129

LIST OF TABLES

Table 1. Parameters for the vessels and summary of the protocols used in the RV surveys of the northern Gulf of St. Lawrence.	26
Table 2. Parameters for the trawls used in the RV surveys of the northern Gulf of St. Lawrence.	27
Table 3. A set of binomial models with various assumptions for the length effect and station effect in the relative catch efficiency. A smoothing length effect can be considered and the station effect can be added to the intercept, without interaction with the length effect, or added to both the intercept and smoother to allow for interaction between the two effects.....	28
Table 4. A set of beta-binomial models with various assumptions for the length effect and station effect in the relative catch efficiency, and the length effect on the variance parameter. A smoothing length effect can be considered in both the conversion factor and the variance parameter. A possible station effect can be added to the intercept, without interaction with the length effect, or added to both the intercept and the smoother to allow for interaction between the two effects.....	28
Table 5. Difference in AIC between converged candidate models and the best model in each comparative fishing analysis. The best model (indicated in bold) was selected by lowest AIC. For a description of the models see Tables 3 and 4.	29
Table 6. Proportion of Sentinel fixed gear survey hauls with zero catch of cod, as a function of cod age, for longline (LLS) and gillnet (GNS) surveys.	30
Table 7. Number of individuals hauls in the Sentinel longline survey using set amounts of hooks.	30
Table 8. Stratum weights used for the stratified Sentinel fixed gear indices, based on the linear distance in km between Zone boundaries (see text)	30
Table 9. Number of hauls used in the fall Zones 1 and 2 (only site 8 used) Sentinel longline survey index, as a function of year and time-block. Duration is 10 days in the first time block and 21 days in the others.....	31
Table 10. Diagnostics for the models to calibrate the relative efficiency of J and circle hooks in the longline Sentinel survey based on quantile residuals: zero-inflation (ZI) and dispersion statistics and associated p-values	31

LIST OF FIGURES

- Figure 1. Stratification scheme for the northern Gulf of St. Lawrence multi-species bottom-trawl survey. Strata 401-408, 801-824 and 827-832 constitute a core group of strata included annually in the sampling design since at least 1985. Additional strata, located in NAFO area 3Pn (southwest Newfoundland) and sampled only in 1987 and 1993-2003 are not shown..... 32
- Figure 2. Summary of the number of survey sets made in each stratum and year in the northern Gulf of St. Lawrence RV survey. Strata indicated in red are not used in the estimation of survey abundance series for any taxa because of inconsistent sampling over the years. 33
- Figure 3. Catches (numbers) of cod by the Alfred Needler (left) and Lady Hammond (right) in paired tows from the comparative fishing survey in 1990, aggregated in four length groups (rows). Solid points with color intensity scale are used for positive catches, while zero catches are indicated by open circles. 34
- Figure 4. Catches (numbers) of cod by the Alfred Needler (left) and Teleost (right) in paired tows from the comparative fishing surveys in 2004 and 2005, aggregated in four length groups (rows). Solid points with color intensity scale are used for positive catches, while zero catches are indicated by open circles. 35
- Figure 5. Proportion of cod catch made by the Lady Hammond-WIIA in paired hauls during the 1990 comparative fishing experiment, as a function of fish length (cm), for individual haul pairs (light grey dots) and for the length-specific sample average (circles). The solid red solid line indicates the estimated conversion based on the selected best model, while the blue dashed lines are for other converged models. 36
- Figure 6. Proportion of cod catch made by the Alfred Needler-URI in paired hauls during the 2004-2005 comparative fishing experiment, as a function of fish length (cm), for individual haul pairs (light grey dots) and for the length-specific sample average (circles). The solid red solid line indicates the estimated conversion based on the selected best model, while the blue dashed lines are for other converged models and the orange line indicates the previously used conversion based on the exponential model by Bourdages et al. (2007). 37
- Figure 7. Estimated catch efficiency of the replaced vessel and gear tandem relative to the replacement vessel and gear tandem. The grey bands indicate one standard deviation and the red lines indicate equal efficiency for the replaced and replacement vessels and gear. 38
- Figure 8. Analysis for the 1990 comparative fishing between Lady Hammond-WIIA and Alfred Needler-URI: normalized randomized quantile residuals for each length bin (top panel) and for each station (bottom panel) for the selected model. 39
- Figure 9. Analysis for the 2004-2005 comparative fishing between Alfred Needler-URI and Teleost-Campelen: normalized randomized quantile residuals for each length bin (top panel) and for each station (bottom panel) for the selected model. 40
- Figure 10. Catch-at-length (cm) composition comparison between the uncalibrated replaced and replacement vessels-gear tandems in the 1990 comparative fishing experiment (top panel) and between calibrated replaced and replacement vessels (bottom panel). 41
- Figure 11. Catch-at-length (cm) composition comparison between the uncalibrated replaced and replacement vessels-gear tandems in the 2004-2005 comparative fishing experiment (top panel) and between calibrated replaced and replacement vessels (bottom panel). 42
- Figure 12. Estimated catch efficiency relative to Teleost-Campelen for each vessel-gear based on sequential multiplication of the estimated relative catch efficiencies from the analyses of the two comparative fishing experiments, as a function of length (cm). 43

Figure 13. Age-specific abundance indices for cod from the RV survey for 1984-2020 for the reduced suite of strata (black line and dots) compared to former indices presented in Brassard et al. (2020) for 1990-2018 for the full suite of strata (blue line). Age 13 represents a 13+ group.	44
Figure 14. Age-aggregated abundance index with 95% confidence intervals for cod from the RV survey for 1984-2020 based on the reduced suite of strata (black dots) and for 1990-2020 based on all consistently sampled strata (grey dots). The stratum numbers are indicated in the legend.	45
Figure 15. Annual RV survey length frequencies in numbers per tow for 1984-2020 based on the reduced suite of strata (black lines) and for 1990-2020 based on all consistently sampled strata (blue lines).	46
Figure 16. Annual RV survey length frequencies expressed as proportions, for 1984-2020 based on the reduced suite of strata (black lines) and for 1990-2020 based on all consistently sampled strata (blue lines).	47
Figure 17. Catch at age in the RV survey for a) 1984-2020 based on the reduced suite of strata and b) 1990-2020 based on all consistently sampled strata. The left panels show catch proportional to circle size, while the right panels show standardized proportions at age and year (SPAY) with grey circles indicating above average catch and black below average. The blue lines indicate some consistently tracked above average cohorts in the survey	48
Figure 18. Abundance of individual cohorts (ages 3 to 13+) from the RV survey catch at age for a) 1984-2020 based on the reduced suite of strata and b) 1990-2020 based on all consistently sampled strata. The year of the 1990 comparative fishing experiment is indicated by a vertical dashed line in a). Cohorts are identified by birth year for every 5 th year.	49
Figure 19. Age-specific abundance of cohorts at a given age and year, as a function of their abundance one year later in the RV survey, for 1984-2020. The correlation between the two sets of estimates is indicated in each panel.	50
Figure 20. Estimates of total mortality (Z ; with 95% confidence intervals) for ages 5 to 10 from the RV survey for 1984-2020 based on the reduced suite of strata (black) and 1990-2020 based on all consistently sampled strata (grey).	51
Figure 21. Relationship between catch rates (number per unit effort, NUE) based on the reduced set of strata used to derive indices for the 1984-2020 period and for the full suite of strata traditionally used for cod, by age (rows; age indicated in the lower corner of the leftmost panel). Left column: Biplots of the two series, where the black line is a 1:1 relationship and the dashed blue line is the estimated conversion (correction) to a full-stratum suite equivalent. Middle column: Time series of the abundance indices for the full suite of strata (black), the reduced set (grey) and the 'corrected' reduced set (blue). Right panel: Residuals of the adjusted model in left column (full suite minus corrected indices) as a function of year. DW is the Durbin-Watson statistic for temporal autocorrelation, with associated p-value. Results indicated for age 13 represent a 13-plus group.	52
Figure 22. Mean depth occupied by cod in the RV survey year and age (panels). The series means are indicated with a dashed blue line. Results indicated for age 13 represent a 13-plus group.	55
Figure 23. Relationship between mean occupied depth and the residuals for the abundance index based on the full suite of strata minus the corrected index, as a function of age (panels). The associated correlation coefficient and p-value are indicated in each panel. Results indicated for age 13 represent a 13-plus group.	56

Figure 24. Distribution of Atlantic cod catches (kg/tow) in the MV Gadus Atlantica January survey, 1978-1994.	57
Figure 25. Catch at age in the Gadus Atlantica winter survey for 1984-1994 for a) unadjusted catches and b) catches adjusted to Teleost-Campelen equivalents based on Warren (1997). The left panels show catch proportional to circle size, while the right panels show standardized proportions at age and year (SPAY) with grey circles indicating above average catch and black below average. The blue lines indicate some consistently tracked above average cohorts in the RV survey (see Figure 17).	58
Figure 26. Relative catch curves (composition as a function of age) for historical research surveys, by NAFO area and period of years, as reported in Wiles and May (1968). The blue lines are regressions of the log relative catch curves, the slope of which provides a cross-sectional estimate of total mortality, Z. The estimate of Z and associated standard error are provided in each plot.	59
Figure 27. Coastal strata used in the northern Gulf of St. Lawrence Sentinel bottom-trawl survey in addition to the other strata employed in the nGSL multi-species survey (Figure 1), with the exception of strata in the Estuary).	60
Figure 28. Age aggregated abundance indices for the Sentinel mobile gear survey, including (blue) and excluding (black) the coastal strata indicated in Figure 27.	60
Figure 29. Relationship between Sentinel mobile gear survey abundance index values for series excluding (x-axis) and including (y-axis) the coastal strata indicated in Figure 27, by age (panels). The black line is a 1:1 relationship while the dashed blue line is a model-estimated correction. The coefficients of determination (R^2) values for the 1:1 relationship and for the model-estimated correction are indicated in each panel.	61
Figure 30. Catch at age in the Sentinel mobile gear survey for 1995-2020. The left panel shows catch proportional to circle size, while the right panel shows standardized proportions at age and year (SPAY) with grey circles indicating above average catch and black below average. The blue lines indicate some consistently tracked above average cohorts in the RV survey (see Figure 17).	62
Figure 31. Age-specific abundance of cohorts at a given age and year, as a function of their abundance one year later in the Sentinel mobile gear survey, for 1995-2020. The correlation between the two sets of estimates is indicated in each panel.	63
Figure 32 . Abundance of individual cohorts (ages 3 to 13+) from the Sentinel mobile gear survey catch at age, 1995-2020. Cohorts are identified by birth year for every 5 th year.	64
Figure 33. Estimates of total mortality (Z; with 95% confidence intervals) for ages 5 to 10 from the Sentinel mobile gear survey, 1995-2020.	64
Figure 34. Spatial distribution of surveys in the nGSL in 2018.	65
Figure 35. Zone boundaries for the sentinel fixed gear surveys, and revised stratum limits for zones 6 and 6b (blue), along with the location of sampling sites in 2018, as a function of gear type.	65
Figure 36. Location of individual Sentinel fixed gear hauls by longlines using J hooks (red) and longlines using circle hooks (orange) in two year blocks in Zone 1 (Channel-Port aux Basques). Site numbers associated with each haul are indicated.	66
Figure 37. Location of individual Sentinel fixed gear hauls by longlines using J-hooks (red), longlines using circle hooks (orange) and gillnets (blue) in two year blocks in Zone 2 (Cape Ray to Port au Port Bay). Site numbers associated with each haul are indicated.	67

Figure 38. Location of individual Sentinel fixed gear hauls by longlines using J-hooks (red), longlines using circle hooks (orange) and gillnets (blue) in two year blocks in Zone 3 (Bay of Islands to Flower’s Cove). Site numbers associated with each haul are indicated.	68
Figure 39. Location of individual Sentinel fixed gear hauls by longlines using J-hooks (red), longlines using circle hooks (orange) and gillnets (blue) in two year blocks in Zone 4 (Belle-Isle Straight). Site numbers associated with each haul are indicated.	69
Figure 40. Location of individual Sentinel fixed gear hauls by longlines using J-hooks (red), longlines using circle hooks (orange) and gillnets (blue) in two year blocks in Zone 5 (Blanc Sablon to St-Augustin). Site numbers associated with each haul are indicated.	70
Figure 41. Location of individual Sentinel fixed gear hauls by longlines using J-hooks (red), longlines using circle hooks (orange) and gillnets (blue) in two year blocks in Zone 6 (St-Augustin to La Romaine). Site numbers associated with each haul are indicated.....	71
Figure 42. Location of individual Sentinel fixed gear hauls by longlines using J-hooks (red) and gillnets (blue) in two year blocks in Zone 6b (Sept-Îles area). Site numbers associated with each haul are indicated.....	72
Figure 43. Gear soak (immersion) times for the Sentinel fixed gear surveys, a) longlines, b) gillnets.....	73
Figure 44. Boxplots of the estimated a) catch (numbers) of fish per haul, all species combined, per 1000 hooks, and b) the proportion of cod in the catches, for each year in the Sentinel longline survey.	74
Figure 45. Boxplots of cod catch rates (numbers per 1000 hook) in individual hauls as function of gear soak (immersion) time in the Sentinel longline survey. The red line is the smoother estimated from a GAMM analysis of catch rates as a function of soak time (dashed lines are 95% confidence intervals on the smoother).	75
Figure 46. Number of individual hauls by zone (panels) and month (coloured lines) in the Sentinel longline survey.	76
Figure 47. Number of individual hauls by zone (lines) in August and September (days of year 210 to 270) in the Sentinel longline survey.	77
Figure 48. Age-specific mean catch rates (number per unit effort, NUE) using J-hooks (x-axes) and using circle hooks (y-axes) in sampling units defined by year, week and site, where age13p and age10p designate plus groups, for ages 13+ and 10+ respectively. The blue lines indicate a 1:1 relationship, the dashed red line is the estimated age-specific relative efficiency from model A, while the dotted red line is the estimate from model B. The inset in the panel for age3 shows a close-up of the biplot excluding the two outlier values.	78
Figure 49. a) Estimated age-specific log efficiency of circle hooks relative to J hooks based on the models (dots with 95% confidence intervals) and based on sample means (crosses). The grey values are for the estimates that exclude two outlier units for age 3 and that group ages 10+ (model B). The dashed grey line is the estimated value for the 10+ group. b) Annual proportion of longline hauls made with J-hooks.	79
Figure 50. Catch rates of age 4 cod (number per 1000 hooks) in individual hauls by zone (panels) and year in Sentinel longline (August-September) summer hauls. Colours distinguish individual sites within zones.	80
Figure 51. Catch rates of age 12 cod (number per 1000 hooks) in individual hauls by zone (panels) and year in Sentinel longline (August-September) summer hauls. Colours distinguish individual sites within zones.	81

Figure 52. Catch rates of age 4 cod (square root, number per unit effort, 1000 hooks) in individual hauls by year (panels) and day of the year in Sentinel longline zone 1 + site 8 fall hauls. Colours distinguish individual sites. The dashed lines delineate the time blocks used to define the temporal strata.	82
Figure 53. Catch rates of age 12 cod (square root, number per unit effort, 1000 hooks) in individual hauls by year (panels) and day of the year in Sentinel longline zone 1 + site 8 fall hauls. Colours distinguish individual sites. The dashed lines delineate the time blocks used to define the temporal strata.	83
Figure 54. Age aggregated 3-plus abundance index (number per unit effort, NUE; 1000 hooks) with 95% confidence intervals for the Sentinel longline survey summer index, 1995-2019.....	84
Figure 55. Catch at age in the Sentinel longline survey (summer index) 1995-2019. The left panel shows catch proportional to circle size, while the right panel shows standardized proportions at age and year (SPAY) with grey circles indicating above average catch and black below average. The blue lines indicate some consistently tracked above average cohorts in the RV survey (see Figure 17).	84
Figure 56. Abundance of individual cohorts (ages 6 to 13+) in the Sentinel longline survey (summer index) catch at age, 1995-2019. Cohorts are identified by birth year for every 5 th year.	85
Figure 57. Age-specific abundance of cohorts at a given age and year, as a function of their abundance one year later in the Sentinel longline survey (summer index), for 1995-2019. The correlation between the two sets of estimates is indicated in each panel.....	86
Figure 58. Estimates of total mortality (Z; with 95% confidence intervals) for ages 8 to 12 from the Sentinel longline survey (summer index), 1995-2019.	87
Figure 59. Age aggregated 3-plus abundance index (number per unit effort, NUE; 1000 hooks) with 95% confidence intervals for the Sentinel longline survey zone 1 fall index, 1995-2019. ...	87
Figure 60. Catch at age in the Sentinel longline survey (fall index) 1995-2019. The left panel shows catch proportional to circle size, while the right panel shows standardized proportions at age and year (SPAY) with grey circles indicating above average catch and black below average. The blue lines indicate some consistently tracked above average cohorts in the RV survey (see Figure 17).....	88
Figure 61. Abundance of individual cohorts (ages 6 to 13+) in the Sentinel longline survey (fall) catch at age, 1995-2019. Cohorts are identified by birth year for every 5 th year.	88
Figure 62. Age-specific abundance of cohorts at a given age and year, as a function of their abundance one year later in the Sentinel longline survey (fall), for 1995-2019. The correlation between the two sets of estimates is indicated in each panel.	89
Figure 63. Estimates of total mortality (Z; with 95% confidence intervals) for ages 8 to 12 from the Sentinel longline survey (zone 1 fall index), 1995-2019.	90
Figure 64. Frequency distribution of the number of nets used for individual hauls in the Sentinel gillnet survey.	90
Figure 65. Boxplots of the estimated a) catch (numbers) of fish per haul and net, all species combined, and b) the proportion of cod in the catches, for each year in the Sentinel gillnet survey.	91
Figure 66. Boxplots of cod catch rates (shown as the square root of numbers per net) in individual hauls as function of gear soak (immersion) time in the Sentinel gillnet survey. The red	

line is the smoother estimated from a GAMM analysis of catch rates as a function of soak time (dashed lines are 95% confidence intervals on the smoother).	92
Figure 67. Number of individual hauls by zone (panels) and month (coloured lines) in the Sentinel gillnet survey.	93
Figure 68. Number of individual hauls by zone (panels) and time block (coloured lines) in the Sentinel gillnet survey. Time blocks were defined based on the day of the year: block 1 [165, 195], block 2 [196, 226], and block 3 [227, 257].	94
Figure 69. Catch rates of age 4 cod (number per net) in individual hauls by zone (rows), time block (columns) and year in Sentinel gillnet hauls. Colours distinguish individual sites. Time blocks were defined based on the day of the year: block 1 [165, 195], block 2 [196, 226], and block 3 [227, 257].	95
Figure 70. Catch rates of age 12 cod (number per net) in individual hauls by zone (rows), time block (columns) and year in Sentinel gillnet hauls. Colours distinguish individual sites. Time blocks were defined based on the day of the year: block 1 [165, 195], block 2 [196, 226], and block 3 [227, 257].	96
Figure 71. Age aggregated 3-plus abundance index (number per unit effort, NUE; per net) with 95% confidence intervals for the Sentinel gillnet survey summer index, 1995-2019.	97
Figure 72. Catch at age in the Sentinel gillnet survey 1995-2019. The left panel shows catch proportional to circle size, while the right panel shows standardized proportions at age and year (SPAY) with grey circles indicating above average catch and black below average. The blue lines indicate some consistently tracked above average cohorts in the RV survey (see Figure 17).	97
Figure 73. Abundance of individual cohorts (ages 7 to 13+) in the Sentinel gillnet survey catch at age, 1995-2019. Cohorts are identified by birth year for every 5 th year.	98
Figure 74. Age-specific abundance of cohorts at a given age and year, as a function of their abundance one year later in the Sentinel gillnet survey, for 1995-2019. The correlation between the two sets of estimates is indicated in each panel.	99
Figure 75. Estimates of total mortality (Z; with 95% confidence intervals) for ages 8 to 12 from the Sentinel gillnet survey, 1995-2019.	100
Figure 76. Comparison of total mortality estimates for each of the five principal fishery independent survey indices.	100
Figure A1. Annual age-length observation in the RV survey.	101
Figure A1 continued.	102
Figure A2. Standardized results and distribution of estimated random effects in the GAMM analysis of catch rates as a function of soak (immersion) time in the Sentinel longline survey.	103
Figure A3. Summary of quantile residuals from model A for the calibration of two hook types in the Sentinel longline program: a) quantile residual Q-Q plots; b) distribution of quantile residuals as a function of rank transformed predicted values, where the solid red line indicates the expected mean value of 0.5, the dashed line is a smooth of the simulated mean value and asterisks indicate significant deviations or outliers; and, c) box plots of quantile residuals as a function of cod age (note that age 13 is actually a 13-plus group), where a correctly fitting model should result in a uniform distribution of residuals for each age, and hence a median (solid black line) at 0.5 and boxes delimited at 0.25 and 0.75.	104

Figure A4. Summary of quantile residuals from model B for the calibration of two hook types in the Sentinel longline program: a) quantile residual Q-Q plots; b) distribution of quantile residuals as a function of rank transformed predicted values, where the solid red line indicates the expected mean value of 0.5, the dashed line is a smooth of the simulated mean value and asterisks indicate significant deviations or outliers; and, c) box plots of quantile residuals as a function of cod age (note that age 13 is actually a 13-plus group), where a correctly fitting model should result in a uniform distribution of residuals for each age, and hence a median (solid black line) at 0.5 and boxes delimited at 0.25 and 0.75.	105
Figure A5. Site-specific annual mean numbers per unit effort (NUE) by zone for cod age 3 in the Sentinel longline program. Values for individual sites are distinguished by colour in each zone.	106
Figure A6. Site-specific annual mean numbers per unit effort (NUE) by zone for cod age 4 in the Sentinel longline program. Values for individual sites are distinguished by colour in each zone.	107
Figure A7. Site-specific annual mean numbers per unit effort (NUE) by zone for cod age 5 in the Sentinel longline program. Values for individual sites are distinguished by colour in each zone.	108
Figure A8. Site-specific annual mean numbers per unit effort (NUE) by zone for cod age 6 in the Sentinel longline program. Values for individual sites are distinguished by colour in each zone.	109
Figure A9. Site-specific annual mean numbers per unit effort (NUE) by zone for cod age 7 in the Sentinel longline program. Values for individual sites are distinguished by colour in each zone.	110
Figure A10. Site-specific annual mean numbers per unit effort (NUE) by zone for cod age 8 in the Sentinel longline program. Values for individual sites are distinguished by colour in each zone.	111
Figure A11. Site-specific annual mean numbers per unit effort (NUE) by zone for cod age 9 in the Sentinel longline program. Values for individual sites are distinguished by colour in each zone.	112
Figure A12. Site-specific annual mean numbers per unit effort (NUE) by zone for cod age 10 in the Sentinel longline program. Values for individual sites are distinguished by colour in each zone.	113
Figure A13. Site-specific annual mean numbers per unit effort (NUE) by zone for cod age 11 in the Sentinel longline program. Values for individual sites are distinguished by colour in each zone.	114
Figure A14. Site-specific annual mean numbers per unit effort (NUE) by zone for cod age 12 in the Sentinel longline program. Values for individual sites are distinguished by colour in each zone.	115
Figure A15. Site-specific annual mean numbers per unit effort (NUE) by zone for cod age 13+ in the Sentinel longline program. Values for individual sites are distinguished by colour in each zone.	116
Figure A16. Boxplots of the number of hauls per site and stratum in the summer Sentinel longline (LLS) and gillnet (GNS) data used to generate abundance indices.	117
Figure A17. Standardized results and distribution of estimated random effects in the GAMM analysis of catch rates as a function of soak (immersion) time in the Sentinel gillnet survey... 117	117

Figure A18. Site-specific annual mean numbers per unit effort (NUE) by zone and seasonal block for cod age 3 in the Sentinel gillnet program. Values for individual sites are distinguished by colour in each zone and block.....	118
Figure A19. Site-specific annual mean numbers per unit effort (NUE) by zone and seasonal block for cod age 4 in the Sentinel gillnet program. Values for individual sites are distinguished by colour in each zone and block.....	119
Figure A20. Site-specific annual mean numbers per unit effort (NUE) by zone and seasonal block for cod age 5 in the Sentinel gillnet program. Values for individual sites are distinguished by colour in each zone and block.....	120
Figure A21. Site-specific annual mean numbers per unit effort (NUE) by zone and seasonal block for cod age 6 in the Sentinel gillnet program. Values for individual sites are distinguished by colour in each zone and block.....	121
Figure A22. Site-specific annual mean numbers per unit effort (NUE) by zone and seasonal block for cod age 7 in the Sentinel gillnet program. Values for individual sites are distinguished by colour in each zone and block.....	122
Figure A23. Site-specific annual mean numbers per unit effort (NUE) by zone and seasonal block for cod age 8 in the Sentinel gillnet program. Values for individual sites are distinguished by colour in each zone and block.....	123
Figure A24. Site-specific annual mean numbers per unit effort (NUE) by zone and seasonal block for cod age 9 in the Sentinel gillnet program. Values for individual sites are distinguished by colour in each zone and block.....	124
Figure A25. Site-specific annual mean numbers per unit effort (NUE) by zone and seasonal block for cod age 10 in the Sentinel gillnet program. Values for individual sites are distinguished by colour in each zone and block.....	125
Figure A26. Site-specific annual mean numbers per unit effort (NUE) by zone and seasonal block for cod age 11 in the Sentinel gillnet program. Values for individual sites are distinguished by colour in each zone and block.....	126
Figure A27. Site-specific annual mean numbers per unit effort (NUE) by zone and seasonal block for cod age 12 in the Sentinel gillnet program. Values for individual sites are distinguished by colour in each zone and block.....	127
Figure A28. Site-specific annual mean numbers per unit effort (NUE) by zone and seasonal block for cod age 13+ in the Sentinel gillnet program. Values for individual sites are distinguished by colour in each zone and block.....	128

ABSTRACT

Fisheries and Oceans Canada in the Quebec region undertook in 2021-2022 a review of the assessment framework for the Northwest Atlantic Fisheries Organization (NAFO) 3Pn4RS Atlantic cod (*Gadus morhua*) stock in the northern Gulf of St. Lawrence. A review of assessment inputs, including information on reported and non-reported fishery catches, tagging information and fishery independent monitoring results took place in the spring of 2021. The principal objective of the present document was to review the availability, duration and quality of fishery independent survey indices and information for the stock. In doing so, we considered how these sources of information contribute to understanding population dynamics, via trends in abundance, demographic composition and mortality rates. Several advances were made as part of the review and which are expected to improve the quality of the assessment. First, the principal age-disaggregated indices obtained from a bottom-trawl research vessel survey were extended back in time from 1990 to 1984 by analyzing and applying results of a comparative fishing experiment that allowed to calibrate the series for the vessel used in the early years of the survey. This extends the time series to before the period when the stock collapsed. Second, a single coherent set of age-disaggregated indices for a Sentinel bottom trawl survey was obtained by combining two sets of indices covering different periods of years. Third, data from a winter survey that ran in the 1980s and 1990s and which had been disregarded were found to produce useful information on the age-composition for the cod stock over the 1983-1994 period. Fourth, results from historical surveys conducted in the 1950s and 1960s, the period during which trawls were introduced into the fishery and landings increased considerably, were found to provide useful estimates of mortality rates, notably an estimate of an upper bound for the natural mortality rate. Fifth, an overhaul of the methods used to estimate age-disaggregated indices of abundance from the Sentinel fixed gear program resulted in the creation of three independent sets of indices, two based on longline catches and one based on gillnet catches. The overhaul was motivated by several issues that had arisen over time with the traditionally used catch-rate standardization approach. Overall, the revised indices provide a coherent picture of stock dynamics, including very similar trends across indices in the estimated rate of total mortality. Furthermore, the extension of information on the stock to the 1950s and abundance indices to the 1980s prior to stock collapse, is likely to provide a more accurate picture of the historical size and productivity of the stock, which in turn should allow for the establishment of more pertinent reference points for its management.

1. INTRODUCTION

Fisheries and Oceans Canada (DFO) undertook in 2021 and 2022 a review of the assessment framework for Atlantic cod (*Gadus morhua*) in NAFO 3Pn4RS (hereafter northern Gulf of St. Lawrence, nGSL, cod). This review, which will take place in two parts, will evaluate appropriateness and utility of a new assessment model for the stock and existing and new inputs to that model. The present document evaluates the information, data and indices that are available from fishery independent surveys and that can contribute to the renewed assessment. This includes data and results from historical surveys that have not been used to assess the stock for more than two decades. Three classes of surveys are examined: research vessel (RV) bottom-trawl surveys, Sentinel bottom-trawl surveys and Sentinel fixed-gear surveys undertaken using gillnets and longlines. These are presented in turn in separate sections. For each of these classes of surveys we provide revised or new indices of abundance or status. This information was reviewed at the Canadian Science Advisory Secretariat regional peer review meeting which took place on April 21 to 22, 2021, and May 12, 2021.

2. SUMMER RESEARCH VESSEL SURVEYS

The current assessment for nGSL cod relies on age-dependent indices from an RV survey undertaken annually in August by DFO's Quebec Region. That survey follows a stratified random design with strata based on depth and area (Figure 1). The current indices begin in 1990 when the Canadian Coast Guard Ship (CCGS) *Alfred Needler* was adopted as the survey vessel. That vessel was replaced after 2005 by the CCGS *Teleost*, which remains the designated vessel for the survey. To date the assessment has not used data collected from 1984 to 1990 in surveys undertaken annually in August using the motor vessel (MV) *Lady Hammond*, and which followed the same stratification scheme as currently used, albeit with fewer strata, notably excluding many strata with depths <100 m. There were concerns that absence of the shallower strata covering depths favoured by cod could result in a significant bias in the index of cod abundance. Furthermore there have been doubts as to whether it would be possible to calibrate the *Lady Hammond*, which fished a Western IIA trawl, and the *Alfred Needler*, which fished a URI trawl, to maintain a standardized series. Although there was a paired-tow comparative fishing experiment involving these two vessels in 1990, researchers at that time concluded, based on limited analysis, that the data were too variable to derive reliable size-based calibrations (Gascon et al. 1991¹, unpublished document). Recently, an analysis of these data using current statistical approaches that are adapted to dealing with different sources of uncertainty concluded that suitable size-based calibrations could be obtained for two other taxa, Greenland halibut, *Reinhardtius hippoglossoides*, and Redfish, *Sebastes spp.* (Yin and Benoît 2021, 2022). In the present report we analyse the comparative fishing data for cod from the 1990 experiments. We also re-analyse comparative fishing data from 2004 and 2005 between the CCGS *Alfred Needler* and the CCGS *Teleost* fishing the Campelen trawl, revising slightly the size-based calibration previously estimated for cod (Bourdages et al. 2007). We then evaluate the magnitude of bias that could result from the excluded strata prior to 1990 and propose an approach to address this bias. We present age-specific and age-aggregated indices

¹ Gascon, D., Gagnon, P., Bernier, B., and Savard, L. 1991. Le relevé conjoint crevette/poisson de fond du nord du golfe du Saint-Laurent (divisions de l'OPANO 4RST). CSCPCA Document de travail 91/70 (unpublished working paper).

of abundance, age-specific indices of depth distribution and estimates of total mortality, derived from the survey data

2.1. METHODS

2.1.1. General

A summary of survey protocols and details of the vessels and trawls used in the RV surveys are provided in Tables 1 and 2. Figure 2 summarizes the number of successful surveys sets in each year and stratum. Only strata numbered 801 to 841 (excluding 825 and 826) are pertinent for nGSL cod. Strata 401 to 414 and 851 to 855 occur in NAFO Division 4T, outside the stock area (Figure 1). Strata 302 to 305 are in NAFO Subdivision 3Pn and could have been relevant for the stock, However, these strata were not sampled for the majority of the time series.

To date, abundance indices for nGSL cod were based on sampling in strata 801-824 and 827 to 841, excluding 840 (Figure 3). Of these strata, 835 to 841 (excl. 840) represent the shallower strata that were not sampled prior to 1990. Here we construct two sets of indices, one covering 1990 to present, based on the traditionally employed strata (8910824; 827-841), and another based on the reduced suite of strata, covering 1984 to present and excluding strata 835-841.

Details for the survey are provided in annual research documents (for the most recent, see Bourdages et al. 2020). The survey is also described more generally in Chadwick et al. (2007).

2.1.2. Comparative fishing

Comparative fishing between the *Lady Hammond* with Western IIA trawl and the CCGS *Alfred Needler* with the URI trawl took place between August 22 and 29, 1990. The results of these experiments have not previously been published (Gascon et al. 1991¹, unpublished document). During the paired tows, the vessels fished simultaneously and in parallel separated by the shortest distance considered practical and safe. Standard fishing procedures proper to each vessel were employed (see Table 1). A tow on the *Lady Hammond* was considered initiated when the winches deploying the trawl warps were blocked and completed when the winches began hauling in the gear. In contrast, a tow on the CCGS *Alfred Needler* was considered initiated when parameters reported by trawl-mounted Scanmar sensors indicated the trawl was on bottom and adequately open, and completed when the trawl left the bottom. Effects on catchability of this and other differences in protocol (e.g., tow speed and duration; Table 1) should implicitly be accounted for in conversion factors estimated from comparative fishing data. A total of 80 valid paired tows were completed, at depths ranging from 74 to 486 m (average 267 m). The location of paired sets and resulting catches of cod by each vessel are presented in Figure 3.

Comparative fishing between the CCGS *Alfred Needler* with the URI trawl and the CCGS *Teleost* took place in August in both 2004 and 2005, with the majority of comparative sets accomplished in the second year. The details of these experiments are available in Bourdages et al. (2007) and are not repeated here. The location of paired sets and resulting catches of cod by each vessel are presented in Figure 4.

2.1.3. Comparative fishing data analysis

2.1.3.1. Binomial models

In the analysis of comparative fishing data, the goal is to estimate the relative fishing efficiency between a pair of vessels-gear combinations (referred to as gear in this section for simplicity). We assume the expected catch from gear g ($g \in \{A, B\}$) at length l and at station i is

$$E[C_{gi}(l)] = q_{gi}(l)D_{gi}(l)f_{gi}$$

where, $q_{gi}(l)$ is the catchability of gear g , D_{gi} is the underlying population density sampled by gear g , and f_{gi} is a standardization term which usually includes the swept area of a tow, and if applicable, the proportion of sub-sampling for size measurement on-board. In a binomial model (e.g., Miller 2013), the catch from gear A at station i , conditioning on the combined catch from both gears at this station, $C_i(l) = C_{Ai}(l) + C_{Bi}(l)$, is binomial-distributed

$$C_{Ai}(l) \sim BI(C_i(l), p_{Ai}(l))$$

where $p_{Ai}(l)$ is the expected proportion of catch from gear A . Tows in a pair are generally assumed to fish the same underlying densities at the station, as the paired vessels typically fish within a small distance of each other: $D_{Ai}(l) = D_{Bi}(l) = D_i(l)$. Then the logit-probability of catch by gear A is

$$\text{logit}(p_{Ai}(l)) = \log\left(\frac{E[C_{Ai}(l)]}{E[C_{Bi}(l)]}\right) = \log(\rho_i(l)) + o_i$$

Where $\rho_i(l)$ is the ratio of catchabilities between gear A and B at length l and at station i , or the conversion factor, the quantity of interest,

$$\rho_i(l) = q_{Ai}(l)/q_{Bi}(l)$$

and $o_i = \log(f_{Ai}/f_{Bi})$ is an offset term derived from known standardization terms for swept area and subsampling.

For a length-based conversion factor, we consider a smooth length effect based on a general additive smooth function,

$$\log(\rho(l)) = \sum_{k=0}^K \beta_k X_k(l) = \mathbf{X}^T \boldsymbol{\beta},$$

where $\boldsymbol{\beta}$ are the coefficient parameters and are estimated, \mathbf{X} , or $\{X_k(l), k = 0, 1, \dots, K\}$, are a set of smoothing basis functions, and K is the dimension of the basis that controls the number of coefficient parameters and is usually pre-defined. Here a cubic spline smoother was used (Hastie et al. 2009), with the basis functions and penalty matrices generated by the R package (R core team 2021).

The estimation of a cubic spline smoother is based on the penalized sum of squares smoothing objective, but in practice, this is usually replaced by a penalized likelihood objective (Green and Silverman 1993):

$$\mathcal{L}(\boldsymbol{\beta}, \lambda) = f(\mathbf{Y}|\mathbf{X}, \boldsymbol{\beta})e^{-\frac{\lambda}{2}\boldsymbol{\beta}^T\mathbf{S}\boldsymbol{\beta}}$$

\mathcal{L} denotes the likelihood objective function. $f(\mathbf{Y}|\mathbf{X}, \boldsymbol{\beta})$ is the joint probability function of the survey data \mathbf{Y} conditional on the basis functions and coefficient parameters. \mathbf{S} is the penalty matrix defined by the smoother and the dimension of the basis, and λ is the smoothness parameter. This smoothness parameter is estimated by maximum likelihood along with other model parameters but may be sensitive to the data. In such cases, it can be determined by other criteria such as generalized cross-validation (Wood 2000).

The penalized maximum likelihood smoother can also be re-parameterized into a mixed effects model (Verbyla et al. 1999; Wood 2017) to facilitate implementation as well as incorporation of additional random effects:

$$\log(\rho_i(l)) = \mathbf{X}_f^T \boldsymbol{\beta}_f + \mathbf{X}_r^T \mathbf{b}$$

where $\boldsymbol{\beta}_f$ are fixed effects and \mathbf{b} are random effects. \mathbf{X}_f and \mathbf{X}_r are transformed from the basis functions \mathbf{X} and an eigen-decomposition of the penalty matrix \mathbf{S} , $\mathbf{X}_f = \mathbf{U}_f^T \mathbf{X}$ and $\mathbf{X}_r = \mathbf{U}_r^T \mathbf{X}$, where \mathbf{U}_f and \mathbf{U}_r are the eigenvectors that correspond to the zero and positive eigenvalues of \mathbf{S} . The random effects $b \sim N(0, \mathbf{D}_+^{-1}/\lambda)$ where \mathbf{D}_+ is the diagonal matrix of the positive eigenvalues of \mathbf{S} . In the mixed effects model representation of the cubic spline smoother, the number of fixed effects is 2 and the number of random effects is bounded by $K - 2$. Smoothing effects are transformed into shrinkage of random effects in the fitting of random deviations, and can be integrated into complex mixed effects models commonly used in fisheries science (Thorson and Minto 2015).

Additional random effects can be incorporated into the mixed effects model to address variations in the relative catch efficiency related to each station,

$$\log(\rho_i(l)) = \mathbf{X}_f^T(\boldsymbol{\beta}_f + \boldsymbol{\delta}_i) + \mathbf{X}_r^T(\mathbf{b} + \boldsymbol{\epsilon}_i).$$

where $\boldsymbol{\delta}_i \sim N(\mathbf{0}, \boldsymbol{\Sigma})$ and $\boldsymbol{\epsilon}_i \sim N(\mathbf{0}, \mathbf{D}_+^{-1}/\xi)$. From a similar re-parameterization of the cubic spline smoother, these random effects allow for deviations of the length-based conversion at each station. $\boldsymbol{\Sigma}$ is the covariance matrix of the random effects corresponding to the random deviations and contains three parameters. ξ controls the degree of smoothness of the random smoothers and the smoother at each station can differ.

A summary of the above binomial mixed model is as follows,

$$\begin{aligned} C_i(l) &= C_{Ai}(l) + C_{Bi}(l) \\ C_{Ai}(l) &\sim BI(C_i(l), p_{Ai}(l)) \\ \text{logit}(p_{Ai}(l)) &= \log(\rho_i(l)) + o_i \\ \log(\rho_i(l)) &= \mathbf{X}_f^T(\boldsymbol{\beta}_f + \boldsymbol{\delta}_i) + \mathbf{X}_r^T(\mathbf{b} + \boldsymbol{\epsilon}_i) \end{aligned}$$

The model is estimated via maximum likelihood and the marginal likelihood integrating out random effects is

$$\mathcal{L}(\boldsymbol{\beta}_f, \boldsymbol{\Sigma}, \lambda, \xi) = \int \left(\prod_{i=1}^m \int \int f(\mathbf{Y}_i | \mathbf{X}_f, \mathbf{X}_r, \boldsymbol{\beta}_f, \mathbf{b}, \boldsymbol{\delta}_i, \boldsymbol{\epsilon}_i) f(\boldsymbol{\delta}_i | \boldsymbol{\Sigma}) f(\boldsymbol{\epsilon}_i | \xi) d\boldsymbol{\delta}_i d\boldsymbol{\epsilon}_i \right) f(\mathbf{b} | \lambda) d\mathbf{b}$$

The binomial mixed model can be adapted for various assumptions on the smoother and potential station variation to accommodate different underlying density of a species and data limitations especially in length measurements. A set of binomial models considered in the present analyses is provided in Table 3.

2.1.3.2. Beta-binomial models

The binomial assumption of the catch can be extended to a beta-binomial distribution to explain over-dispersion at the stations (Miller 2013):

$$C_{A,i}(l) \sim BB(C_i(l), p_{A,i}(l), \phi_i(l)).$$

The beta-binomial distribution is a compound of the binomial distribution and a beta distribution. More specifically, it assumes a beta-distributed random effect in the expected proportion of catch from gear A across stations. As a result, the expected catch by gear A has a variance of

$$\text{var}(C_{A,i}) = C_i p_i (1 - p_i) \frac{\phi_i + C_i}{\phi_i + 1}$$

where ϕ is the over-dispersion parameter that captures the extra-binomial variation.

The same smoothing length effect can be applied to the over-dispersion parameter,

$$\log(\phi_i(l)) = \mathbf{X}_f^T \boldsymbol{\gamma} + \mathbf{X}_r^T \mathbf{g}$$

where $\boldsymbol{\gamma}$ are fixed effects and \mathbf{g} are random effects, $\mathbf{g} \sim N(0, \mathbf{D}_+^{-1}/\tau)$. This length effect models the variance heterogeneity and is particularly useful for projecting uncertainty to poorly sampled lengths. However, estimation of a length-based variance parameter typically requires sufficient catch at length data, which is usually not available for less abundant species.

A summary of the beta-binomial mixed model is as follows,

$$\begin{aligned} C_i(l) &= C_{Ai}(l) + C_{Bi}(l) \\ C_{Ai}(l) &\sim BB(C_i(l), p_{Ai}(l), \phi_i(l)) \\ \text{logit}(p_{Ai}(l)) &= \log(\rho_i(l)) + o_i \\ \log(\rho_i(l)) &= \mathbf{X}_f^T (\boldsymbol{\beta}_f + \boldsymbol{\delta}_i) + \mathbf{X}_r^T (\mathbf{b} + \boldsymbol{\epsilon}_i) \\ \log(\phi_i(l)) &= \mathbf{X}_f^T \boldsymbol{\gamma} + \mathbf{X}_r^T \mathbf{g} \end{aligned}$$

The marginal likelihood is

$$\begin{aligned} &\mathcal{L}(\boldsymbol{\beta}_f, \boldsymbol{\gamma}, \boldsymbol{\Sigma}, \lambda, \xi, \tau) \\ &= \int \int \left(\prod_{i=1}^m \int \int f(\mathbf{Y}_i | \mathbf{X}_f, \mathbf{X}_r, \boldsymbol{\beta}_f, \mathbf{b}, \boldsymbol{\gamma}, \mathbf{g}, \boldsymbol{\delta}_i, \boldsymbol{\epsilon}_i) f(\boldsymbol{\delta}_i | \boldsymbol{\Sigma}) f(\boldsymbol{\epsilon}_i | \xi) d\boldsymbol{\delta}_i d\boldsymbol{\epsilon}_i \right) f(\mathbf{b} | \lambda) f(\mathbf{g} | \tau) d\mathbf{b} d\mathbf{g} \end{aligned}$$

Likewise, various smoothing assumptions can be applied to the variance parameter. Table 4 presents a set of beta-binomial mixed models.

2.1.3.3. Model fitting and selection

In the analysis of each comparative fishing experiment, the conversion factor was developed for a pre-specified length range at an interval of 1 cm. The length range was selected as the minimum to the maximum observed length from the comparative fishing survey.

The binomial and beta-binomial models in Tables 3 and 4 were implemented in *TMB* (Kristensen et al. 2016) which were compiled into objective functions and subsequently optimized in *R*. The basis functions for the cubic smoothing spline and the corresponding penalty matrices were generated using the *R* package *mgcv* (Wood 2011) based on 10 equally-spaced knots ($K = 9$) within the pre-specified length range depending on the comparative fishing survey. *TMB* automatically calculates a standard error for the maximum likelihood estimation of the conversion factor via the delta method (Kristensen et al. 2016).

There are in total 13 candidate models for estimating the conversion factors, although convergence could not be attained for some of the more complex models. The best model for each comparative fishing survey was selected by AIC (Akaike information criterion) to maximize model fitting, while avoiding over-fitting of more complicated models especially in cases without adequate data. In each analysis, the estimated μ function (length-specific expected proportion of catch by gear *A*) from all converged models were compared along with the sample proportions (aggregated by stations and averaged for each length) to provide a more rigorous interpretation of the results. The estimated ρ (expected relative catch efficiency, or conversion factor) from the best model is presented here and validated with estimation from past studies, if available.

2.1.3.4. Calibration of survey catch

The conversion factors estimated from the comparative fishing experiments were applied to the annual bottom trawl survey catches from the *Lady Hammond* (C_{LW}) and the CCGS *Alfred Needler* (C_{NU}) to calibrate the catches equivalent to those that would be made by the CCGS *Teleost* fishing the Campelen trawl, C_{TC} . For most surveys this involved applying sequential length dependent conversion factors:

$C_{TC} = \rho(l)_{NU \rightarrow TC} C_{NU}$, for catches by the *Alfred Needler* fishing the URI trawl in the nGSL survey;

$C_{TC} = \rho(l)_{NU \rightarrow TC} \rho(l)_{LW \rightarrow NU} C_{LW}$, for catches by the *Lady Hammond* fishing the Western IIA (WIIA) trawl;

In this report we proceed with calibrations as they have traditionally been employed, that is without propagating their uncertainty to the estimated uncertainty in catch-related estimates, such as abundance indices. Propagation of uncertainty is reasonably straightforward in an integrated survey analysis model, or using computer intensive approaches such as bootstrapping, and is planned for the analysis of these survey data in the future.

Length-dependent relative catch efficiency was estimated only over the range of length available in the respective comparative fishing experiments. When applying these estimates to lengths below or above this range to calibrate survey catches, we assumed constant efficiencies equal, respectively, to those at the minimum and maximum lengths of the range in the estimation.

2.1.4. Survey data analysis

2.1.4.1. Abundance indices

Annual abundance indices and associated standard errors were estimated using the standard estimators for stratified sampling

$$\bar{x} = \frac{\sum_{h=1}^L N_h \bar{x}_h}{N} \text{ where } N = \sum_{h=1}^L N_h$$

$$s_{\bar{x}}^2 = \left(\frac{N_h}{N}\right)^2 \left(\frac{N_h - n_h}{N_h}\right) \frac{s_h^2}{n_h} \text{ where,}$$

L = total number of strata

N_h = size of stratum h (here expressed as the number of trawlable units)

\bar{x}_h =sample mean for stratum h based on the standardized catches (standardized for distance towed)

n_h = sample size for stratum h

s_h = sample standard deviation for stratum h

In some years, certain strata were not sampled at all, or were sampled only by one tow, preventing an estimation of s_h (Figure 2). In these cases, values of \bar{x}_h and s_h were imputed using predictions from linear models of the form:

$$\log(\text{catch rate} + 0.5) \sim \text{stratum} + \text{year}$$

which were fit using the data from the year in question and the three preceding years, when three were available, or three adjacent years for cases of missing strata occurring in the first three years of the series.

Total and age-specific annual abundance indices were estimated. Age-specific estimates were derived by first producing length-specific estimates, to which annual age-length keys were applied. Survey lengths were recorded in 3-cm intervals for 1985-1987, in 1 cm intervals in 1984 and 1988-1995, and by 1 mm intervals thereafter, but rounded to cm for the current analyses. Annual age-length keys were derived for the entire survey area based on length-group stratified sampling. Greater variation in lengths at age are evident for the first three years of the survey using the *Lady Hammond* (Figure A1).

2.1.4.2. Catch at age and standardized proportion at age per year (SPAY)

Catches at age were plotted using traditional bubble plots in which bubble size was proportional to mean catch for each age and year. These values were also converted to standardized proportion at age per year (SPAY) by first calculating proportions at age in each year, subtracting the mean proportion at each age and dividing by the standard deviation of the proportions computed across years.

2.1.4.3. Total mortality

A modified catch curve analysis was used to estimate annual values of total mortality, Z (Sinclair 2001). The approach is an extension of a typical catch curve analysis (regression of log-abundance on age), whereby Z is estimated as the common slope from an analysis of covariance that includes several year classes (cohorts) treated as a factor. The analytical model employed was:

$$\log A_{ij} = \beta_0 + \beta_{1y} + \beta_2 age + \varepsilon$$

where A_{ij} is the stratified mean catch per tow in the RV survey of cod age i in year j . The vector β_{1y} provides separate estimates of intercepts for each year class (treated as fixed effects). The parameter β_2 is the estimator of Z . Following the approach of Sinclair (2001), this analysis was repeated in successive 4-year blocks providing an estimate of the average Z experienced by the cohorts during the time block. The age range included in the analysis was restricted to include those ages that appear to be fully recruited to each survey included in the analysis (i.e., age-specific catch rates linearly declining with age within cohort; see Sinclair 2001), specifically ages 5 to 10 for the RV survey. Assuming that mortality is the same over the ages, departures from linearity in the catch curve analysis suggest a change in catchability across ages (Ricker 1975). As such we visually examined the residuals of the analysis with respect to age to confirm the appropriateness of the age ranges for each survey.

2.2. RESULTS

2.2.1. Comparative fishing data analysis

The comparative fishing survey in 1990 (nGSL 1990) resulted in 80 pairs of successful tows and 53 effective pairs (with a positive combined catch of cod) which were used for the analysis. The nGSL 2004-2005 analysis had 161 successful pairs and retained 86 effective pairs for the analysis. These effective tows were mostly located within 4RS (Figures 3, 4), where population density was relatively higher. A 15-80 cm size range was selected for modeling based on frequencies of measured lengths from both surveys. In the analysis of each dataset, the 13 candidate binomial and beta-binomial models were fit to paired catches within the specified length range and the best model was selected as the one with the lowest AIC among all models that properly converged (Table 5).

The best model in the nGSL 1990 analysis was BB5 (Table 5), with a marginal difference in AIC from BB4. The expected proportion of catch by *Lady Hammond-WIIA* was estimated from each converged model and then compared to the best model (Figure 5). The length effect in the

relative catch efficiency between *Lady Hammond*-WIIA and *Alfred Needler*-URI was significant, where *Lady Hammond*-WIIA was increasingly more efficient for large sizes. The estimated length-effect was nearly identical for models BB5 and BB4, and quite similar for the other length-dependent models.

In the nGSL 2004-2005 analysis, the best model selected by AIC was BI3 (Table 5) but estimates were almost identical to BB4. Improvements in model fit were mostly explained by the length effect (comparing to BI1 and BB1) and the random station effect (comparing to BI2, BB2, BB3). As the more parsimonious model, BI3 was chosen to estimate the calibrations. The estimated proportion of catch by *Alfred Needler*-URI (Figure 6) from that model indicated an increased relative catch efficiency with length up to 50 cm. For cod greater than 50 cm, *Teleost*-Campelen consistently caught about three times the catches compared to the *Alfred Needler*-URI (estimated relative catch efficiency of *Teleost* compared to *Alfred Needler* of around 4 for length range 50-80 cm). This was a notable improvement from models BB2, BB3 and the exponential model used previously (Bourdages et al. 2007), all of which did not include a station effect. Relative to the results of the exponential model which were previously used for cod, the new estimates predict less catch by the *Alfred Needler* compared to the *Teleost* at larger sizes (Figure 6).

The estimated relative catch efficiencies (conversion factors) were derived from the estimated catch proportions in each analysis with their respective standard deviations (Figure 7). Estimation for larger sizes were subject to higher estimation uncertainty due to limited catches or population presence. Prediction residuals were calculated for the best models in each case in order to assess model fits and residual diagnostics using the normalized randomized quantile residuals (Dunn and Smyth 1996). These residuals did not indicate significant deviations related to either length or station (Figures 8, 9). To demonstrate the effectiveness of the conversion factors, catches from the old vessel were calibrated to the new vessel in each comparative fishing survey and the subsequent catch-at-length composition was compared to the new vessel. In both cases, catch compositions matched up between the calibrated old vessels and the new vessels (Figures 10, 11). For calibration of the survey index, conversion from *Lady Hammond*-WIIA to *Teleost*-Campelen was derived by a sequential multiplication of relative catch efficiencies from two comparative fishing analyses so that all historical survey catches were eventually calibrated to *Teleost*-Campelen equivalent. The conversion factors were also extended over the range 1-120 cm to cover lengths outside of the model range that may appear in annual survey catches (Figure 12).

2.2.2. RV survey indices

The new RV survey indices compare very favorably with the ones previously used for the stock assessment (Figures 13, 14). In some years and for some ages (Figure 13), and for overall numbers (Figure 14), the new values are somewhat lower in the new series as a result of not including the shallower strata where higher cod densities are expected. This is examined in more detail below. The effect is often to attenuate spikes in abundance at age that occurred in the previous indices (Figure 13). For ages 4 and older, the addition of the 1984-1989 period considerably increases the span of time at which the stock was at higher abundance, prior to the collapse in the early 1990s. Previously the assessment of the stock relied on survey indices that included only two years of pre-collapse abundances. Notably, survey numbers per tow at ages 6 and older are considerably higher in the newly added period.

Survey length frequencies for estimates based on the reduced suite of strata and all consistently sampled strata are very similar (Figure 15). Although numbers are typically somewhat higher in the latter estimates, again because of the exclusion of shallower strata favored by cod, proportions at length are generally nearly identical (Figure 16). Compared to the 1980s, surveys

in the most recent decade, have shown a reduced proportion of larger cod. The length frequencies also show the progression of a rather large cohort first seen at a mode of around 12 cm in 1988 and which tracked through the length frequencies until at least 1991.

Survey catch at age, particularly when standardized as SPAY were nearly identical for the two sets of estimates (Figure 17). As noted above, the new extended series provides estimates of catches at older ages in the 1980s that are well above average both numerically and as standardized proportions. They also show the progression of at least two large cohorts that are not otherwise seen in the series that begins in 1990.

The progression of cohorts is also illustrated as catch curves in Figure 18. From these it is evident that the survey tracks cohorts consistently over time, i.e., with few exceptions, abundance is decreasing with age. Furthermore, the absence of breaks or unusual patterns in typical cohort decline around the years 1990 and 2004-2005 supports/confirms the efficacy and reliability of the conversions used to adjust the relative efficiency of survey vessels and trawls for the changes that occurred in those years. Finally, changes over time in the slopes of individual cohort trends indicate changes in total mortality, which is specifically analyzed below.

The ability to track cohorts, often called internal consistency, is also evident (Figure 19). One must bear in mind that the measure of correlation from one age to the next depends in part on the contrasts in the data, i.e., the range of abundances. The correlation coefficients presented in Figure 19 may therefore underrepresent true internal consistency, which is better evaluated by looking at longer term tracking of cohort abundance, as was presented in Figure 18.

Estimated Z for ages 5 to 10 has cycled since the mid-1980s, with a peak in values leading to the collapse of the stock in the early 1990s, lower values around 0.6 during the moratorium, followed by an increasing trend when the fishery was re-opened (Figure 20). Z then decreased associated with the 2003 moratorium, before increasing rapidly again after 2004. Values then decreased to 2015 before increasing again in the last five years to values that are among the highest in the series.

The remaining results relate to the relationship between age-specific survey indices based on the reduced versus full suite of strata. The goal is to find a method that might allow values for the 1984 to 1989 period to be adjusted to values equivalent of the full suite of strata. As noted above, survey indices for the reduced suite of strata were generally smaller than those for the full suite (Figure 21). A linear model regressing the log survey index for the full suite on the log index for the reduced suite was used to estimate possible age-specific conversions. While these conversions generally adjusted the 'reduced suite' index to values much closer to those of the full suite, they failed particularly to correct for cases in which there was a spike in abundance in the latter indices (Figure 21, middle column). This is especially true for older ages. With the exception of ages 11 and 13-plus, there was no autocorrelation in the residuals from the models indicating that there were no significant temporal patterns in the errors associated with an adjustment.

Instances in which the reduced suite and full survey indices differed the most indicate that the stock is distributed in more shallow waters in those years. We therefore reasoned that the depth distribution of cod in the reduced suite of strata might serve as an indicator of overall depth distribution and might therefore be a predictor in these instances. We estimated the mean depth occupied by cod for each age and year using depths measured in the survey, weighted by survey catches and survey design weights (sensu Perry and Smith 1994). Age-specific trends in the mean depth occupied are presented in Figure 22. As predicted there was generally a negative relationship between the mean depth occupied and residuals from the model used to calibrate the two sets of survey indices (Figure 23). That is, the corrected index tended to underestimate the index for the full suite when the occupied depth was shallowed. However the

relationship between the residuals and mean depths was not statistically significant, except for age 3. Nonetheless, the general pattern suggests that it might be possible to develop more reliable corrections by incorporating information on depth distribution as measured in the reduced suite of strata.

3. JANUARY RESEARCH VESSEL SURVEYS

From 1978 to 1994, excluding 1982, bottom-trawl surveys were undertaken annually in January in the nGSL and NAFO Subdivision 3Pn. These surveys, initially operated by DFO's Newfoundland and Labrador region and then DFO's Quebec region, used the MV *Gadus Atlantica*, which fished an Engel 145 High Lift otter trawl. Although these surveys were largely focused on redfish, catches of cod and certain other species were recorded. Beginning in 1983, length frequencies of cod catches and cod ages were also taken. While this survey had been used in the assessment of nGSL cod (e.g., Fréchet and Schwab 1989), this practice was discontinued in 1998 in favor of using only the August RV survey, along with Sentinel fishery indices (Fréchet and Schwab 1998). An important reason for this was that coverage of the survey area had varied considerably over time because of constraints caused by seasonal formation of sea ice. During the last five years of the survey, coverage was largely concentrated in the eastern portion of the area (Figure 24). Furthermore, there was evidence of important shifts in the distribution of cod associated with cooling ocean conditions and earlier formation of sea ice, raising concerns that a non-negligible portion of the stock may have been outside the survey area at the time of the survey (Fréchet 1990; Castonguay et al. 1999).

The shifts in survey coverage and cod distribution are such that it is very likely that the survey did not sample a constant proportion of the stock, and in fact this proportion likely diminished over time. Although attempts were made to infer representative annual spatial distributions of cod using spatio-temporal modelling to try and develop a consistent abundance index, the uncertainty associated with these predictions was far too great to yield a useful result (Rivest et al. 2021). Although four covariates of the distribution of cod were examined – depth, bottom temperature and presence or thickness of sea ice – non proved to be good predictors. Consequently inferences were largely based on estimated spatial and temporal correlations, which results in ballooning uncertainty as distances (in space or time) for predictions increase.

Although it is not possible to construct a reliable index of abundance for the January RV surveys, the age-composition data available since 1983 may nonetheless provide information for the assessment, provided that the survey sampled the different ages proportionately. Furthermore, conversions are available to adjust for the relative efficiency of the *Gadus Atlantica* fishing the Engel and the CCGS *Teleost* fishing the Campelen for size-dependent differences in relative catchability (Warren 1997). The age composition information from the January surveys might therefore provide validation of the age composition information from the August RV survey for the overlapping period of 1984-1994. It might also provide one additional year of information, for 1983.

Catch at age in the January RV surveys displays important year effects characterized by unusually large catches across most ages in 1986 and parts of the early 1990s, and low catches in 1988 for example (Figure 25, left panels). This illustrates the problems associated with partial and variable coverage of the stock by the survey. In contrast the SPAY plot for the survey is largely consistent with that of the August RV survey (compared Figure 17 and Figure 25, right panels). Both surveys tracked the progression of the same cohorts, although the January survey did not track the 1991 cohort over the three years during which the RV survey sampled it.

4. HISTORICAL RESEARCH SURVEYS

Scientific bottom-trawl surveys were undertaken in NAFO Divisions 4RS during a number of years from 1947 to the mid to late 1960s (Wiles and May 1968). These surveys have the potential to provide important information on the stock for a period that begins before the introduction of bottom-trawls to the fishery in 1954 and that spans an important intensification of fishing on the stock (Wiles and May 1968; Lear 1998). Unfortunately documentation of these surveys is not extensive and attempts to locate the original data in DFO's Newfoundland and Labrador Region were unsuccessful.

Wiles and May (1968) provide summaries of the survey results that inform on various demographic properties of the stock at the time, notably size and age composition and maturity. This information could provide a historical basis for changes in growth and maturation properties of the stock associated with intensification of fishing. Of note for the assessment, the authors provided survey catch curves for specific time periods. Extracting the data from their Figure 14, we used these catch curves to estimate total mortality, Z , under the assumption that the age composition for each period was approximately stationary. This cross-sectional approach to analyzing catch curves (unlike the longitudinal approach of Sinclair 2001) has the potential to provide biased estimates of Z if the different cohorts composing the curve had different initial abundance or experienced a different mortality schedule. Although we cannot rule out the former, it is reasonable to assume that mortality schedules could have been largely stationary at least prior to the intensification of commercial fishing. Furthermore, aggregating age-specific catches over several years as was done by the authors might 'average out' differences.

From the catch curves we estimate $Z=0.25$ (SE 0.02) for 1947 to 1951 (Figure 26). Because the stock was fished at the time, this value provides an upper bound for natural mortality, M . That value is consistent with values estimated for neighboring cod stocks at the time, which were estimated to be around 0.1 to 0.2 (northern cod, Pinhorn 1975; NAFO Divisions 4TVn cod, Dickie 1963, Paloheimo and Kohler 1968). We are not aware of any other sources of information on the natural mortality level for the 3Pn 4RS stock prior to the 1980s. Values of Z estimated for the periods 1957-1961 ($Z=0.39$) and 1962-1966 ($Z=0.59$ for 4R and $Z=0.44$ for 4S) were increasing in time (Figure 26), consistent with the increased intensification of fishing.

5. SENTINEL MOBILE GEAR SURVEYS

The Sentinel mobile gear (bottom-trawl) survey began in its current form in 1995. It involves sampling annually in July. There is also some sampling at other times of the year in many years, but the associated data are not used to derive indices of abundance and are not further discussed in this document. The July Sentinel mobile gear survey involves commercial fishery bottom-trawlers (typically nine vessels in a given year), that undertake a random stratified survey using the strata from the DFO RV surveys (Figure 1), with additional strata in NAFO Subdivision 3Ps, and coastal strata around Newfoundland added in 2003 (Figure 27) following a review of the program (Gillis 2002). Fishing procedures are standardized in the survey and all vessels fish the same type of trawl. Despite selecting vessels with similar fishing power, an evaluation of trawl performance using trawl mounted sensors in 1995 found that wingspread could vary among vessels by up to 20% (Fréchet 1996). A restrictor cable was thus implemented in the survey and found to be effective for standardizing wingspread among vessels (Fréchet 1997). The vessel are thus assumed to have equivalent fishing efficiency in the analysis of the survey data. A description of the history of the program and other details on survey procedures are available in Gillis (2002).

5.1. METHODS

Currently two distinct sets of abundance indices are derived from the sentinel mobile gear surveys, one for 1995-2002 based on the original suite of strata and one for 2003-present that includes catches in the coastal strata added in 2003. These two indices are treated as independent in the assessment model. This is not ideal because it increases the number of survey selectivity parameters to be estimated and especially because it eliminates information on abundance and especially mortality rates that would be available if the cohorts present in 2003 were tracked over their full course. As was done for the August RV survey, we estimated survey abundance indices for the 2003-2020 period excluding and retaining the coastal strata to examine the extent to which the latter can be predicted from the former.

5.2. RESULTS

On an age-aggregated basis, the two sets of indices generally correspond, but in some years (e.g., 2007, 2008, 2015), the values for the index that includes the coastal strata are considerably greater (Figure 28). On an age-specific basis, the differences are not as important for any given age (Figure 29). The indices excluding the coastal strata generally explain 90% or more of the variation of the indices based on all strata for ages 5 and up, and somewhat lower percentages for ages 2 to 4. Conversion factors were estimated using linear models. These improved the prediction of indices equivalent to those using all strata, especially for younger ages. Overall, and regardless of whether the indices excluding the coastal strata are assumed to be directly equivalent to those that include the strata, or equivalent following application of conversion factors, it is clear from Figure 29 that they predict well the indices based on all strata. For the younger ages (2 to 4), when there are deviations, these do not affect the rank order of values much. There may be benefits to converting 1995-2002 indices for these ages to full-stratum equivalents; however, for the older ages converting would change the values almost imperceptibly and is not worthwhile.

The catch at age and SPAY for the 1995-2020 series are presented in Figure 30. From this figure it is apparent that the Sentinel mobile gear survey was able to track at least two cohorts that were tracked by the August RV survey, those born in 1993 and 1998 (Figure 17). The surveys also tracked some above average cohorts born in the mid 2002 which were also evident, though perhaps to a lesser extent in the RV survey.

Overall the internal consistency for the Sentinel mobile-gear survey, based on biplots of survey abundance one year to the next, is moderate for ages 2 to 5 and 9 and above, but low for intervening ages (Figure 31). Recall however that the magnitude of these correlations depends on contrasts in the data, and that abundance over the period has not varied tremendously (Figures 28, 29). Trends in the abundance of individual cohorts show that the survey tracks abundance quite well (Figure 32).

Trends in estimated Z for the Sentinel mobile gear survey (Figure 33) are very similar to those from the August RV survey (Figure 20). Unlike the RV survey, the values for 2011 and 2012 are not declining, but this may reflect the higher uncertainty associated with them.

6. SENTINEL FIXED GEAR SURVEYS

A Sentinel fixed gear survey program involving commercial gillnet and longline harvesters was also initiated (at least in its current form) in 1995. It provides information on the abundance of cod in coastal areas that are not well sampled, if at all, by either the August RV or Sentinel mobile-gear surveys (Figure 34). The program involves largely standardized fishing procedures and fishing at or around defined sites. Sites were chosen to be roughly representative of

historical fishing grounds within each of six zones (Figure 35). Zones were defined based on geography and patterns in cod distribution inferred from historical knowledge in the fishery and surveys. Initially, in most zones, fishing occurred from the late spring to the fall, while in others (e.g., zone 1) it was almost year around. A general description of the program is available in Bérubé et al. (2000) and Gillis (2002).

Traditionally in the assessment for nGSL cod, abundance indices for each of the gillnets and longlines surveys were estimated using classical catch rate standardization (Gavaris 1980). This involved the use of linear models based on the log of catch standardized to effort (number of nets or hooks) in individual hauls, as a function of main fixed effects for year, month and zone. For longlines an additional effect for the use of J-hooks versus circle hooks was also included. In some years main effects for classes of gear immersion times were also included. Interactions between the main effects were usually tested and variously reported to be unimportant, even when they were statistically significant. The linear model was used to standardize total catch rate. Age composition was estimated in a manner equivalent to the way it is done for commercial catches (Ouellette-Plante et al. 2022). The length composition of catches from individual hauls were aggregated by season (month), zone and gear type, and an overall length composition was estimated by weighing these value by catch amounts. Age composition was then inferred by applying an age length key.

A review of these methods and data inputs leading up to the current review of the assessment framework revealed a number of important deficiencies with the traditionally used approach. There has been an overall reduction in sampling over time as a result of budgetary constraints that resulted in an increasing absence of sampling for a number of levels of the main effects in the linear model, resulting in turn, in a highly imbalanced design matrix. This can produce biases in the standardized series. Notably the effect for several month classes became increasingly informed from sampling in fewer zones. There were also important interactions between the main effects in the model, notably between zone, month and year, reflecting changes in the seasonal migration patterns between zones over time. The presence of interactions involving the effect of year prevent the production of a reliable time series of standardized catches. In addition, the approach to estimating age composition explicitly did not account for the effects on catch for which the linear model was trying to account.

It is not clear why catch rate standardization was applied to the Sentinel fixed gear survey data, although this is the practice in the other DFO regions that have such programs (Mello et al. 2019; Swain et al. 2019). Standardization of catch per unit effort in commercial fishery data (*sensu* Gavaris 1980) is used to standardize for many of the factors that are otherwise accounted for by the sampling design for Sentinel fisheries, such as spatial and temporal stratification of sampling. In many respects, the Sentinel fixed gear surveys are much more akin to the stratified RV and mobile gear surveys, than to commercial fishing. Fortunately, the estimation of indices based on a stratified design is also the main method advocated for producing standardized catch per unit effort series when there are interactions involving the effect of year (Maunder and Punt 2004). This requires defining meaningful statistical weights for the strata, which is possible for the Sentinel fixed gear surveys. Here we have revised the estimation of abundance indices using stratified estimation.

For the analyses, catches of cod in each haul were disaggregated by age using length frequencies that were typically haul specific or based on hauls nearby in space and time and assumed to be representative. Appropriate age-length keys were then applied to these length frequencies to obtain an estimated age composition (see Appendix II).

The indices derived here cover ages 3 to a 13+ group. Catches of cod ages 1 and 2 were nil or too infrequent to derive meaningful abundance indices (Table 6). Although indices were derived

for cod age 3 in the gillnet surveys, they may not be very reliable given a high proportion of nil catches.

For the analyses described in the next sub sections, we treat observations (individual hauls) as clustered by fishing site, and stratified according to zone and some sub-annual temporal unit. Analyses were kept separate for longline and gillnet data, and the definition of the temporal unit was specific to each, according to data availability (details below). Overall, there was a general reduction over the years in the number of sites fished in each zone, and the number of hauls undertaken annually per site in all zones and by both types of gear (Figures 36 to 42). A switch from J hooks to circle hooks in longlines is also evident in all zones.

Selection of the spatial (zone) and temporal strata for the abundance indices was based on the availability of data over the whole series beginning in 1995 and is described below. Before making this selection, we first selected the observations which were considered to constitute valid Sentinel fixed gear fishing hauls. This selection was based on criteria associated with gear soak times and the amount of gear used for a haul. Soak times can affect catch rates because times that are too short will not allow for the complete capture of fish in the area, thereby under-representing catch as a function of abundance, while soak times that are too long may result in the loss of captured fish due to depredation and drop-out of decaying fish. The non-linear relationships that likely exist between catch rates and soak times are such that it is often not possible to account for variable soak time in fixed-gear survey standardization (Ward et al. 2004; Peterson et al. 2017). Instead, soak times are often standardized in surveys to control for their effect.

6.1. LONGLINE SENTINEL

Soak times for longlines were generally clustered around four hours, although there was also a secondary peak at 24 hours and a much smaller one at 48 hours (Figure 43a). Limiting soak times to between one and 25 hours retained 96% of the available data.

Most sentinel longline hauls were made using 1000 hooks, and nearly all involved some multiple of 250, between 500 and 2000 hooks (Table 7). Retaining hauls using 500 to 2000 hooks eliminated fewer than 90 observations out of 9,147. The criteria we used to select data based on the amount of gear employed are the same as the criteria used previously.

6.1.1. Methods

6.1.1.1. Gear saturation

Unlike bottom-trawls, fixed gear hauls are susceptible to saturation of the gear, generating hyperstability that can make catch rates increasingly less proportional to abundance as competition for slots on the gear increases. This competition can be intraspecific (other cod) or with other species and is perhaps more poignant for longlines where bait may be taken from hooks, causing them to cease fishing. Methods exist to account for competition for bait and gear saturation, but these require data for the total number of fish caught (all species) as well as the number of hooks that were empty and still baited and hooks that were empty and unbaited when the gear was retrieved (Étienne et al. 2013; Smith 2016). The later information is not collected in the Sentinel program. Brulotte and Fréchet (2000) previously considered saturation in the nGSL Sentinel fixed gear surveys by looking at the relationship between catch rates and soak times, concluding that saturation did not appear important. Catches of species other than cod are recorded as total catch weight, which Brulotte and Fréchet (2000) converted to estimated numbers of fish by applying species-specific average individual weights. Using the weights they employed, we examined the catch rates (all species) in longline catches. Since the early 2000s, median catches per 1000 hooks have varied without trend, around or below 200 fish (Figure

44). Most hauls caught 500 or fewer fish per 1000 hooks, well below saturation levels, assuming limited bait loss. Since 1998, most of the catch has been cod, indicating that interspecific competition for hooks is likely limited. To evaluate whether catch rates (all species) were related to soak times, we used a model of the form:

$$\log(\text{catch per 1000 hooks}) \sim s(\text{soak time}) + (1|\text{unit})$$

where $s(\text{soak})$ is a cubic regression spline for soak time and $(1|\text{unit})$ is a random effect grouping hauls at the same site, month and year, and which was included to account for local density of fish. Residuals from the model fish and the distribution of the random effects are presented in Figure A2. Although the model seems to fit well, there was some heteroscedasticity in residuals for larger fitted values and the distribution of random effects was slightly skewed compared to Normal.

Although there was a statistically significant effect of soak time, the patterns were not consistent with a systematic trend (Figure 45). This was equally apparent in the distribution of catch rates which did not vary systematically with soak time (boxplots in Figure 45). There is consequently no adjustment or accounting for soak times in the subsequently analyses.

6.1.1.2. Strata for the abundance indices

Longline sampling has occurred consistently in all zones except zone 6. For zones 1 to 5, the number of hauls undertaken each month has declined over the years (Figure 46). Over the history of the survey sampling across all five zones has only occurred concurrently in August and September. In contrast there has been consistent monthly sampling from June to December at sites in zone 1 and the most southerly site (site 8) in zone 2, which is located off of Codroy Newfoundland (Figure 37). Based on the availability of data, and to maximize their use, we derived two separate abundance indices for Sentinel longlines.

The first used sampling in August to September (specifically days of the year 210 to 270) in each of the five zones. The availability of data prevented the use of temporal strata (e.g., month), and consequently zones were treated as the only strata for the estimates of abundance indices. Annual sample sizes by stratum are provided in Figure 47. This abundance index has the advantage that it should reflect the abundance of cod in coastal waters during the late summer, and therefore complement the index for cod in mid and offshore waters provided by the August RV and Sentinel mobile gear surveys. The statistical weights for the strata defined by zone were established based on the linear distance between zone boundaries (Table 8; see Figure 35 for the boundaries). For Zone 4 it was based on the distance from the boundary with Zones 3 and 5, and the tip of the Strait of Belle Isle. The rationale for Zone 6 is provided later when discussing gillnets.

The second index was based on data from the late fall (days of the year 271 to 365) from sites in Zone 1 and site 8 in Zone 2. Dates were chosen to eliminate overlap of data with the other index. Although these data are more spatially concentrated than for the first index, they may nonetheless be representative of the cod stock given that it migrates through the area in the late fall and early winter to reach its overwintering grounds in the deeper waters of NAFO Subdivision 3Pn. Given the migratory movement of cod through the area, catch rates vary over the fall and early winter period. To address this we defined five sequential time blocks to serve as strata, based on availability of data and consistent with seasonal changes in catches rates. While the first block represented 10 days, the four subsequent ones were each of 21 day duration (more details are provided below). The number of hauls available for each time block stratum and year are given in Table 9.

6.1.1.3. Relative fishing efficiency of J hooks and circle hooks

Circle and J-hooks are known to have differing length-dependent, and thus age-dependent, efficiency. To account for these difference, we estimated age-specific relative efficiencies which were then applied to catches by J-hooks to produce circle hook-equivalent catches. Circle hooks were chosen as the standard given their overwhelming use in the past 20 year in Sentinel surveys.

For the analysis we defined sampling units based on hauls undertaken at the same site, year and week. The assumption for the analysis is that hauls in the same unit fished the same density of cod. For this analysis, data from all zones and dates were used to maximize the availability of data given that it is unlikely that age-specific relative efficiency varied over time and among locations since size at age of cod has not varied much (Brassard et al. 2020). Only units that had hauls using circle hooks and hauls using J-hooks were retained, regardless of whether there were any cod caught. This retained data for 995 hauls.

The model employed was of the form:

$$\text{catch} \sim \text{gear} + \text{age} + (\text{gear} \times \text{age}) + (1|\text{unit}) + \text{offset}(\log(\text{hooks}/1000))$$

where, gear was a factor for hook type, cod age was included as a factor, unit was included as a random effect, and an offset term was included to account for effort. Catches were assumed to follow a Tweedie distribution (with a log link function), which is a continuous distribution with a density at values of zero. Although catches are meant to be counts, the estimations of catches at age for the Sentinel fixed gear data results in non-integer values. For this reason, and due to model performance issues in preliminary analyses, the Tweedie distribution was chosen over the negative binomial. The analysis was undertaken using the glmmTMB package (Brooks et al. 2019). Results are presented in Figures 48 and 49.

The analysis was first run for ages 3 to 12 and for 13-plus, and is referred to as model A. Quantile residuals estimated using the R DHARMA package (Hartig 2021) were used to evaluate model adequacy. The distribution of quantile residuals indicated some model inadequacy in particular for ages 3 and 13-plus, and more minor inadequacy (tendency towards larger quantiles) for ages 5 to 11 (Figure A3). Diagnostic tests indicated that the model adequately captured the prevalence of zeros, but that the models was associated with a statistically significant level of under-dispersion (dispersion metric <1 ; Table 10). Under-dispersion is statistically conservative in that standard errors for model parameters will tend to be overestimated. This is less of a concern here. A second model (model B), removing two outlier hauls for age 3 (Figure 49) and grouping cod aged 10-plus was also fitted. The distribution of quantile residuals as a function of age was improved compared to model A (Figure A4), although zero-inflation and dispersion characteristics were similar (Table 10).

The models, which estimate the log relative efficiency of circle hooks, fit the relationship between mean catch rates by the two gears in the respective units well (Figure 48). (Note the model is fit to individual catches, while Figure 48 contrasts the average of individual catches in units). The estimated log relative efficiency values for both models increased for ages 3 and 4, leveling off for subsequent ages and corresponded to sample (empirical) means calculated directly from the data, providing confidence in the results (Figure 49a). Nonetheless, the estimates from model A for ages 11 and above were characterized by higher uncertainty, and more variability between ages, motivating the fitting of model B. Furthermore, the results for age 3 were sensitive to the removal of the two outlier sets. Consequently these estimated relative efficiencies from model B were applied to subsequent analyses.

Taking the exponent of the estimated parameter, we find that relative to J-hooks, circle hooks caught 10% less cod of age 3, but 16% more at age 4, between 26 and 33% more at ages 5 to

9, and 15% more at ages 10-plus. The corrections apply to all or almost all longline hauls prior to 2000, but a much reduced proportions of hauls since 2003 (Figure 49b).

6.1.1.4. Abundance index estimation

Although sites were initially chosen by fishing industry participant in a manner that might be akin to random within zones, these were largely fixed subsequently. New sites were rarely added and many were dropped over time. For the late summer index we therefore chose not to treat sites as random clusters, but instead as strata nested within zone, with each site receiving a weight equal to 1 over the number of sites for a given zone and year. This is meant to account for some intra-site correlation in catch rates that is evident for those longline data (see examples for cod ages 4 and 12 in Figures 50, 51). (Note that these figures also illustrate some of the interaction between Zone and year on catch rates, which motivated us to abandon the previously used catch-rate standardization approach.) Stratification by site was not employed for the late fall index as there was little evidence of intra-site correlation in catch rates (Figures 52, 53). In fact catch rates for a given year and date are remarkably consistent among hauls, regardless of site, especially for more abundant cod ages, here age 4 as an example (Figure 52).

An important consideration when employing stratification by site when the number of sites varies across years is that catch rates at sites that are not sampled every year are approximately equal to average catch rates in the zone. For instance, cessation of sampling at a site that normally has above average catch rates will produce a decrease in zonal mean catch rate relative to what would have otherwise been obtained. To evaluate whether this might be a concern for the late summer indices, we calculated and plotted zone and site specific annual mean catch rates for cod of different ages. (Note that this was not undertaken for the late fall zone 1 index given little evidence for site-specific differences in Figures 52 and 53, nor for that same zone in the late summer, which we show below.) For zones 1 and 5, and to a more variable degree zone 3, annual mean catch rates were consistent between sites, regardless of cod age (Figures A5 to A15). For zones 2 and 4, there were site-specific differences, particularly for ages 3 to 6, which may have affected the zonal annual means before 2000 and after 2012, years when one of more key sites were not sampled. The solution to this deficiency is not straightforward. Simply selecting sites for which there are data over all or most years would result in a large loss of data. Alternatively, model-based index estimation, in which site effects are modelled using an autoregressive process to estimate annual values in the absence of data could be explored, but was not feasible as part of the current project. Instead, we simply argue that because zones 2 and 4 constitute only a third of the survey area weight (Table 8) and that the impacts of site exclusion on zonal means are likely to be on the order 2 to 3 fold differences (based on Figures A5 to A8), consequences of variable site sampling on the overall abundance index are likely to be small. Furthermore, as we show below, the late summer abundance indices correspond well to the late fall indices, suggesting that the impacts of variable site sampling may be minor.

The majority of sites within a stratum and year were associated with at least two hauls in the summer index (Figure A16). Only 5.5% year-stratum-site groups had only 1 haul. To obtain estimates of the mean and variance for those sites we used a predictions from a linear model of the form

$$\log(\text{catch rate} + 0.01) \sim \text{year} + \text{site}$$

Model parameters were estimated using data limited to the year in question and three years preceding in the zone in question.

A stratified mean and variance were first estimated for each zone and year, based on site levels means and variances. In cases involving a single site, the site mean and variance were imputed for the stratum using results from the above multiplicative model. A second stratified calculation involving the statistical weights for the zones (Table 8) was then used to estimate annual means and standard errors.

There were a limited number of cases in which certain zones were not sampled in a given year. A mean and variance value for these cases were imputed using predictions from a linear model of the form

$$\log(\text{catch rate} + 0.01) \sim \text{year} + \text{zone} + (1|\text{site})$$

where $1|\text{site}$ is a site specific random intercept. Model parameters were estimated using data limited to the year in questions and three years preceding across all zones.

Stratified mean abundance estimates (in numbers per haul) were undertaken separately by age and for total cod catch. As with the trawl surveys, we estimated trends in total mortality using a catch-curve analysis, assuming that cod ages 8 to 12 were fully recruited to the surveys

6.1.2. Results - Sentinel longline indices

The ages 3+ age-aggregated summer index increased over the 1995 to 2005 period, declined until 2010, before rising again and generally declining as of 2012 (Figure 54). The exception was 2011 for which the value was elevated. Catch at age in that index indicates that it tracks cohorts reasonably well, with many but not all cohorts also tracked by the August RV survey (Figure 55). In particular the longline index tracked above average abundance cohorts born in the mid-2005, that were present, but less evident in the catch at age for the mobile gear surveys (Figure 30).

The summer index follows the abundance pattern of cohorts well (Figure 56), indicative of a reasonable internal consistency also seen in biplots (Figure 57).

Estimates of Z were very smooth over time, declining from the mid-1995 to the 2003 moratorium to a value around 0.1 (Figure 58). They then increased rapidly to a peak around a value of 2 in 2009, before declining in the early 2010s and increasing to values of around 1 more recently. Although the trends in Z are very similar to those obtained from the RV and Sentinel mobile-gear survey indices, values of Z peaked at a higher level in the longline index.

The ages 3+ age-aggregated fall index followed a similar trends as the summer index (Figure 59). Patterns in catches at age and SPAY (figure 60) were also quite similar. The fall index follows the abundance pattern of cohorts well (Figure 61), indicative of a generally good internal consistency also seen in biplots for many ages (Figure 62). The trend in Z was similar to that of the summer index, although the extremes were reduced (Figure 63). Unlike the summer index, Z in the fall index only reached value around 0.5 around the 2003 moratorium, and the subsequent peak in Z was of lower magnitude.

6.2. GILLNET SENTINEL

Most gillnet soak times were just below or at 24 hours, with a secondary peak at 48 hours (Figure 43b). Some values extent much beyond 48 hours. Limiting soak times to between 8 and 48 hours retained 97.3% of available data. The larger allowance for soak times in the gillnet surveys compared to longline surveys was based on the distribution of soak time values and reflects the fact that longlines actively attract fish, thereby accumulating catch more quickly, but also loose fishing power more quickly as the bait deteriorates.

Retaining gillnet hauls that involved between 5 and 30 nets retained 15,317 of 15,402 total observations (Figure 64).

6.2.1. Gear saturation

The potential for gear saturation was also examined for gillnets, although unlike longlines it is less clear how to define a net as being saturated. Catches, expressed as numbers of fish (all species) per net, did not vary much over the years, although there were more slightly larger values during the middle of the 2000s and 2010s (Figure 65). The majority of hauls did not exceed 25 fish per net and few had more than 100. These numbers appear to represent levels well below net saturation. Cod generally represented a smaller fraction of the catch in gillnets compared to longlines (bottom panels of Figures 44 and 65). Regardless, the potential for intra or inter-specific competition for net meshes seems very low.

As was done for longlines, a general additive mixed effects model was used to assess the relationship between net soak time and catch rate (cod number per haul). The model was identical as that for longlines, specifically:

$$\log(\text{catch per haul}) \sim s(\text{soak time}) + (1|\text{unit})$$

where $s(\text{soak})$ is a cubic regression spline for soak time and $(1|\text{unit})$ is a random effect grouping hauls at the same site, month and year, and which was included to account for local fish density. A small constant of 0.1 was added to the catch prior to taking the logarithm to address a small number of zero values. Residuals from the model and the distribution of the random effects are presented in Figure A17. The model seems to fit well, with no patterns in standardized residuals and approximately normally-distributed random effects.

Although there was a statistically significant effect of soak time, it suggested a small and uncertain decrease in catch rates with increasing immersion times from 8 to 20 hours, and a slight increase thereafter (Figure 66). The soak times associated with the decrease are too low to be associated with significant drop out of deteriorating fish, and the subsequent stabilization or slight increase in catch rates for larger soak times is inconsistent with depredation loss, which should increase as predators become increasingly attracted to the nets. Consequently we applied no adjustment or accounting for soak times in the subsequently analyses.

6.2.2. Strata for the abundance indices

Gillnet sampling has occurred consistently in zones 3 to 6 from June to September, and into later months in Zone 3 (Figure 67). Decreases in the number of annual hauls occurred primarily before 2005. Based on the availability of data, and to account for seasonal effects on catch rates, we defined three sequential time blocks for the summer period: block 1 for days 165 to 195, block 2 for days 196 to 226 and block 3 for days 227 to 257 (Figure 68). Catch rates have varied by block, zone and year, and there is clear evidence of an interaction between these factors in the data (Figure 69 and 70). It is also clear from these figures that catch rates show some within-site correlation.

Zone 6 includes fish at geographically disparate sites, notably one off Sept-Îles in the western end of the zone, and other sites more clustered in the eastern end (Figure 35). The zone is also very long, which would give it a disproportionate weight in stratified estimates. To address this, we split the zone into three parts. The first, which we call hereafter Zone 6, is based on the established border with Zone 5 on the eastern end and a border set half way between Natashquan and Havre Saint-Pierre on the western end (see blue arrow in Figure 35). The choice of this western border was based on a discontinuity in cod density that is often evident in August RV survey catch rates around that location (see Brassard et al. 2020). The second zone,

which we term 6b, was defined using the existing western border and assigning the distance separating the site from that border to define the eastern border. The third zone, lying between Zones 6 and 6.2 and never sampled, was simply not assigned to any strata and therefore not represented in the analysis. The statistical weights for all strata are provided in Table 8.

The stratified mean was estimated as described for the longline summer index but with concurrent seasonal (time block) and zonal stratification. Time blocks were given equal weight. As with the summer longline index, a two stage stratified estimation was employed, first for catches within site and then for sites within Zones and time block. There were only 31 out of the 1402 year-time block-site pairs associate with a single haul, representing 2.2% of hauls. Imputation for single haul cases and for instances of missing stratum and year combinations was performed as described for longlines.

As with the longlines, we examined whether there was evidence for site-specific differences in mean catch rates within strata defined by zone and season block and which could influence the abundance indices as a result of inter-annual variability in which sites were sampled. Unlike the results for longlines, there was a high degree of consistency among sites in annual mean catch rates for all ages, except age 3 cod which are not common in the Sentinel gillnet catches (Figures A18 to A28). Furthermore, unlike Sentinel longlines, there was less inter-annual variability in which sites were sampled. Overall, this suggests that the stratified approach to estimating gillnet abundance indices is likely to be valid.

6.2.3. Results – Sentinel gillnet indices

The age aggregated index for ages 3-plus was generally low for 1995 to 2002, at a higher level for 2003 to 2009, and then varied considerably before falling to more average levels (Figure 71). Catches at age track the large cohort born in the early 1990s and seen by other surveys (Figure 72). They also somewhat tracked the above average cohorts born in the mid-2000s. Unlike the other surveys, the gillnet Sentinel index shows sudden above average SPAY values for older ages in 2019, indicative of a year effect.

Like the other surveys, the Sentinel gillnet index followed the progression of cohorts well (Figure 73), demonstrating generally decent internal consistency (see also Figure 74). Trends in estimated Z values are remarkably similar to those for the other Sentinel fixed gear indices (Figure 75).

7. COMPARISON OF TOTAL MORTALITY TRENDS

As noted above, the trends in total mortality estimates was remarkably similar between the five principal fishery independent survey indices (Figure 76). However, there is a notable difference in the magnitude of estimated values between the mobile and fixed gear indices, particularly during periods of high mortality. This difference may in part result from differences in the range of ages used for the estimates, which was constrained by selectivity of the gear and the requirement to include only fully recruited ages. Mortality rates for the fixed gear indices are based on older ages which likely experience higher fishing mortality, given that since 1995, the directed fishery has used exclusively fixed gear to which younger cod are not fully recruited. Natural mortality in the older fish may also be higher as a result of senescence. Total mortality rate estimates may also be sensitive to shifts in cod distribution into and out of more coastal waters, whereby a shift inshore would attenuate Z and a shift out would exaggerate Z in summer Sentinel fixed gear indices. This effect is not expected to be as important for the late fall longline index since it includes cod that have migrated out of the Gulf, presumably from both the inshore and offshore. The comparison of Sentinel mobile gear indices for a survey area that includes or excludes coastal strata suggest that cod shifted into coastal waters between about

2004 and 2008 and again in 2014 to 2016 (higher survey mean when coastal strata are included), and out from about 2009 to 2013 (Figure 28). Correspondingly, Z values between 2004 and 2008 were somewhat lower for the Sentinel summer longline and gillnet indices, and higher for 2008 to 2011, compared to estimates from mobile gear surveys (Figure 76). The correspondence is not perfect, but does suggest that the summer fixed gear indices in particular may be sensitive to shifts in cod distribution. This is something that should be explored and possibly accounted for in forthcoming population dynamics modelling. Finally, differences in Z estimates between surveys could occur if cod of the ages included in the analysis are not fully recruited in some surveys, as otherwise assumed.

8. SUMMARY AND CONCLUSIONS

The principal objective of this document was to review the availability, duration and quality of fishery independent survey indices and information for NAFO 3Pn4RS cod. In doing so we considered how these sources of information contribute to understanding population dynamics, via trends in abundance, demographic composition and mortality rates. We did not consider, at this time, how these sources inform other changes in the stock such as changes in maturation, growth rates, seasonal/interannual changes in distribution and somatic condition.

In the last stock assessment, catch at age indices from the RV survey beginning in 1990 were a primary input to the assessment model for nGSL cod (Brassard et al. 2020). These indices begin at a time when the collapse of the stock was well underway and during which natural mortality is felt to have changed. Absence of indices covering the pre-collapse period risks producing biases in historical estimates of the productivity and size of the stock, and hence in key reference points. Here, we have successfully extended the standardized series back to 1984 by including results of the 1990 comparative fishing experiments. The longer series track cohorts very well and provide a very useful perspective on the stock prior to collapse. A difference in the number and bathymetric coverage of strata sampled prior to and following 1990 should be accounted for in subsequent assessment modelling of the stock, and a path to doing so for the years 1984-1990 was provided here.

The Sentinel mobile gear survey, initiated in 1995, was shown to track cohorts very well. In the last stock assessment, indices from the survey for 1995-2002 and 2003-present were treated as independent, as a result of the addition of coastal strata to the survey in 2003. Analyses presented here support joining these series, perhaps with some adjustments for younger cod. The single series will provide more coherent information on cohort dynamics for the assessment model.

Surveys undertaken each January from 1978 to 1994, except 1982, appear to provide coherent information of the age composition of the population for 1983-1994, the years for which age data were available. Inclusion of these compositional estimates in the assessment model will provide some redundant information with the RV survey which could increase the precision of some estimated parameters, such as model estimated age composition and age-specific mortality rates. At present, it does not appear appropriate to use information on catch amounts from this survey in the assessment model given important inter-annual differences in survey coverage that appear to produce important year effects in the catch at age matrix. However, it may be possible to model the catchability of cod to this survey as time-varying, and an evaluation of the benefits of doing so for the assessment could be explored eventually.

Historical surveys of this stock were also undertaken during the 1950s and 1960s, a period which straddles the introduction of a trawl fleet to the fishery and a general increase in landings and likely fishing mortality (Wiles and May 1968). Unfortunately the raw data from these surveys could not be located; however, published estimates of catches-at-age allow for the estimation of

catch curves from surveys prior to, during and following the expansion of the fishery, and which can provide estimates of total mortality (Z). Notably, the estimate of Z for years prior to fishery expansion, can represent an upper bound on natural mortality, with a value consistent with that of neighboring cod stocks in the 1950s and 1960s (Dickie 1963; Paloheimo and Kohler 1968; Pinhorn 1975).

Perhaps the most significant changes arising from this review are those affecting the estimation of abundance indices from the fixed-gear Sentinel program. Previously, traditional catch-rate standardization was used to derive a gillnet and a longline index and catch at age series. However, over time, uneven reductions in sampling intensity seasonally and spatially have caused the standardization model design-matrix to become severely imbalanced, which can lead to biased estimates of parameters. Furthermore, changes in the seasonal spatial distribution of cod over the years led to the appearance of interactions between main effects in the model, including with the factor *year* such that it was no longer possible to reliably interpret the effect of the factor *year* or other effects. Also, while total catch was standardized, catch composition was not. To remedy these issues, we applied stratified design-based estimation, which is appropriate as Sentinel fixed-gear surveys resemble structured (stratified) surveys much more so than they do fisheries, for which catch rate standardization is used to control for effects on catchability. Using this approach, three independent age-disaggregated survey indices could be estimated. These indices track cohorts very well and remarkably similarly in the case of the two summer indices. Furthermore, the indices produce very smooth trends in Z which are similar amongst each other. While the trend in Z is also consistent with that obtained from the trawl surveys, the amplitude of variation in Z is greater, possibly related to difference in the ages included in the estimates but also to movements by cod in and out of the sentinel fixed gear zones. Accounting for these interannual difference in availability (catchability) to the surveys in the assessment model could go a long way to resolving some of the existing model diagnostic issues (Brassard et al. 2020).

Overall we feel that the improvements to key assessment model inputs brought about by this review are manifold and collectively important. Beneficial future developments include the use of spatio-temporal modelling to account for interannual differences in the strata sampling in bottom-trawl surveys, and for variability in the season sampling of sites in the Sentinel fixed program. A subsequently extension would be the integration of data from all fishery independent monitoring using spatio-temporal modelling, which would directly account for shifts in cod distribution with respect to coastal waters and which affects availability to the different surveys.

9. ACKNOWLEDGEMENTS

We wish to thank the reviewers and participants at the spring 2021 meeting for their comments and suggestions on the analyses presented here. We thank J-M Chamberland and H. Bourdages for their review of the penultimate draft of the document.

10. REFERENCES CITED

- Bérubé, M., Bourdages, H., and Fréchet, A. 2000. [Effects of soak time on catch per unit effort using longline and gillnets for the Northern Gulf of St. Lawrence cod stock](#). DFO Can. Stock Assess. Sec. Res. Doc. 2000/150. 28 p.
- Bourdages, H., Savard, L., Archambault, D., and Valois, S. 2007. Results from the August 2004 and 2005 comparative fishing experiments in the northern Gulf of St Lawrence between the CCGS *Alfred Needler* and the CCGS *Teleost*. Can. Tech. Rep. Fish. Aquat. Sci. 2750: ix + 57 pp.
- Bourdages, H., Brassard, C., Desgagnés, M., Galbraith, P., Gauthier, J., Nozères, C., Scallon-Chouinard, P.-M. and Senay, C. 2020. [Preliminary results from the ecosystemic survey in August 2019 in the Estuary and northern Gulf of St. Lawrence](#). DFO Can. Sci. Advis. Sec. Res. Doc. 2020/009. iv + 93 p.
- Brassard, C., Lussier, J-F., Benoît, H, Way, M. and Collier, F. 2020. [The status of the Northern Gulf of St. Lawrence \(3Pn, 4RS\) Atlantic cod \(*Gadus morhua*\) stock in 2018](#). DFO Can. Sci. Advis. Sec. Res. Doc. 2019/075. xi + 117 p.
- Brooks, M.E., Kristensen, K., van Benthem K.J., Magnusson, A., Berg, C.W., Nielsen, A., Skaug, H.J., Maechler, M., and Bolker, B.M. 2017. glmmTMB Balances Speed and Flexibility Among Packages for Zero-inflated Generalized Linear Mixed Modeling. *The R Journal* 9:, 378–400
- Brulotte, S., and Fréchet. 2000. [Saturation index for longlines and gillnets from Sentinel Fisheries of cod in the northern Gulf of St. Lawrence](#). DFO Can. Stock Assess. Sec. Res. Doc. 2000/118.
- Castonguay, M., Rollet, C., Fréchet, A., Gagnon, P., Gilbert, D., and Brêthes, J.-C. 1999. Distribution changes of Atlantic cod (*Gadus morhua* L.) in the northern Gulf of St-Lawrence in relation to an oceanic cooling. *ICES J. Mar. Sci.* 56:333–344.
- Chadwick, E.M.P., Brodie, W., Colbourne, E, Clark, D., Gascon, D., and Hurlbut, T. 2007. History of annual multi-species trawl surveys on the Atlantic coast of Canada. *Atlantic Zonal Monitoring Program Bulletin* 6: 25–42.
- Dickie, L.M. 1963. Estimation of mortality rates of Gulf of St. Lawrence cod from results of a tagging experiment. *Spec. Publ. Int. Comm. Northwest Atl. Fish.* 3:71–80
- Dunn, P.K. and Smyth, G.K. 1996. Randomized quantile residuals. *J. Comput. Graph. Stat* 5: 236-244.
- Etienne, M.P., Obradovich, S.G., Yamanaka, K.L., and McAllister, M.K. 2013. [Extracting abundance indices from longline surveys: a method to account for hook competition and unbaited hooks](#). arXiv 1005.0892v3: 1–35.
- Fréchet, A. 1990. Catchability variations of cod in the marginal ice zone. *Can. J. Fish. Aquat. Sci.* 47:1678–1683.
- Fréchet, A. 1996. [Intercalibration of eight otter trawlers participating in the Sentinel fisheries in the northern Gulf of St. Lawrence \(3Pn,4RS\) in 1995 through the use of Scanmar sensors](#). DFO Atl. Fish. Res. Doc. 96/67
- Fréchet. 1997. [Standardization of otter trawlers participating in the Sentinel fisheries in the Northern Gulf of St. Lawrence in 1996](#). DFO Can. Stock Assess. Sec. Res. Doc. 97/72.
- Fréchet, A., and Schwab, P. 1989. [Évaluation du stock de morue de 3Pn, 4RS en 1988](#). CAFSAC Res. Doc. 89/55

-
- Fréchet, A., and Schwab, P. 1998. [Assessment of the northern Gulf of St. Lawrence cod stock \(3Pn, 4RS\) in 1997](#). DFO Can. Stock Assess. Sec. Res. Doc. 98/127.
- Gavaris, S. 1980. Use of a Multiplicative Model to Estimate Catch Rate and Effort from Commercial Data. Can. J. Fish. Aquat. Sci. 37: 2272-2275.
- Gillis, D.J. 2002. [Workshop on the groundfish Sentinel Program](#). DFO Can. Sci. Adv. Sec. Proc. Ser 2002/003.
- Green, P.J., and Silverman, B.W. 1993. Nonparametric regression and generalized linear models. Chapman and Hall/CRC, 184 p.
- Hartig, F. 2021. DHARMs: Residual diagnostics for hierarchical (multi-level/mixed) regression models. R package version 0.4.1
- Hastie, T., Tibshirani, R. and Friedman, J., 2009. The elements of statistical learning: data mining, inference, and prediction. Springer Science and Business Media.
- Kristensen, K., Nielsen, A., Berg, C.W., Skaug, H., and Bell, B.M. 2016. TMB: Automatic differentiation and Laplace approximation. J. Stat. Softw. 70: 1-21.
- Lear, W.H. 1998. History of fisheries in the northwest Atlantic: the 500-year perspective. J. Northw. Atl. Fish. Sci., 23: 41-73.
- Maunder, M.N., and Punt, A.E. 2004. Standardizing catch and effort data: a review of recent approaches. Fish. Res. 70: 141-159.
- Mello, L.G.S., Maddock Parsons, D., and Simpson, M.R. 2019. [Sentinel Surveys 1995-2018 – Catch rates and biological information on Atlantic Cod \(*Gadus morhua*\) in NAFO Subdivision 3Ps](#). DFO Can. Sci. Advis. Sec. Res. Doc. 2019/053. iv + 28 p.
- Miller, T.J. 2013. A comparison of hierarchical models for relative catch efficiency based on paired-gear data for US Northwest Atlantic fish stocks. Can. J. Fish. Aquat. Sci. 70: 1306-1316.
- Ouellette-Plante, J., van Beveren, E., Benoît, H.P. and Brassard, C. 2022. [Details of catchR, an R package to estimate the age and length composition of fishery catches, with an application to 3Pn4RS Atlantic cod](#). DFO Can. Sci. Advis. Sec. Res. Doc. 2022/015. iv + 69 p.
- Paloheimo, J.E., and Kohler, A.C. 1968. Analysis of the southern Gulf of St. Lawrence cod population. J. Fish. Res. Board. Can. 25: 555–578.
- Perry, R.I. and Smith, S.J. 1994. Identifying habitat associations of marine fishes using survey data: an application to the northwest Atlantic. Can. J. Fish. Aquat. Sci. 51:589– 602.
- Peterson, C.D., Gartland, J., and Latour, R.J. 2017. Novel use of hook timers to quantify changing catchability over soak time in longline surveys. Fish. Res. 194: 99-111.
- Pinhorn, A.T. 1975. Estimates of Natural Mortality for the Cod Stock Complex in ICNAF Divisions 2J, 3K and 3L. ICNAF Res. Bull. 11: 31-36.
- R Core Team. 2021. [R: A language and environment for statistical computing](#). R Foundation for Statistical Computing, Vienna, Austria.
- Ricker, W.E. 1975. Computation and Interpretation of Biological Statistics of Fish Populations. Bull. Fish. Res. Bd. Can. 191.
-

-
- Rivest, L.-P., Boivin A., and Benoît H.P. 2021. A Spatiotemporal Investigation of the Cod Stock in the Northern Gulf of St-Lawrence. In Y. P. Chaubey et al. (eds.), Applied Statistics and Data Science. Springer Proceedings in Mathematics and Statistics 375
- Sinclair, A.F. 2001. Natural mortality of cod (*Gadus morhua*) in the southern Gulf of St. Lawrence. ICES J. Mar. Sci. 58:1-10.
- Smith, S. J. 2016. Review of the Atlantic Halibut longline survey index of exploitable biomass. Can. Tech. Rep. Aquat. Sci. 3180: v + 56 p.
- Swain, D.P., Ricard, D., Rolland, N., and Aubry, É. 2019. [Assessment of the southern Gulf of St. Lawrence Atlantic Cod \(*Gadus morhua*\) stock of NAFO Div. 4T and 4Vn \(November to April\), March 2019](#). DFO Can. Sci. Advis. Sec. Res. Doc. 2019/038. iv + 105 p.
- Thorson, J.T. and Minto, C. 2015. Mixed effects: a unifying framework for statistical modelling in fisheries biology. ICES J. Mar. Sci. 72:1245-1256.
- Verbyla, A.P., Cullis, B.R., Kenward, M.G, and Welham, S.J. 1999. The analysis of designed experiments and longitudinal data by using smoothing splines. J. Roy. Stat. Soc. Ser. C 48: 269-311.
- Ward, P., Myers, R.A., and Blanchard, W. 2004. Fish lost at sea: the effect of soak time on pelagic longline catches. Fish. Bull. 102: 179-195.
- Warren, W.G. 1997. Report on the comparative fishing trial between the *Gadus Atlantica* and Teleost. NAFO Sci. Coun. studies 29: 81-92.
- Wiles, B., and May, A.W. 1968. Biology and fishery of the West Newfoundland cod stock. ICNAF Res. Bull. 5: 5-43.
- Wood, S.N. 2000. Modelling and smoothing parameter estimation with multiple quadratic penalties. J. Royal. Statist. Soc. Ser. B Stat. Methodol. 62: 413–428.
- Wood, S.N. 2011. Fast stable restricted maximum likelihood and marginal likelihood estimation of semiparametric generalized linear models. J. R. Stat. Soc. Ser. B Stat. Methodol. 73: 3–36.
- Wood, S.N. 2017. Generalized additive models: An introduction with R, 2nd ed. Chapman and Hall/CRC Press, 496 p.
- Yin, Y. and Benoît, H.P. 2021. Length-specific relative catchabilities of redfish and Atlantic halibut by vessels and bottom trawls in multispecies research surveys in the Gulf of St. Lawrence based on paired-tow comparative fishing and spatio-temporal overlap. Can. Tech. Rep. Fish. Aquat. Sci. 3454: vi + 79 p.
- Yin, Y. and Benoît, H.P. 2022. [Re-analysis of comparative fishing experiments in the Gulf of St. Lawrence and other analyses to derive stock-wide bottom-trawl survey indices beginning in 1971 for 4RST Greenland halibut, *Reinhardtius hippoglossoides*](#). DFO Can. Sci. Advis. Sec. Res. Doc. 2022/002. vii + 45 p.

11. TABLES

Table 1. Parameters for the vessels and summary of the protocols used in the RV surveys of the northern Gulf of St. Lawrence.

Parameters for the vessels	<i>MV Lady Hammond</i>	<i>CCGS Alfred Needler</i>	<i>CCGS Teleost</i>
Regular survey operation	1984-1990	1990-2005	2004-present
Vessel type	Stern trawler	Stern trawler	Stern trawler
Tonnage	897	959	2,405
Length (m)	58	50	63
Operating hours	24-hr	24-hr	24-hr
Standard tow speed (knots)	3.5	1990-1993: 2.5 1994-2005: 3.0	3.0
Standard tow duration (min)	30	1990-1992: 20 1993-2005: 24	15
Standard tow distance (nm)	1.75	1990-1992: 0.83 1993: 1.00 1994-2005: 1.20	0.75

Table 2. Parameters for the trawls used in the RV surveys of the northern Gulf of St. Lawrence.

Parameters for the trawls used	Western IIA	URI 81/114	Campelen
Years in operation	1984-1990	1990-2005	2004-present
Footgear	21 inch (outer) and 18 inch (inner) rubber bobbins and 6.75 inch diameter 7 inch long rubber spacers	Details unavailable to the authors	Rockhopper
Footrope length (m)	32.3	34.8	35.6
Headline length (m)	22.9	24.7	29.5
Headline height (m)	4.6	5.5	
Wingspread (m)	12.5	14-15	16-17
Door type	Portuguese (all steel)	Morgère	Polyvalent
Lengthening piece liner (mm)	31.75	44.0	44.0
Codend liner (mm)	19.0	19.0	12.7

Table 3. A set of binomial models with various assumptions for the length effect and station effect in the relative catch efficiency. A smoothing length effect can be considered and the station effect can be added to the intercept, without interaction with the length effect, or added to both the intercept and smoother to allow for interaction between the two effects.

Model	$\log(\rho)$	Length Effect	Station Effect
B10	β_0	constant	not considered
B11	$\beta_0 + \delta_{0,i}$	constant	intercept
B12	$\mathbf{X}_f^T \boldsymbol{\beta}_f + \mathbf{X}_r^T \mathbf{b}$	smoothing	not considered
B13	$\mathbf{X}_f^T \boldsymbol{\beta}_f + \mathbf{X}_r^T \mathbf{b} + \delta_{0,i}$	smoothing	intercept
B14	$\mathbf{X}_f^T (\boldsymbol{\beta}_f + \boldsymbol{\delta}_i) + \mathbf{X}_r^T (\mathbf{b} + \boldsymbol{\epsilon}_i)$	smoothing	intercept, smoother

Table 4. A set of beta-binomial models with various assumptions for the length effect and station effect in the relative catch efficiency, and the length effect on the variance parameter. A smoothing length effect can be considered in both the conversion factor and the variance parameter. A possible station effect can be added to the intercept, without interaction with the length effect, or added to both the intercept and the smoother to allow for interaction between the two effects.

Model	$\log(\rho)$	$\log(\phi)$	Length Effects	Station Effect
BB0	β_0	γ_0	constant/constant	not considered
BB1	$\beta_0 + \delta_{0,i}$	γ_0	constant/constant	intercept
BB2	$\mathbf{X}_f^T \boldsymbol{\beta}_f + \mathbf{X}_r^T \mathbf{b}$	γ_0	smoothing/constant	not considered
BB3	$\mathbf{X}_f^T \boldsymbol{\beta}_f + \mathbf{X}_r^T \mathbf{b}$	$\mathbf{X}_f^T \boldsymbol{\gamma} + \mathbf{X}_r^T \mathbf{g}$	smoothing/smoothing	not considered
BB4	$\mathbf{X}_f^T \boldsymbol{\beta}_f + \mathbf{X}_r^T \mathbf{b} + \delta_{0,i}$	γ_0	smoothing/constant	intercept
BB5	$\mathbf{X}_f^T \boldsymbol{\beta}_f + \mathbf{X}_r^T \mathbf{b} + \delta_{0,i}$	$\mathbf{X}_f^T \boldsymbol{\gamma} + \mathbf{X}_r^T \mathbf{g}$	smoothing/smoothing	intercept
BB6	$\mathbf{X}_f^T (\boldsymbol{\beta}_f + \boldsymbol{\delta}_i) + \mathbf{X}_r^T (\mathbf{b} + \boldsymbol{\epsilon}_i)$	γ_0	smoothing/constant	intercept, smoother
BB7	$\mathbf{X}_f^T (\boldsymbol{\beta}_f + \boldsymbol{\delta}_i) + \mathbf{X}_r^T (\mathbf{b} + \boldsymbol{\epsilon}_i)$	$\mathbf{X}_f^T \boldsymbol{\gamma} + \mathbf{X}_r^T \mathbf{g}$	smoothing/smoothing	intercept, smoother

Table 5. Difference in AIC between converged candidate models and the best model in each comparative fishing analysis. The best model (indicated in bold) was selected by lowest AIC. For a description of the models see Tables 3 and 4.

Model	nGSL 1990	nGSL 2004-2005
BI0	362	433
BI1	-	76
BI2	146	301
BI3	133	0
BI4	-	-
BB0	261	333
BB1	185	78
BB2	79	238
BB3	64	130
BB4	6	2
BB5	0	-
BB6	-	-
BB7	-	-

Table 6. Proportion of Sentinel fixed gear survey hauls with zero catch of cod, as a function of cod age, for longline (LLS) and gillnet (GNS) surveys.

Age	LLS	GNS
1	1.000	0.983
2	0.884	1.000
3	0.497	0.930
4	0.067	0.571
5	0.039	0.199
6	0.037	0.110
7	0.043	0.106
8	0.050	0.112
9	0.068	0.134
10	0.206	0.186
11	0.268	0.367
12	0.563	0.496
13+	0.502	0.672

Table 7. Number of individuals hauls in the Sentinel longline survey using set amounts of hooks.

Number of hooks	Hauls
500	731
750	160
1000	7601
1500	40
2000	279
Other values (<2000)	246

Table 8. Stratum weights used for the stratified Sentinel fixed gear indices, based on the linear distance in km between Zone boundaries (see text)

Zone	Weight
1	125
2	145
3	295
4	105
5	100
6	335
6.2	80

Table 9. Number of hauls used in the fall Zones 1 and 2 (only site 8 used) Sentinel longline survey index, as a function of year and time-block. Duration is 10 days in the first time block and 21 days in the others.

Year	Time block				
	1	2	3	4	5
1995	19	33	55	21	6
1996	18	47	47	14	9
1997	15	38	48	21	7
1998	18	30	39	24	5
1999	23	26	40	56	16
2000	24	28	33	42	22
2001	23	26	26	53	10
2002	14	14	25	30	13
2003	12	17	25	27	13
2004	10	19	15	20	11
2005	13	18	14	11	7
2006	16	16	16	15	15
2007	16	24	18	19	6
2008	2	10	18	16	11
2009	10	17	16	10	8
2010	8	13	17	15	3
2011	8	15	16	17	3
2012	8	12	12	14	8
2013	10	9	13	9	2
2014	8	11	6	10	9
2015	8	8	16	16	10
2016	12	9	13	17	6
2017	4	14	15	11	4
2018	8	4	5	9	4
2019	10	12	8	4	5

Table 10. Diagnostics for the models to calibrate the relative efficiency of J and circle hooks in the longline Sentinel survey based on quantile residuals: zero-inflation (ZI) and dispersion statistics and associated p-values.

Model	ZI	p-value ZI	Dispersion	p-value Dispersion
A	0.961	0.168	0.329	<2.2E-16
B	0.906	0.128	0.328	<2.2E-16

12. FIGURES

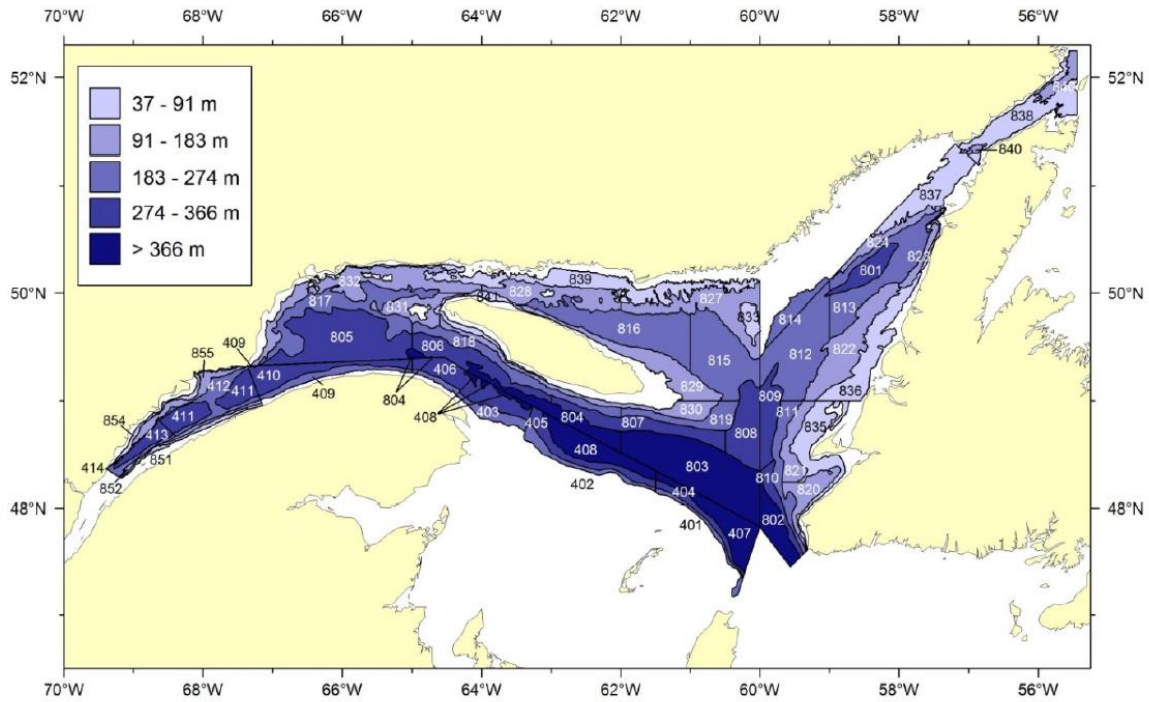


Figure 1. Stratification scheme for the northern Gulf of St. Lawrence multi-species bottom-trawl survey. Strata 401-408, 801-824 and 827-832 constitute a core group of strata included annually in the sampling design since at least 1985. Additional strata, located in NAFO area 3Pn (southwest Newfoundland) and sampled only in 1987 and 1993-2003 are not shown.

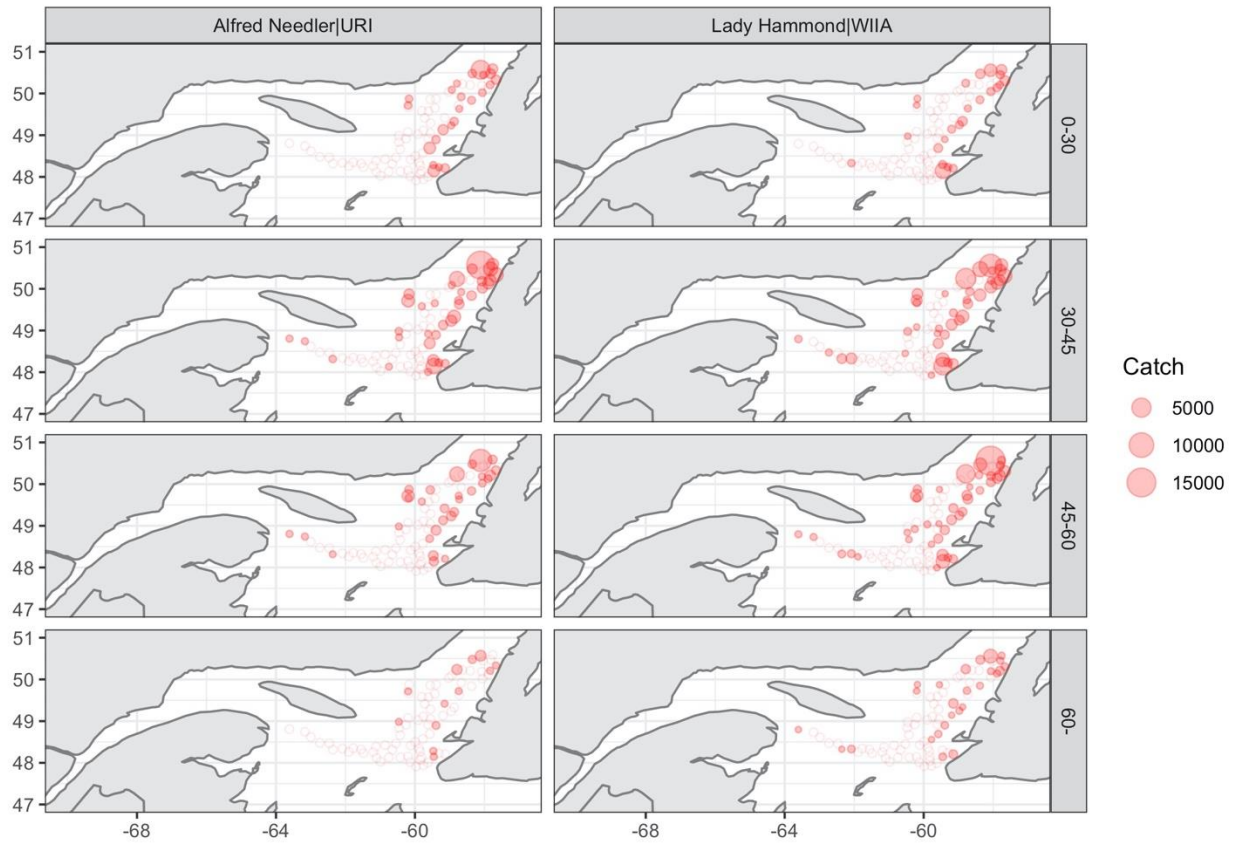


Figure 3. Catches (numbers) of cod by the Alfred Needler (left) and Lady Hammond (right) in paired tows from the comparative fishing survey in 1990, aggregated in four length groups (rows). Solid points with color intensity scale are used for positive catches, while zero catches are indicated by open circles.

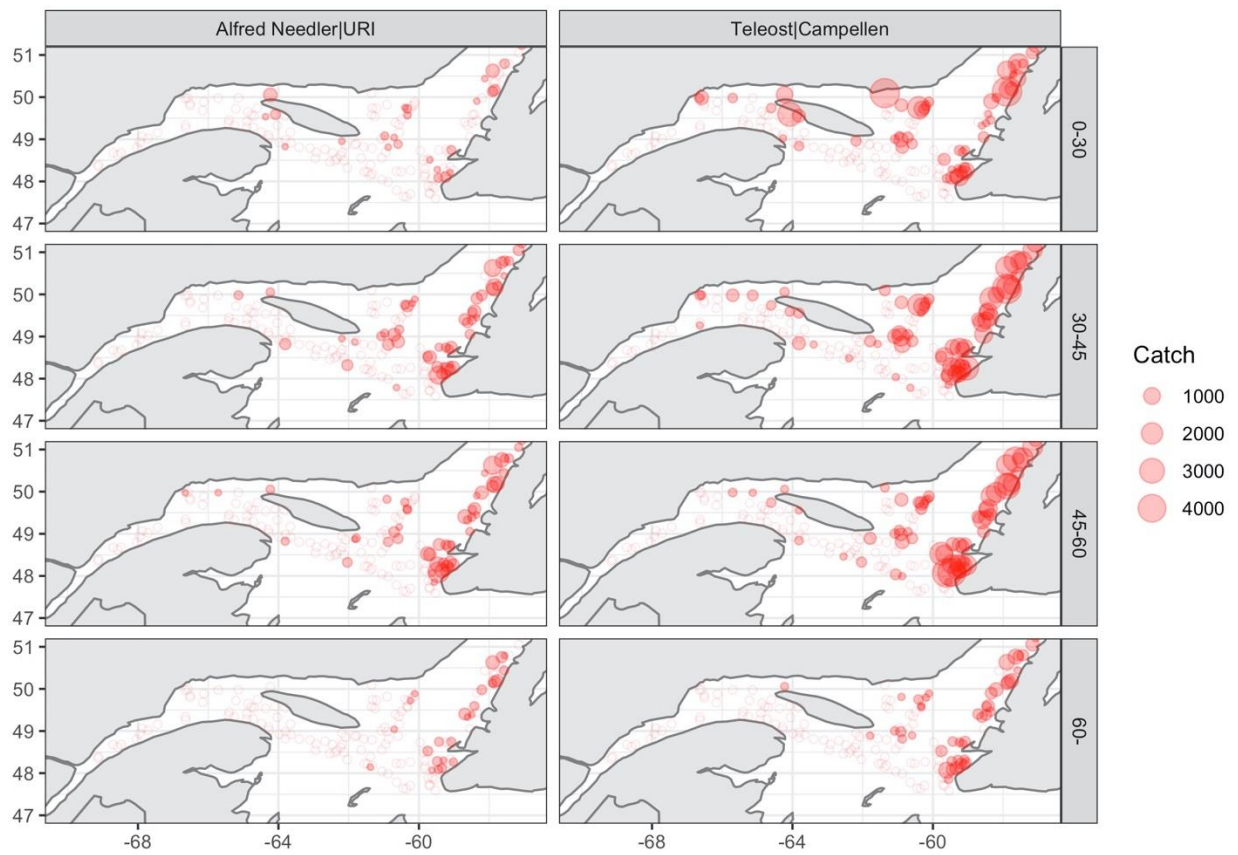


Figure 4. Catches (numbers) of cod by the Alfred Needler (left) and Teleost (right) in paired tows from the comparative fishing surveys in 2004 and 2005, aggregated in four length groups (rows). Solid points with color intensity scale are used for positive catches, while zero catches are indicated by open circles.

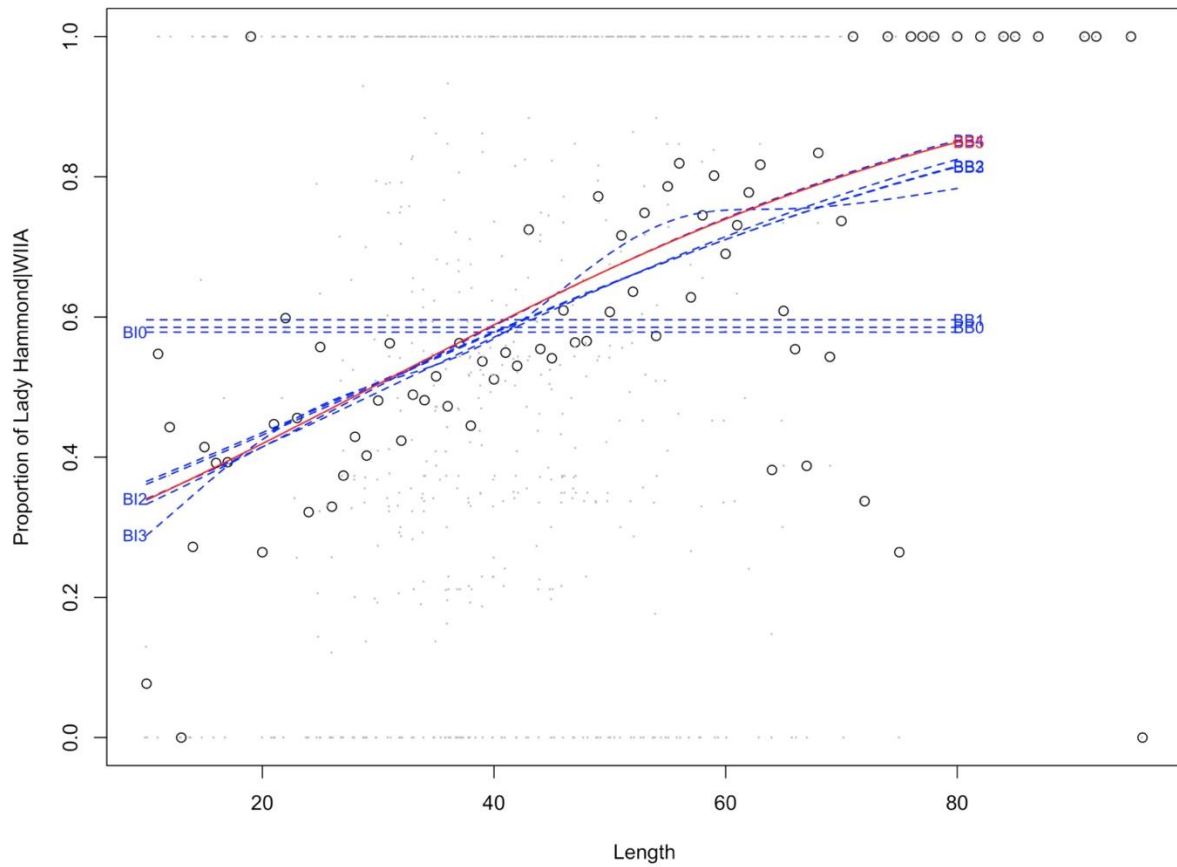


Figure 5. Proportion of cod catch made by the Lady Hammond-WIIA in paired hauls during the 1990 comparative fishing experiment, as a function of fish length (cm), for individual haul pairs (light grey dots) and for the length-specific sample average (circles). The solid red solid line indicates the estimated conversion based on the selected best model, while the blue dashed lines are for other converged models.

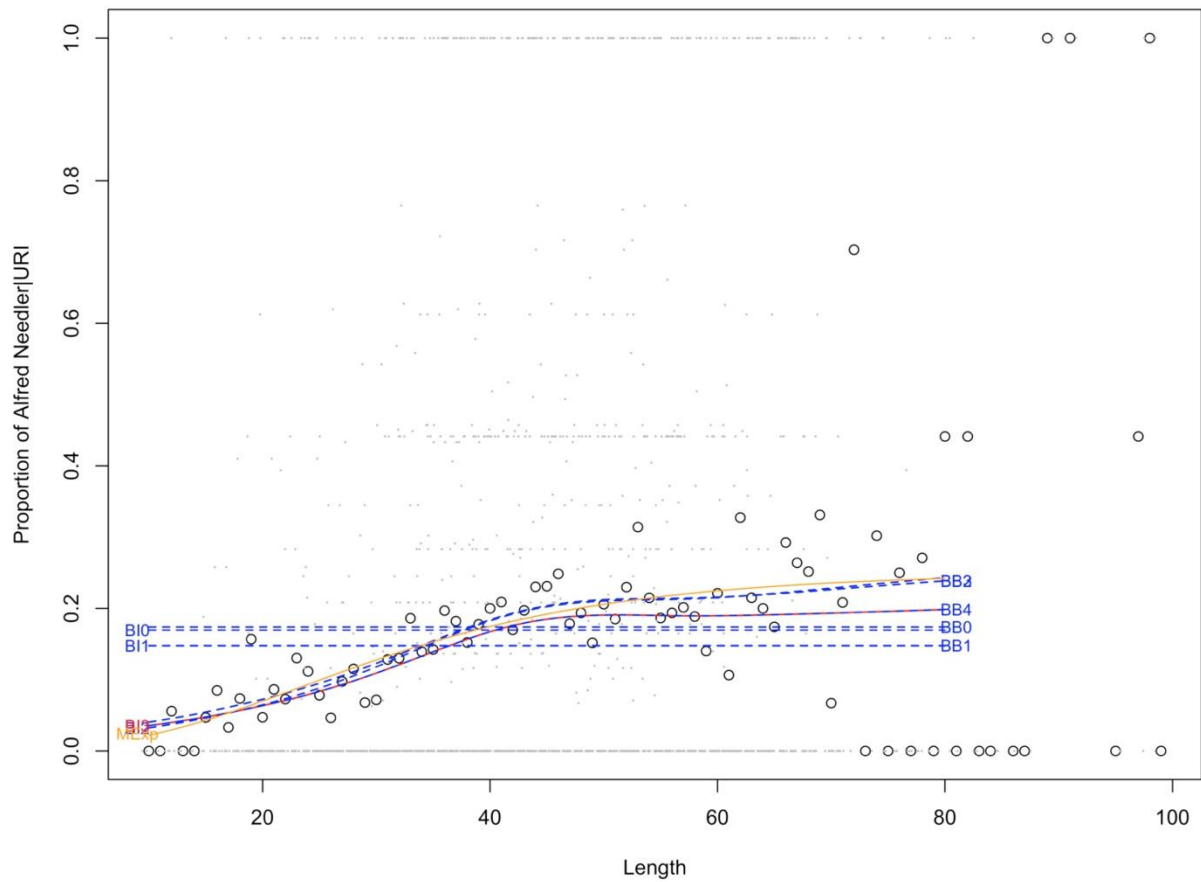


Figure 6. Proportion of cod catch made by the Alfred Needler-URI in paired hauls during the 2004-2005 comparative fishing experiment, as a function of fish length (cm), for individual haul pairs (light grey dots) and for the length-specific sample average (circles). The solid red solid line indicates the estimated conversion based on the selected best model, while the blue dashed lines are for other converged models and the orange line indicates the previously used conversion based on the exponential model by Bourdages et al. (2007).

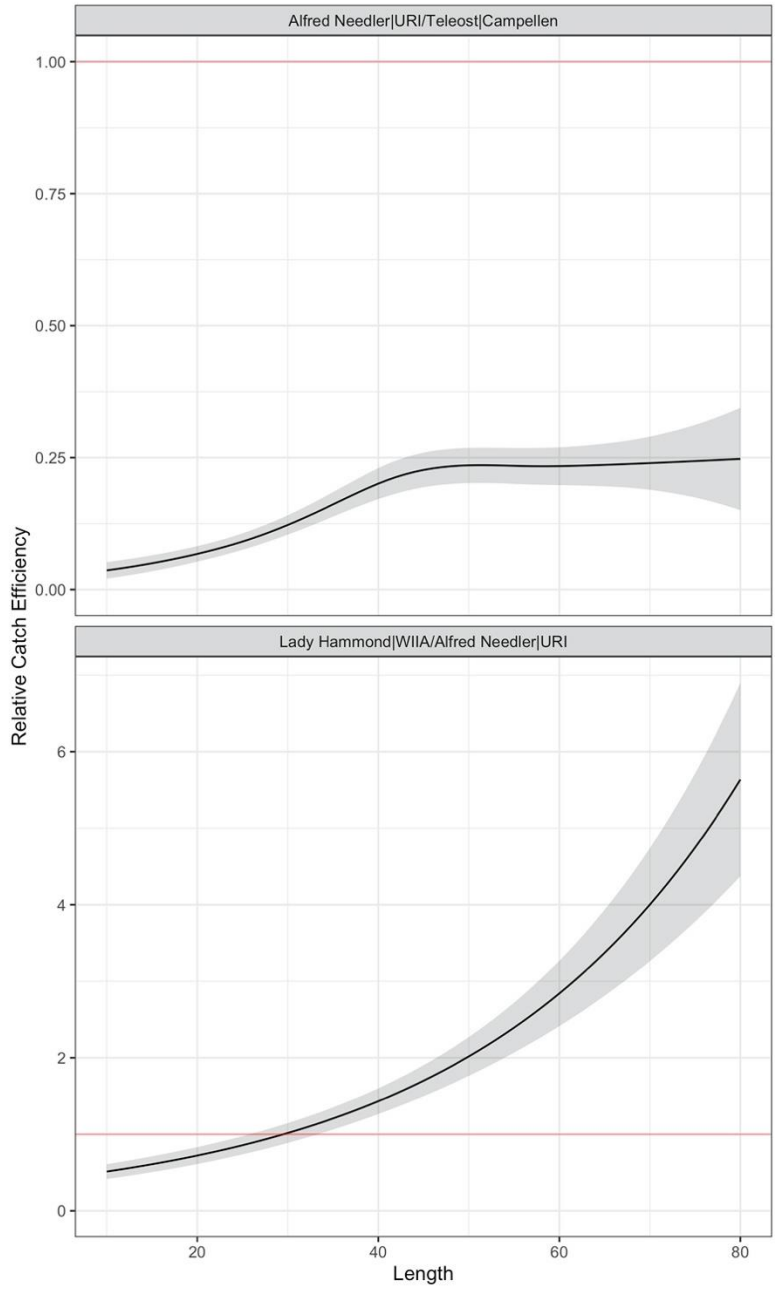


Figure 7. Estimated catch efficiency of the replaced vessel and gear tandem relative to the replacement vessel and gear tandem. The grey bands indicate one standard deviation and the red lines indicate equal efficiency for the replaced and replacement vessels and gear.

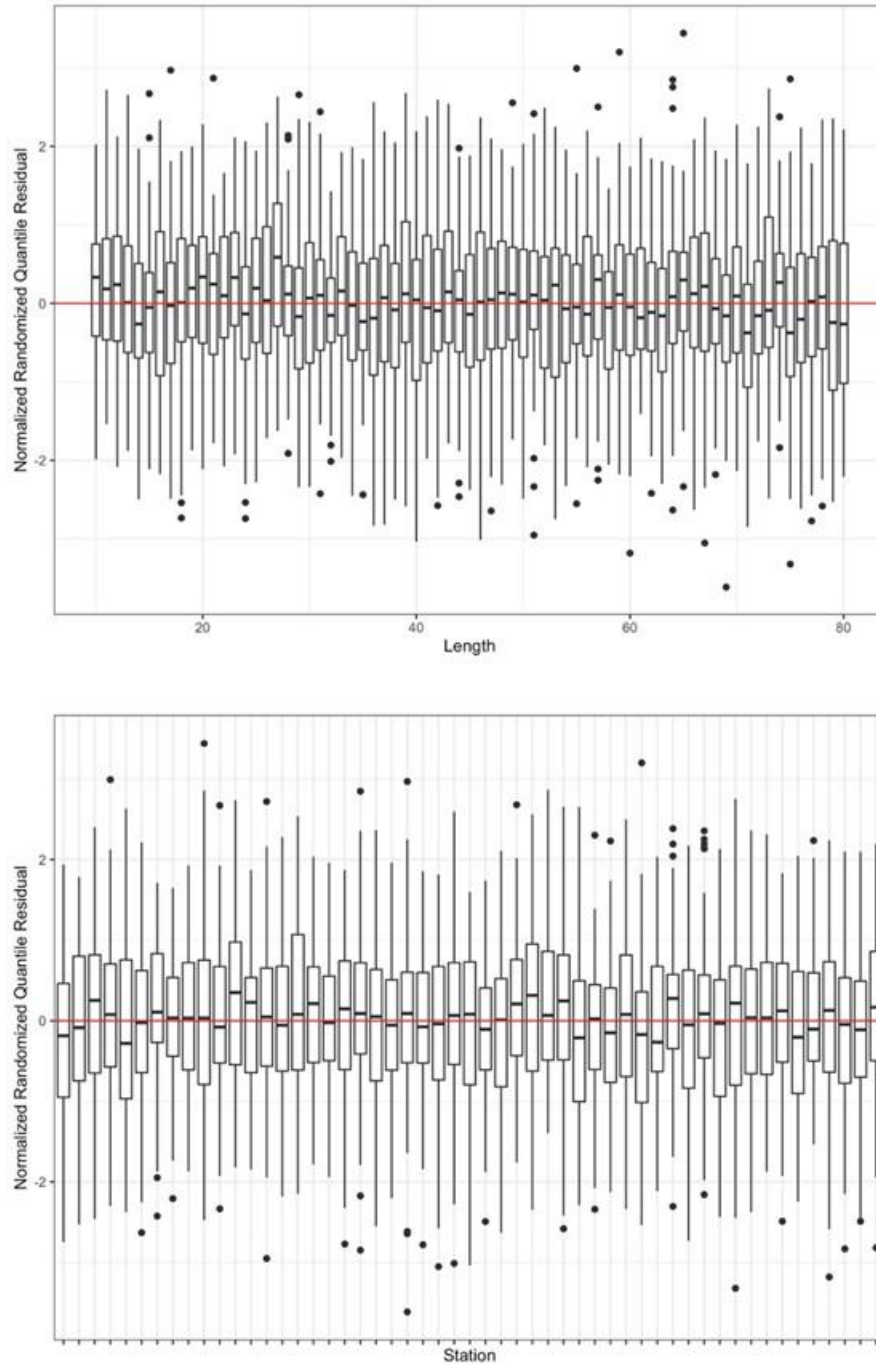


Figure 8. Analysis for the 1990 comparative fishing between Lady Hammond-WIIA and Alfred Needler-URI: normalized randomized quantile residuals for each length bin (top panel) and for each station (bottom panel) for the selected model.

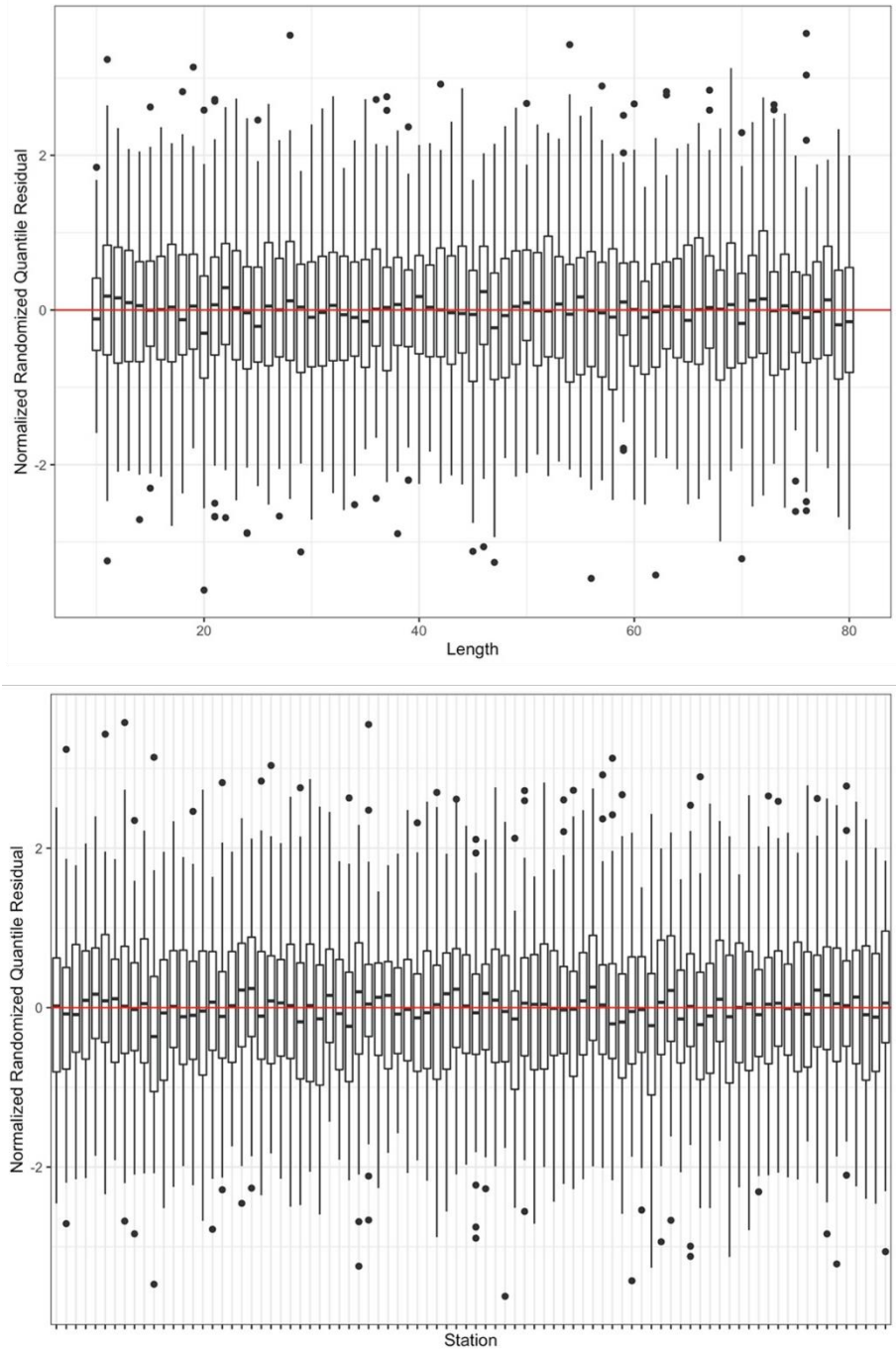


Figure 9. Analysis for the 2004-2005 comparative fishing between Alfred Needler-URI and Teleost-Campelen: normalized randomized quantile residuals for each length bin (top panel) and for each station (bottom panel) for the selected model.

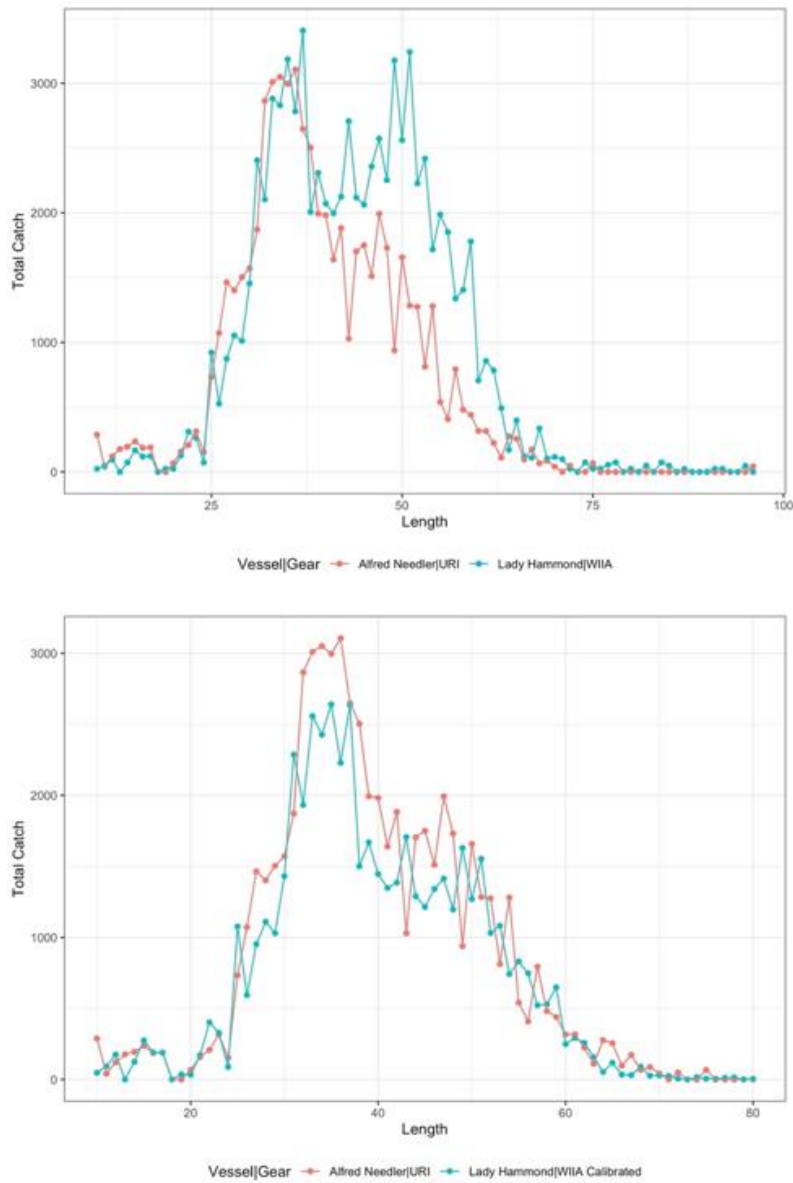


Figure 10. Catch-at-length (cm) composition comparison between the uncalibrated replaced and replacement vessels-gear tandems in the 1990 comparative fishing experiment (top panel) and between calibrated replaced and replacement vessels (bottom panel).

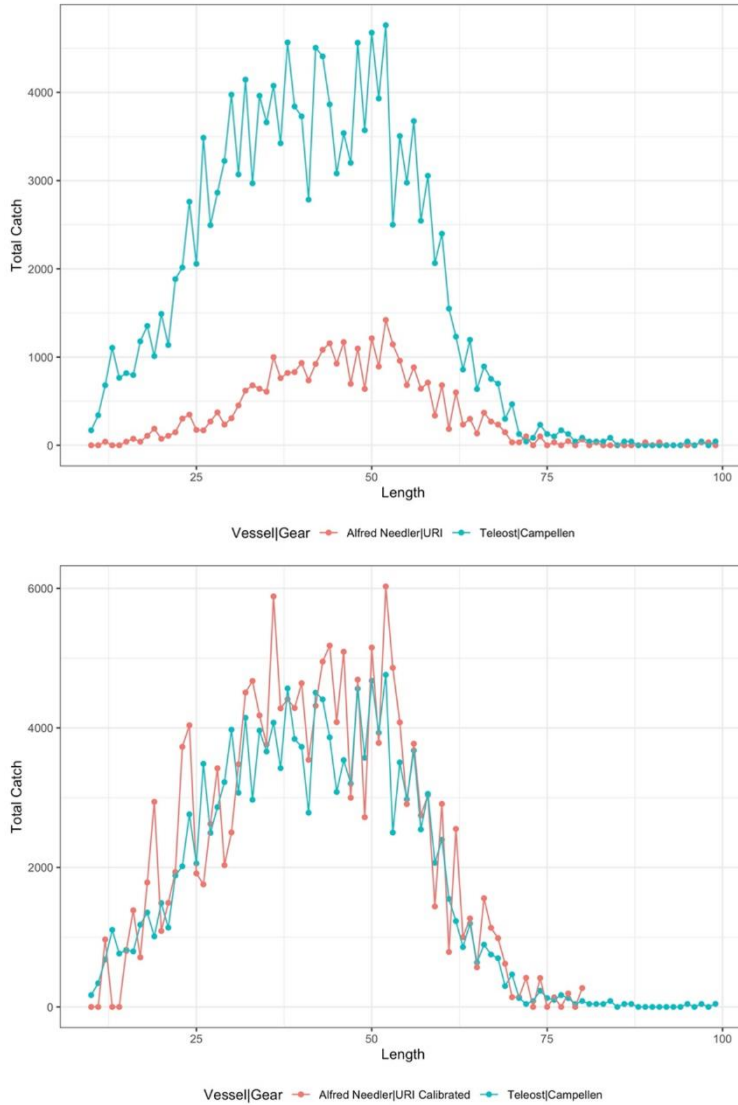


Figure 11. Catch-at-length (cm) composition comparison between the uncalibrated replaced and replacement vessels-gear tandems in the 2004-2005 comparative fishing experiment (top panel) and between calibrated replaced and replacement vessels (bottom panel).

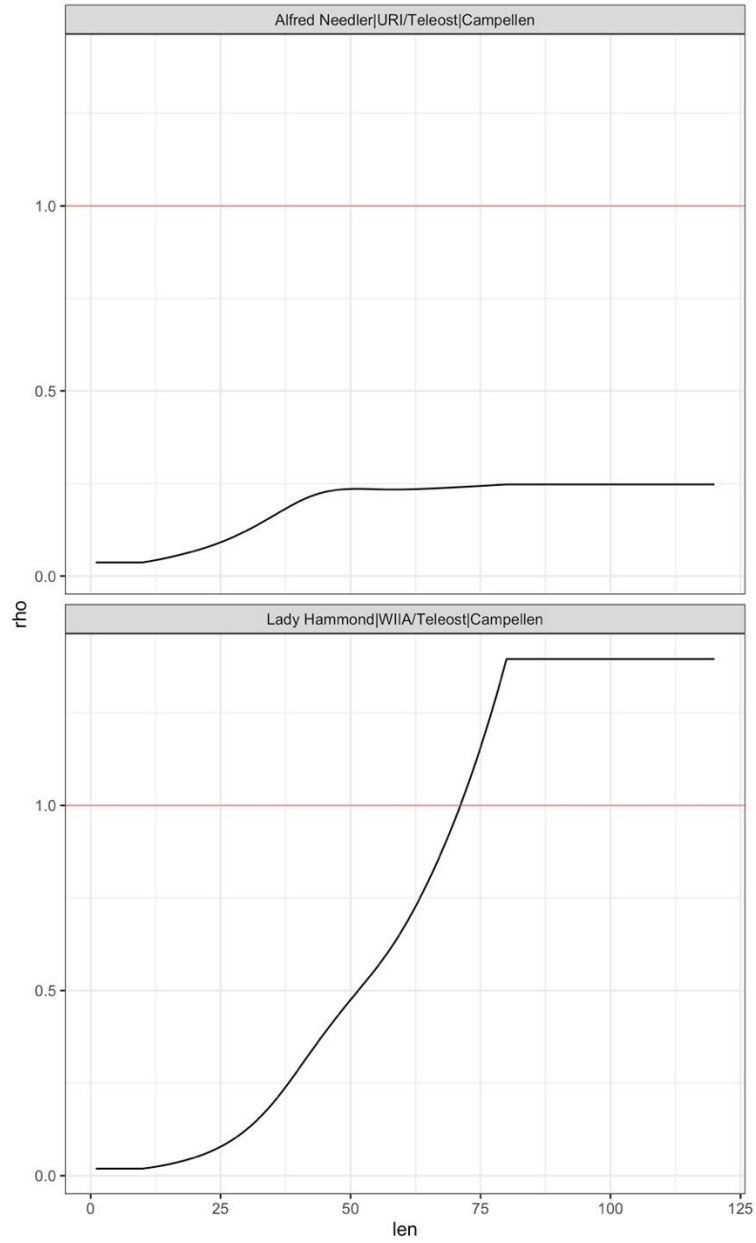


Figure 12. Estimated catch efficiency relative to Teleost-Campelen for each vessel-gear based on sequential multiplication of the estimated relative catch efficiencies from the analyses of the two comparative fishing experiments, as a function of length (cm).

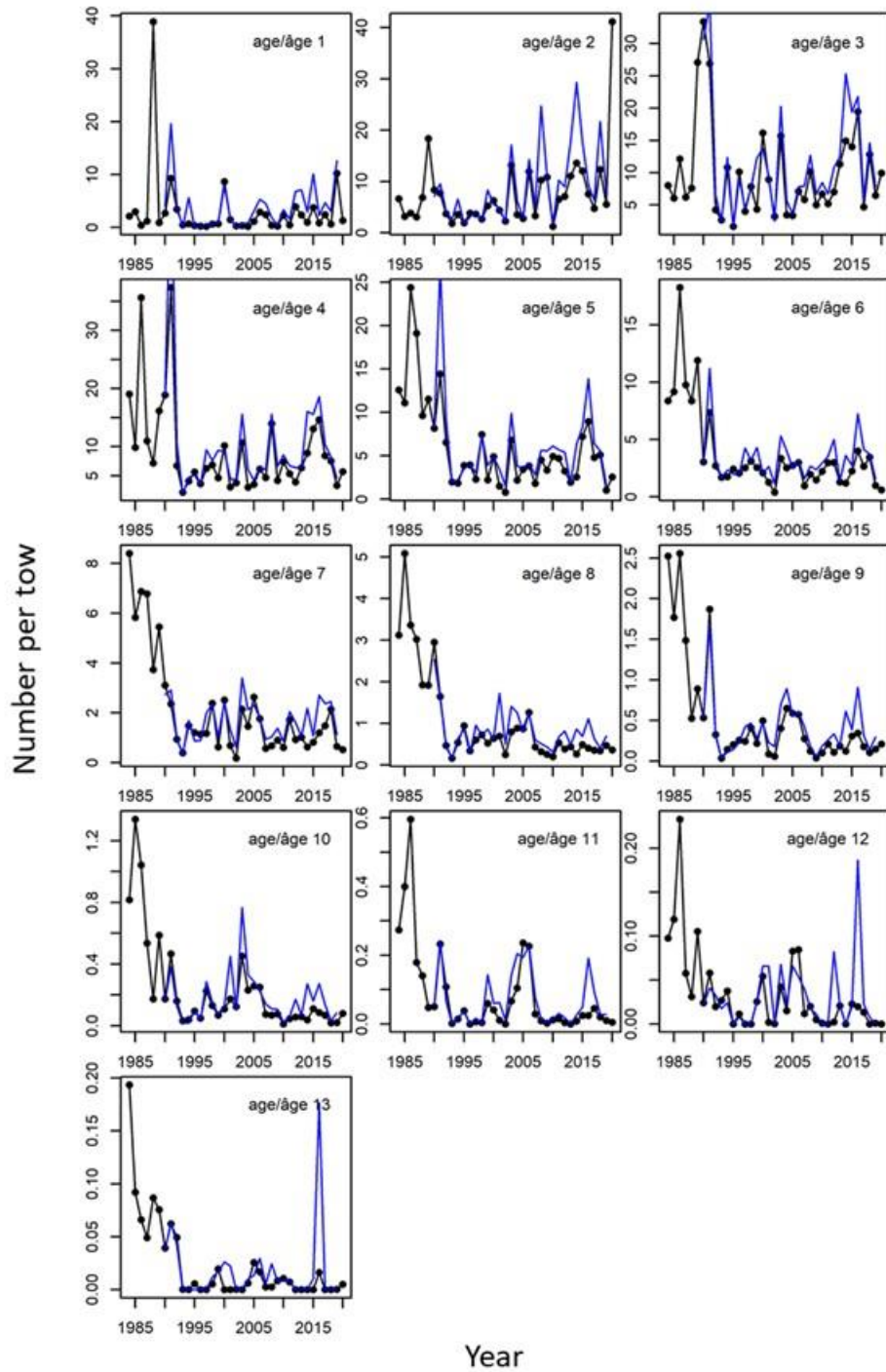


Figure 13. Age-specific abundance indices for cod from the RV survey for 1984-2020 for the reduced suite of strata (black line and dots) compared to former indices presented in Brassard et al. (2020) for 1990-2018 for the full suite of strata (blue line). Age 13 represents a 13+ group.

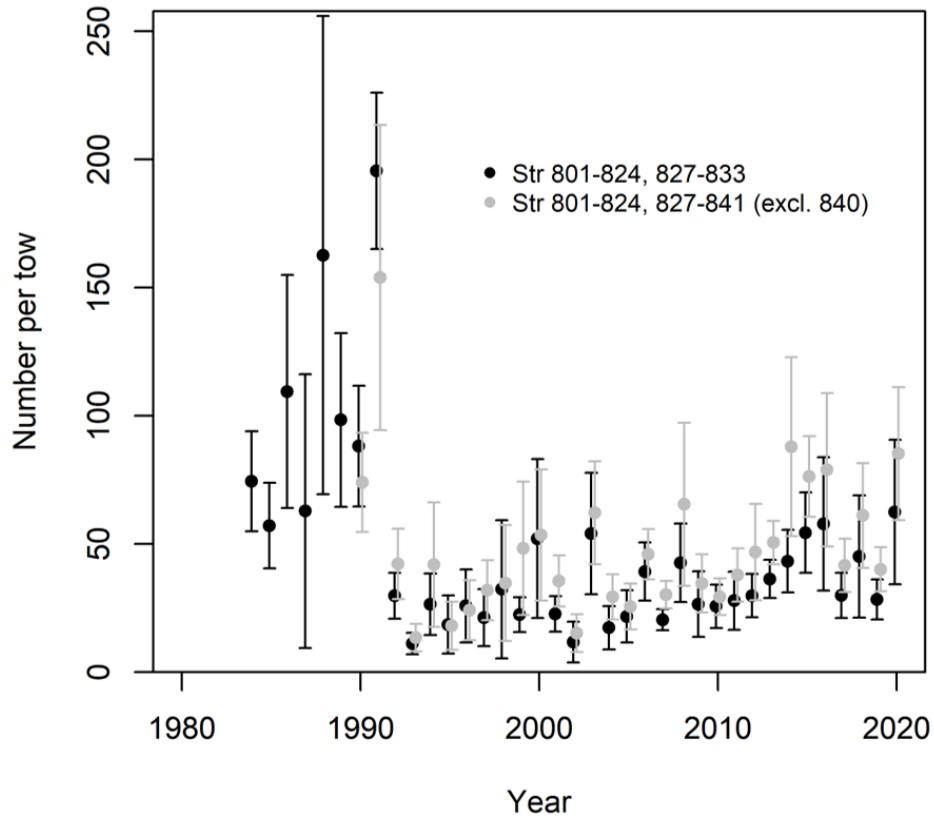


Figure 14. Age-aggregated abundance index with 95% confidence intervals for cod from the RV survey for 1984-2020 based on the reduced suite of strata (black dots) and for 1990-2020 based on all consistently sampled strata (grey dots). The stratum numbers are indicated in the legend.

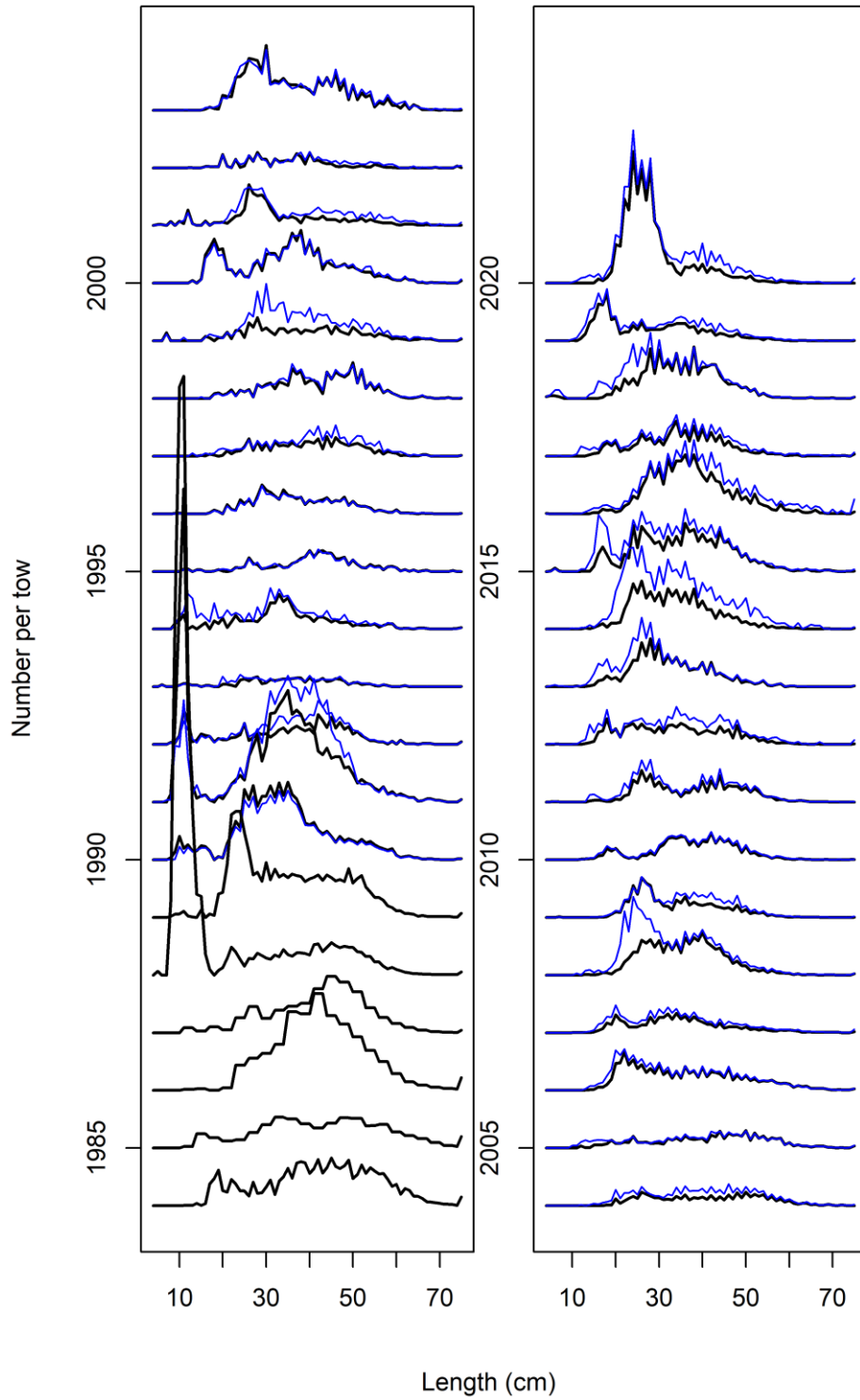


Figure 15. Annual RV survey length frequencies in numbers per tow for 1984-2020 based on the reduced suite of strata (black lines) and for 1990-2020 based on all consistently sampled strata (blue lines).

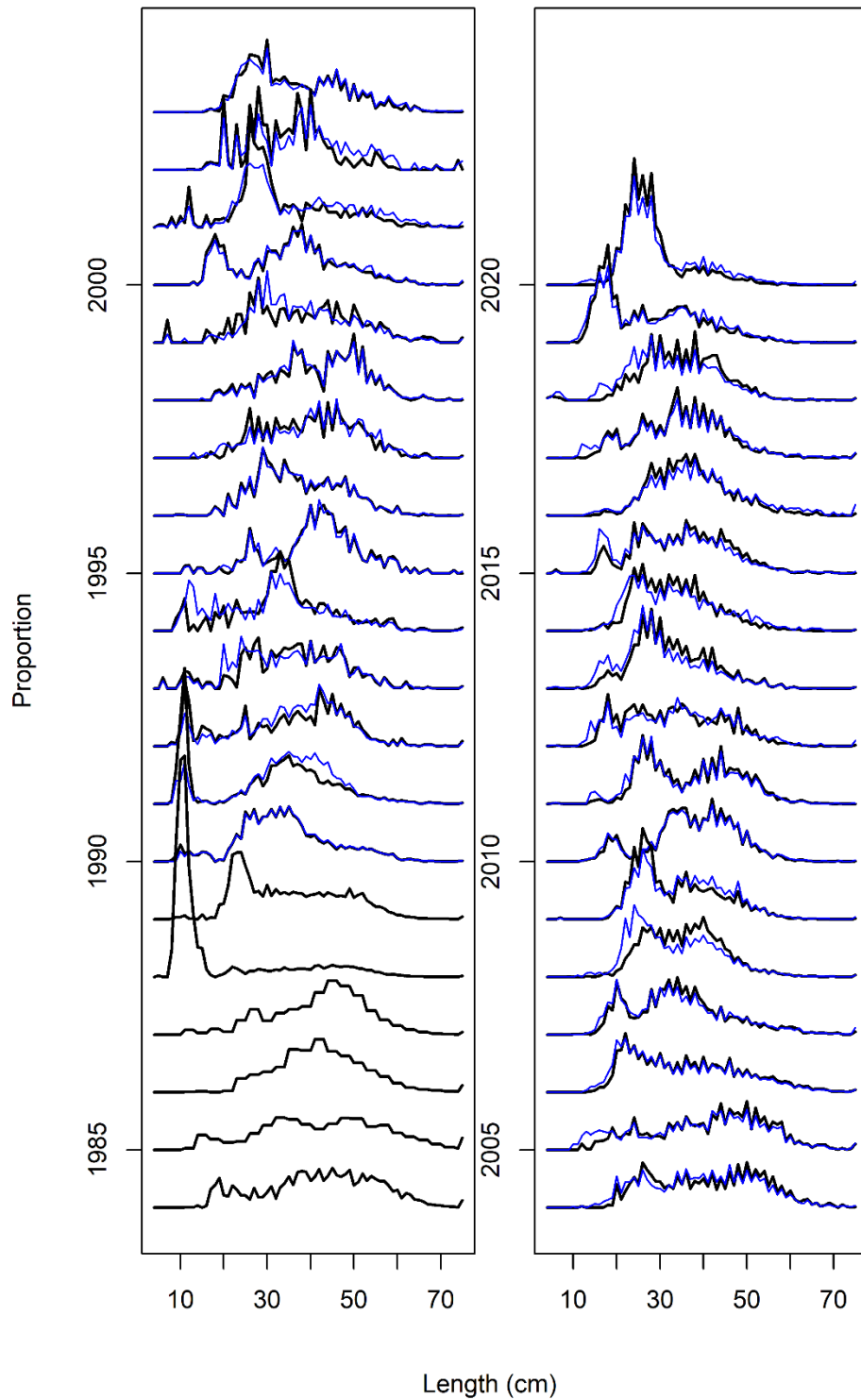
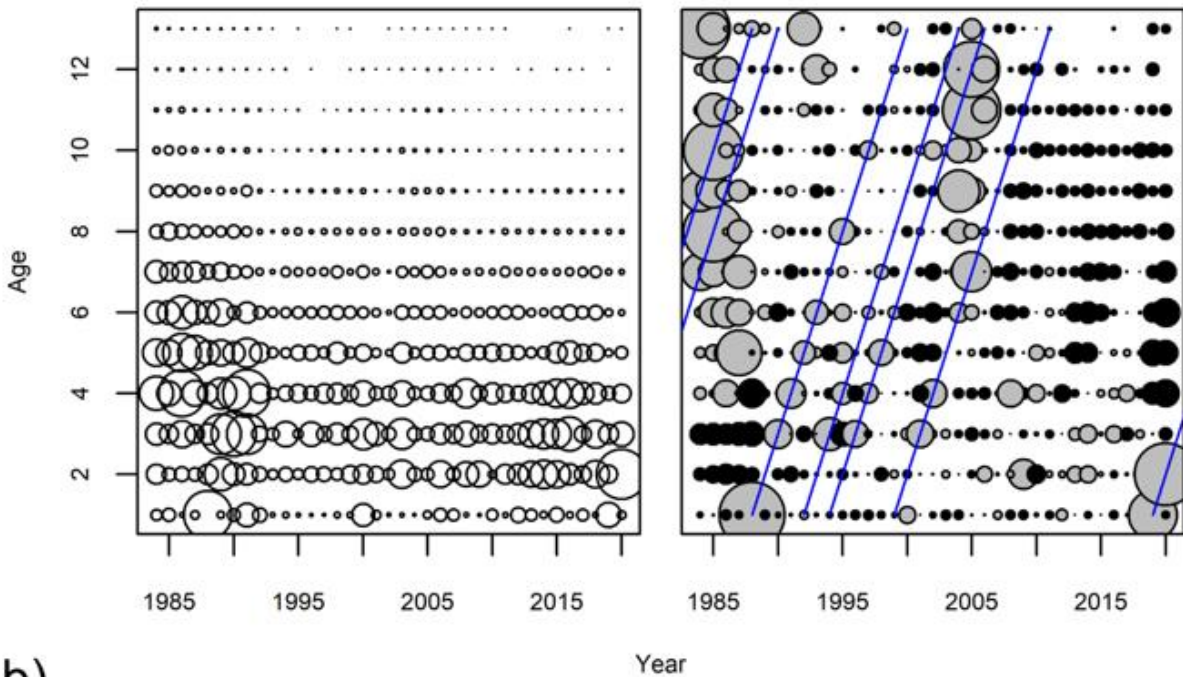


Figure 16. Annual RV survey length frequencies expressed as proportions, for 1984-2020 based on the reduced suite of strata (black lines) and for 1990-2020 based on all consistently sampled strata (blue lines).

a)



b)

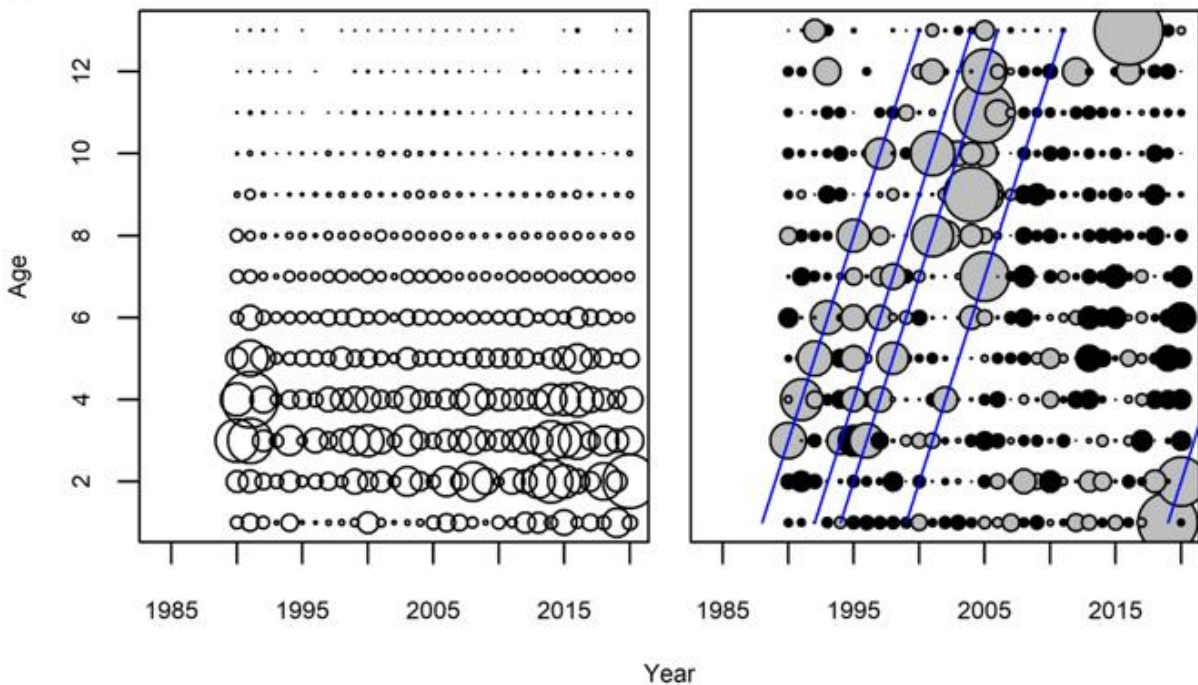


Figure 17. Catch at age in the RV survey for a) 1984-2020 based on the reduced suite of strata and b) 1990-2020 based on all consistently sampled strata. The left panels show catch proportional to circle size, while the right panels show standardized proportions at age and year (SPAY) with grey circles indicating above average catch and black below average. The blue lines indicate some consistently tracked above average cohorts in the survey

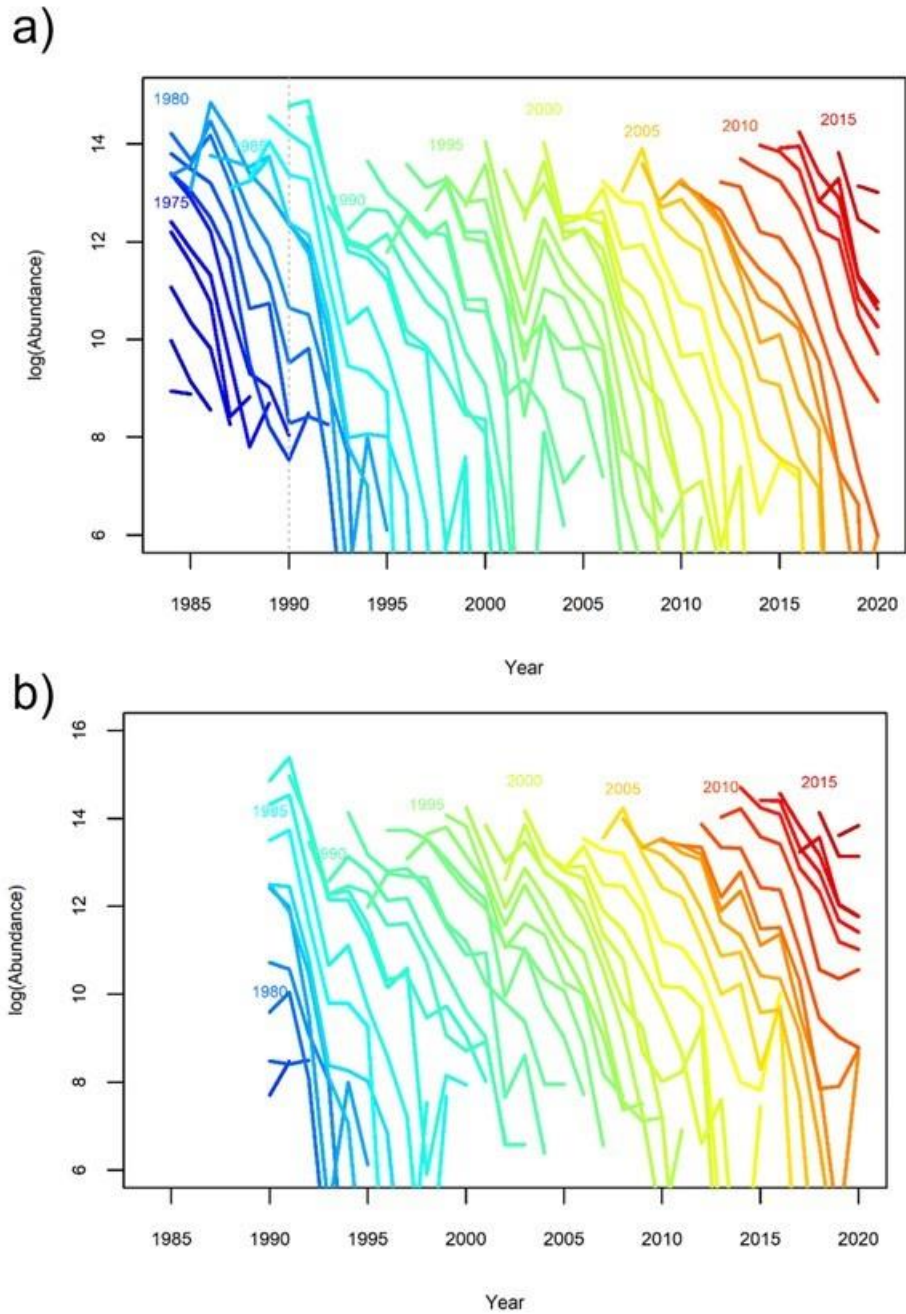


Figure 18. Abundance of individual cohorts (ages 3 to 13+) from the RV survey catch at age for a) 1984-2020 based on the reduced suite of strata and b) 1990-2020 based on all consistently sampled strata. The year of the 1990 comparative fishing experiment is indicated by a vertical dashed line in a). Cohorts are identified by birth year for every 5th year.

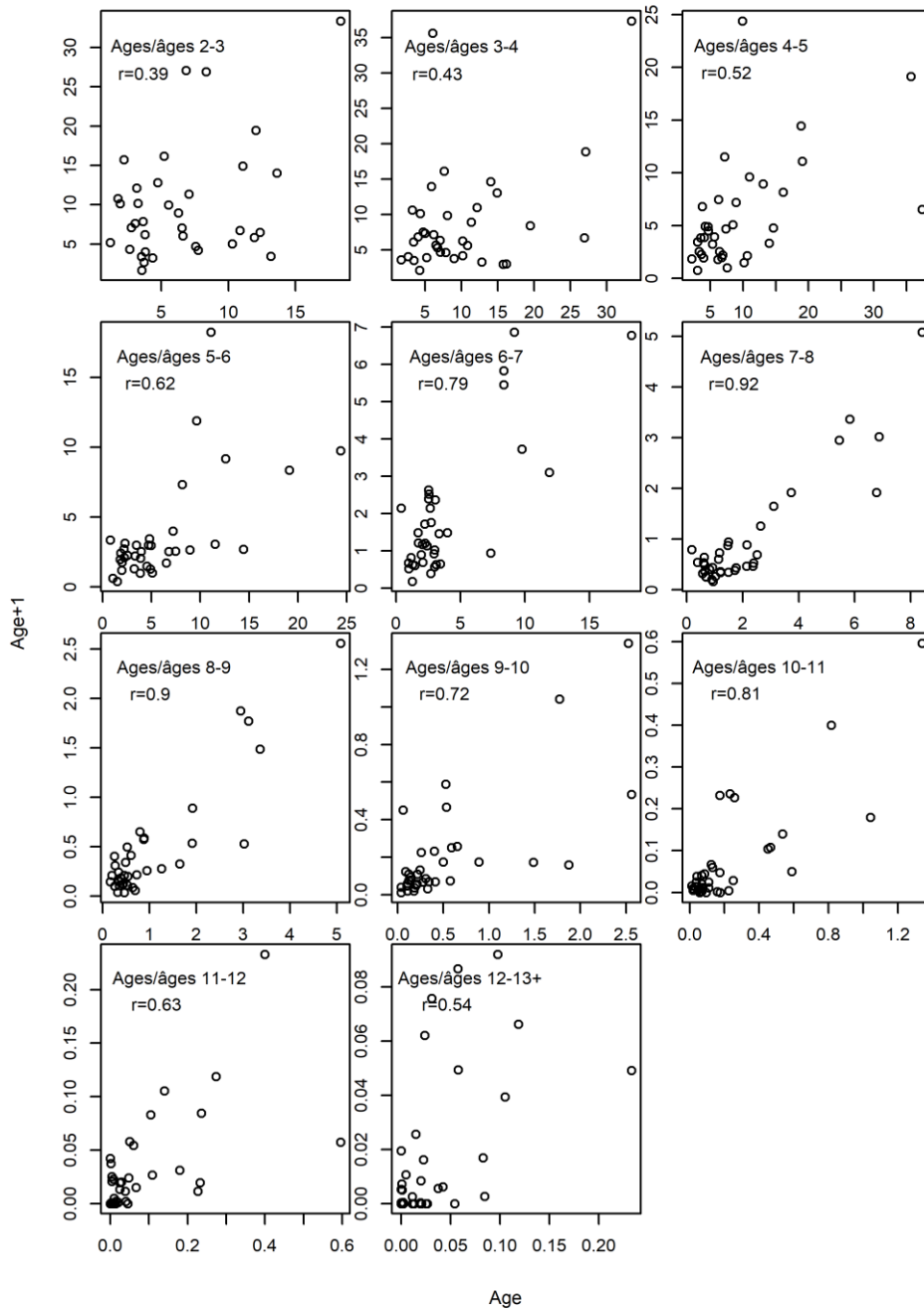


Figure 19. Age-specific abundance of cohorts at a given age and year, as a function of their abundance one year later in the RV survey, for 1984-2020. The correlation between the two sets of estimates is indicated in each panel.

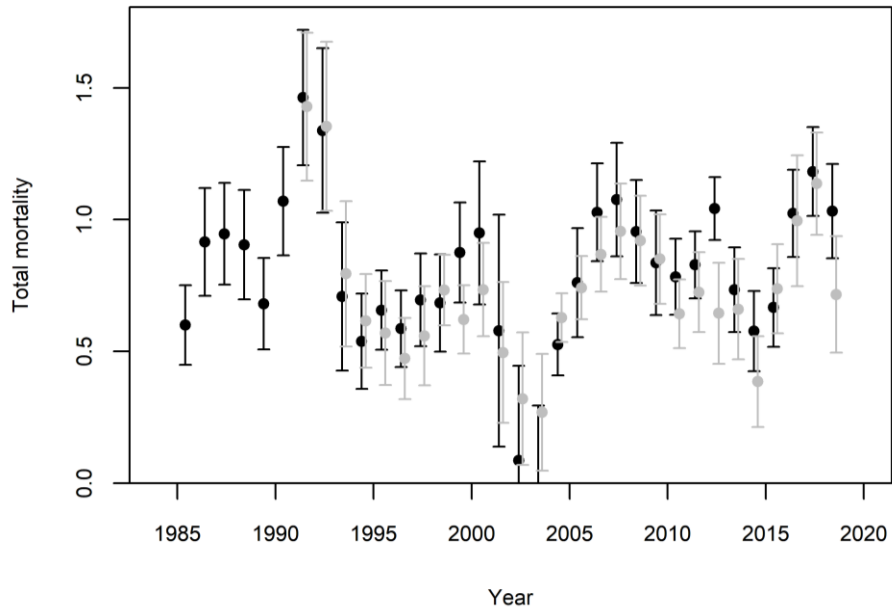


Figure 20. Estimates of total mortality (Z ; with 95% confidence intervals) for ages 5 to 10 from the RV survey for 1984-2020 based on the reduced suite of strata (black) and 1990-2020 based on all consistently sampled strata (grey).

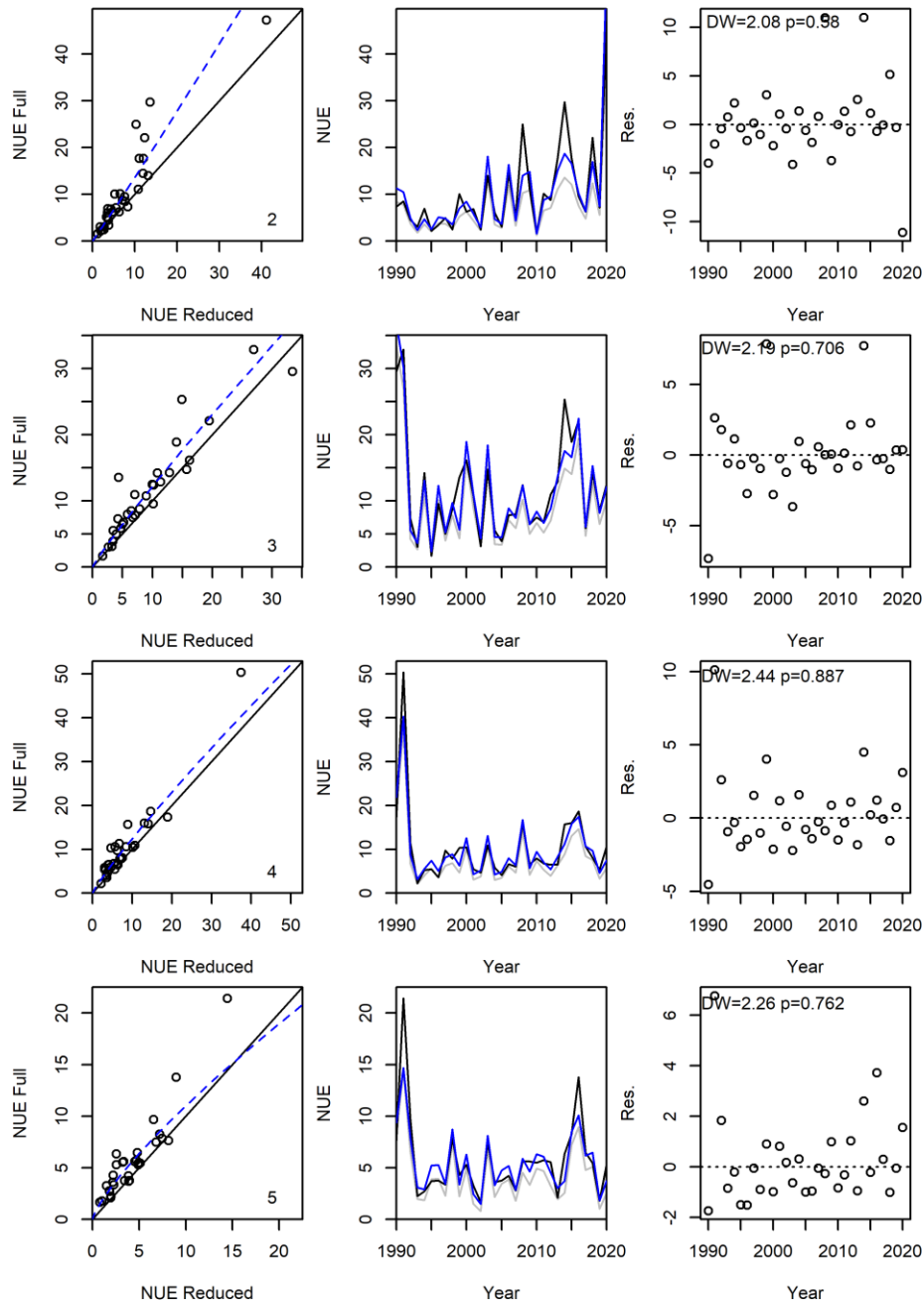


Figure 21. Relationship between catch rates (number per unit effort, NUE) based on the reduced set of strata used to derive indices for the 1984-2020 period and for the full suite of strata traditionally used for cod, by age (rows; age indicated in the lower corner of the leftmost panel). Left column: Biplots of the two series, where the black line is a 1:1 relationship and the dashed blue line is the estimated conversion (correction) to a full-stratum suite equivalent. Middle column: Time series of the abundance indices for the full suite of strata (black), the reduced set (grey) and the 'corrected' reduced set (blue). Right panel: Residuals of the adjusted model in left column (full suite minus corrected indices) as a function of year. DW is the Durbin-Watson statistic for temporal autocorrelation, with associated p-value. Results indicated for age 13 represent a 13-plus group.

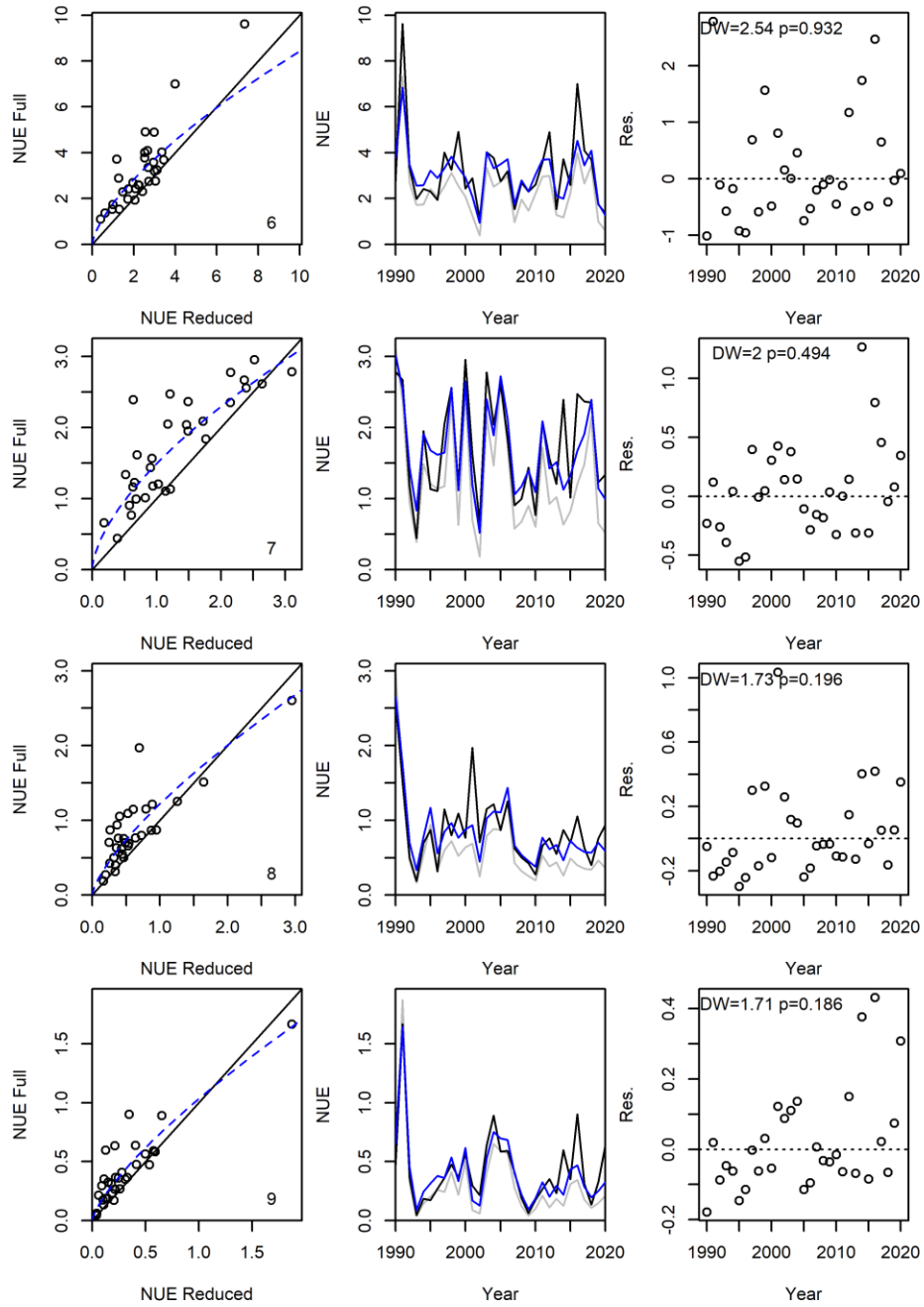


Figure 21. Continued

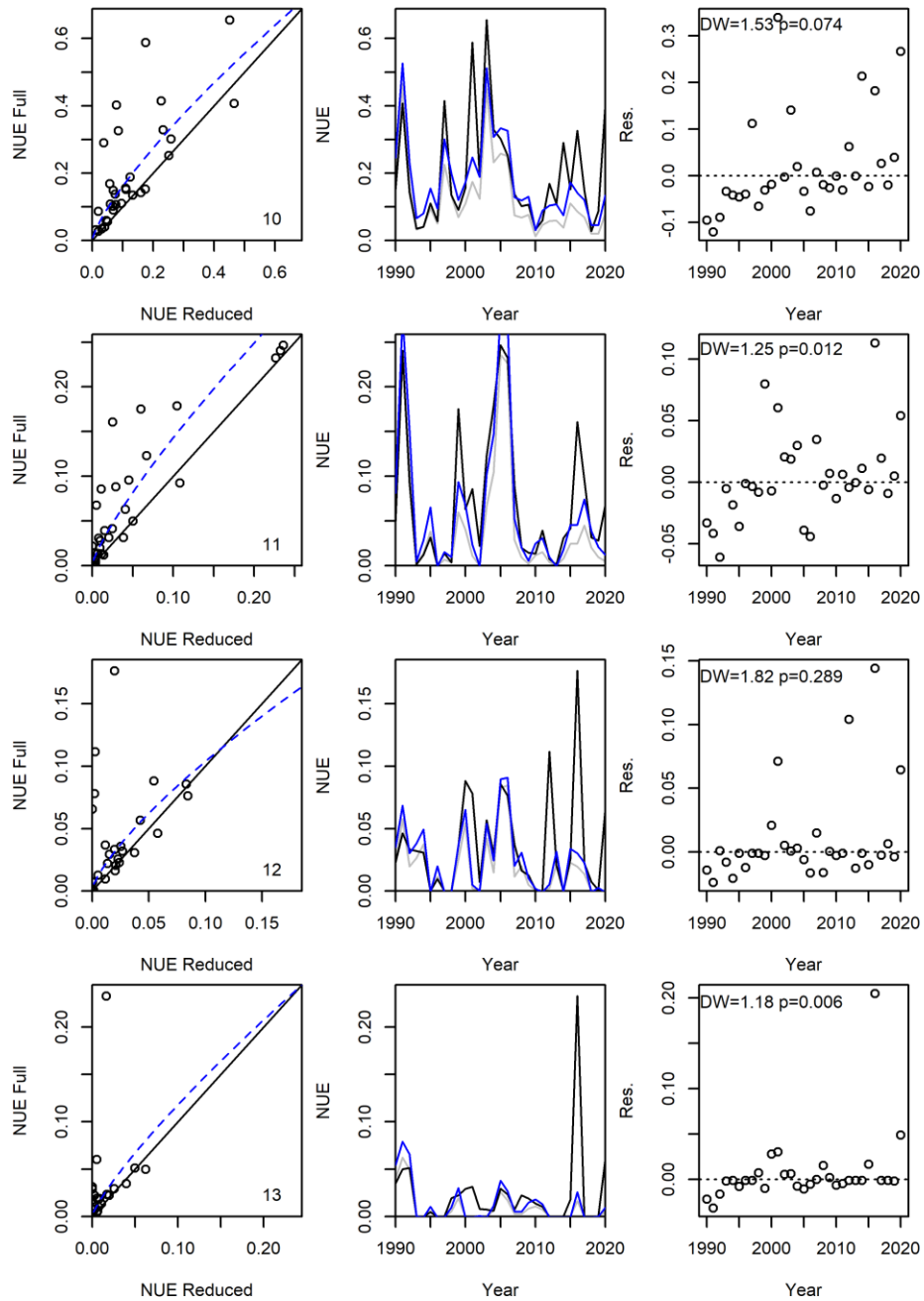


Figure 21. Continued

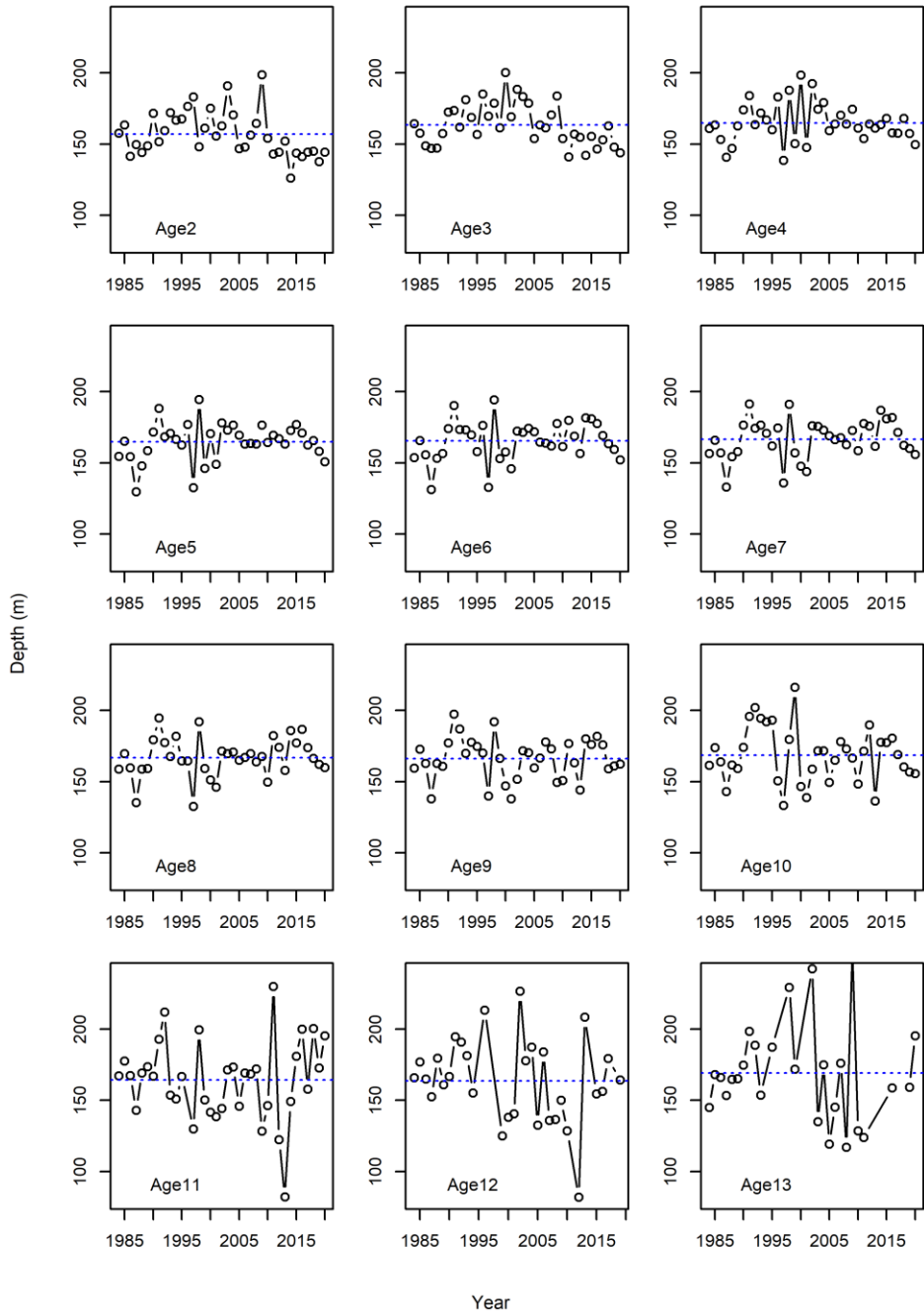


Figure 22. Mean depth occupied by cod in the RV survey year and age (panels). The series means are indicated with a dashed blue line. Results indicated for age 13 represent a 13-plus group.

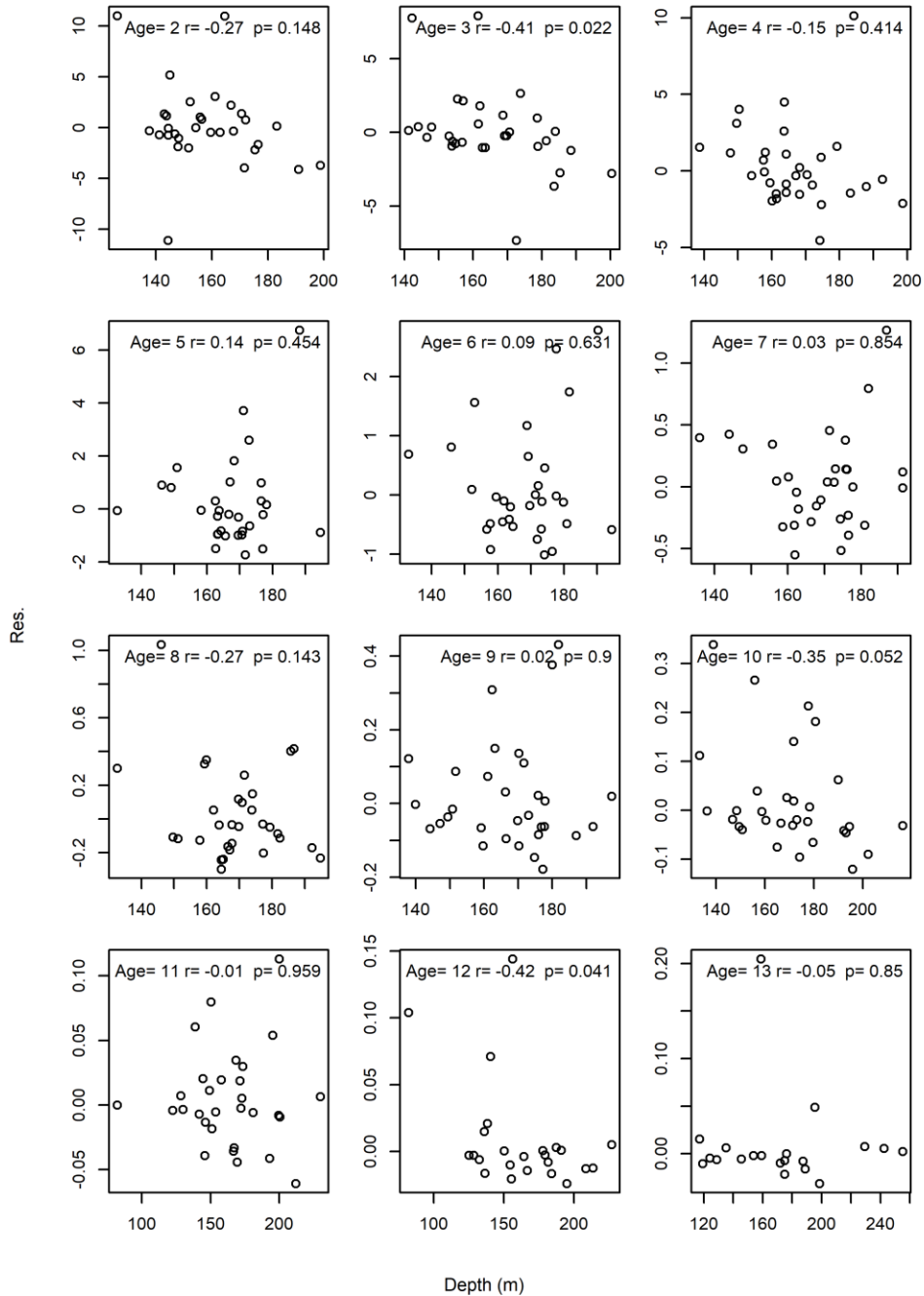


Figure 23. Relationship between mean occupied depth and the residuals for the abundance index based on the full suite of strata minus the corrected index, as a function of age (panels). The associated correlation coefficient and p -value are indicated in each panel. Results indicated for age 13 represent a 13-plus group.

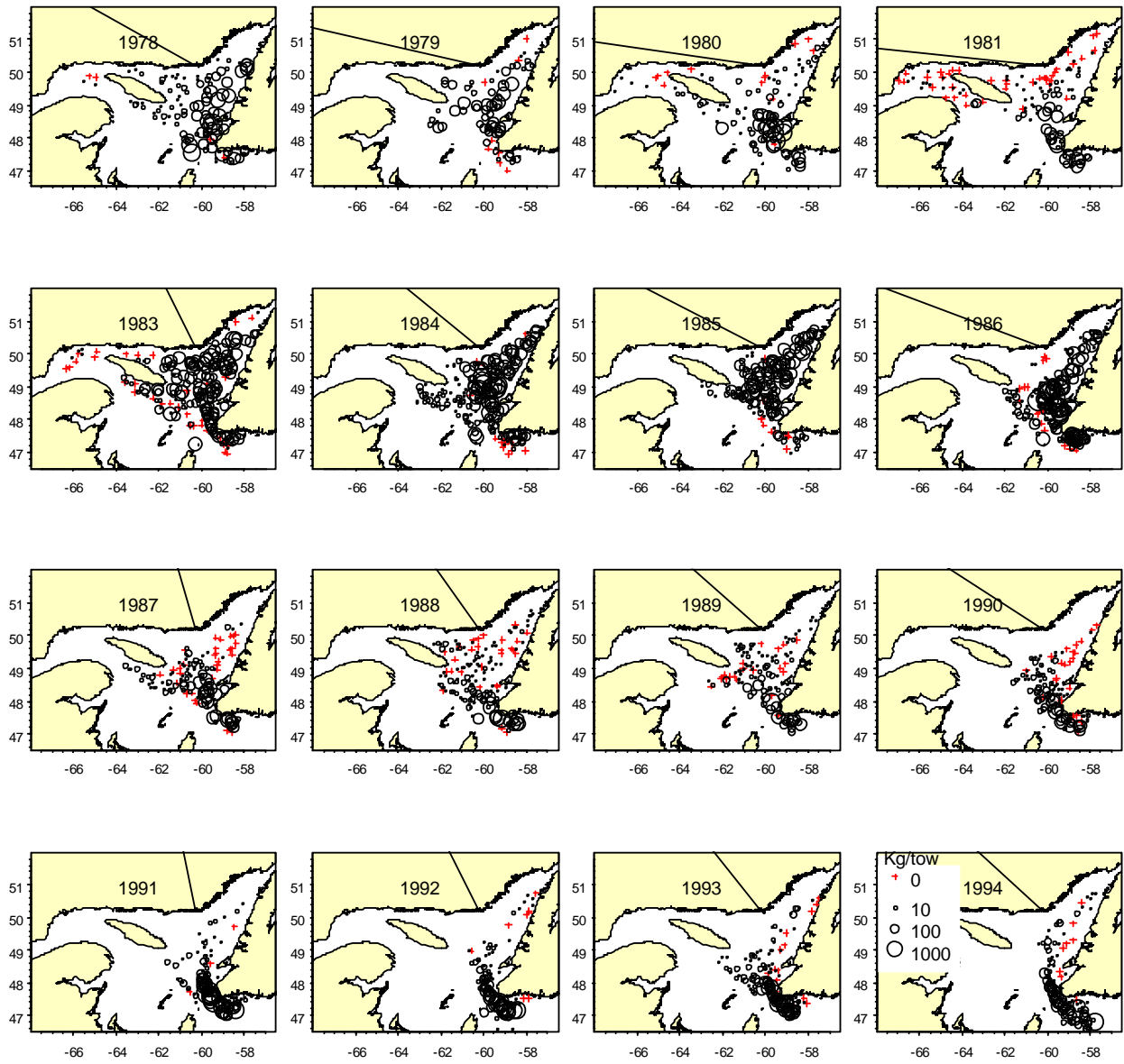


Figure 24. Distribution of Atlantic cod catches (kg/tow) in the MV Gadus Atlantica January survey, 1978-1994.

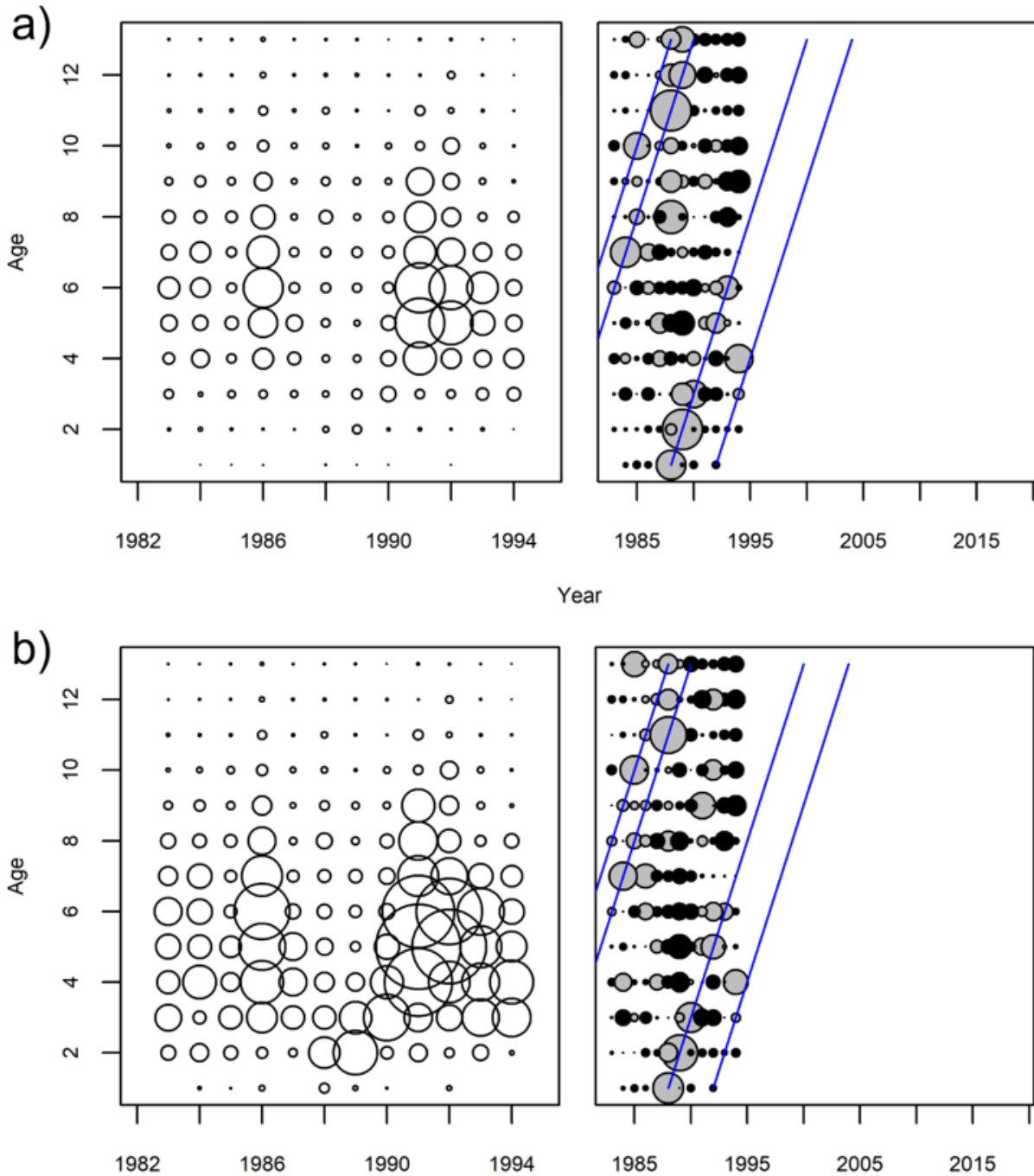


Figure 25. Catch at age in the *Gadus Atlantica* winter survey for 1984-1994 for a) unadjusted catches and b) catches adjusted to Teleost-Campelen equivalents based on Warren (1997). The left panels show catch proportional to circle size, while the right panels show standardized proportions at age and year (SPAY) with grey circles indicating above average catch and black below average. The blue lines indicate some consistently tracked above average cohorts in the RV survey (see Figure 17).

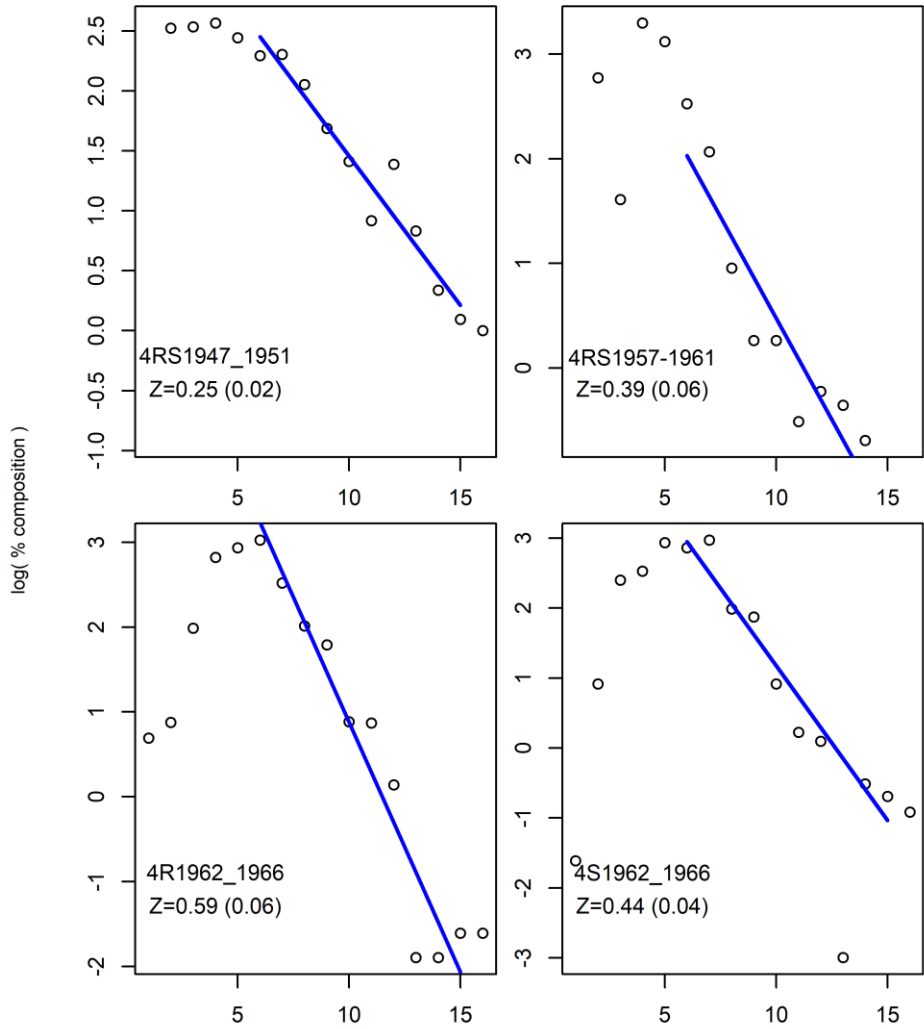


Figure 26. Relative catch curves (composition as a function of age) for historical research surveys, by NAFO area and period of years, as reported in Wiles and May (1968). The blue lines are regressions of the log relative catch curves, the slope of which provides a cross-sectional estimate of total mortality, Z . The estimate of Z and associated standard error are provided in each plot.

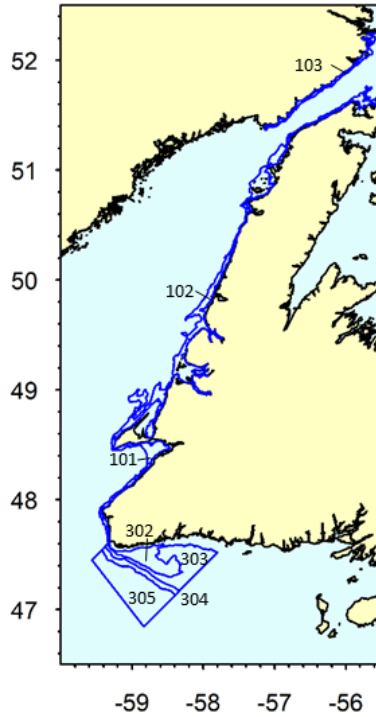


Figure 27. Coastal strata used in the northern Gulf of St. Lawrence Sentinel bottom-trawl survey in addition to the other strata employed in the nGSL multi-species survey (Figure 1), with the exception of strata in the Estuary).

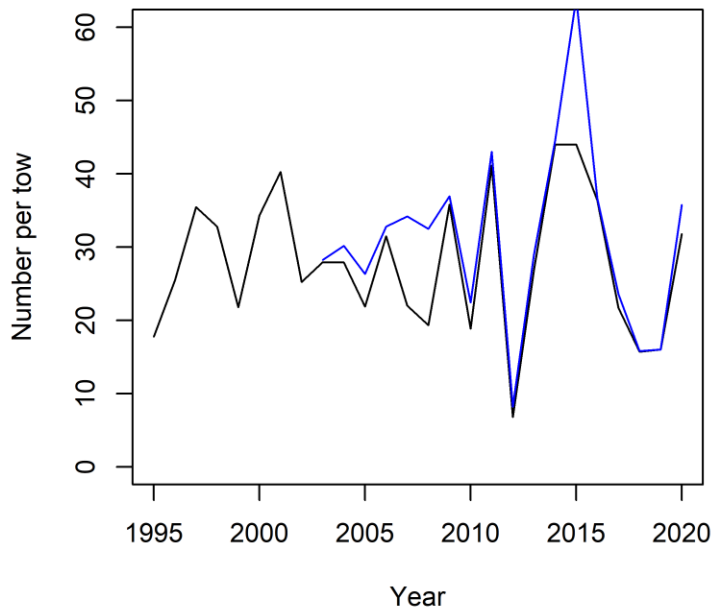


Figure 28. Age aggregated abundance indices for the Sentinel mobile gear survey, including (blue) and excluding (black) the coastal strata indicated in Figure 27.

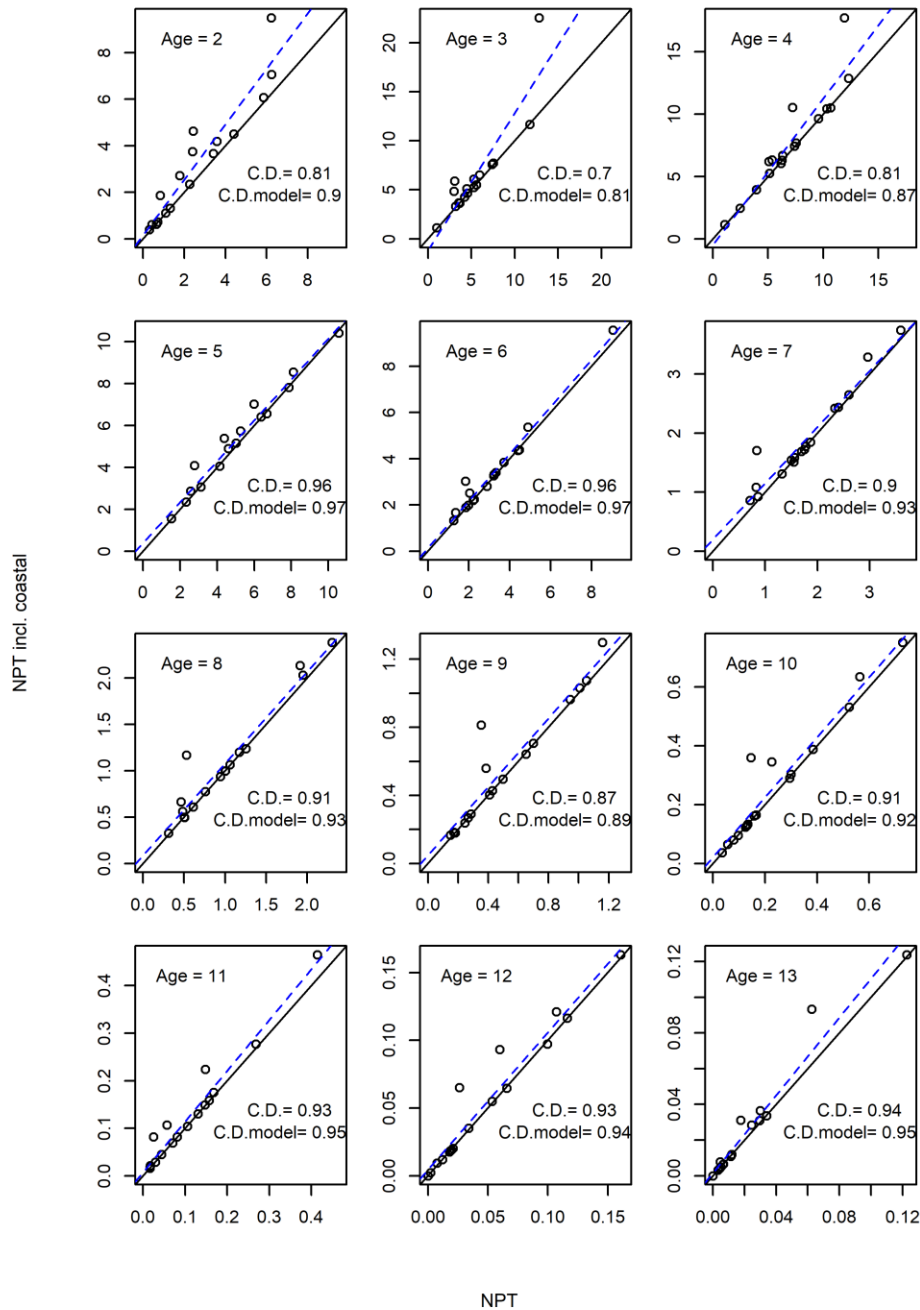


Figure 29. Relationship between Sentinel mobile gear survey abundance index values for series excluding (x-axis) and including (y-axis) the coastal strata indicated in Figure 27, by age (panels). The black line is a 1:1 relationship while the dashed blue line is a model-estimated correction. The coefficients of determination (R^2) values for the 1:1 relationship and for the model-estimated correction are indicated in each panel.

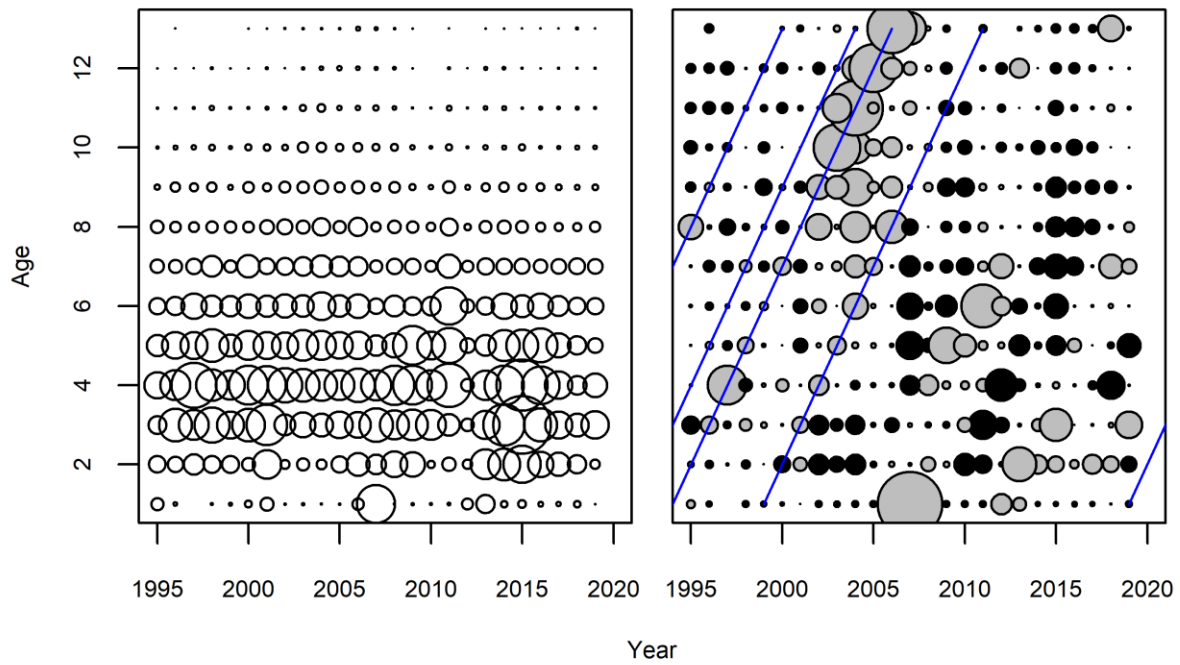


Figure 30. Catch at age in the Sentinel mobile gear survey for 1995-2020. The left panel shows catch proportional to circle size, while the right panel shows standardized proportions at age and year (SPAY) with grey circles indicating above average catch and black below average. The blue lines indicate some consistently tracked above average cohorts in the RV survey (see Figure 17).

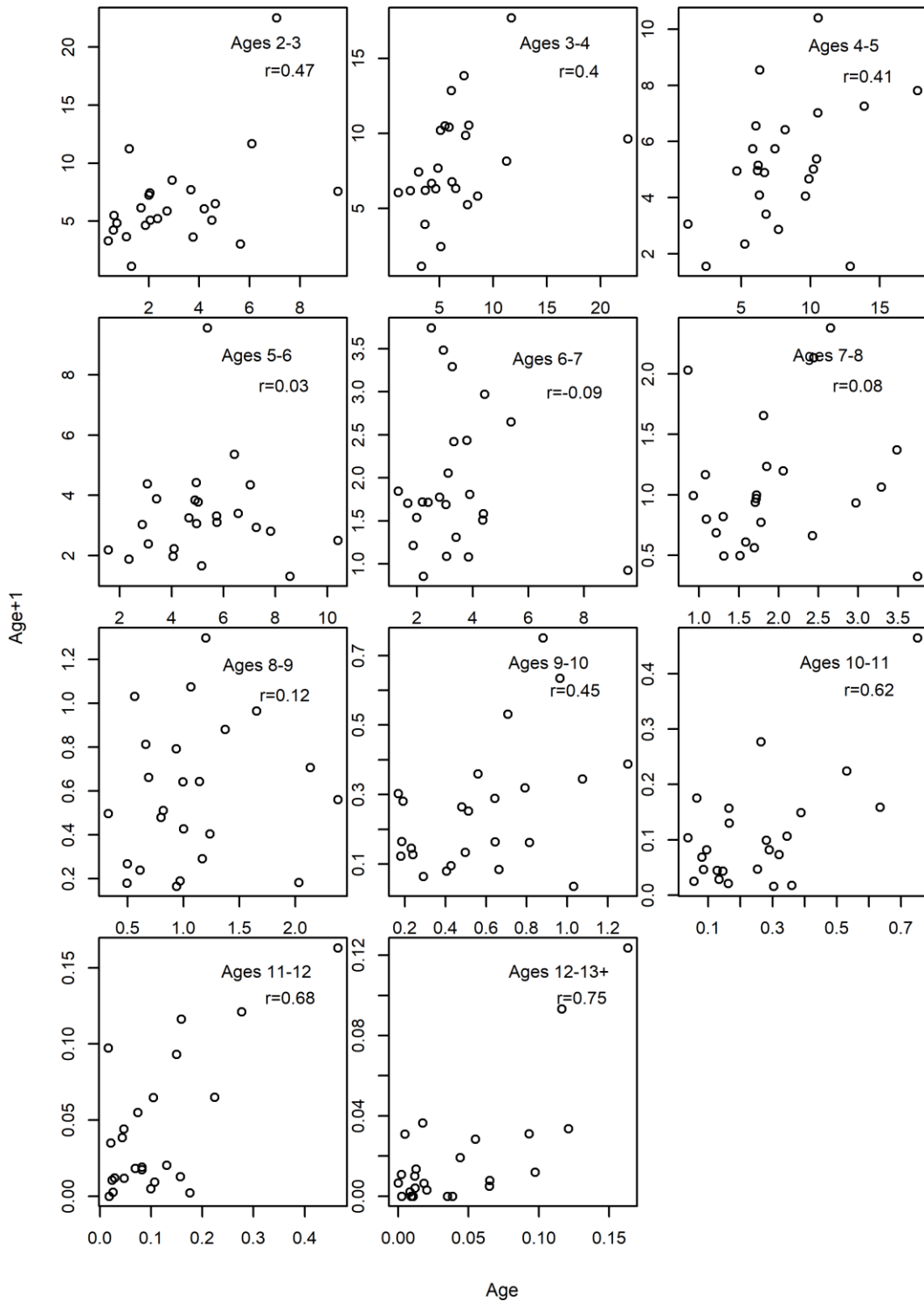


Figure 31. Age-specific abundance of cohorts at a given age and year, as a function of their abundance one year later in the Sentinel mobile gear survey, for 1995-2020. The correlation between the two sets of estimates is indicated in each panel.

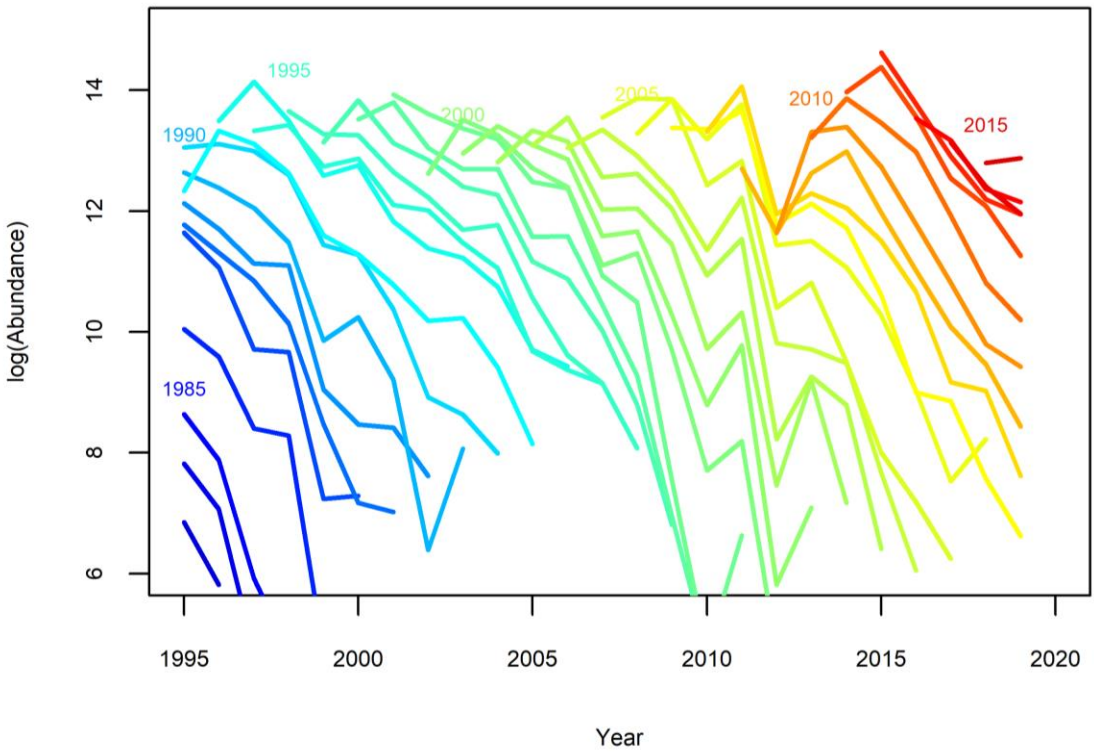


Figure 32 . Abundance of individual cohorts (ages 3 to 13+) from the Sentinel mobile gear survey catch at age, 1995-2020. Cohorts are identified by birth year for every 5th year.

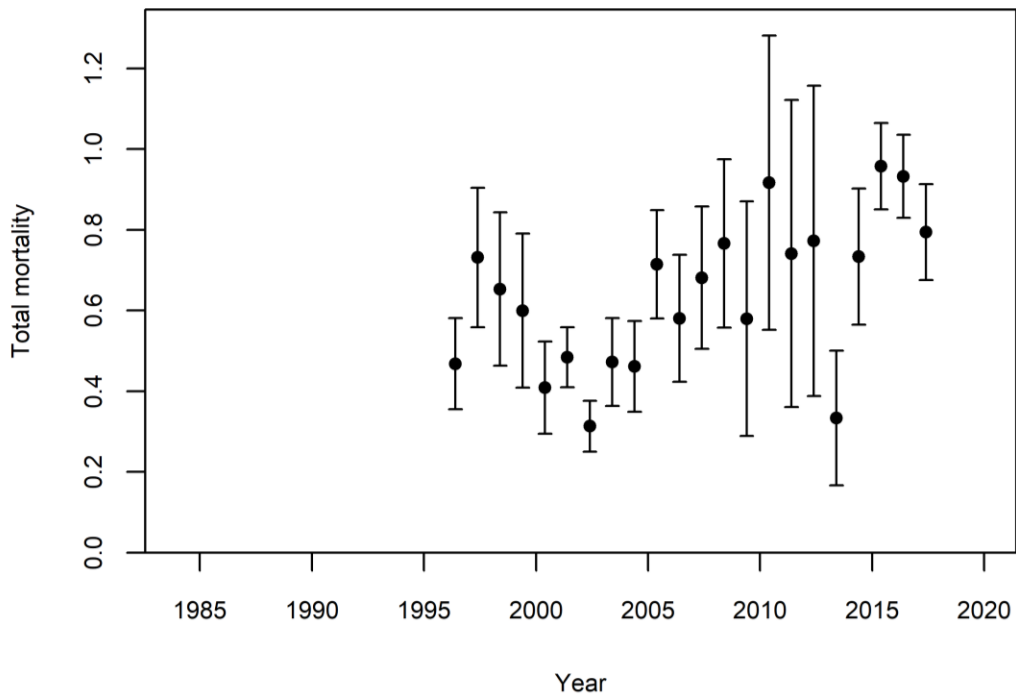


Figure 33. Estimates of total mortality (Z ; with 95% confidence intervals) for ages 5 to 10 from the Sentinel mobile gear survey, 1995-2020.

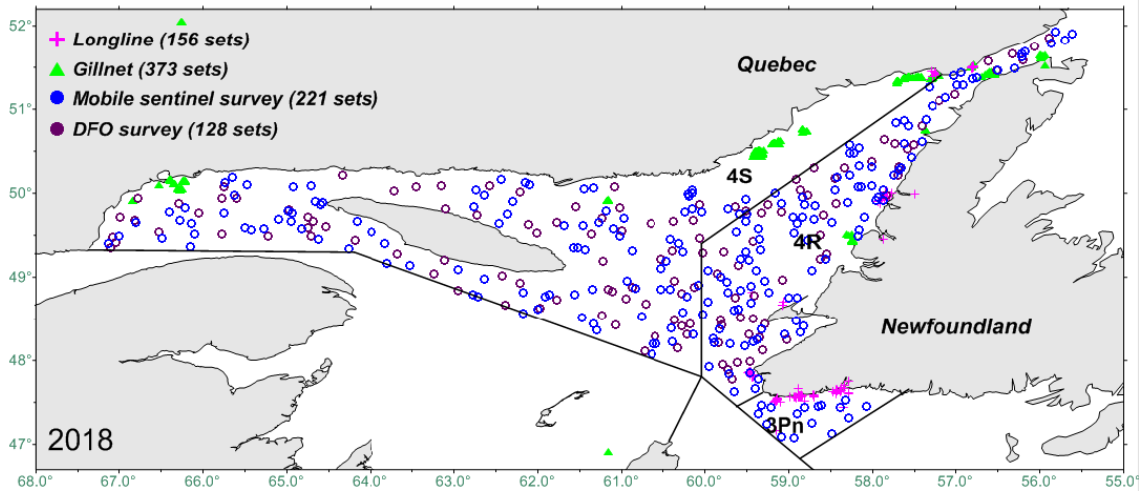


Figure 34. Spatial distribution of surveys in the nGSL in 2018.

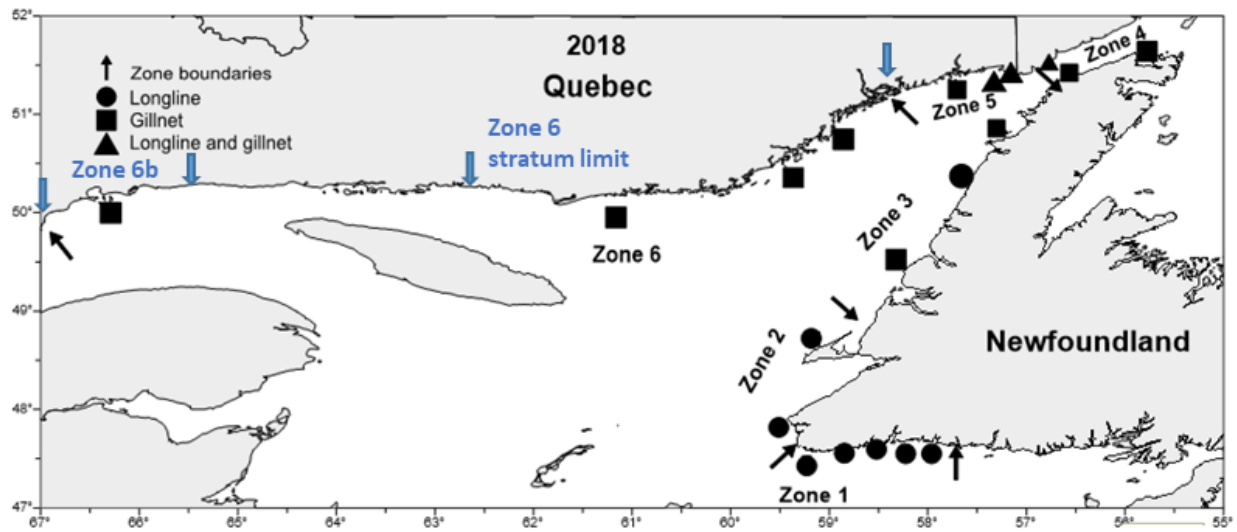


Figure 35. Zone boundaries for the sentinel fixed gear surveys, and revised stratum limits for zones 6 and 6b (blue), along with the location of sampling sites in 2018, as a function of gear type.

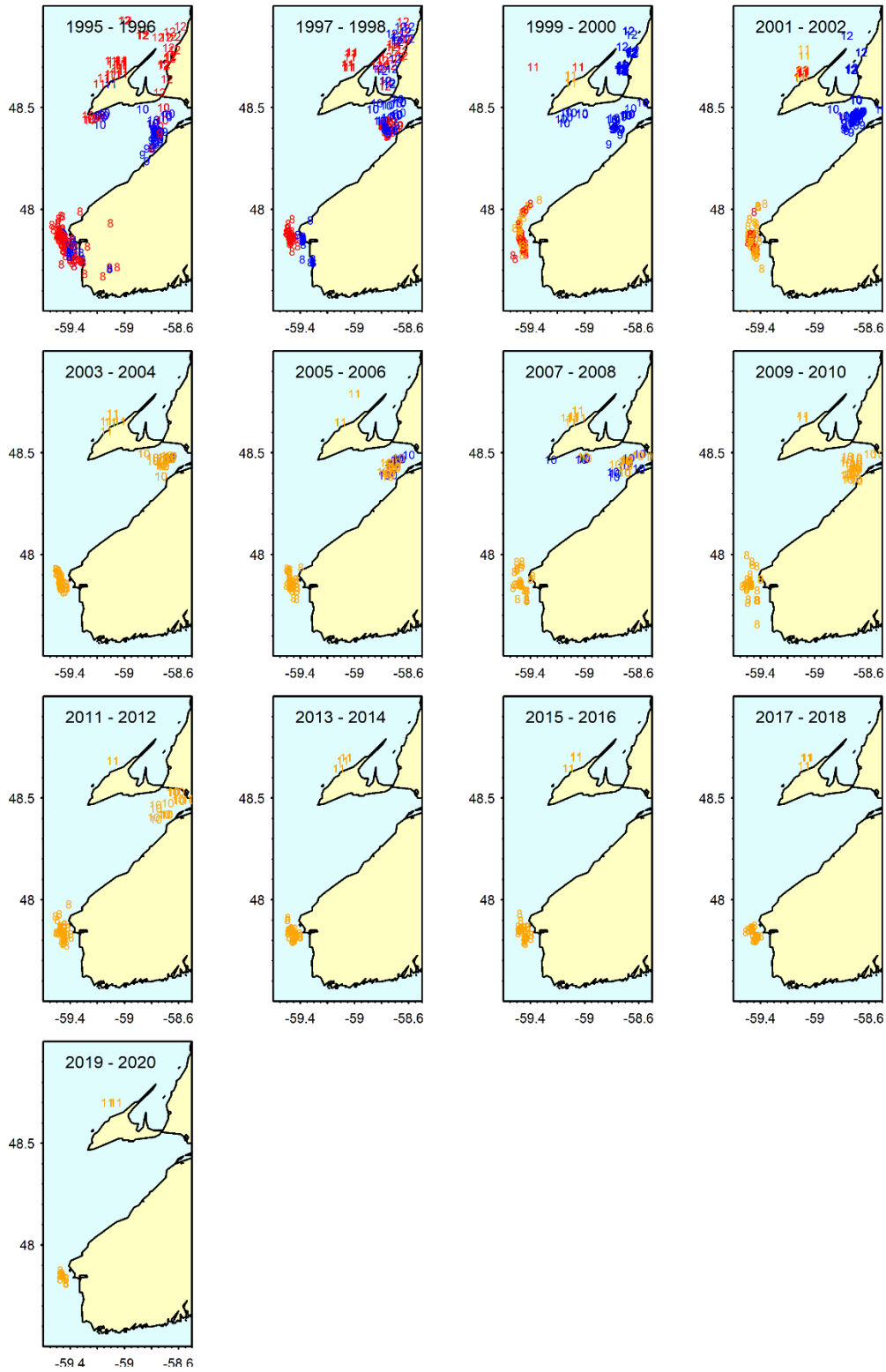


Figure 37. Location of individual Sentinel fixed gear hauls by longlines using J-hooks (red), longlines using circle hooks (orange) and gillnets (blue) in two year blocks in Zone 2 (Cape Ray to Port au Port Bay). Site numbers associated with each haul are indicated.

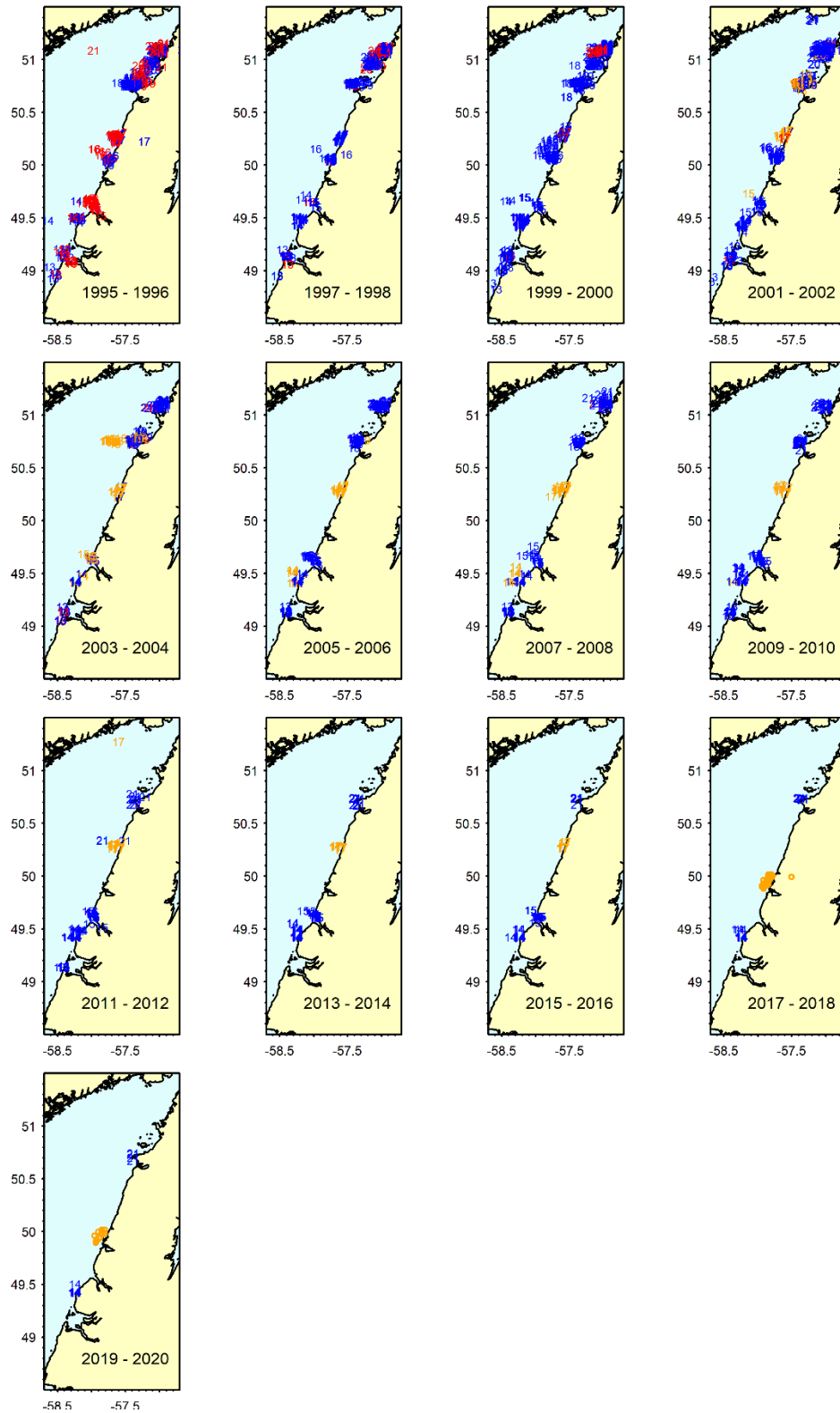


Figure 38. Location of individual Sentinel fixed gear hauls by longlines using J-hooks (red), longlines using circle hooks (orange) and gillnets (blue) in two year blocks in Zone 3 (Bay of Islands to Flower's Cove). Site numbers associated with each haul are indicated.

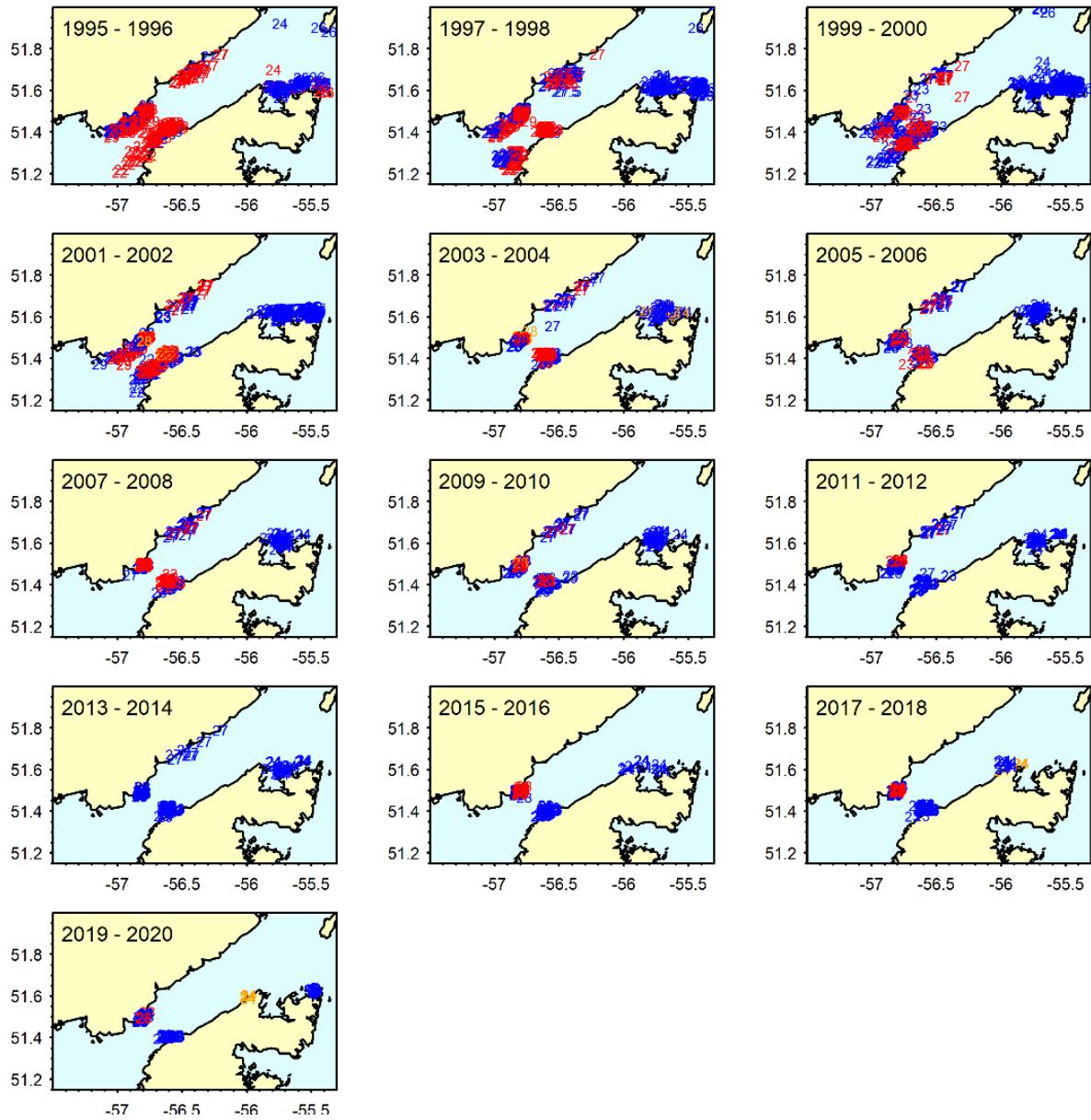


Figure 39. Location of individual Sentinel fixed gear hauls by longlines using J-hooks (red), longlines using circle hooks (orange) and gillnets (blue) in two year blocks in Zone 4 (Belle-Isle Strait). Site numbers associated with each haul are indicated.

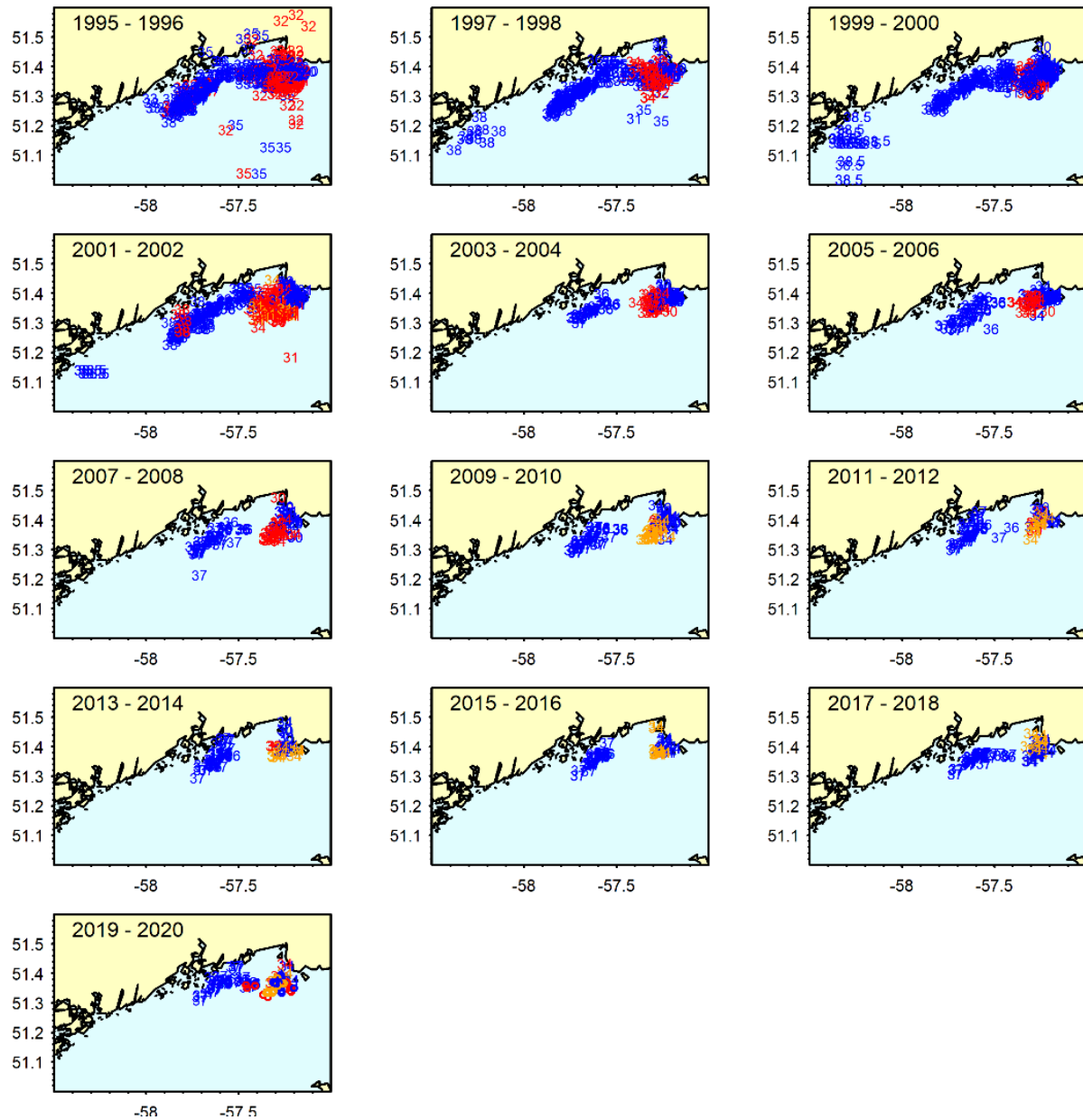


Figure 40. Location of individual Sentinel fixed gear hauls by longlines using J-hooks (red), longlines using circle hooks (orange) and gillnets (blue) in two year blocks in Zone 5 (Blanc Sablon to St-Augustin). Site numbers associated with each haul are indicated.

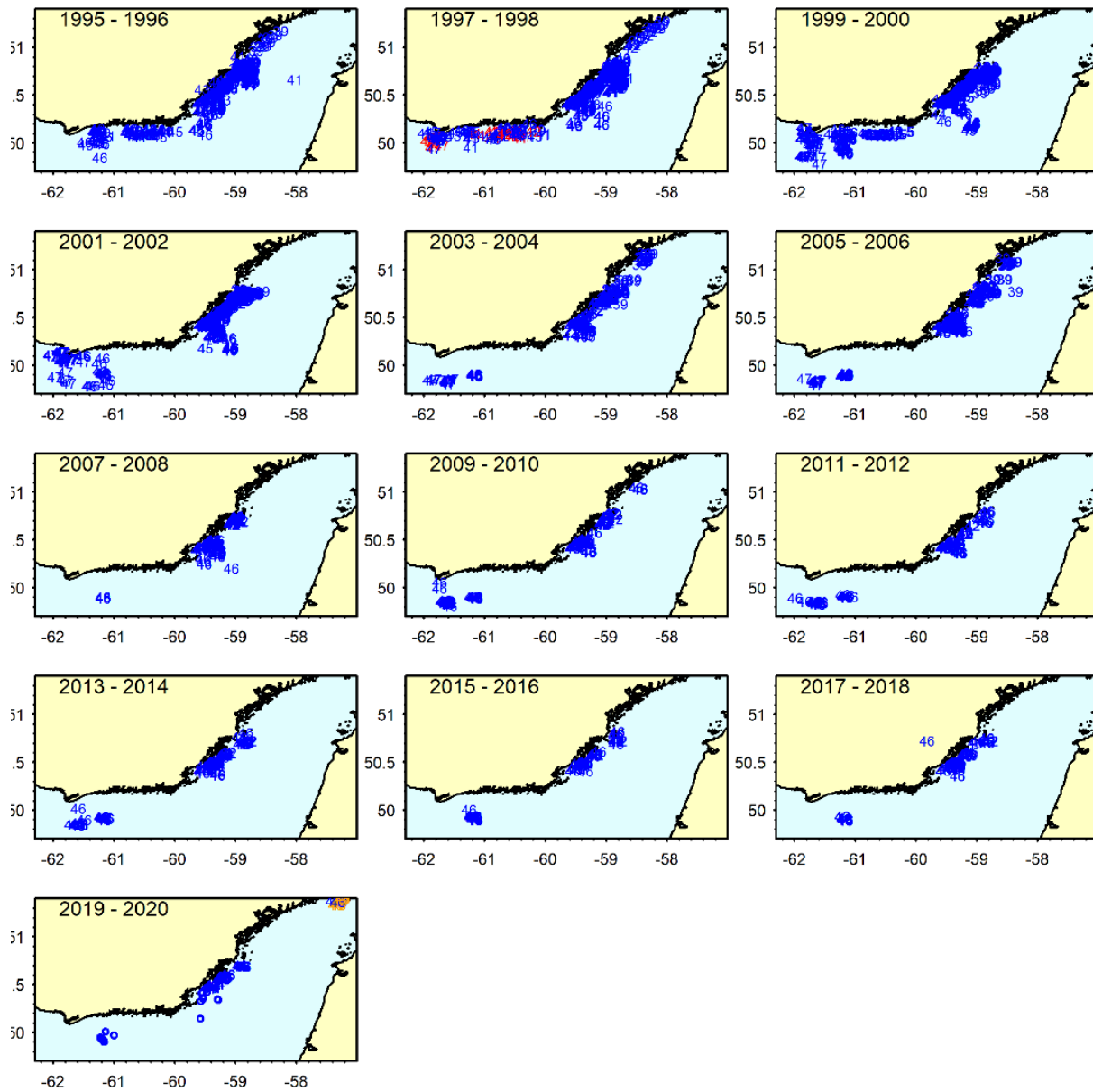


Figure 41. Location of individual Sentinel fixed gear hauls by longlines using J-hooks (red), longlines using circle hooks (orange) and gillnets (blue) in two year blocks in Zone 6 (St-Augustin to La Romaine). Site numbers associated with each haul are indicated.

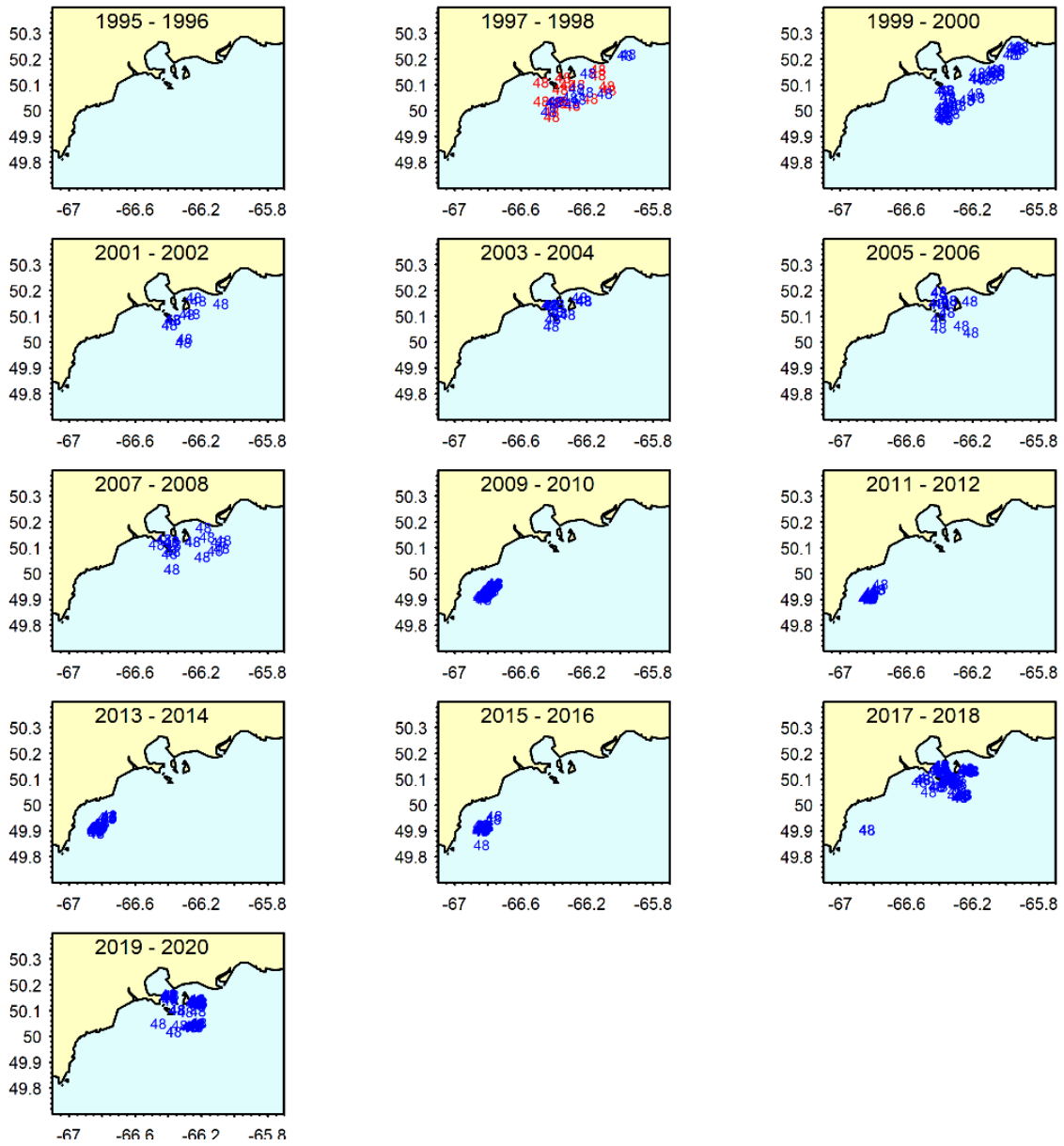


Figure 42. Location of individual Sentinel fixed gear hauls by longlines using J-hooks (red) and gillnets (blue) in two year blocks in Zone 6b (Sept-Îles area). Site numbers associated with each haul are indicated.

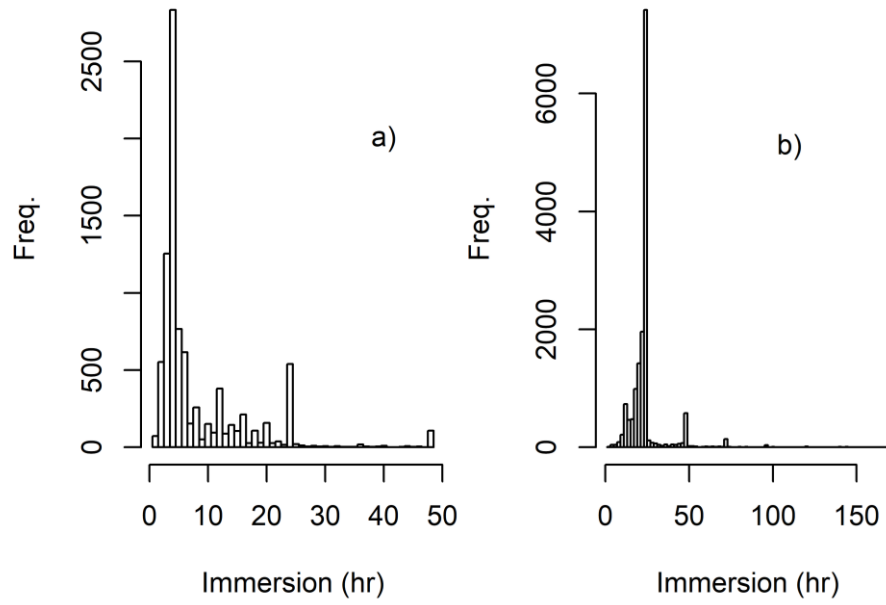


Figure 43. Gear soak (immersion) times for the Sentinel fixed gear surveys, a) longlines, b) gillnets

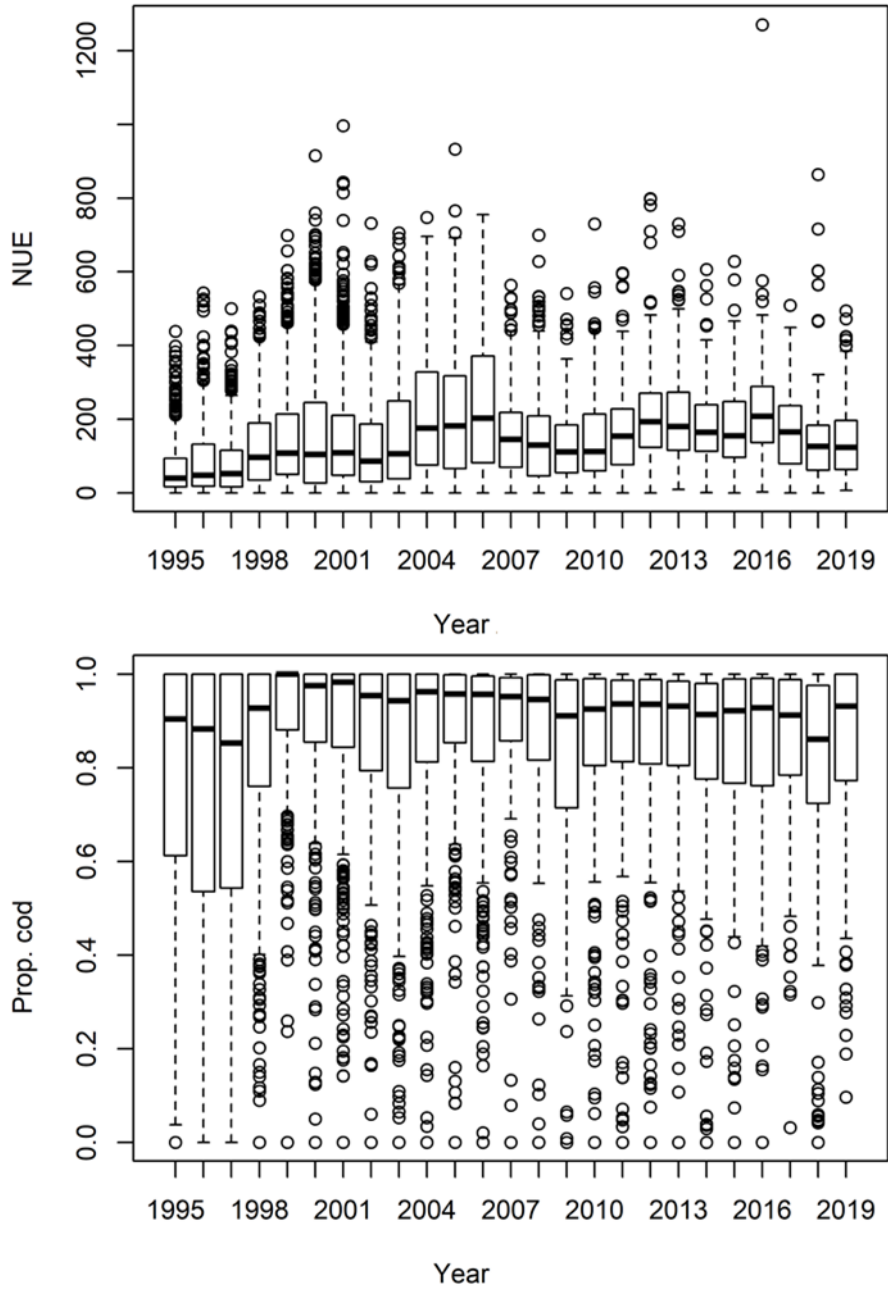


Figure 44. Boxplots of the estimated a) catch (numbers) of fish per haul, all species combined, per 1000 hooks, and b) the proportion of cod in the catches, for each year in the Sentinel longline survey.

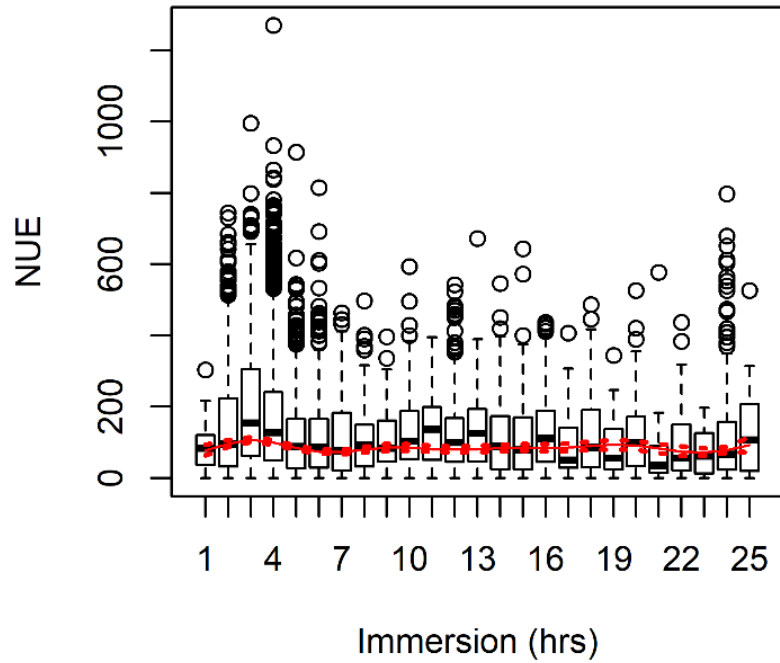


Figure 45. Boxplots of cod catch rates (numbers per 1000 hook) in individual hauls as function of gear soak (immersion) time in the Sentinel longline survey. The red line is the smoother estimated from a GAMM analysis of catch rates as a function of soak time (dashed lines are 95% confidence intervals on the smoother).

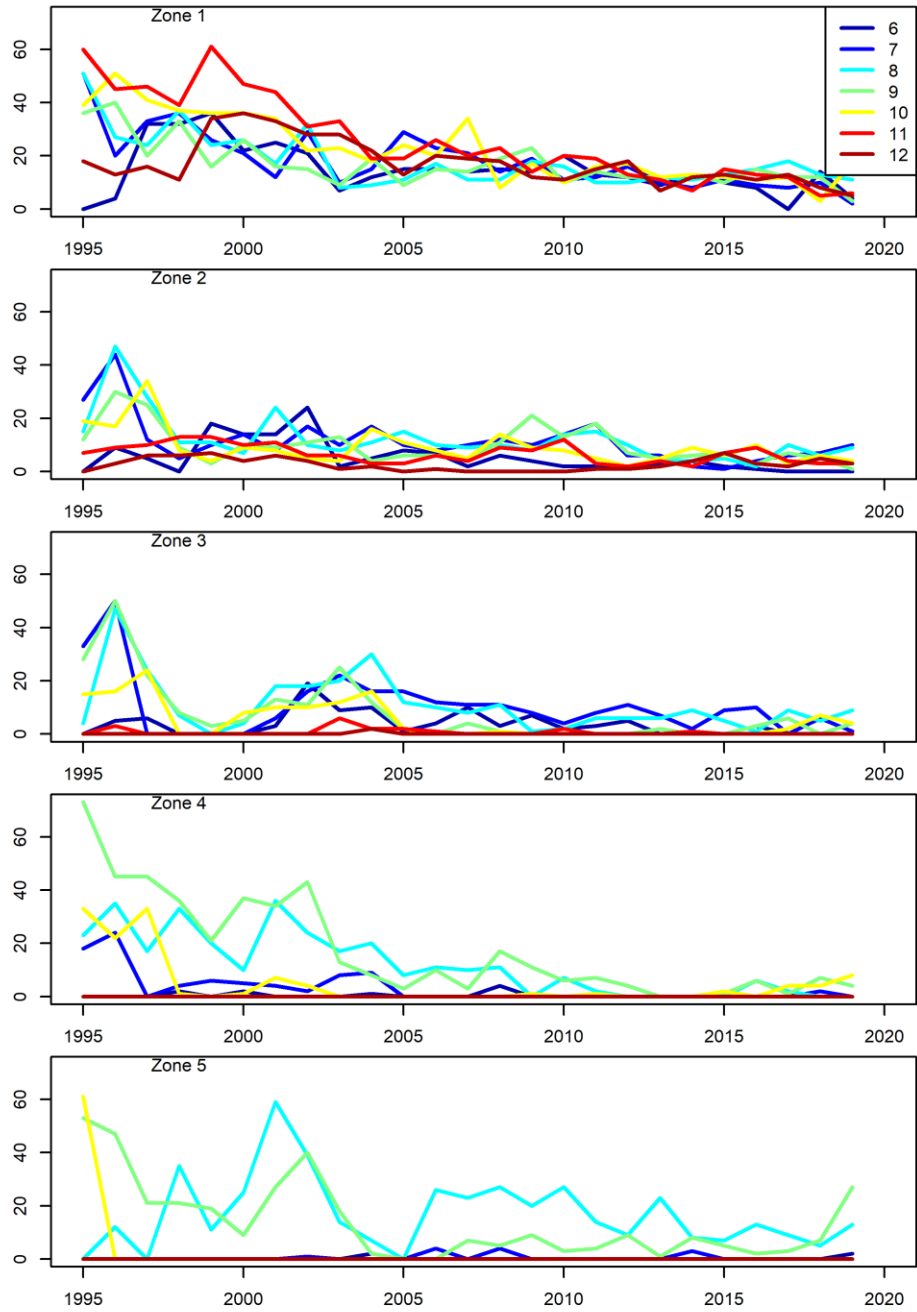


Figure 46. Number of individual hauls by zone (panels) and month (coloured lines) in the Sentinel longline survey.

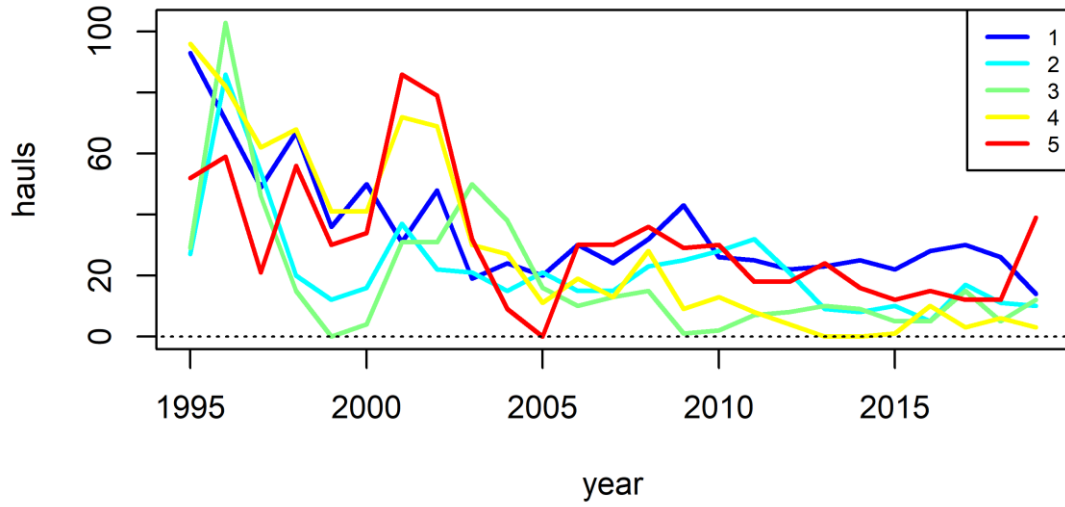


Figure 47. Number of individual hauls by zone (lines) in August and September (days of year 210 to 270) in the Sentinel longline survey.

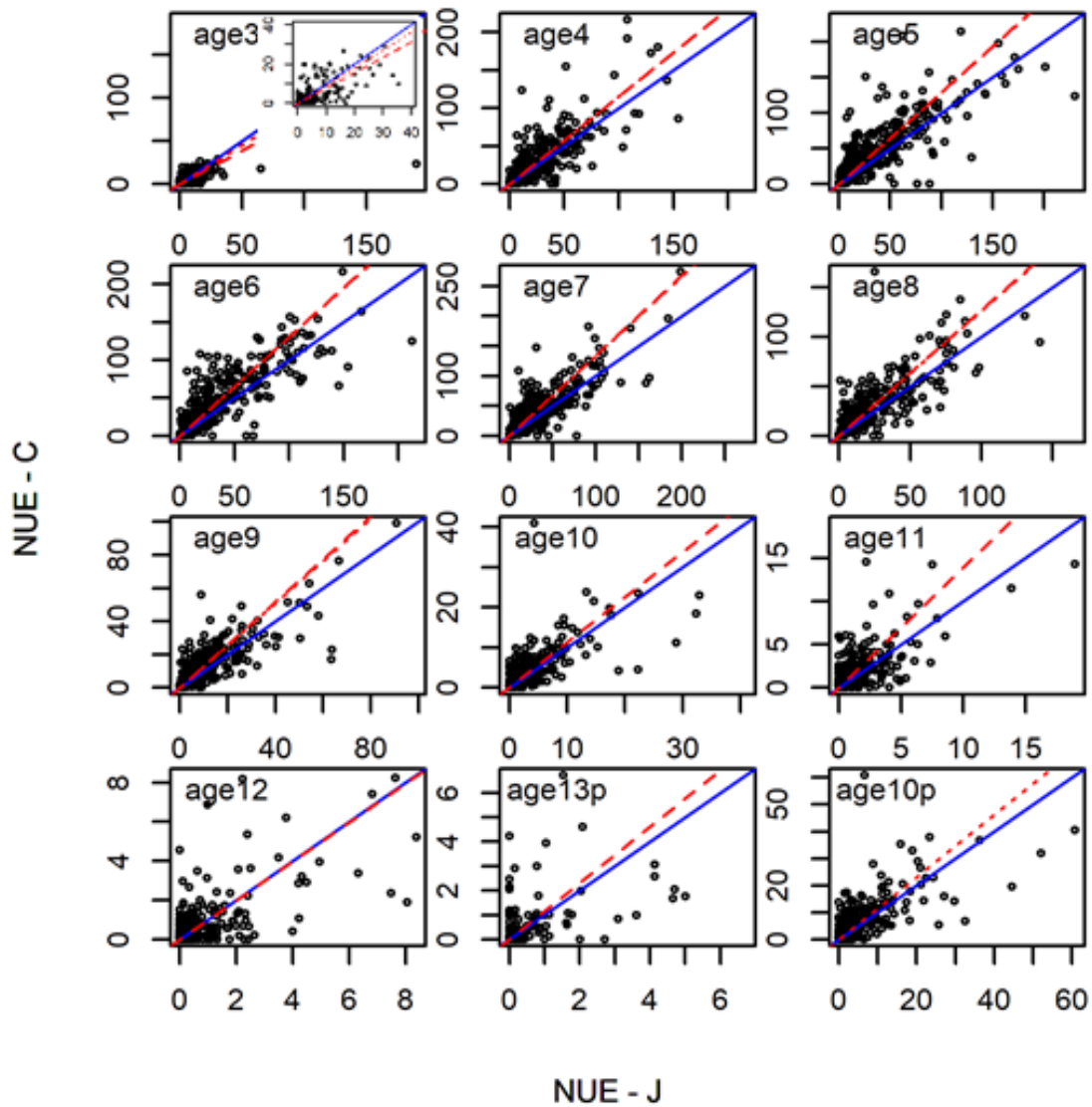


Figure 48. Age-specific mean catch rates (number per unit effort, NUE) using J-hooks (x-axes) and using circle hooks (y-axes) in sampling units defined by year, week and site, where age13p and age10p designate plus groups, for ages 13+ and 10+ respectively. The blue lines indicate a 1:1 relationship, the dashed red line is the estimated age-specific relative efficiency from model A, while the dotted red line is the estimate from model B. The inset in the panel for age3 shows a close-up of the biplot excluding the two outlier values.

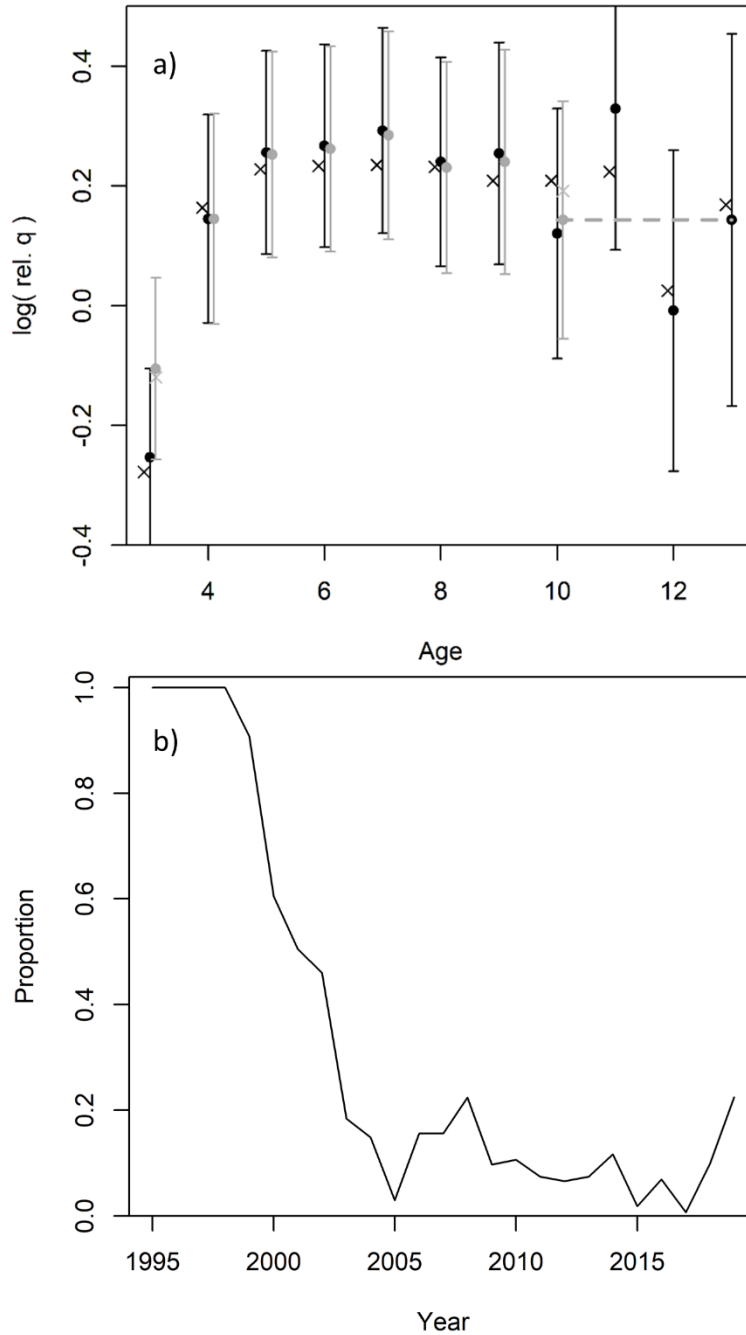


Figure 49. a) Estimated age-specific log efficiency of circle hooks relative to J hooks based on the models (dots with 95% confidence intervals) and based on sample means (crosses). The grey values are for the estimates that exclude two outlier units for age 3 and that group ages 10+ (model B). The dashed grey line is the estimated value for the 10+ group. b) Annual proportion of longline hauls made with J-hooks.

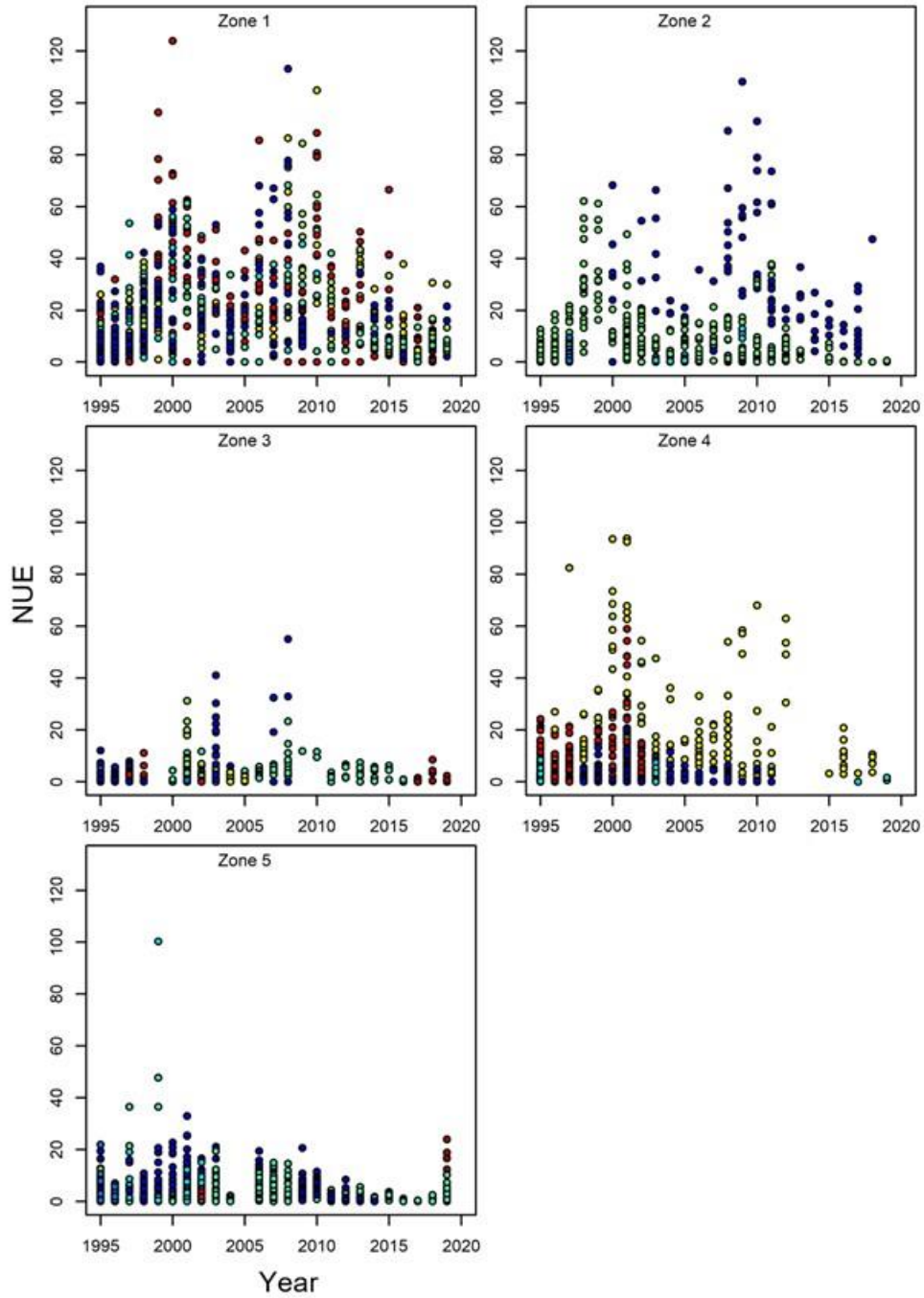


Figure 50. Catch rates of age 4 cod (number per 1000 hooks) in individual hauls by zone (panels) and year in Sentinel longline (August-September) summer hauls. Colours distinguish individual sites within zones.

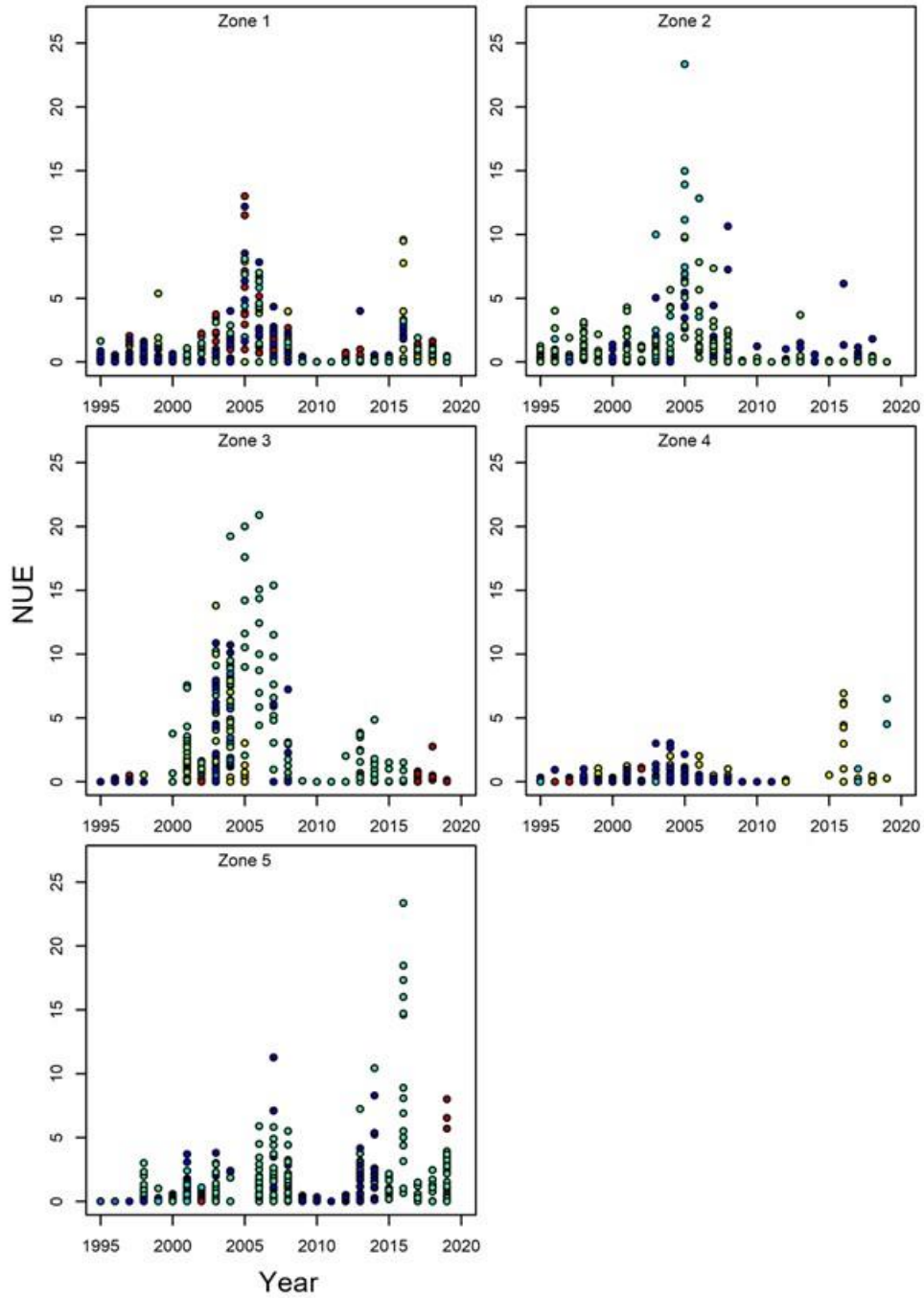


Figure 51. Catch rates of age 12 cod (number per 1000 hooks) in individual hauls by zone (panels) and year in Sentinel longline (August-September) summer hauls. Colours distinguish individual sites within zones.

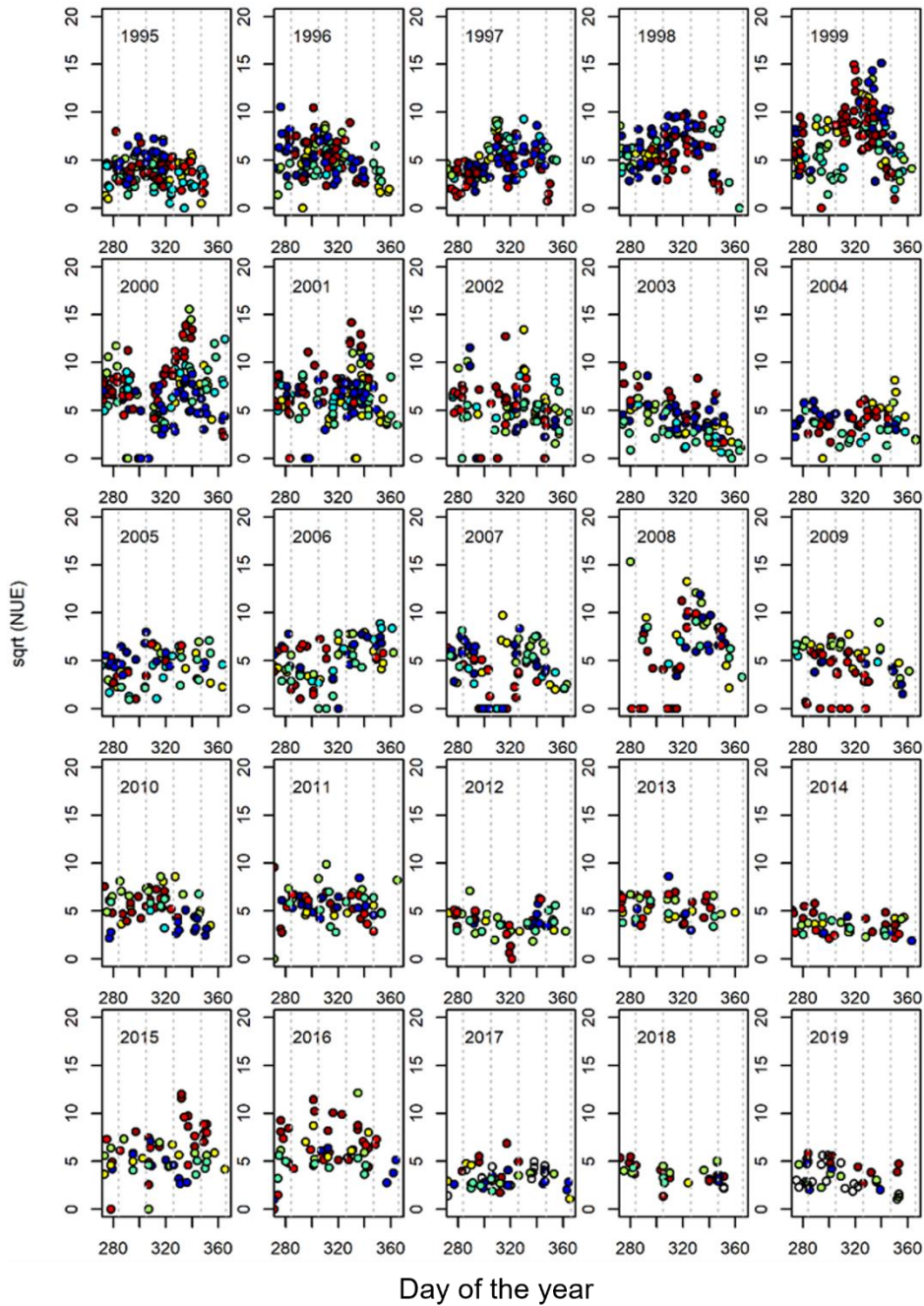


Figure 52. Catch rates of age 4 cod (square root, number per unit effort, 1000 hooks) in individual hauls by year (panels) and day of the year in Sentinel longline zone 1 + site 8 fall hauls. Colours distinguish individual sites. The dashed lines delineate the time blocks used to define the temporal strata.

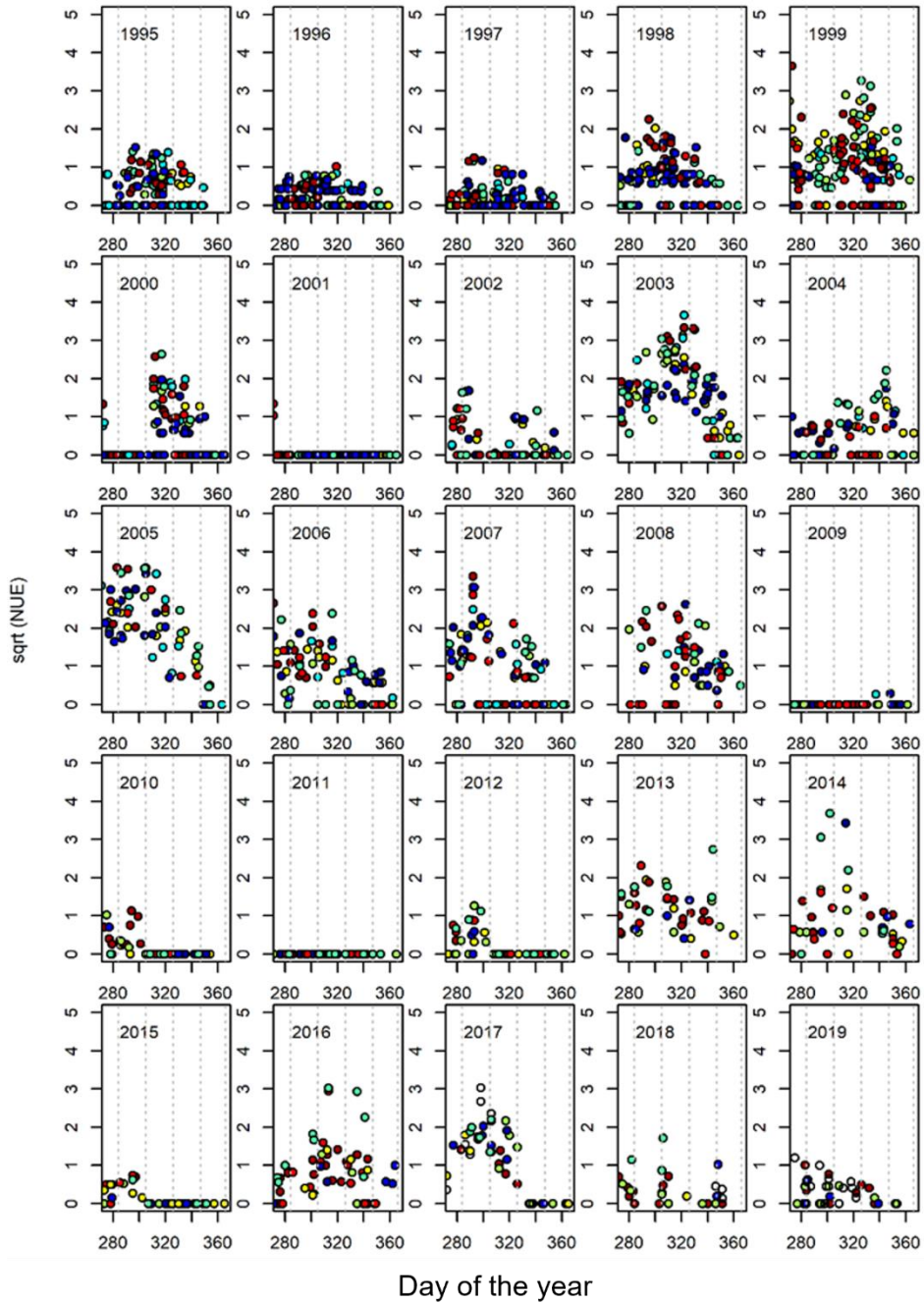


Figure 53. Catch rates of age 12 cod (square root, number per unit effort, 1000 hooks) in individual hauls by year (panels) and day of the year in Sentinel longline zone 1 + site 8 fall hauls. Colours distinguish individual sites. The dashed lines delineate the time blocks used to define the temporal strata.

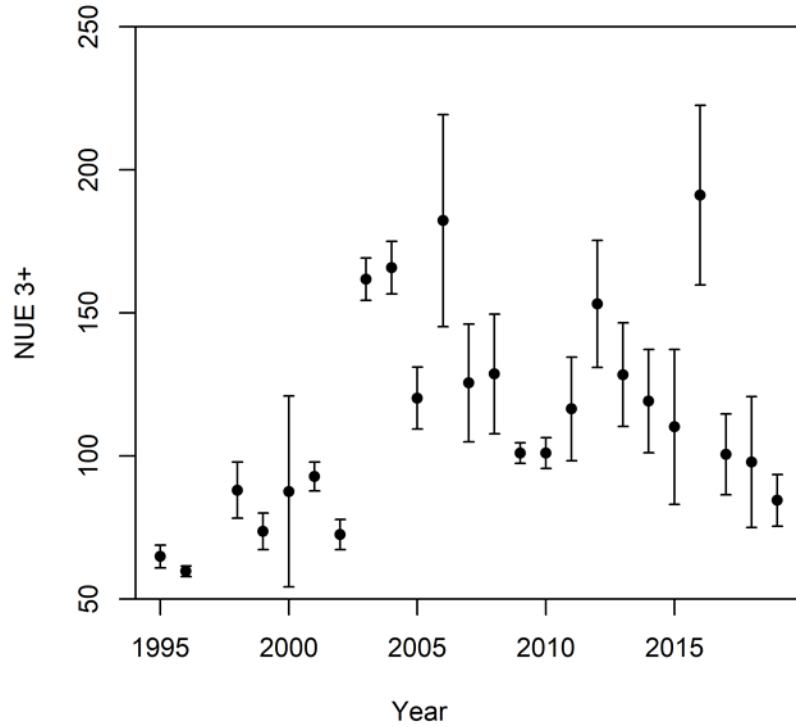


Figure 54. Age aggregated 3-plus abundance index (number per unit effort, NUE; 1000 hooks) with 95% confidence intervals for the Sentinel longline survey summer index, 1995-2019.

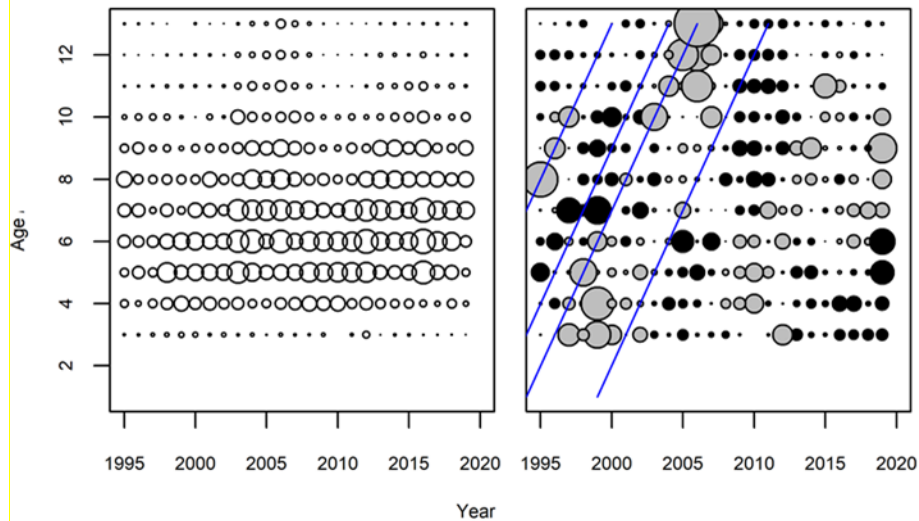


Figure 55. Catch at age in the Sentinel longline survey (summer index) 1995-2019. The left panel shows catch proportional to circle size, while the right panel shows standardized proportions at age and year (SPAY) with grey circles indicating above average catch and black below average. The blue lines indicate some consistently tracked above average cohorts in the RV survey (see Figure 17).

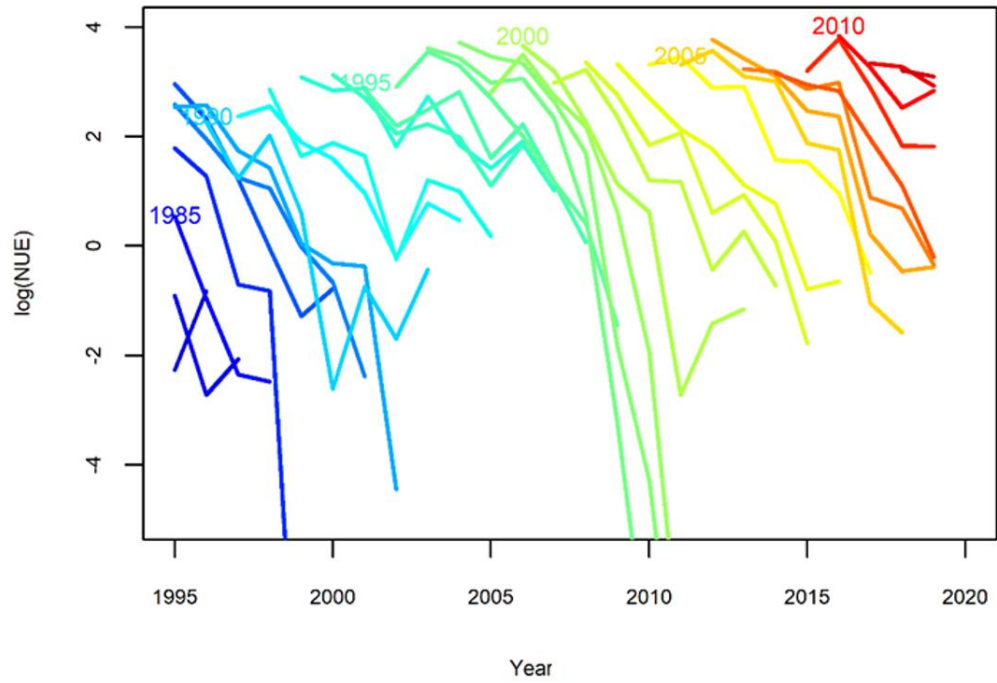


Figure 56. Abundance of individual cohorts (ages 6 to 13+) in the Sentinel longline survey (summer index) catch at age, 1995-2019. Cohorts are identified by birth year for every 5th year.

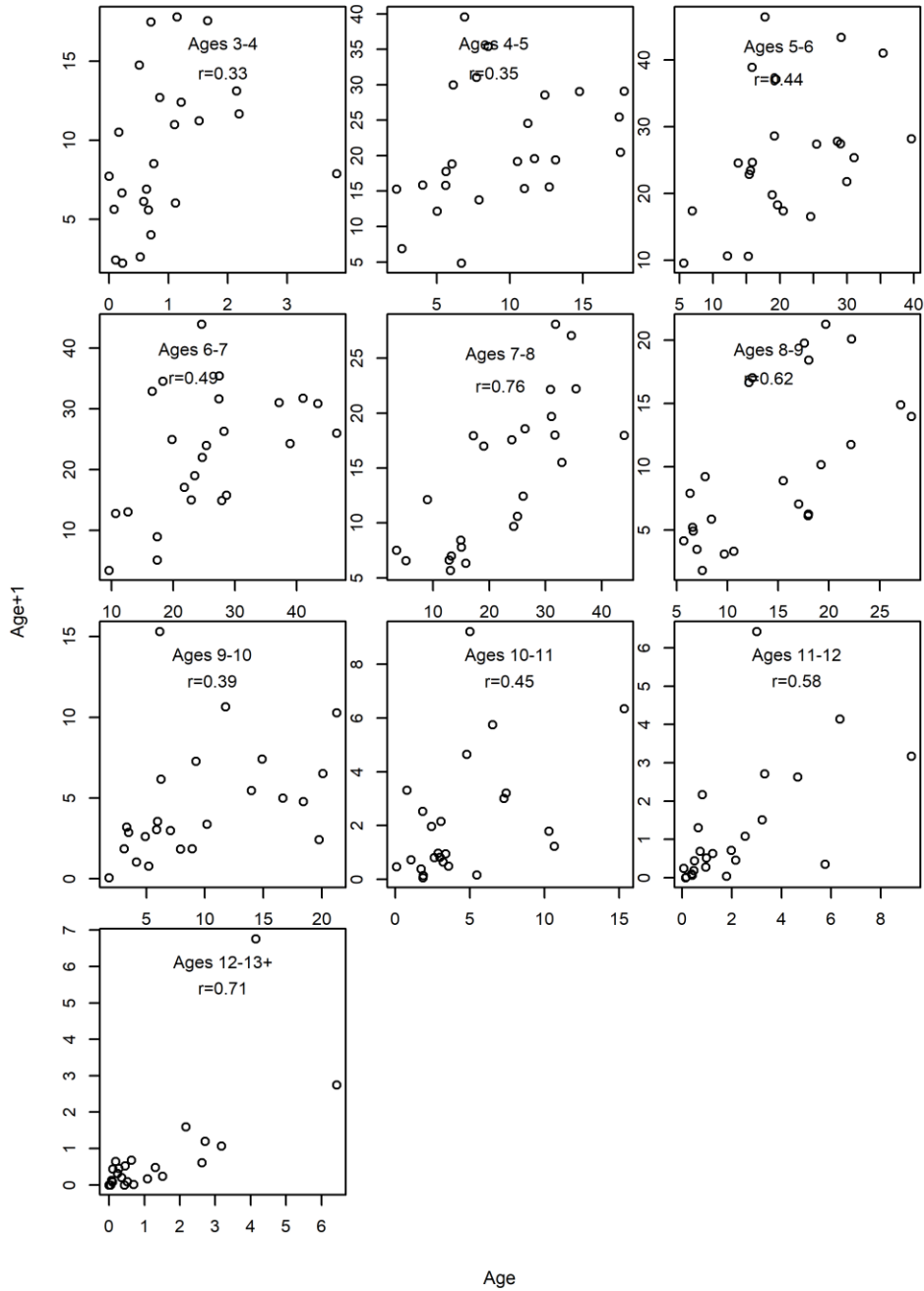


Figure 57. Age-specific abundance of cohorts at a given age and year, as a function of their abundance one year later in the Sentinel longline survey (summer index), for 1995-2019. The correlation between the two sets of estimates is indicated in each panel.

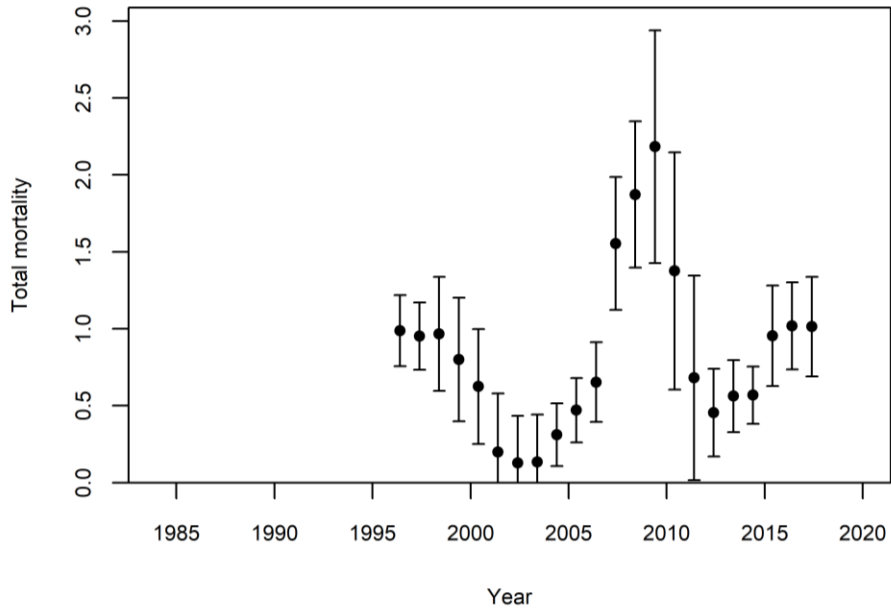


Figure 58. Estimates of total mortality (Z ; with 95% confidence intervals) for ages 8 to 12 from the Sentinel longline survey (summer index), 1995-2019.

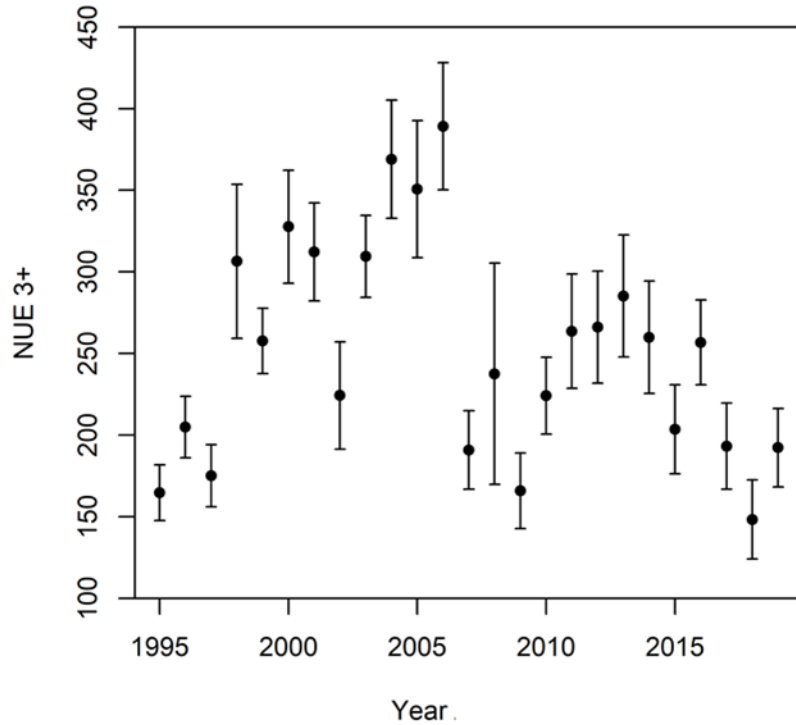


Figure 59. Age aggregated 3-plus abundance index (number per unit effort, NUE; 1000 hooks) with 95% confidence intervals for the Sentinel longline survey zone 1 fall index, 1995-2019.

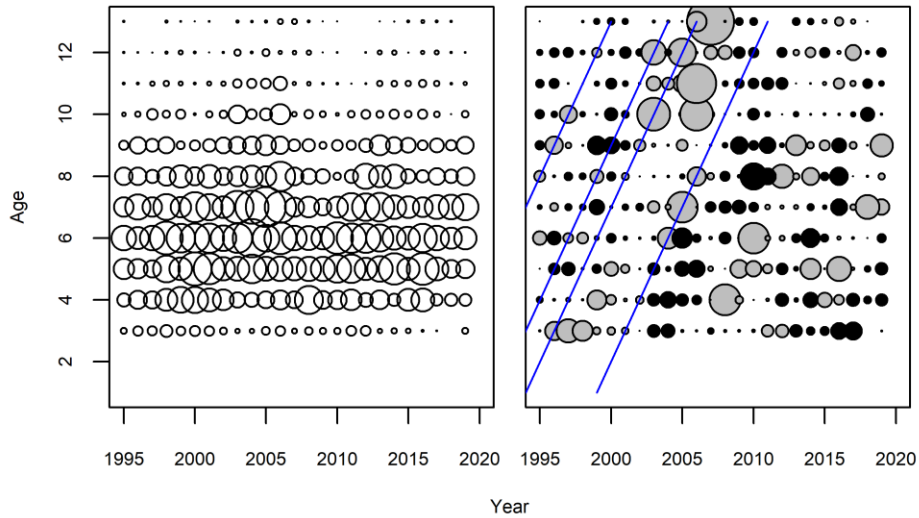


Figure 60. Catch at age in the Sentinel longline survey (fall index) 1995-2019. The left panel shows catch proportional to circle size, while the right panel shows standardized proportions at age and year (SPAY) with grey circles indicating above average catch and black below average. The blue lines indicate some consistently tracked above average cohorts in the RV survey (see Figure 17).

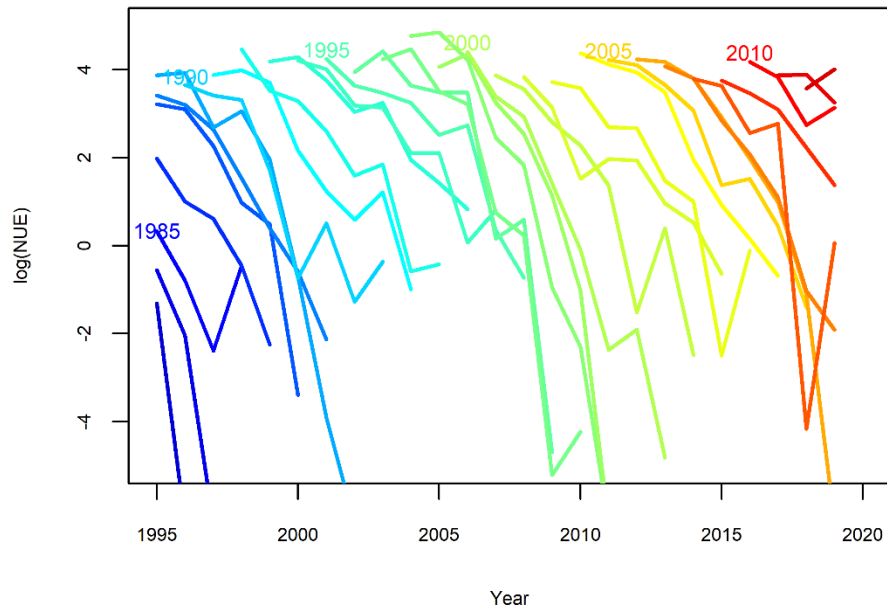


Figure 61. Abundance of individual cohorts (ages 6 to 13+) in the Sentinel longline survey (fall) catch at age, 1995-2019. Cohorts are identified by birth year for every 5th year.

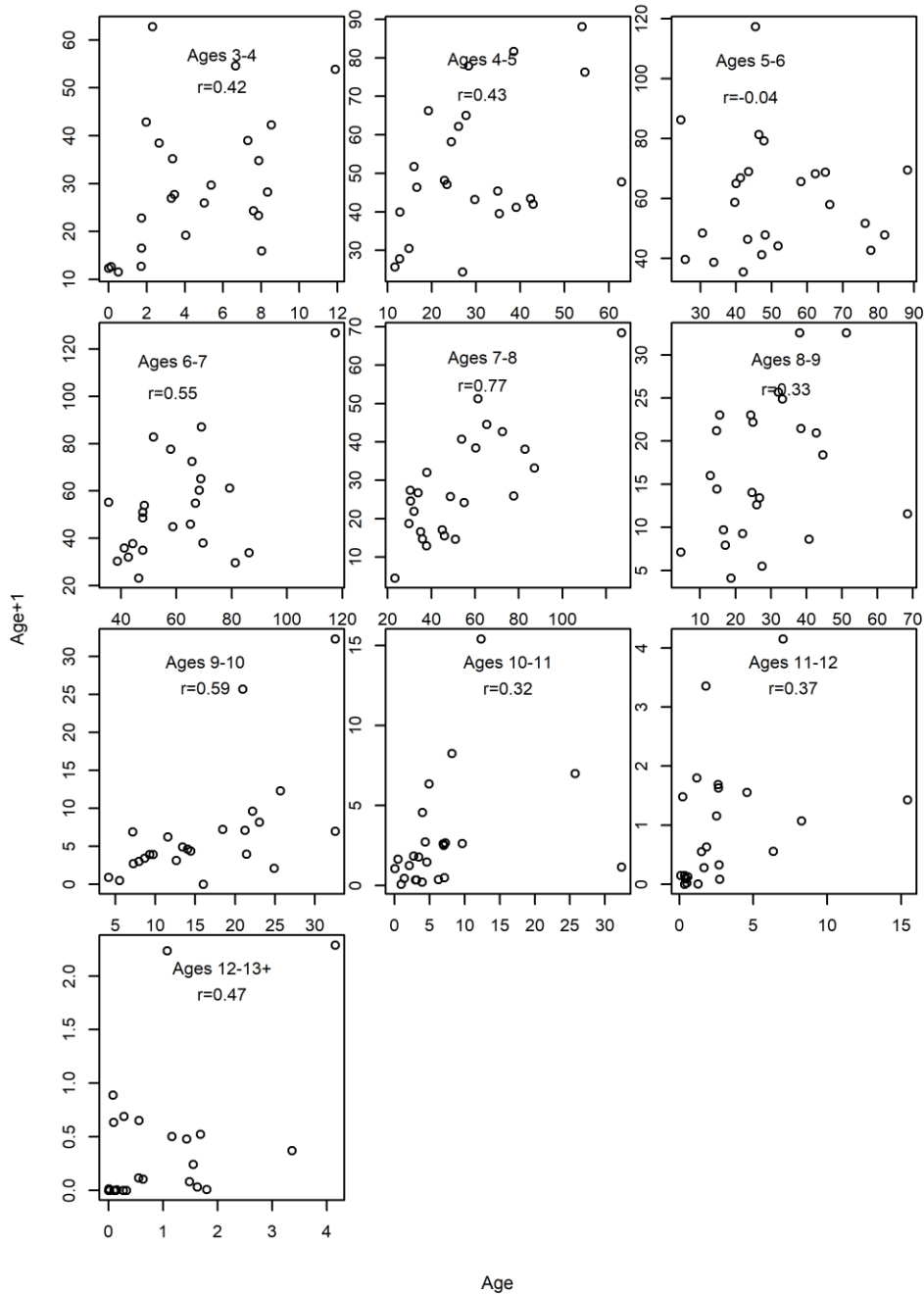


Figure 62. Age-specific abundance of cohorts at a given age and year, as a function of their abundance one year later in the Sentinel longline survey (fall), for 1995-2019. The correlation between the two sets of estimates is indicated in each panel.

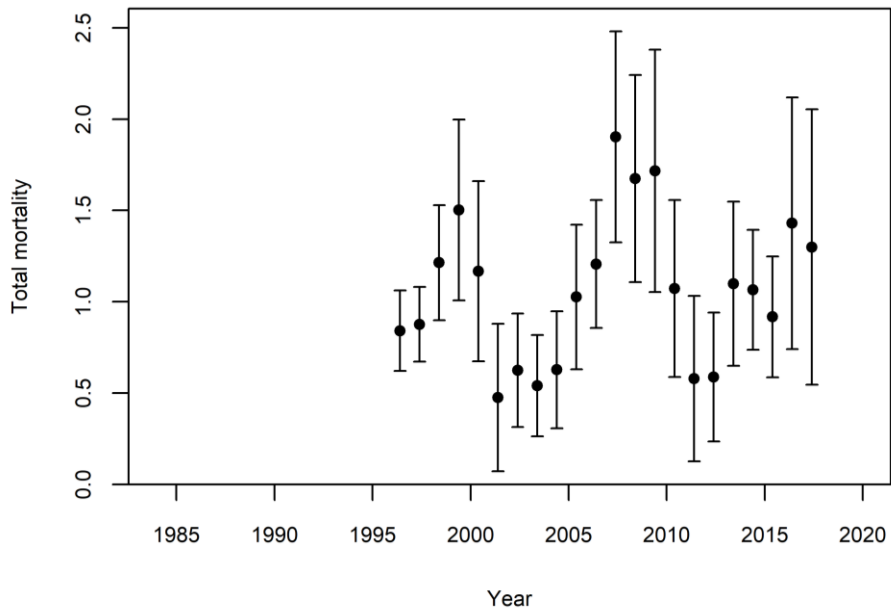


Figure 63. Estimates of total mortality (Z ; with 95% confidence intervals) for ages 8 to 12 from the Sentinel longline survey (zone 1 fall index), 1995-2019.

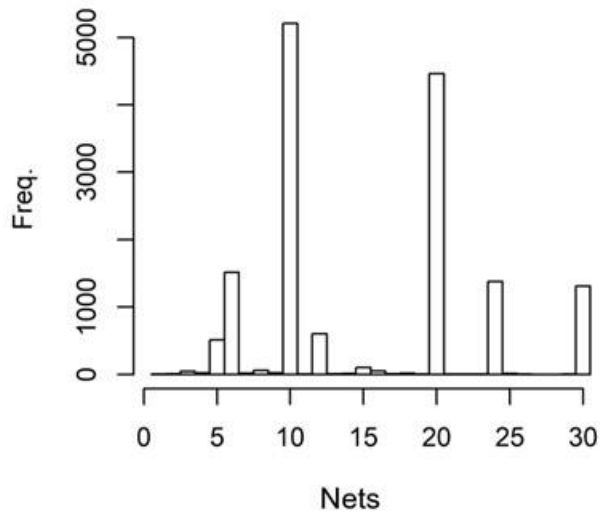


Figure 64. Frequency distribution of the number of nets used for individual hauls in the Sentinel gillnet survey.

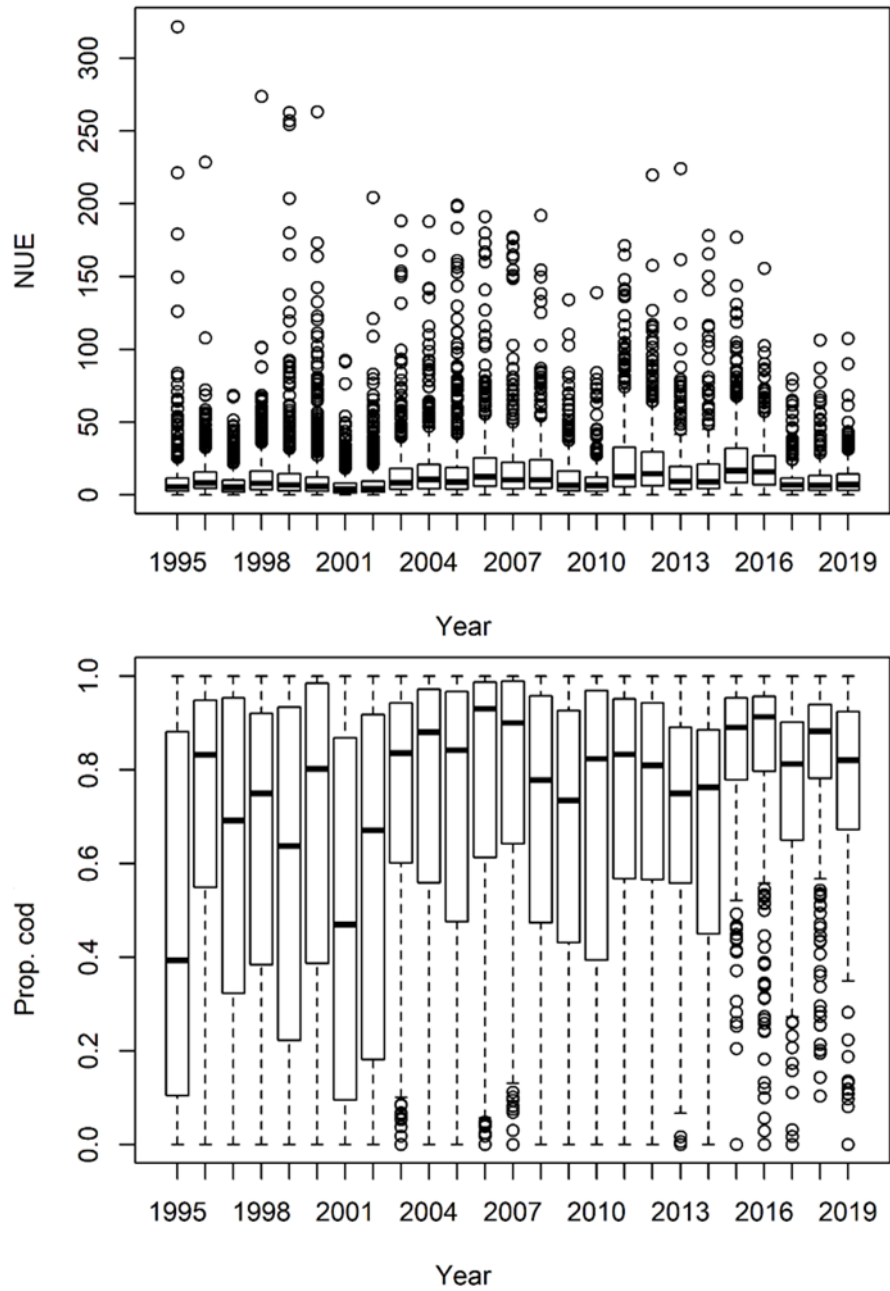


Figure 65. Boxplots of the estimated a) catch (numbers) of fish per haul and net, all species combined, and b) the proportion of cod in the catches, for each year in the Sentinel gillnet survey.

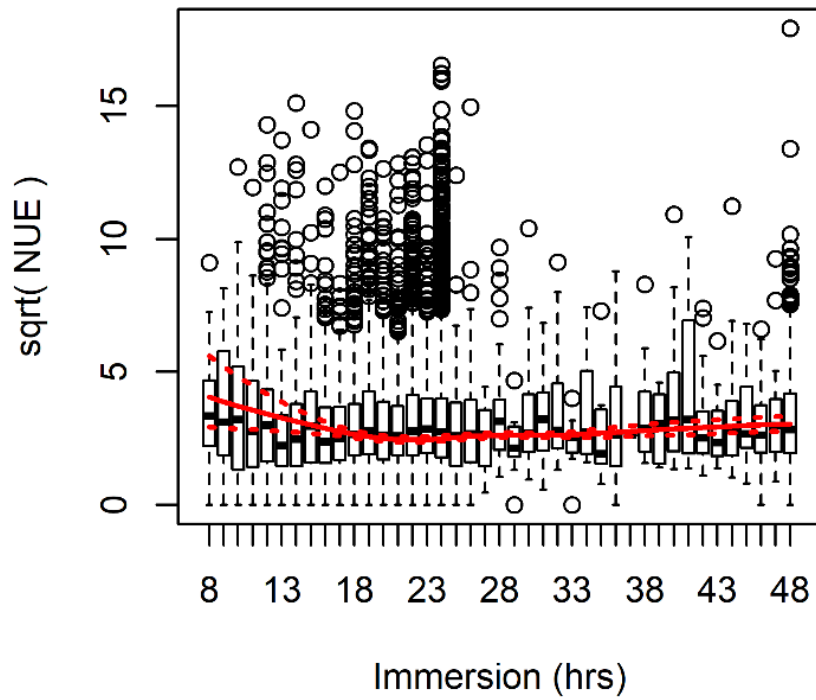


Figure 66. Boxplots of cod catch rates (shown as the square root of numbers per net) in individual hauls as function of gear soak (immersion) time in the Sentinel gillnet survey. The red line is the smoother estimated from a GAMM analysis of catch rates as a function of soak time (dashed lines are 95% confidence intervals on the smoother).

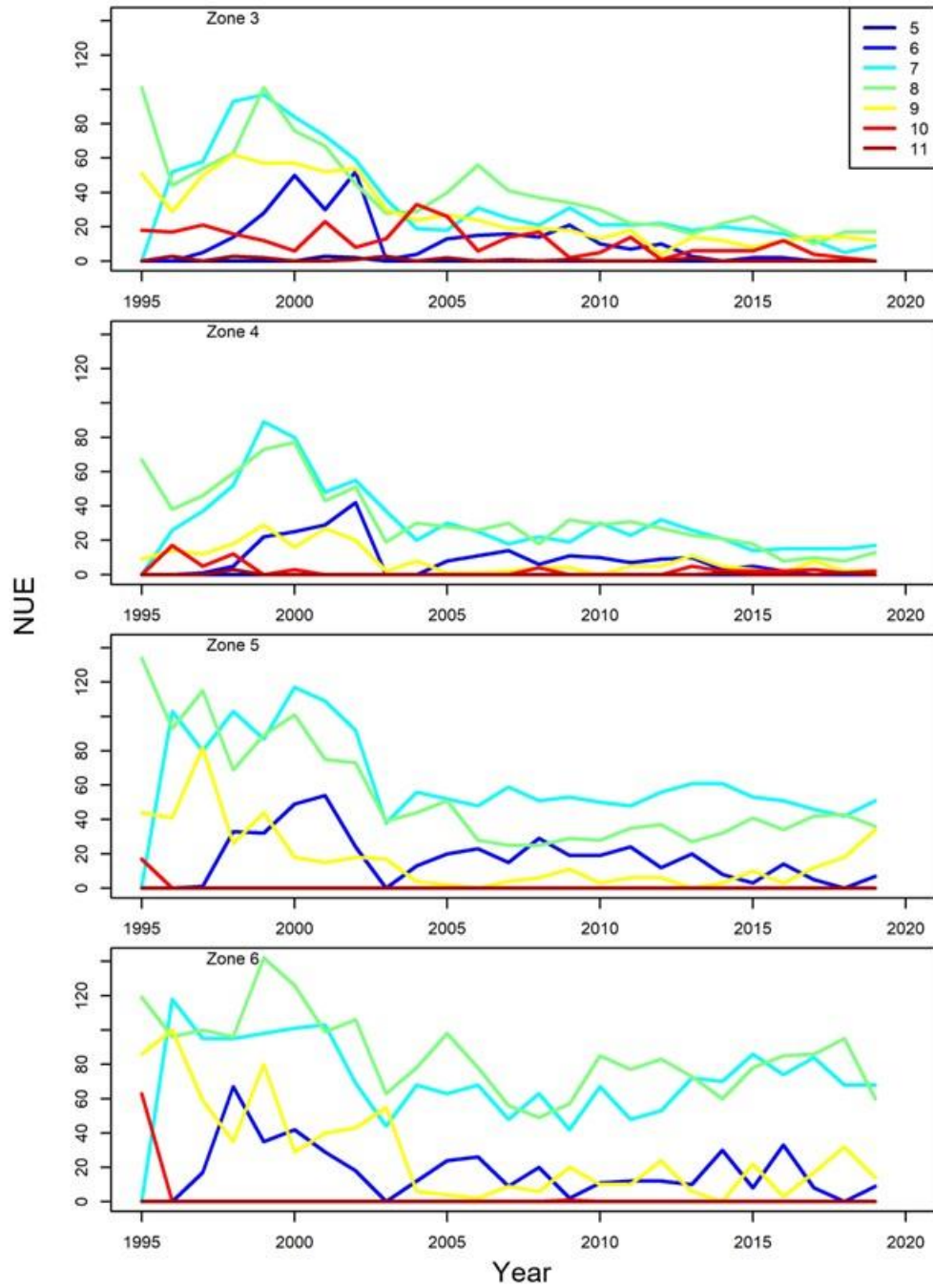


Figure 67. Number of individual hauls by zone (panels) and month (coloured lines) in the Sentinel gillnet survey.

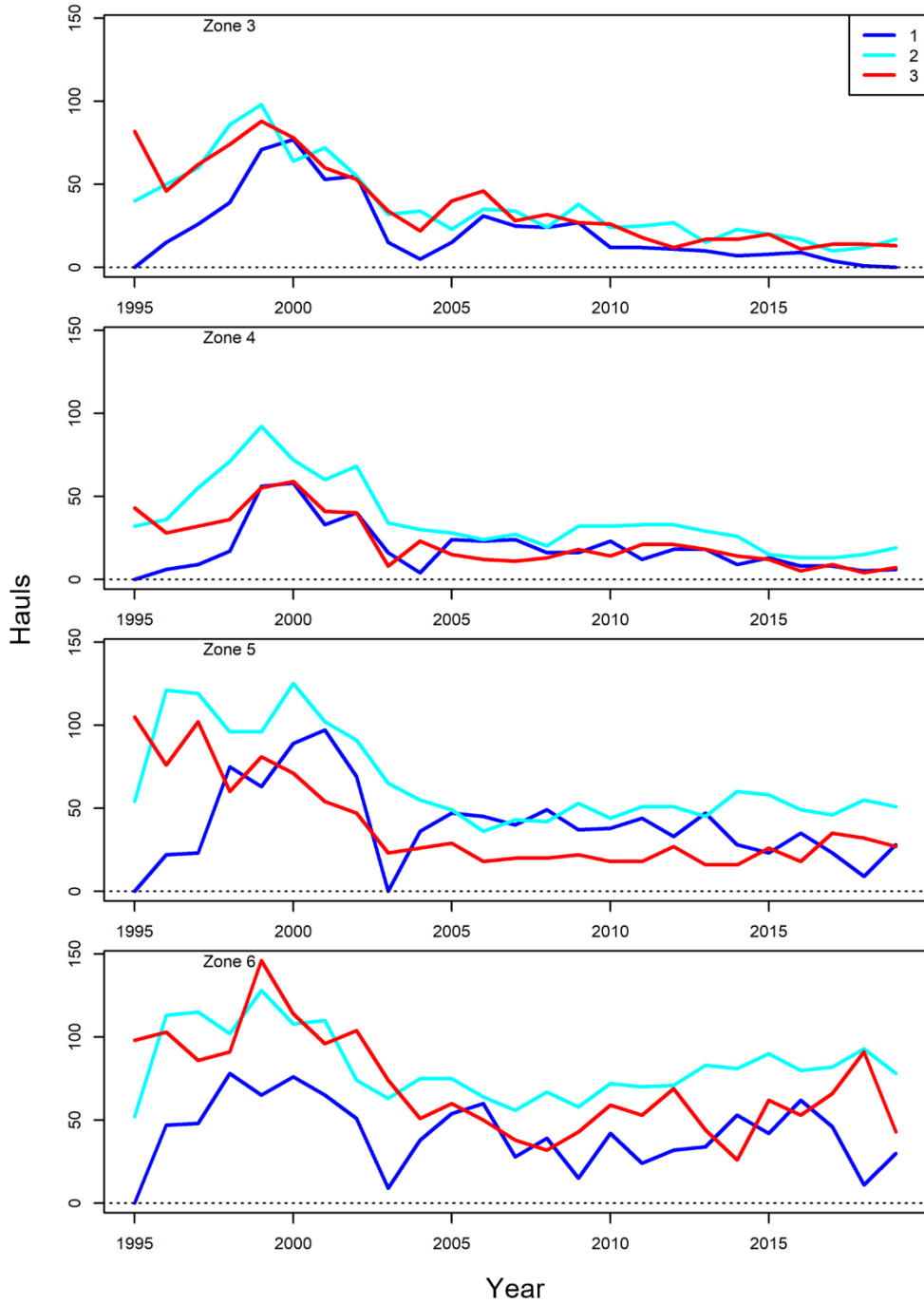


Figure 68. Number of individual hauls by zone (panels) and time block (coloured lines) in the Sentinel gillnet survey. Time blocks were defined based on the day of the year: block 1 [165, 195], block 2 [196, 226], and block 3 [227, 257].

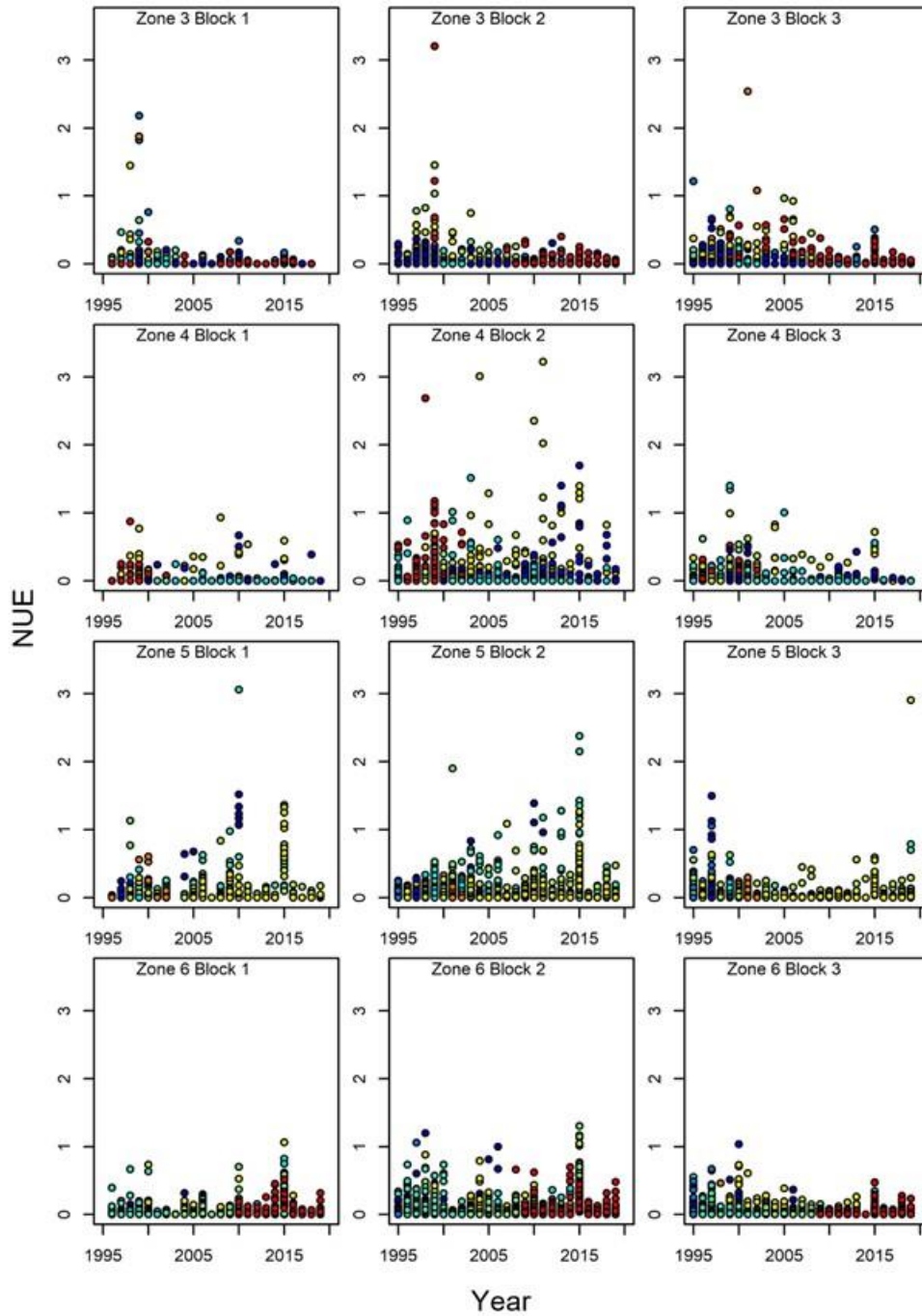


Figure 69. Catch rates of age 4 cod (number per net) in individual hauls by zone (rows), time block (columns) and year in Sentinel gillnet hauls. Colours distinguish individual sites. Time blocks were defined based on the day of the year: block 1 [165, 195], block 2 [196, 226], and block 3 [227, 257].

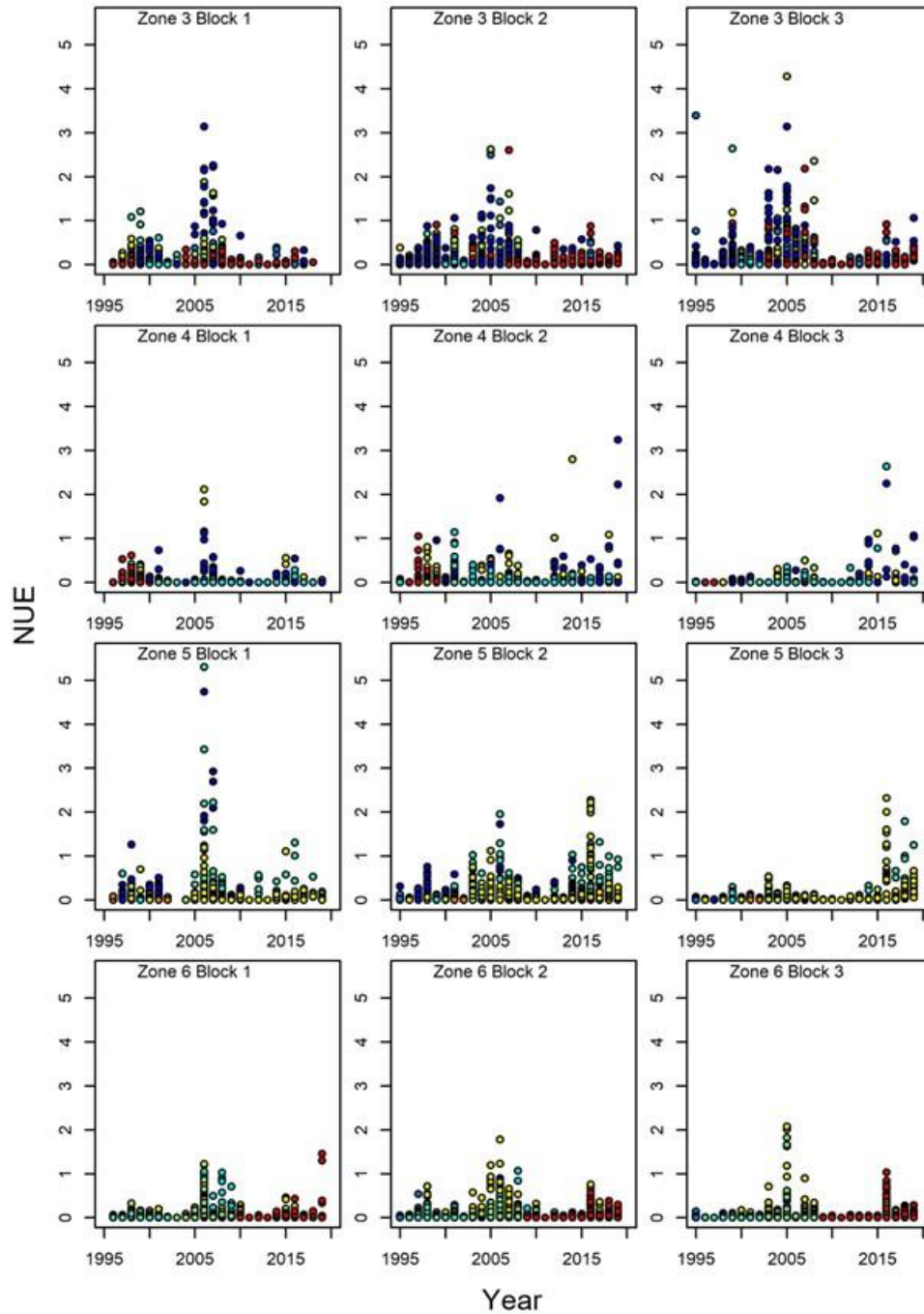


Figure 70. Catch rates of age 12 cod (number per net) in individual hauls by zone (rows), time block (columns) and year in Sentinel gillnet hauls. Colours distinguish individual sites. Time blocks were defined based on the day of the year: block 1 [165, 195], block 2 [196, 226], and block 3 [227, 257].

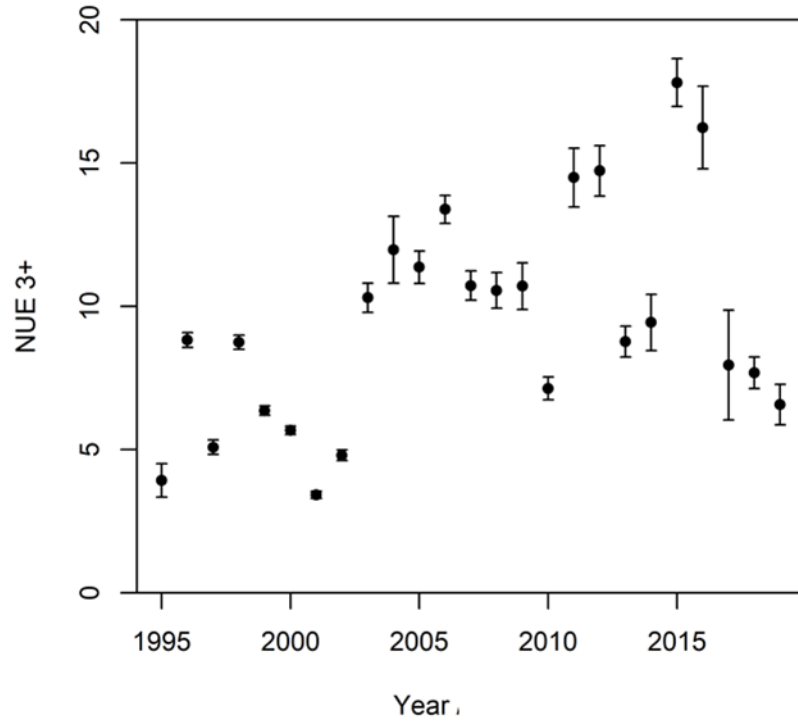


Figure 71. Age aggregated 3-plus abundance index (number per unit effort, NUE; per net) with 95% confidence intervals for the Sentinel gillnet survey summer index, 1995-2019.

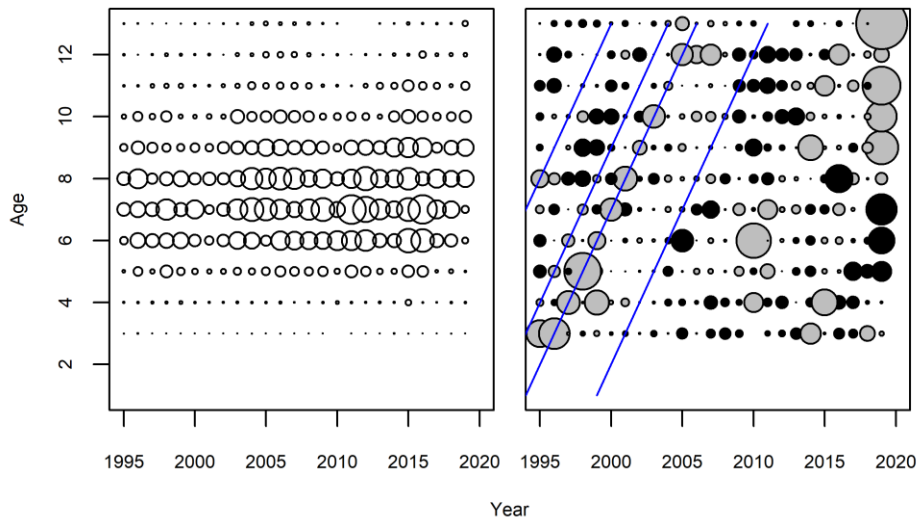


Figure 72. Catch at age in the Sentinel gillnet survey 1995-2019. The left panel shows catch proportional to circle size, while the right panel shows standardized proportions at age and year (SPAY) with grey circles indicating above average catch and black below average. The blue lines indicate some consistently tracked above average cohorts in the RV survey (see Figure 17).

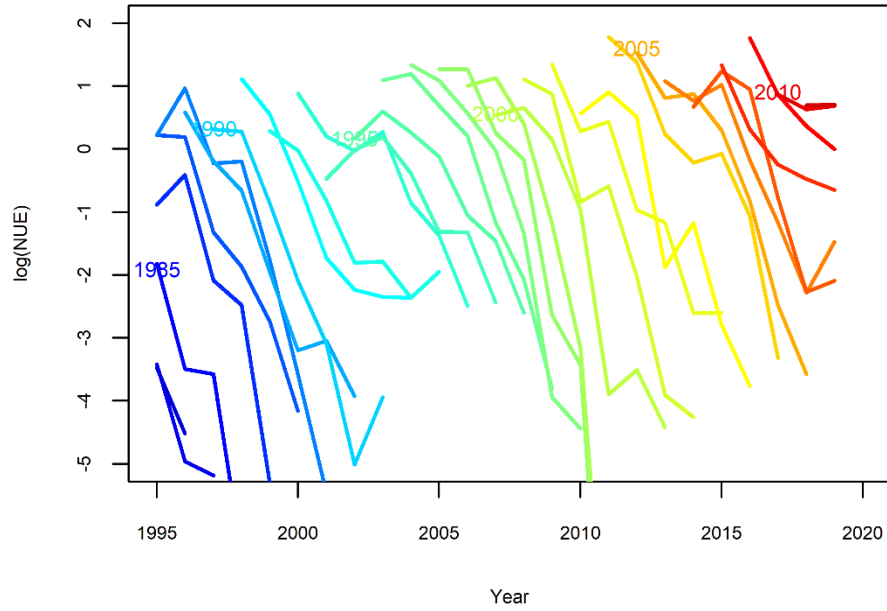


Figure 73. Abundance of individual cohorts (ages 7 to 13+) in the Sentinel gillnet survey catch at age, 1995-2019. Cohorts are identified by birth year for every 5th year.

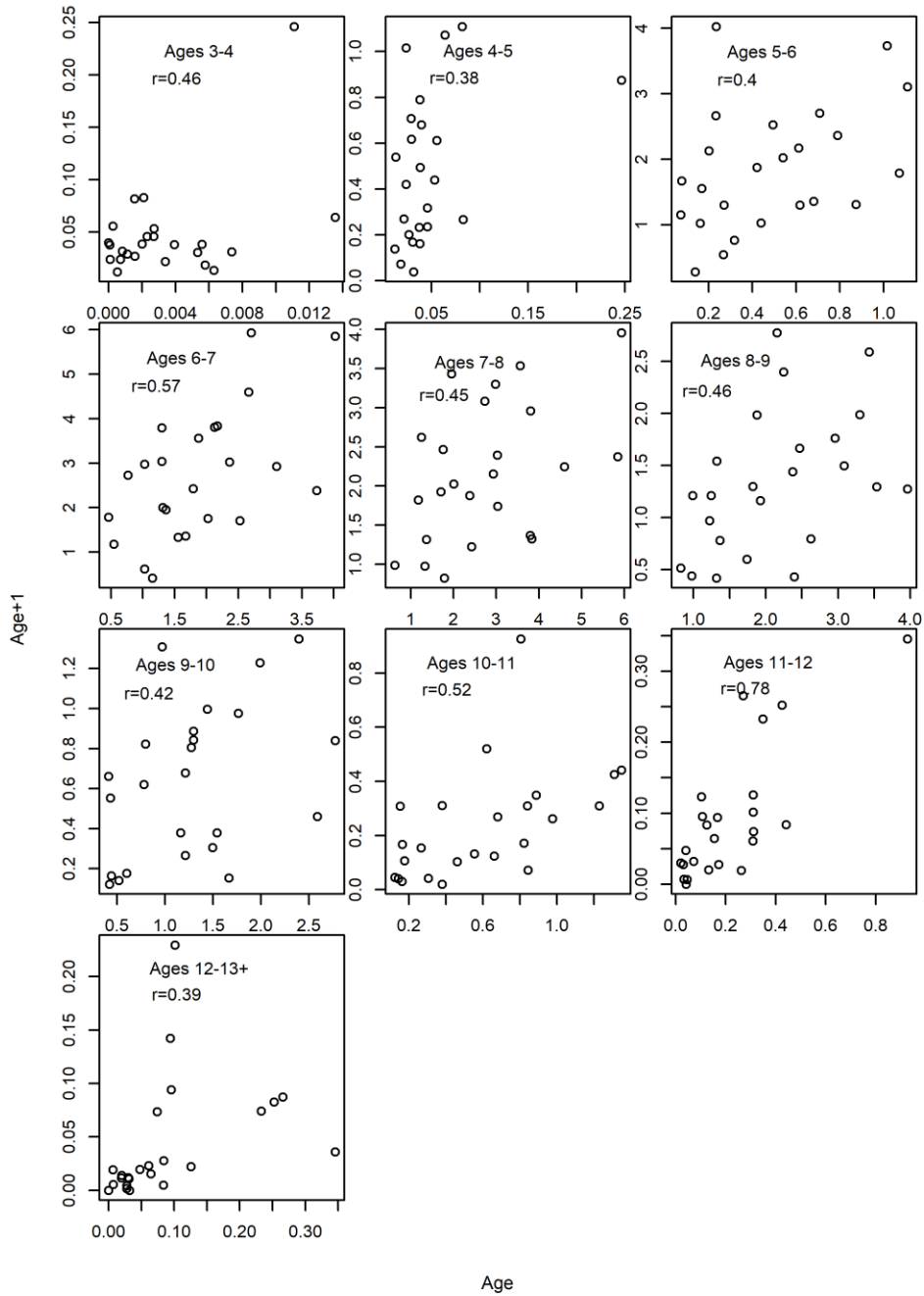


Figure 74. Age-specific abundance of cohorts at a given age and year, as a function of their abundance one year later in the Sentinel gillnet survey, for 1995-2019. The correlation between the two sets of estimates is indicated in each panel.

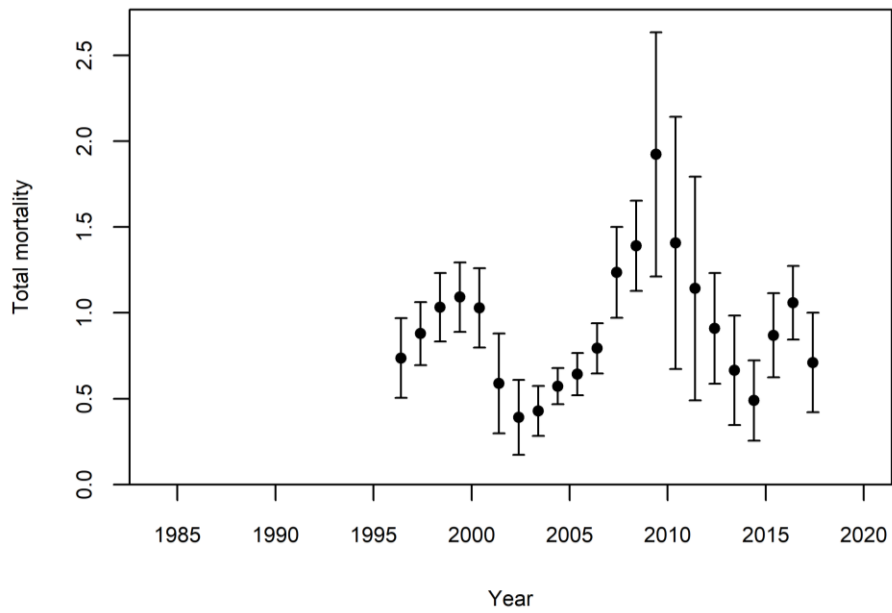


Figure 75. Estimates of total mortality (Z ; with 95% confidence intervals) for ages 8 to 12 from the Sentinel gillnet survey, 1995-2019.

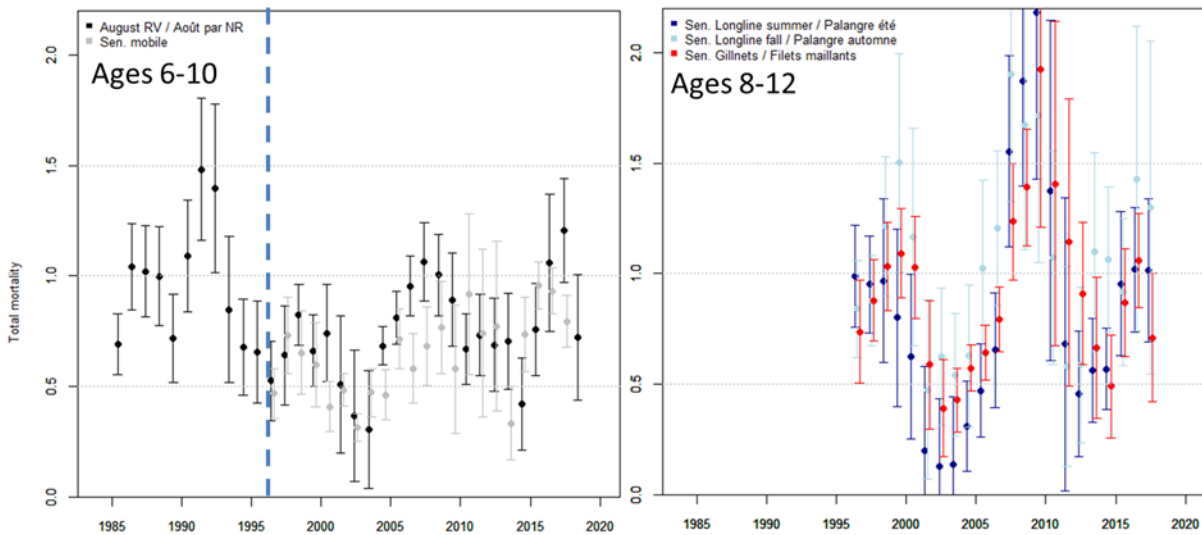


Figure 76. Comparison of total mortality estimates for each of the five principal fishery independent survey indices.

13. APPENDIX I

13.1. SUPPLEMENT FIGURES

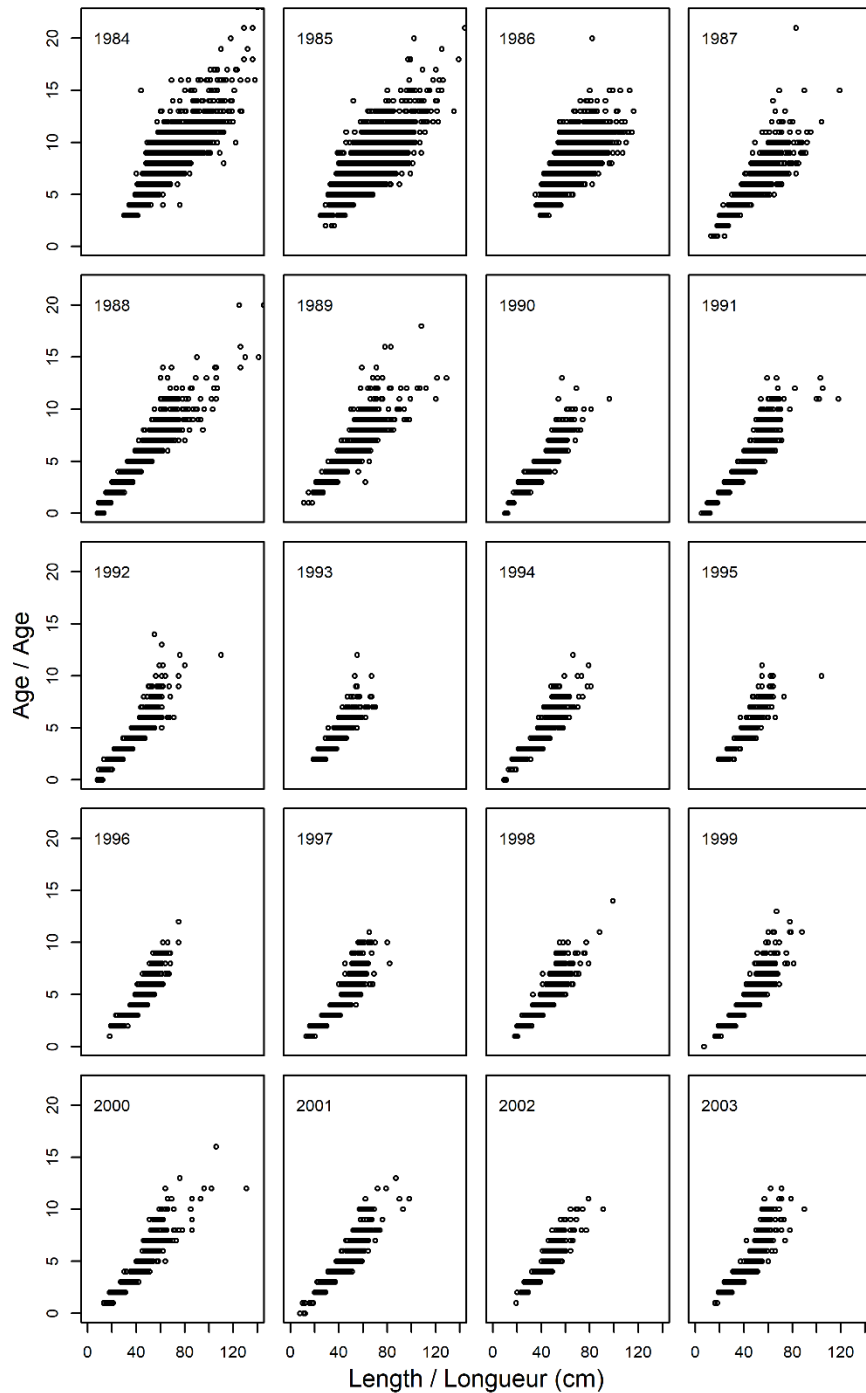


Figure A1. Annual age-length observation in the RV survey.

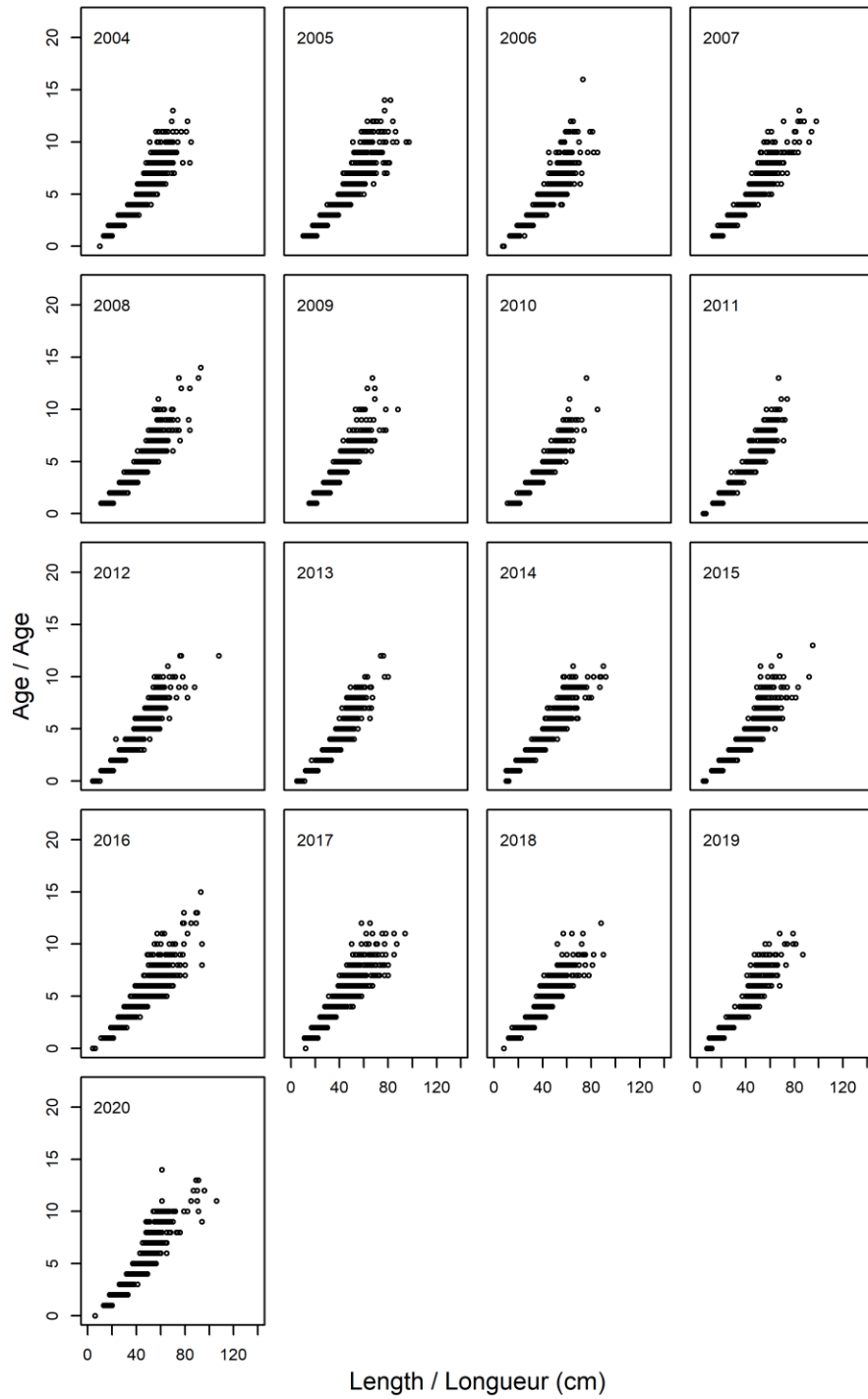


Figure A1 continued.

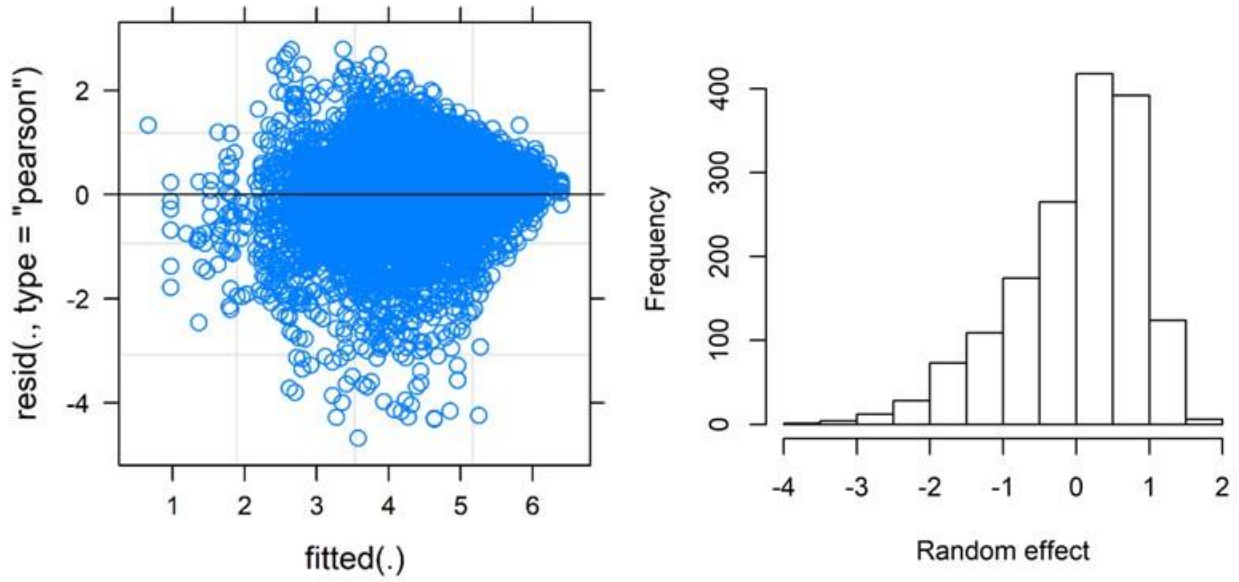


Figure A2. Standardized results and distribution of estimated random effects in the GAMM analysis of catch rates as a function of soak (immersion) time in the Sentinel longline survey.

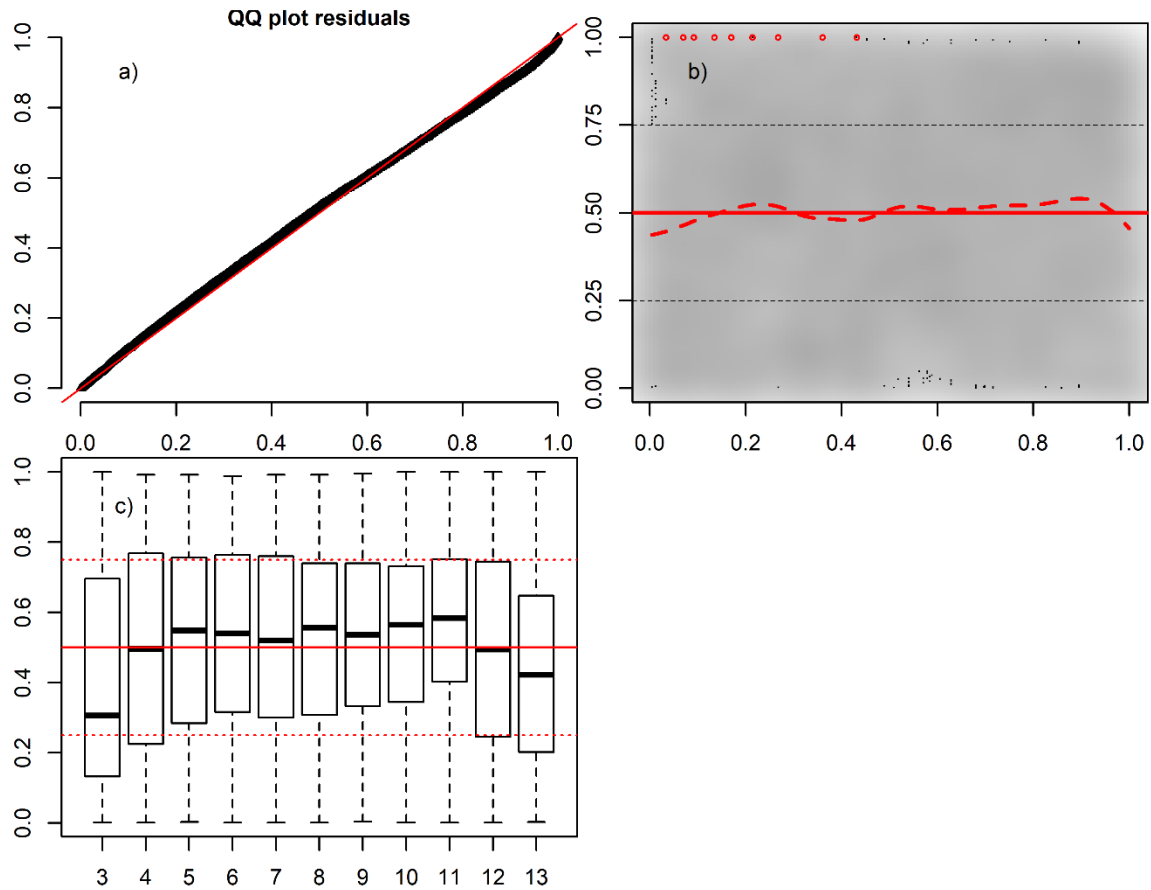


Figure A3. Summary of quantile residuals from model A for the calibration of two hook types in the Sentinel longline program: a) quantile residual Q-Q plots; b) distribution of quantile residuals as a function of rank transformed predicted values, where the solid red line indicates the expected mean value of 0.5, the dashed line is a smooth of the simulated mean value and asterisks indicate significant deviations or outliers; and, c) box plots of quantile residuals as a function of cod age (note that age 13 is actually a 13-plus group), where a correctly fitting model should result in a uniform distribution of residuals for each age, and hence a median (solid black line) at 0.5 and boxes delimited at 0.25 and 0.75.

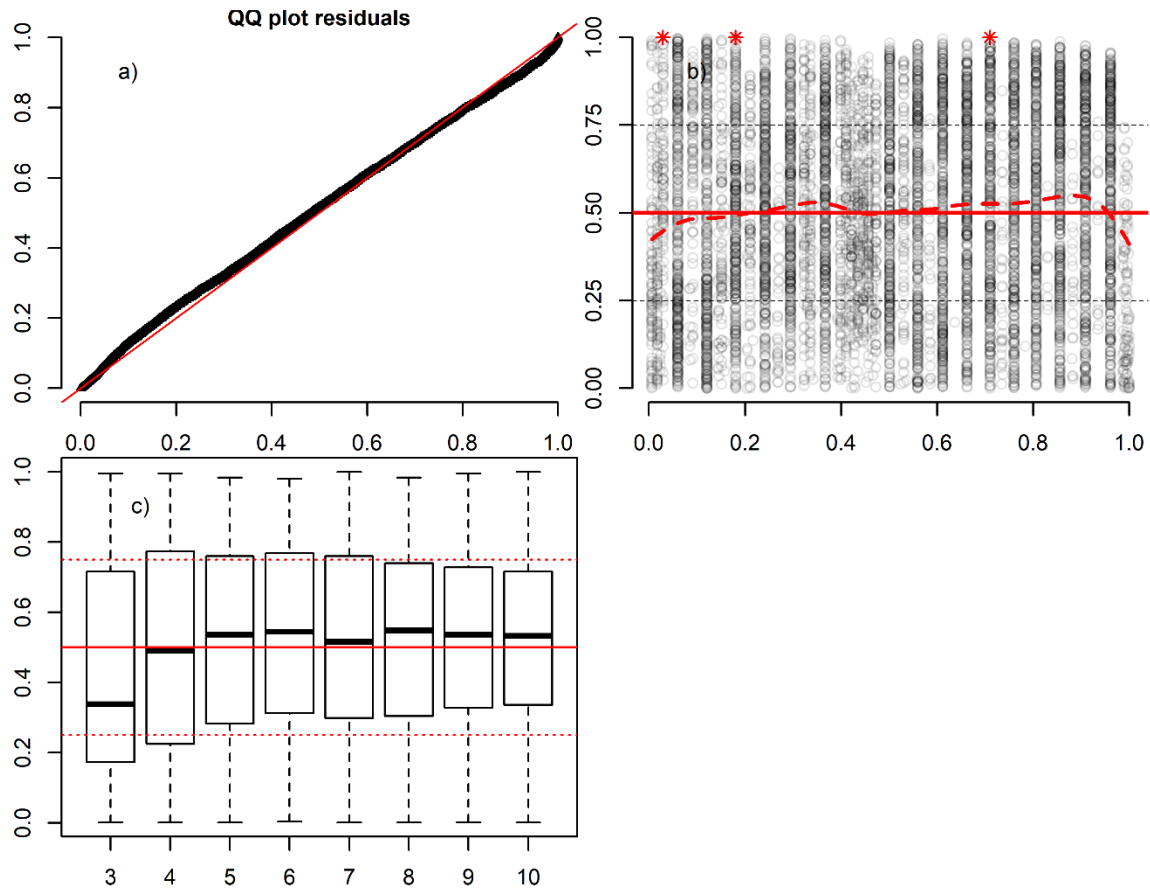


Figure A4. Summary of quantile residuals from model B for the calibration of two hook types in the Sentinel longline program: a) quantile residual Q-Q plots; b) distribution of quantile residuals as a function of rank transformed predicted values, where the solid red line indicates the expected mean value of 0.5, the dashed line is a smooth of the simulated mean value and asterisks indicate significant deviations or outliers; and, c) box plots of quantile residuals as a function of cod age (note that age 13 is actually a 13-plus group), where a correctly fitting model should result in a uniform distribution of residuals for each age, and hence a median (solid black line) at 0.5 and boxes delimited at 0.25 and 0.75.

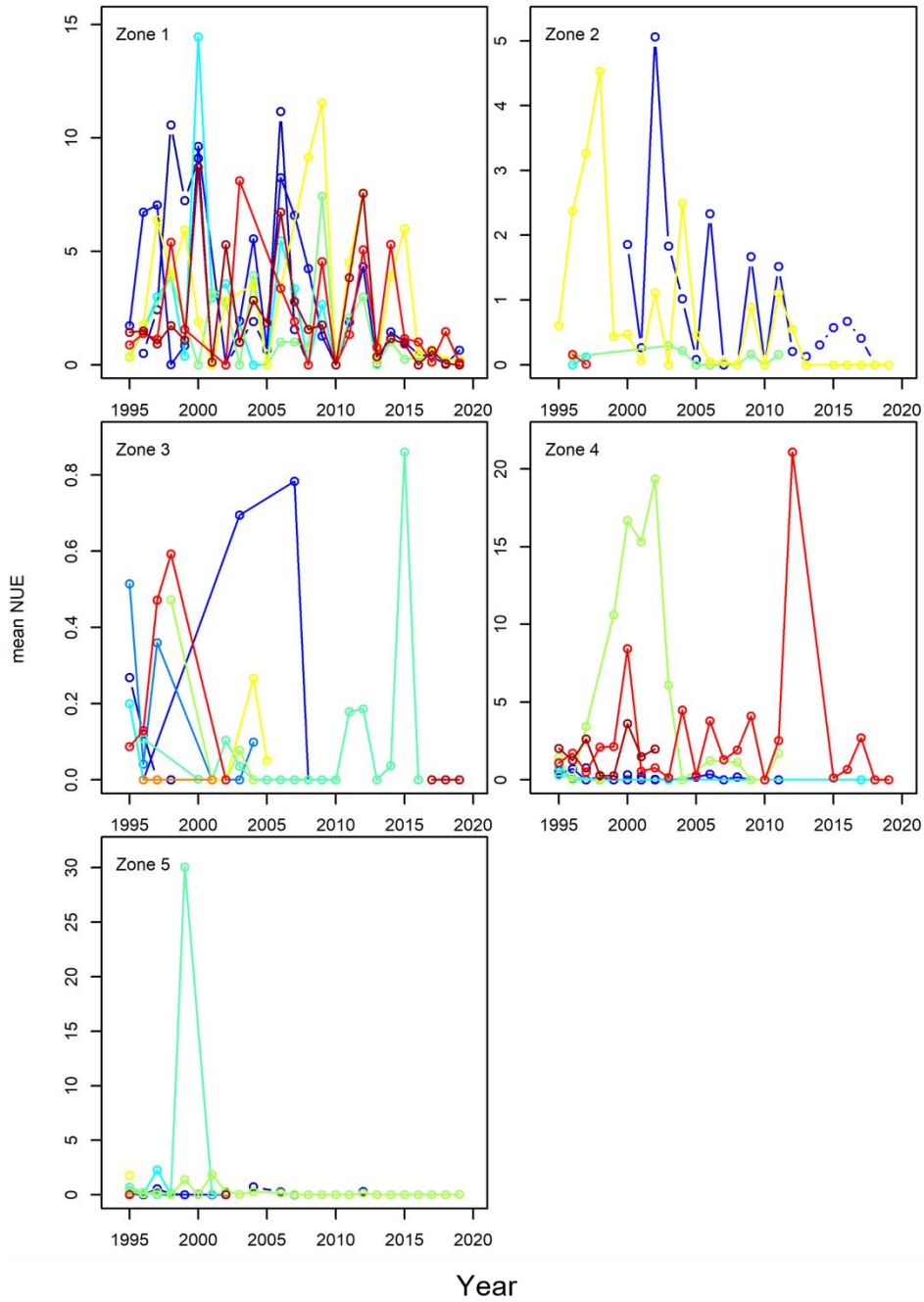


Figure A5. Site-specific annual mean numbers per unit effort (NUE) by zone for cod age 3 in the Sentinel longline program. Values for individual sites are distinguished by colour in each zone.

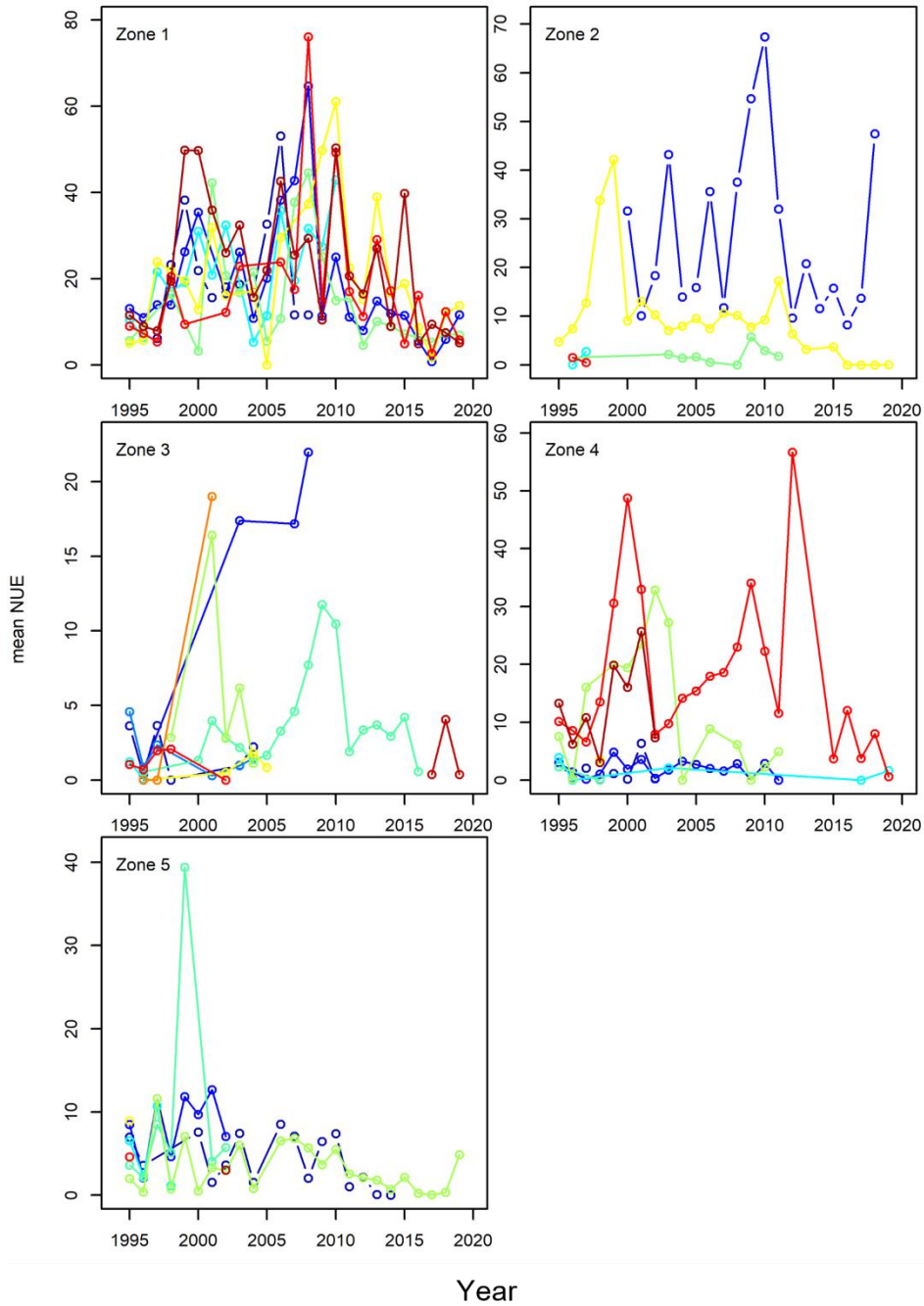


Figure A6. Site-specific annual mean numbers per unit effort (NUE) by zone for cod age 4 in the Sentinel longline program. Values for individual sites are distinguished by colour in each zone.

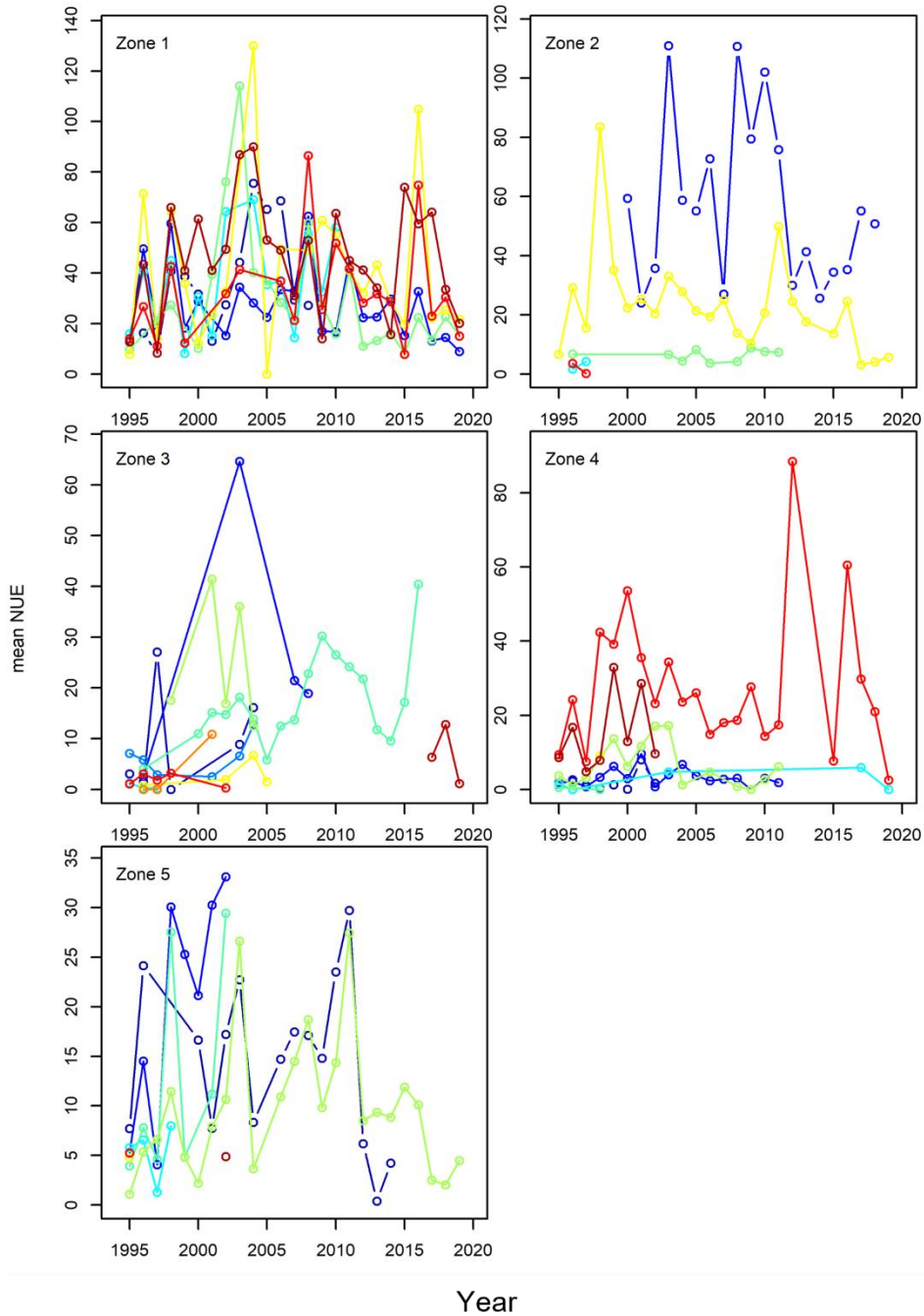


Figure A7. Site-specific annual mean numbers per unit effort (NUE) by zone for cod age 5 in the Sentinel longline program. Values for individual sites are distinguished by colour in each zone.

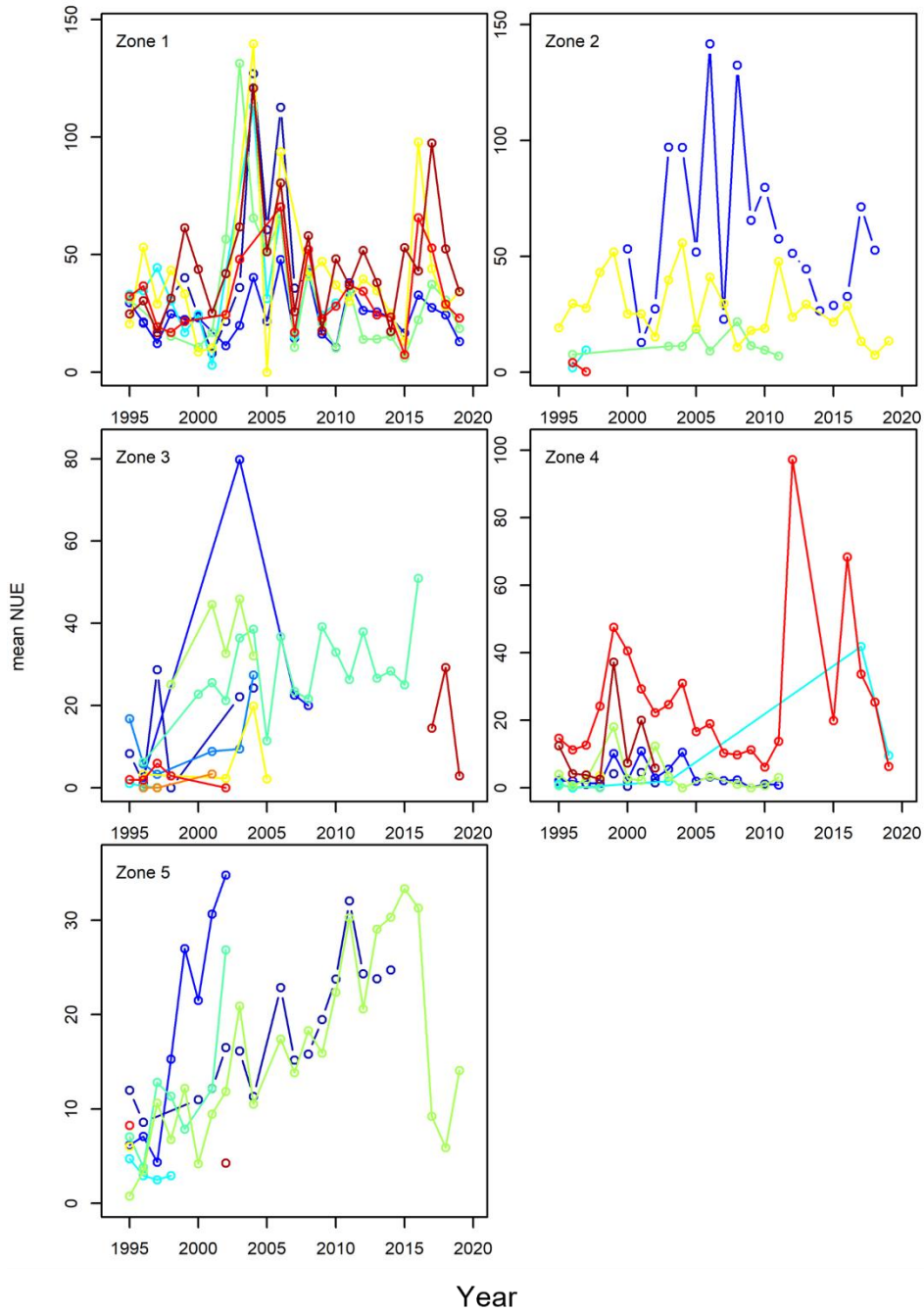


Figure A8. Site-specific annual mean numbers per unit effort (NUE) by zone for cod age 6 in the Sentinel longline program. Values for individual sites are distinguished by colour in each zone.

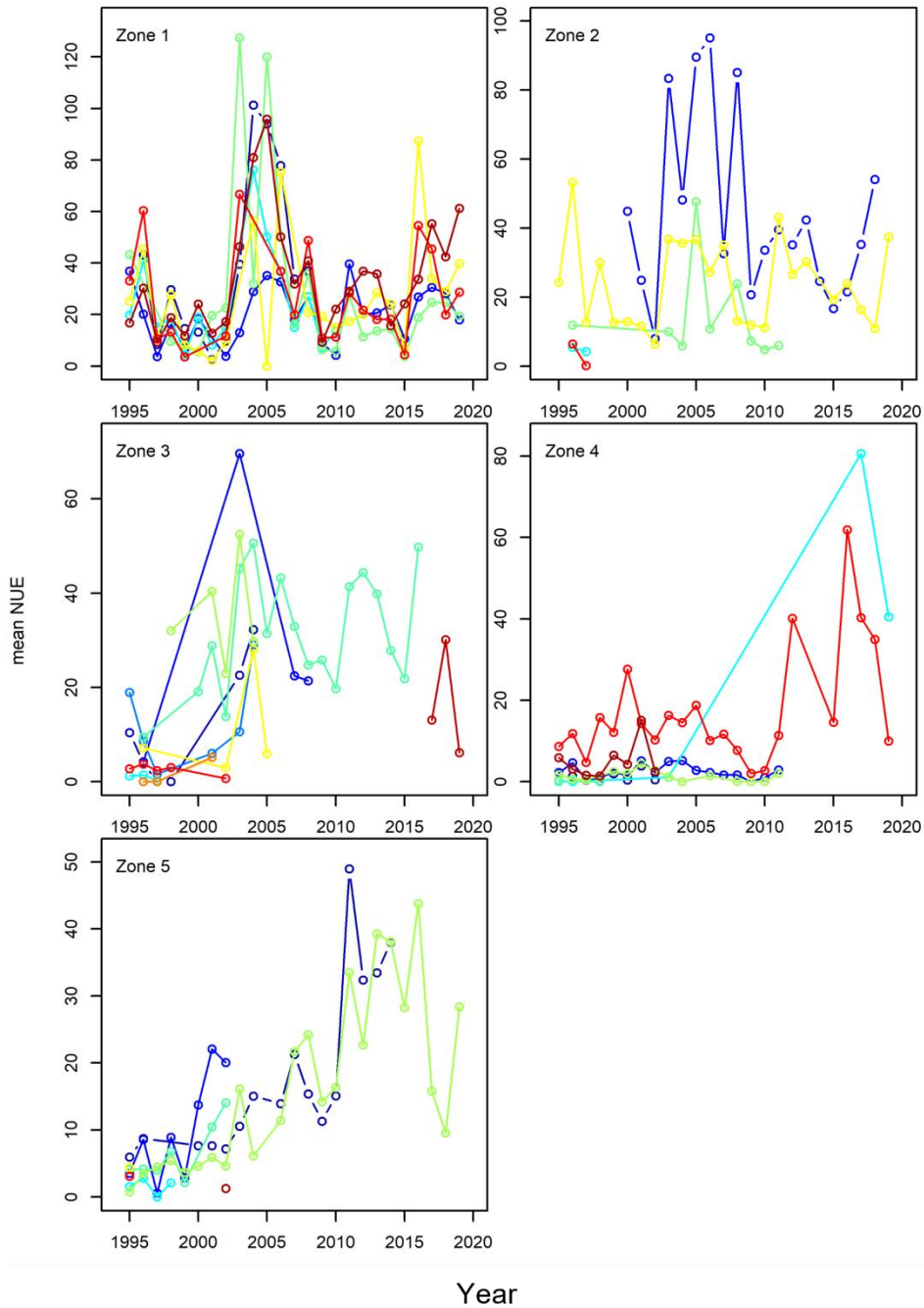


Figure A9. Site-specific annual mean numbers per unit effort (NUE) by zone for cod age 7 in the Sentinel longline program. Values for individual sites are distinguished by colour in each zone.

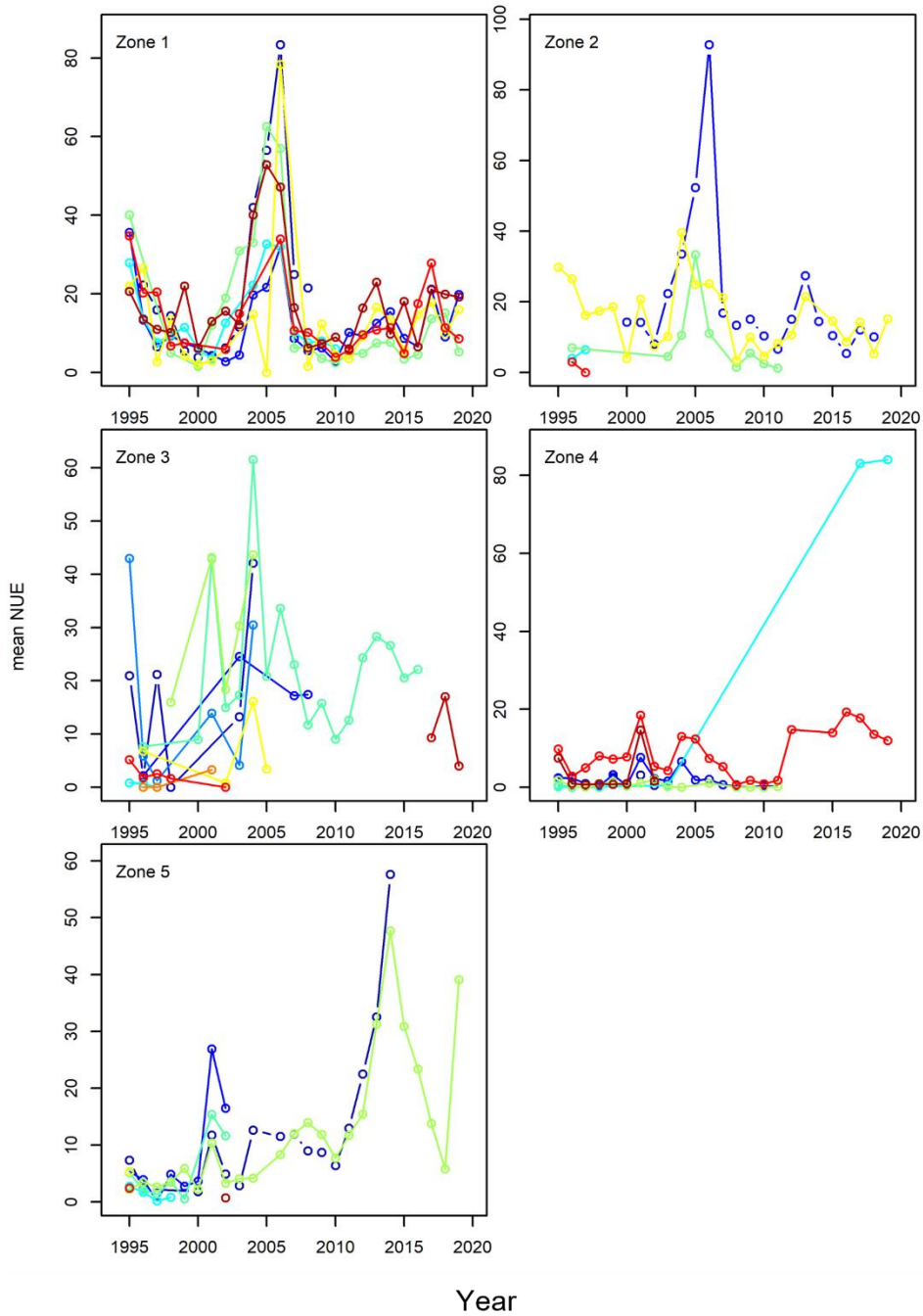


Figure A10. Site-specific annual mean numbers per unit effort (NUE) by zone for cod age 8 in the Sentinel longline program. Values for individual sites are distinguished by colour in each zone.

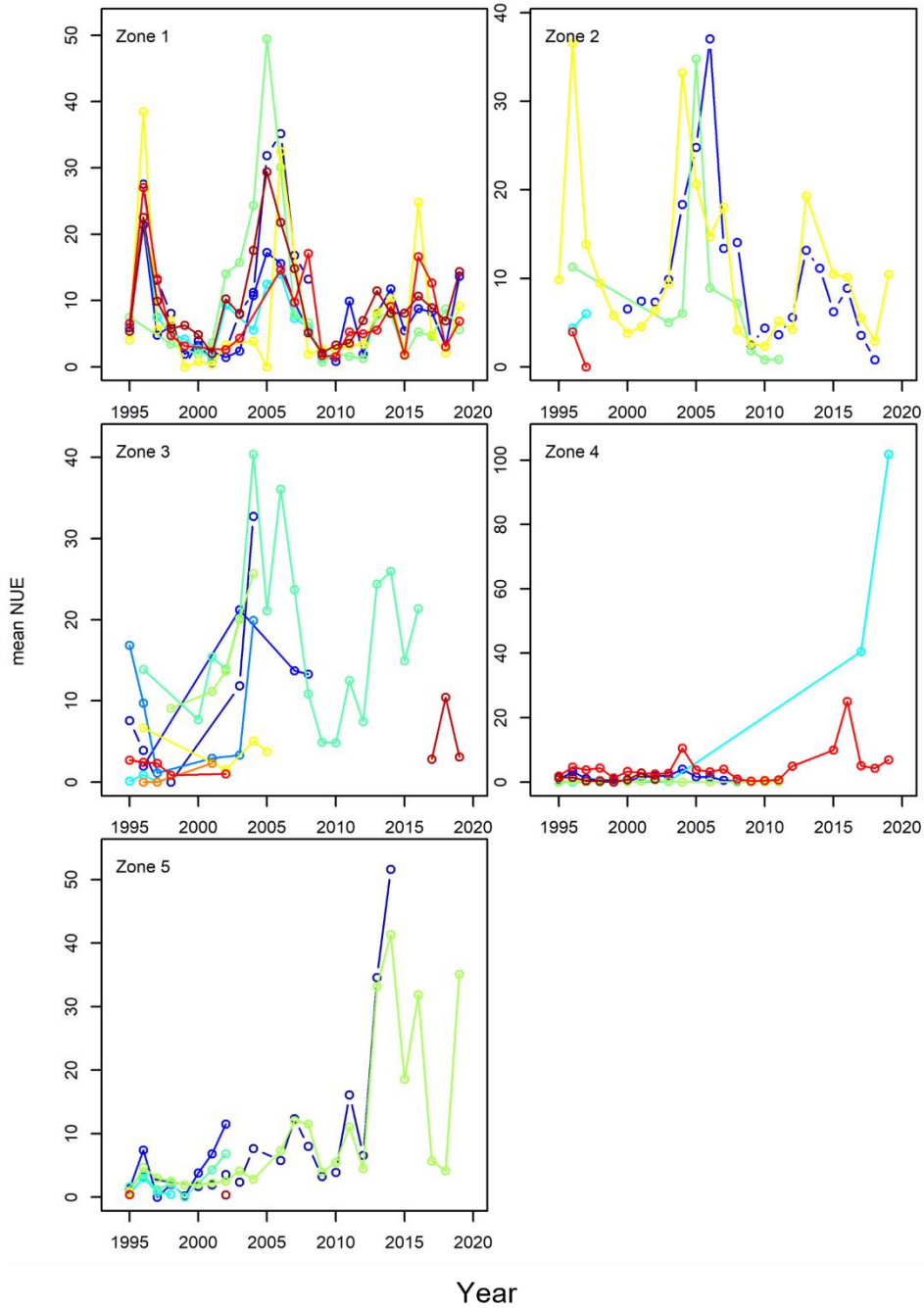


Figure A11. Site-specific annual mean numbers per unit effort (NUE) by zone for cod age 9 in the Sentinel longline program. Values for individual sites are distinguished by colour in each zone.

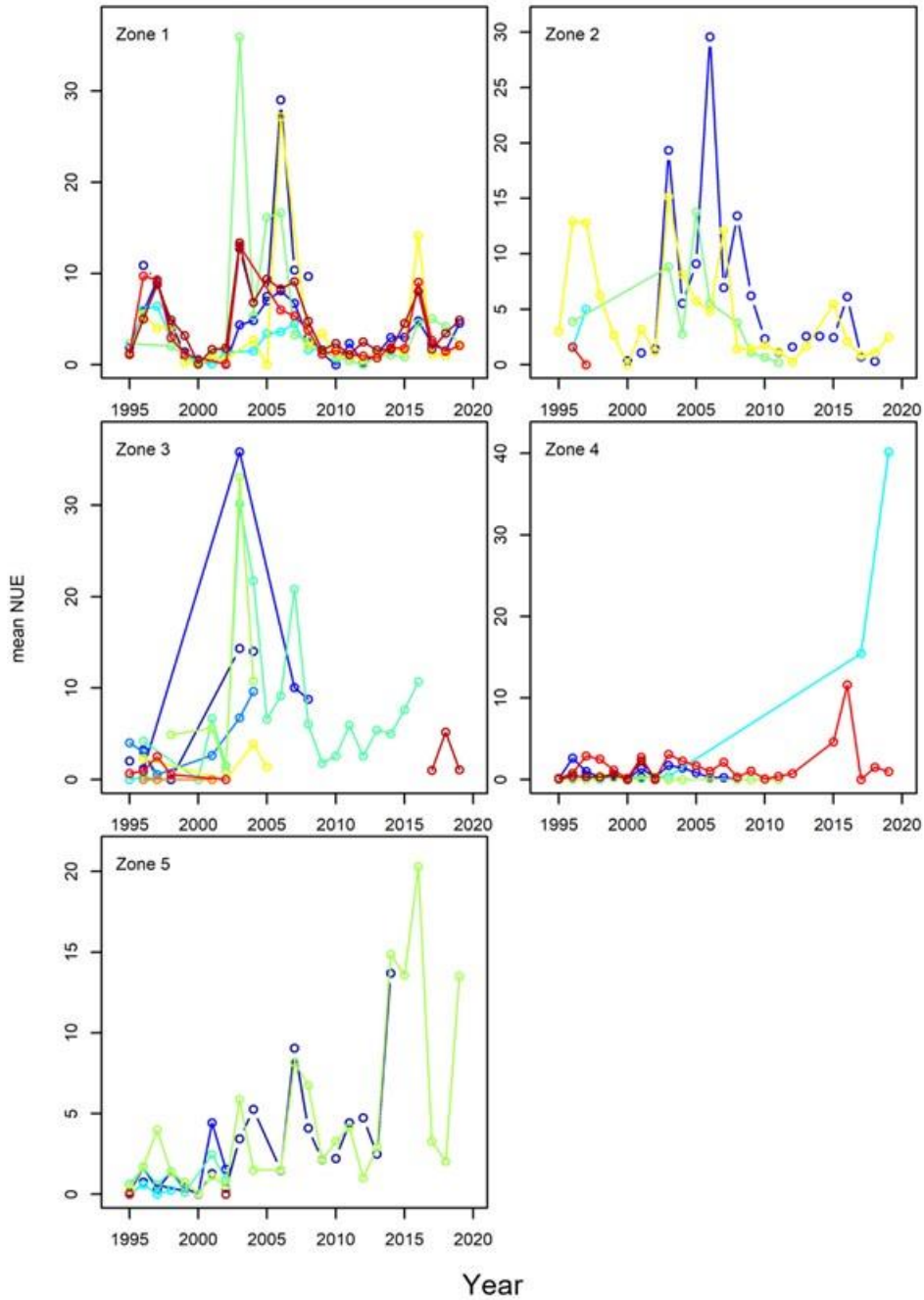


Figure A12. Site-specific annual mean numbers per unit effort (NUE) by zone for cod age 10 in the Sentinel longline program. Values for individual sites are distinguished by colour in each zone.

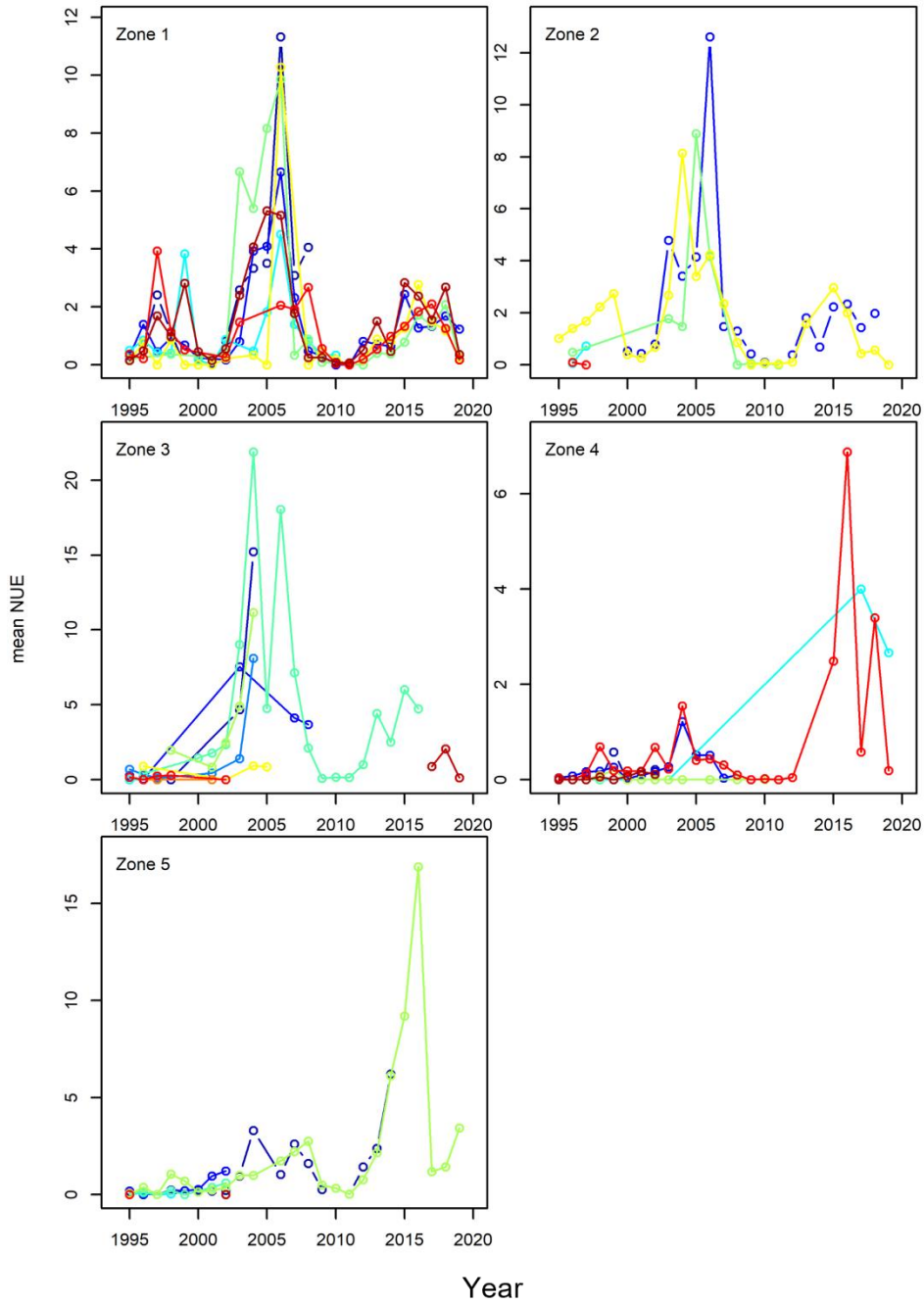


Figure A13. Site-specific annual mean numbers per unit effort (NUE) by zone for cod age 11 in the Sentinel longline program. Values for individual sites are distinguished by colour in each zone.

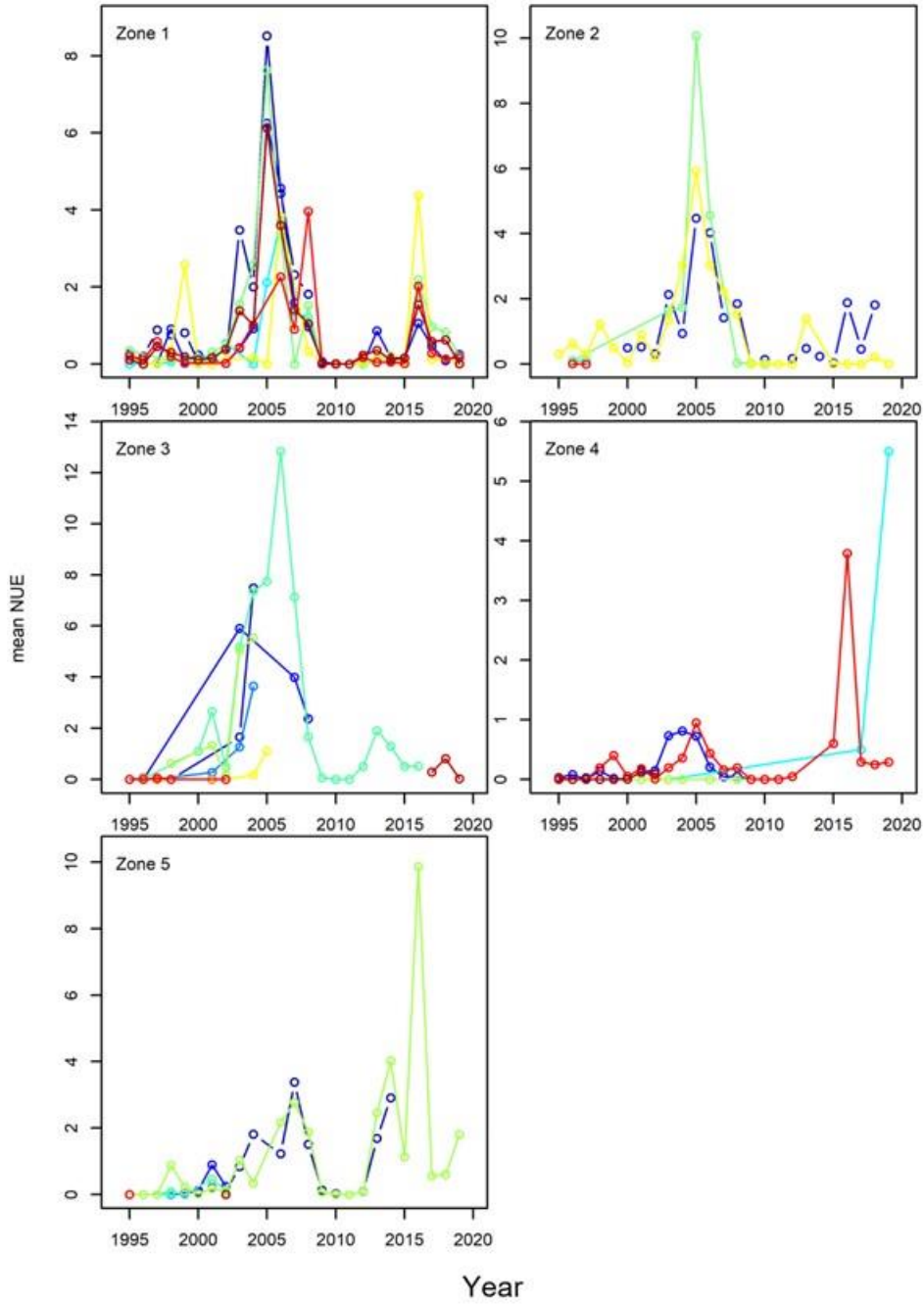


Figure A14. Site-specific annual mean numbers per unit effort (NUE) by zone for cod age 12 in the Sentinel longline program. Values for individual sites are distinguished by colour in each zone.

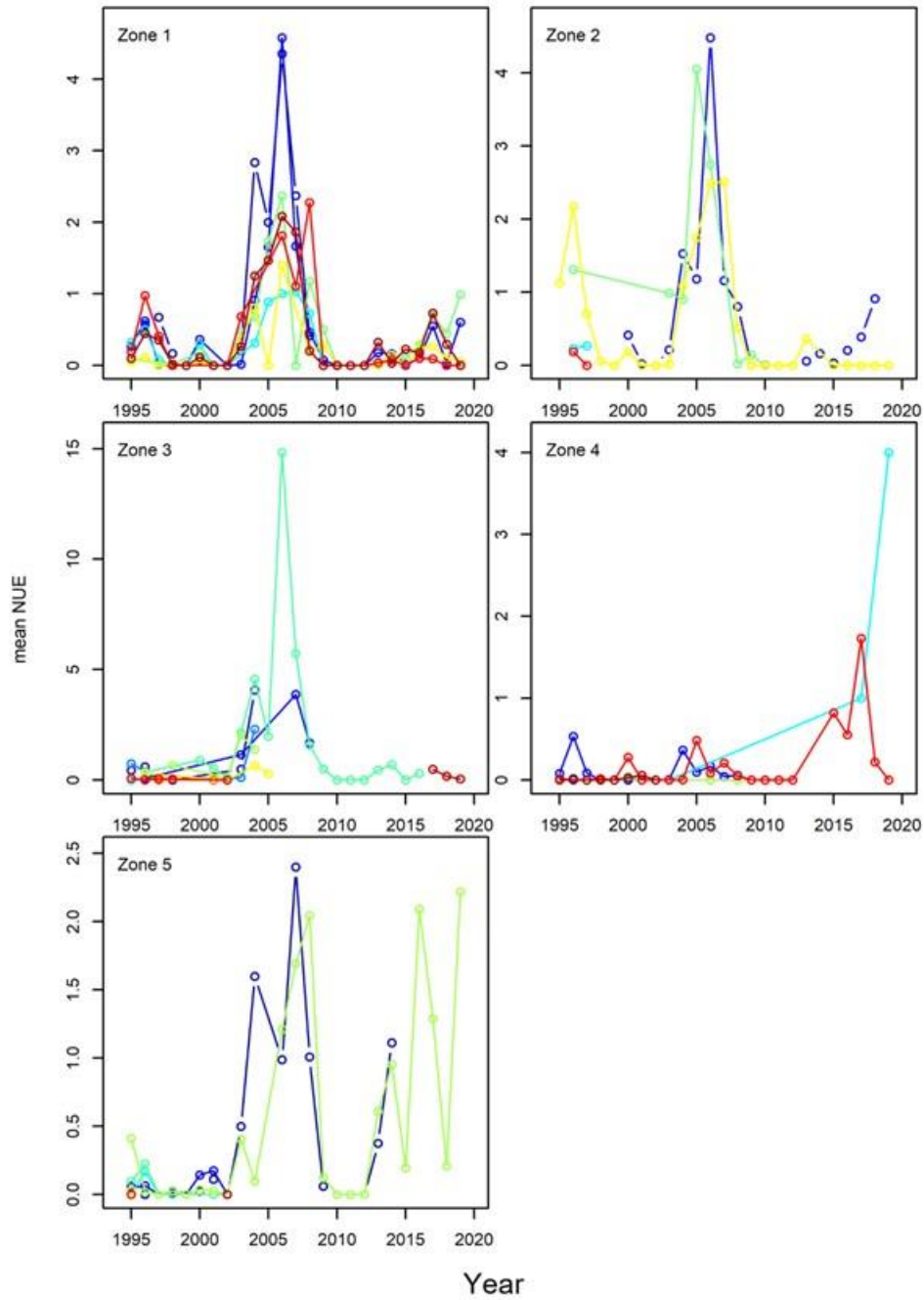


Figure A15. Site-specific annual mean numbers per unit effort (NUE) by zone for cod age 13+ in the Sentinel longline program. Values for individual sites are distinguished by colour in each zone.

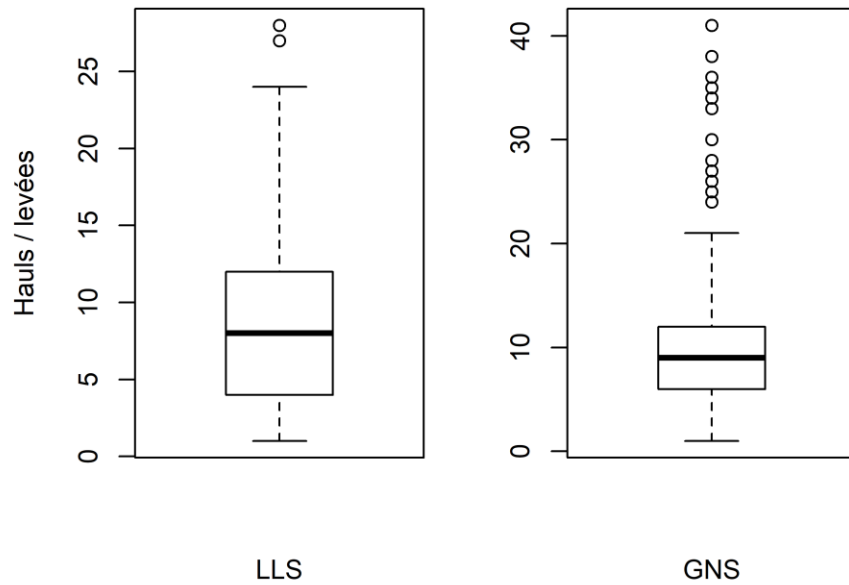


Figure A16. Boxplots of the number of hauls per site and stratum in the summer Sentinel longline (LLS) and gillnet (GNS) data used to generate abundance indices.

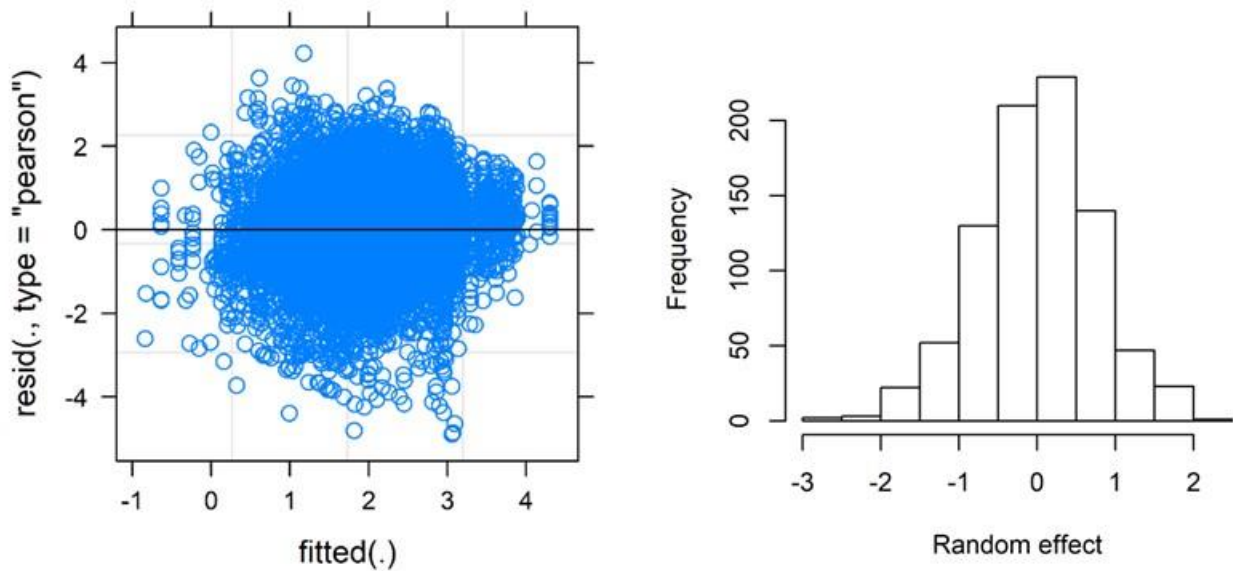


Figure A17. Standardized results and distribution of estimated random effects in the GAMM analysis of catch rates as a function of soak (immersion) time in the Sentinel gillnet survey.

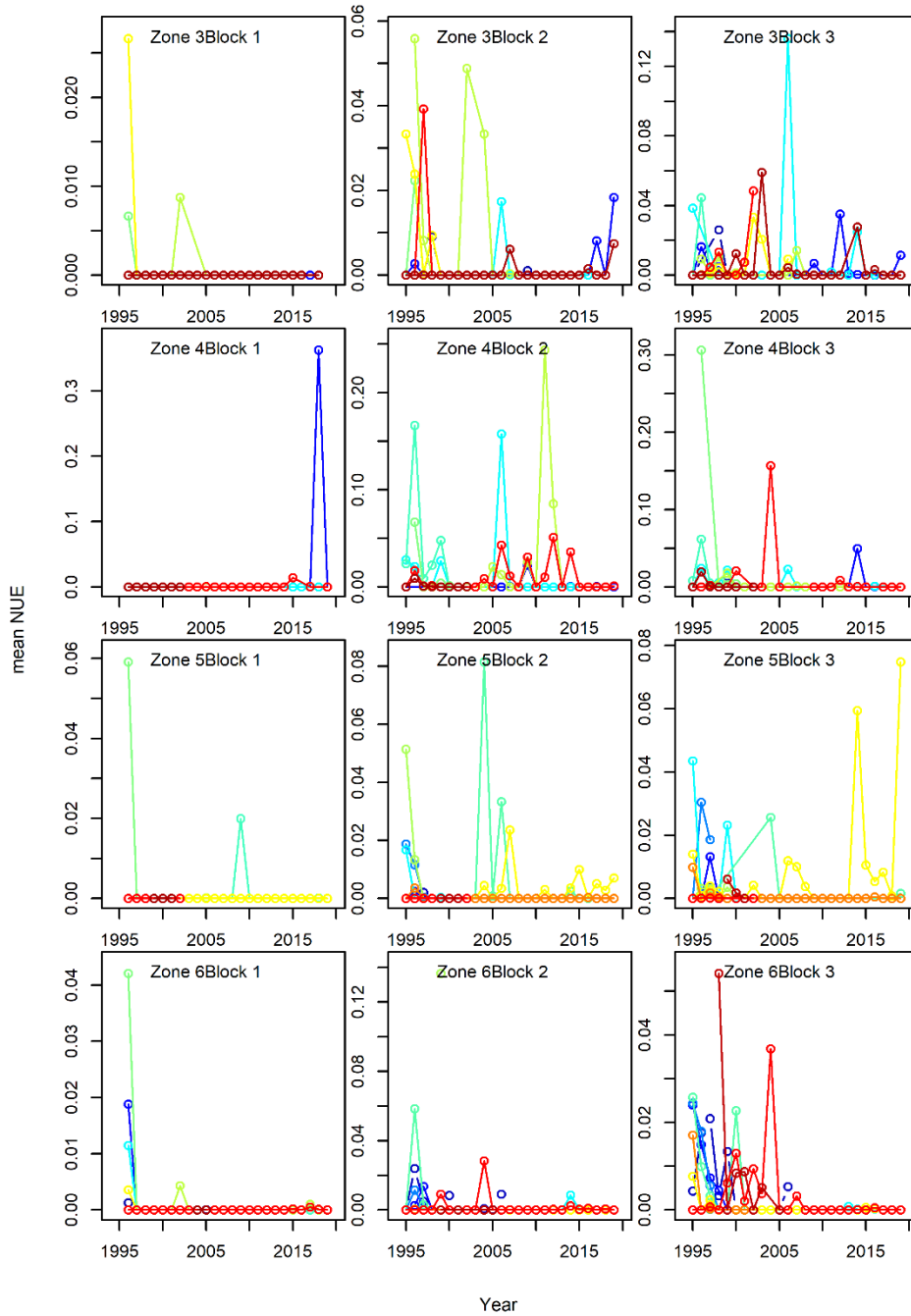


Figure A18. Site-specific annual mean numbers per unit effort (NUE) by zone and seasonal block for cod age 3 in the Sentinel gillnet program. Values for individual sites are distinguished by colour in each zone and block.

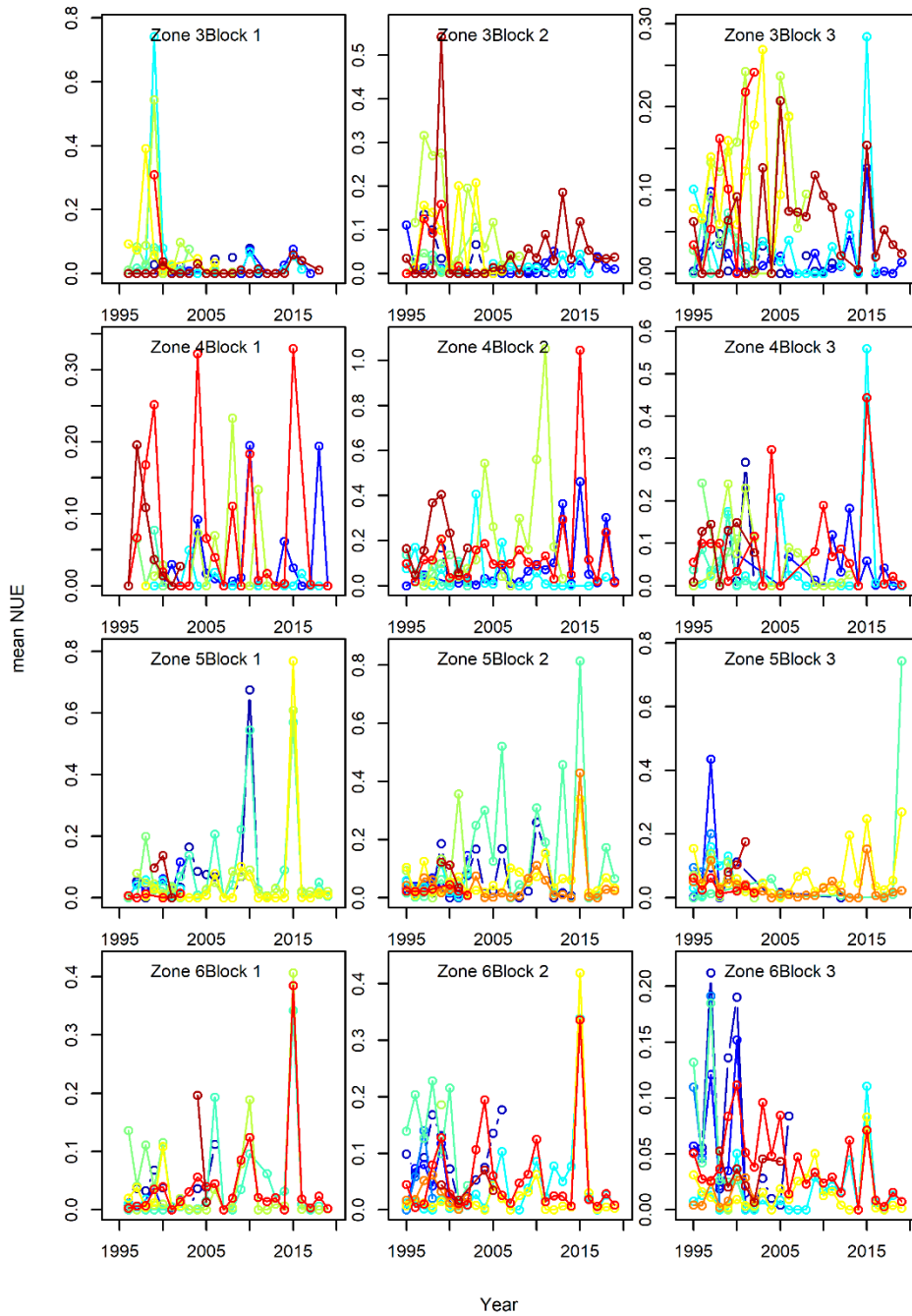


Figure A19. Site-specific annual mean numbers per unit effort (NUE) by zone and seasonal block for cod age 4 in the Sentinel gillnet program. Values for individual sites are distinguished by colour in each zone and block.

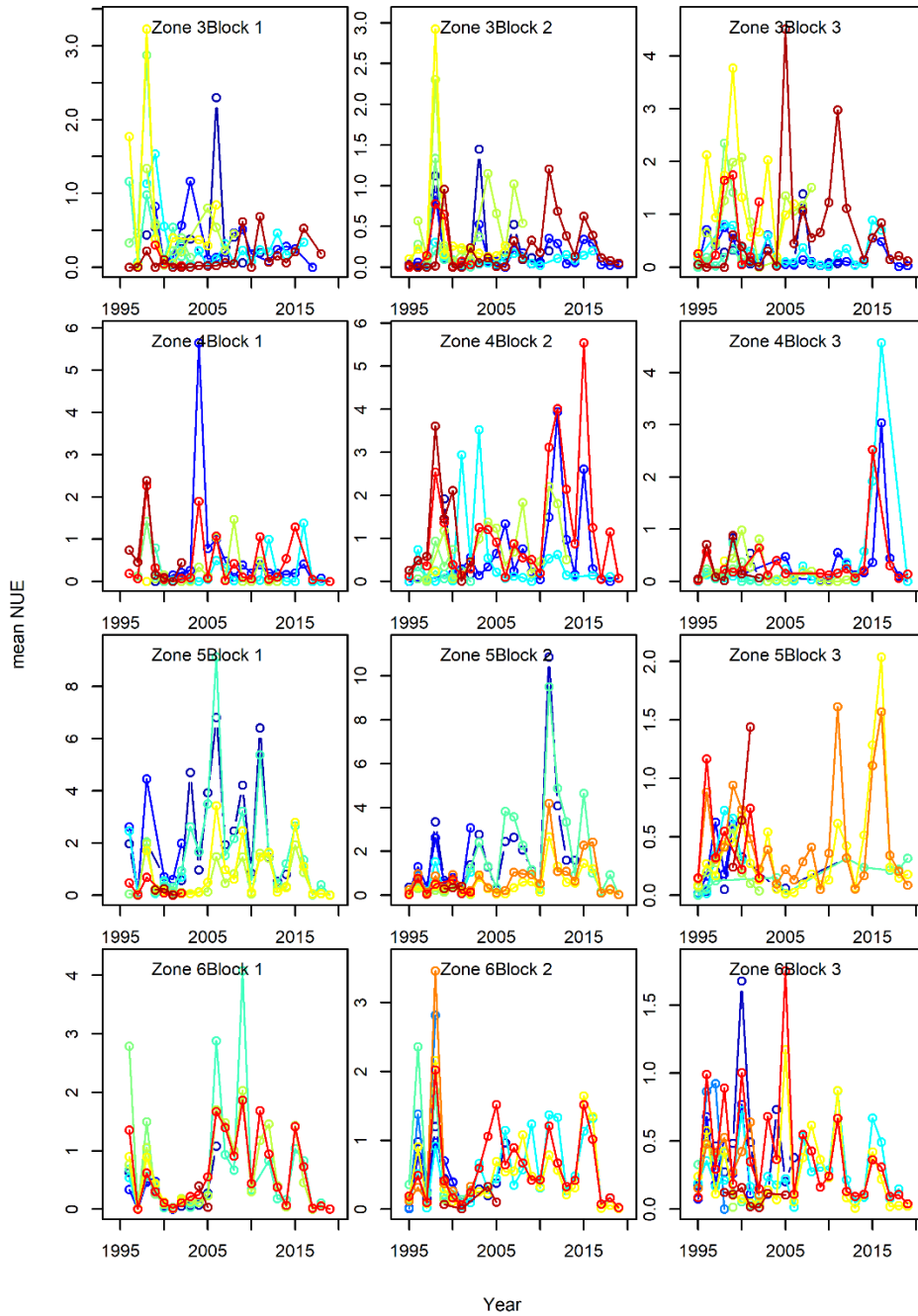


Figure A20. Site-specific annual mean numbers per unit effort (NUE) by zone and seasonal block for cod age 5 in the Sentinel gillnet program. Values for individual sites are distinguished by colour in each zone and block.

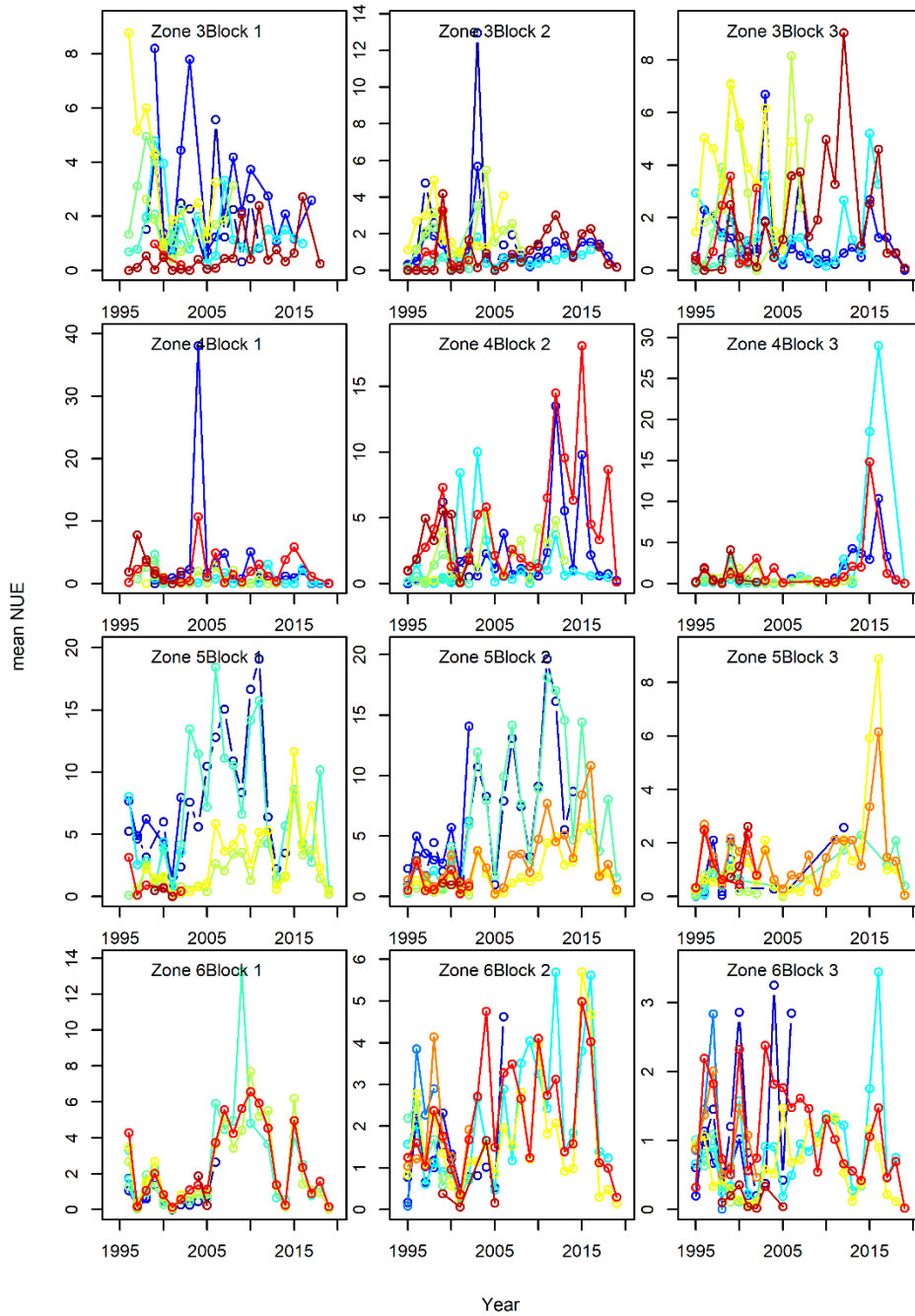


Figure A21. Site-specific annual mean numbers per unit effort (NUE) by zone and seasonal block for cod age 6 in the Sentinel gillnet program. Values for individual sites are distinguished by colour in each zone and block.

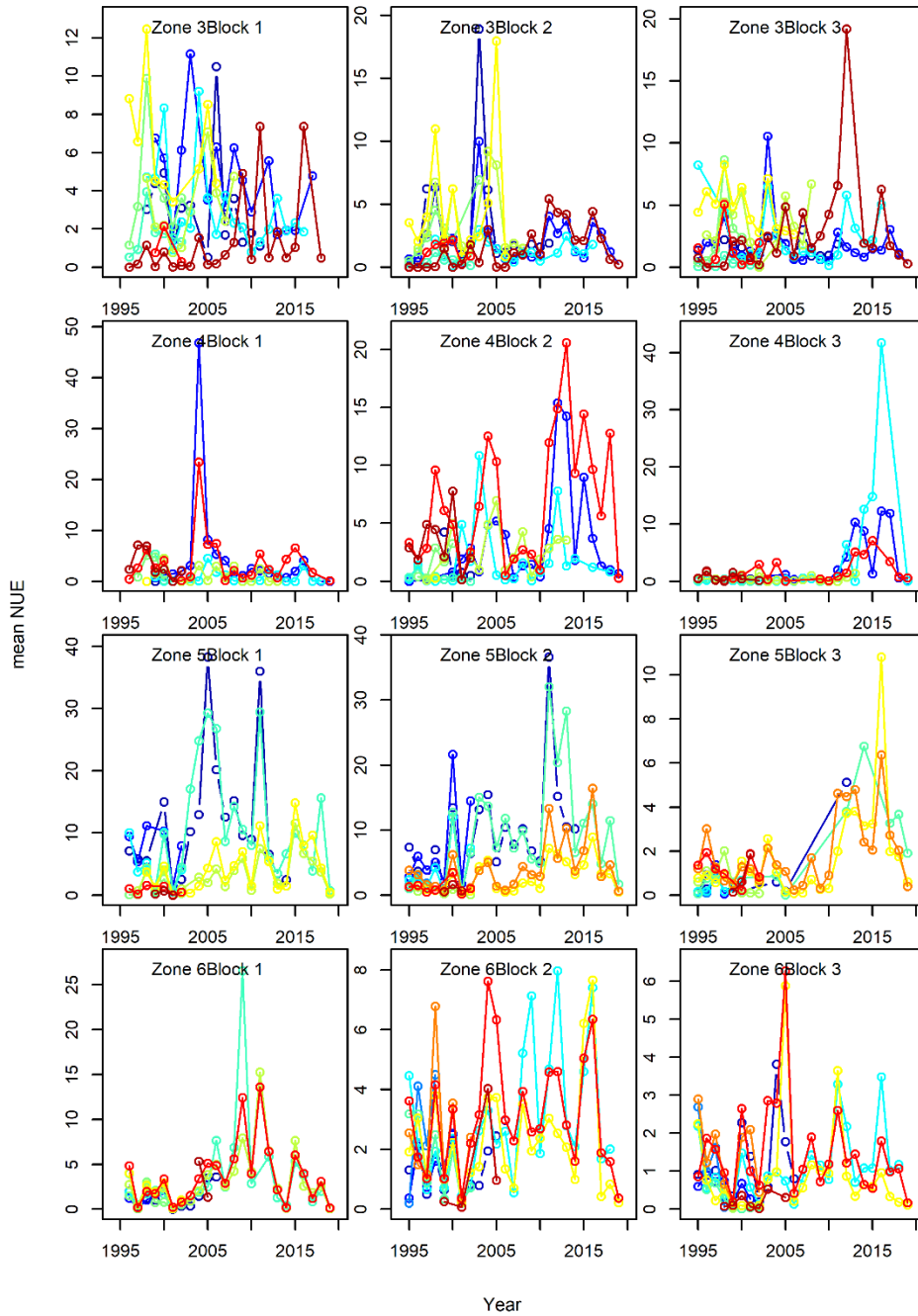


Figure A22. Site-specific annual mean numbers per unit effort (NUE) by zone and seasonal block for cod age 7 in the Sentinel gillnet program. Values for individual sites are distinguished by colour in each zone and block.

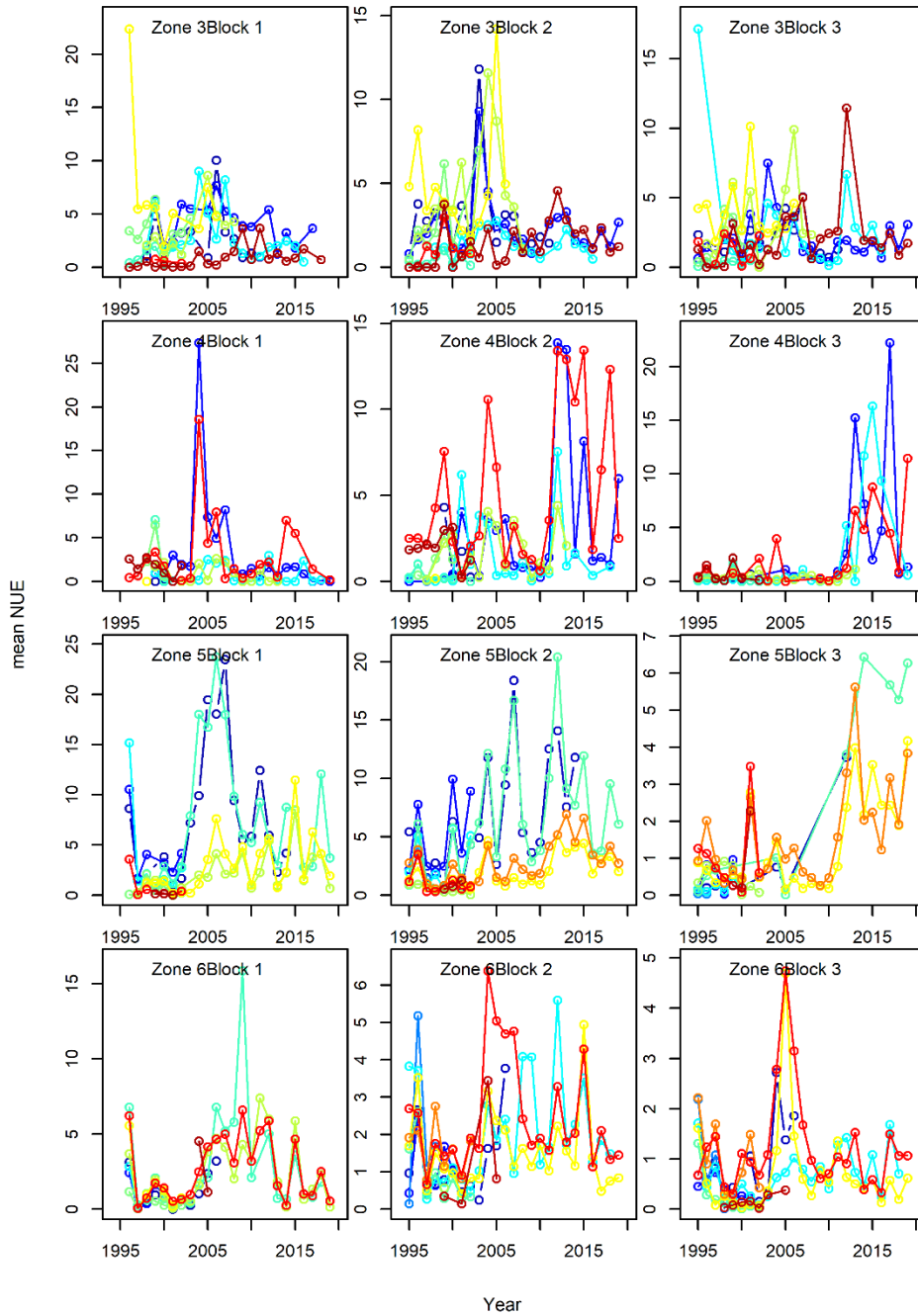


Figure A23. Site-specific annual mean numbers per unit effort (NUE) by zone and seasonal block for cod age 8 in the Sentinel gillnet program. Values for individual sites are distinguished by colour in each zone and block.

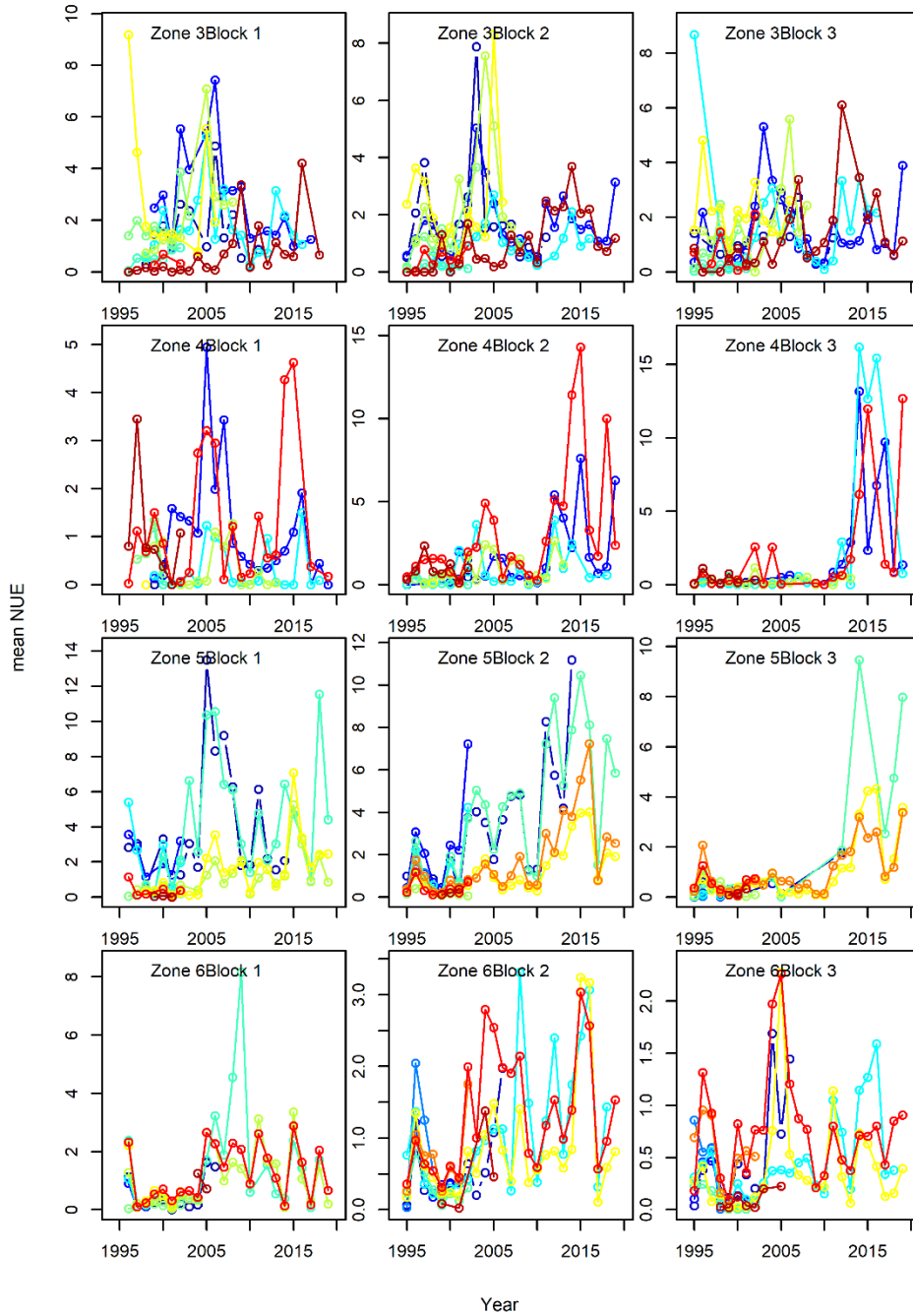


Figure A24. Site-specific annual mean numbers per unit effort (NUE) by zone and seasonal block for cod age 9 in the Sentinel gillnet program. Values for individual sites are distinguished by colour in each zone and block.

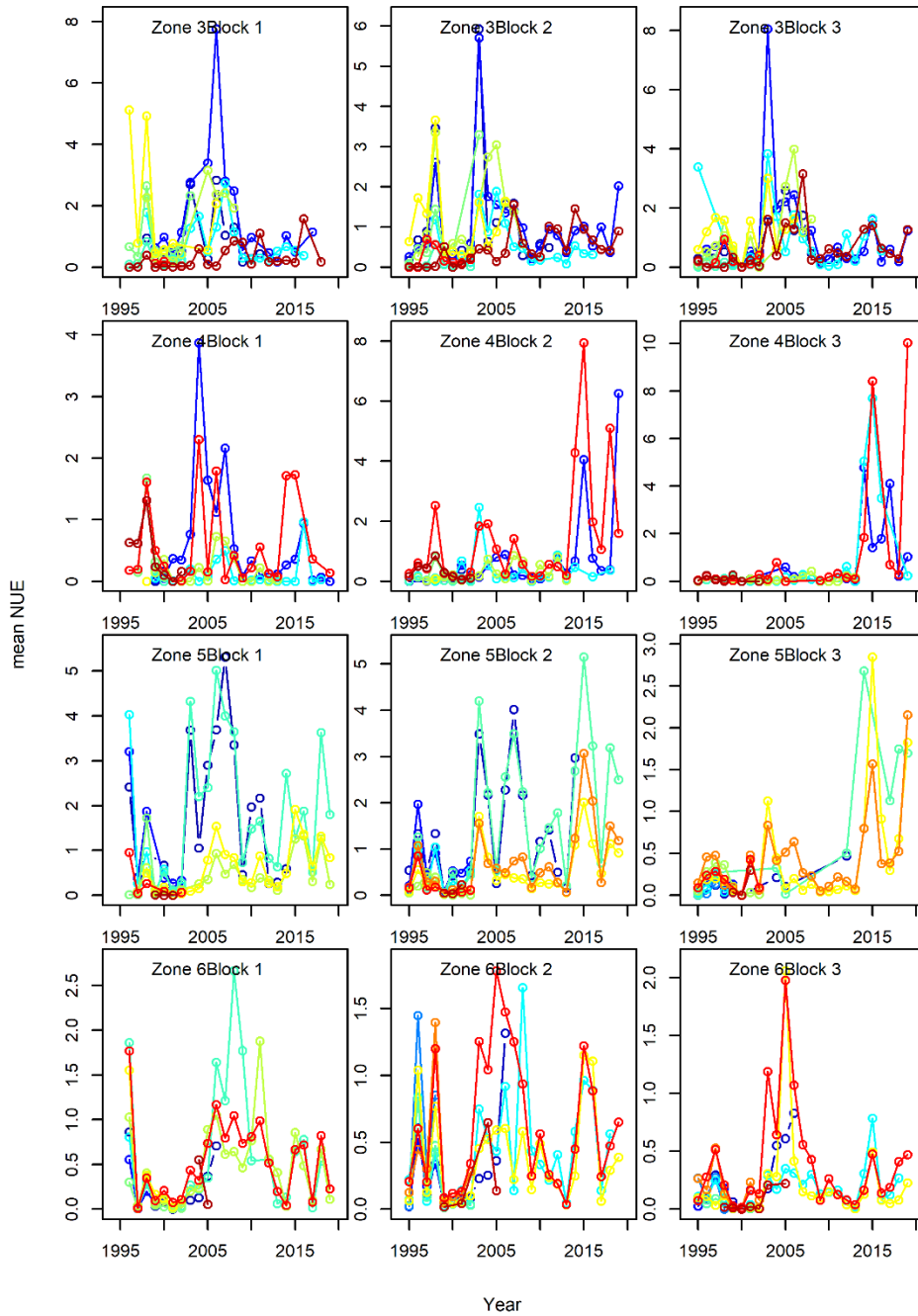


Figure A25. Site-specific annual mean numbers per unit effort (NUE) by zone and seasonal block for cod age 10 in the Sentinel gillnet program. Values for individual sites are distinguished by colour in each zone and block.

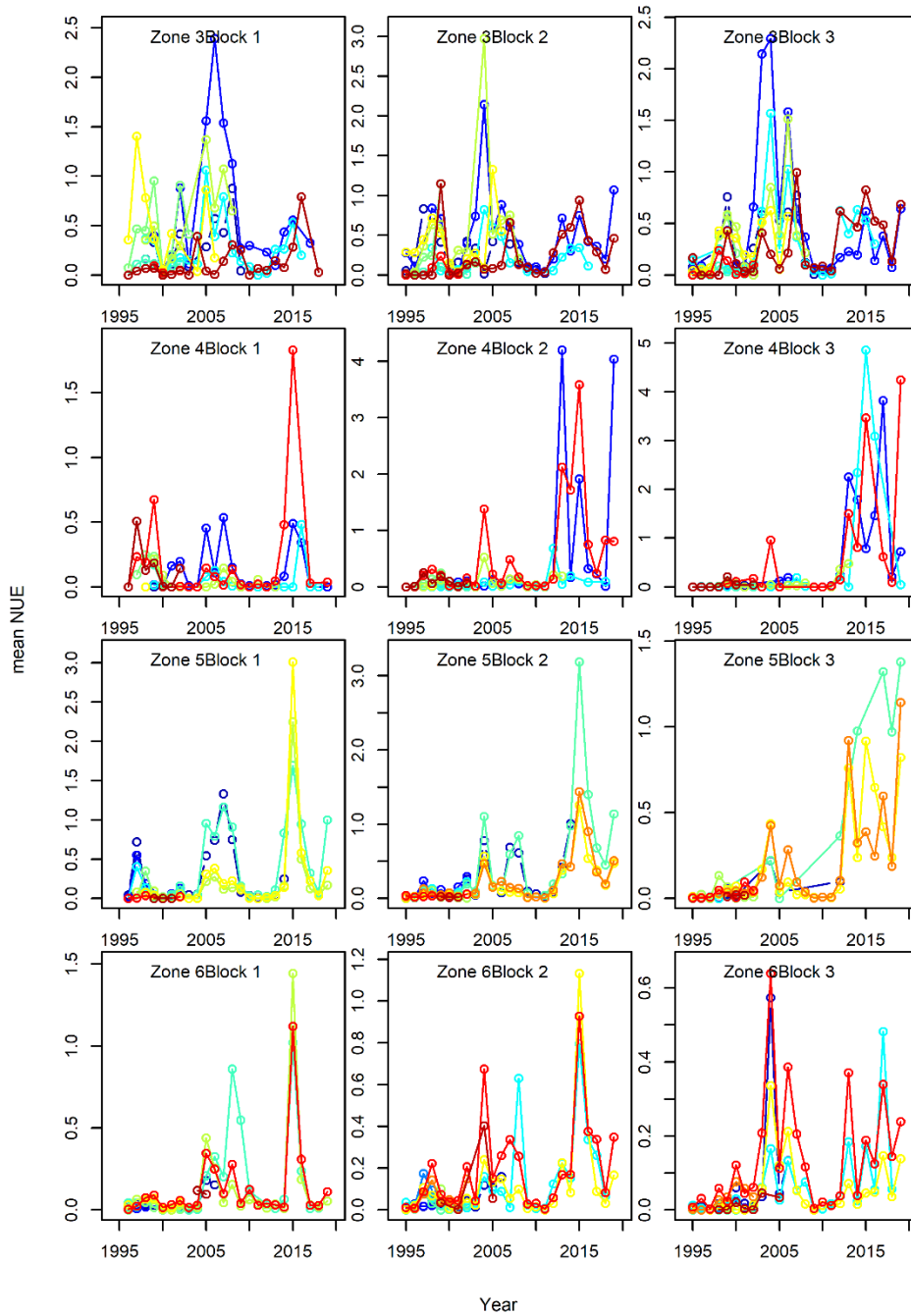


Figure A26. Site-specific annual mean numbers per unit effort (NUE) by zone and seasonal block for cod age 11 in the Sentinel gillnet program. Values for individual sites are distinguished by colour in each zone and block.

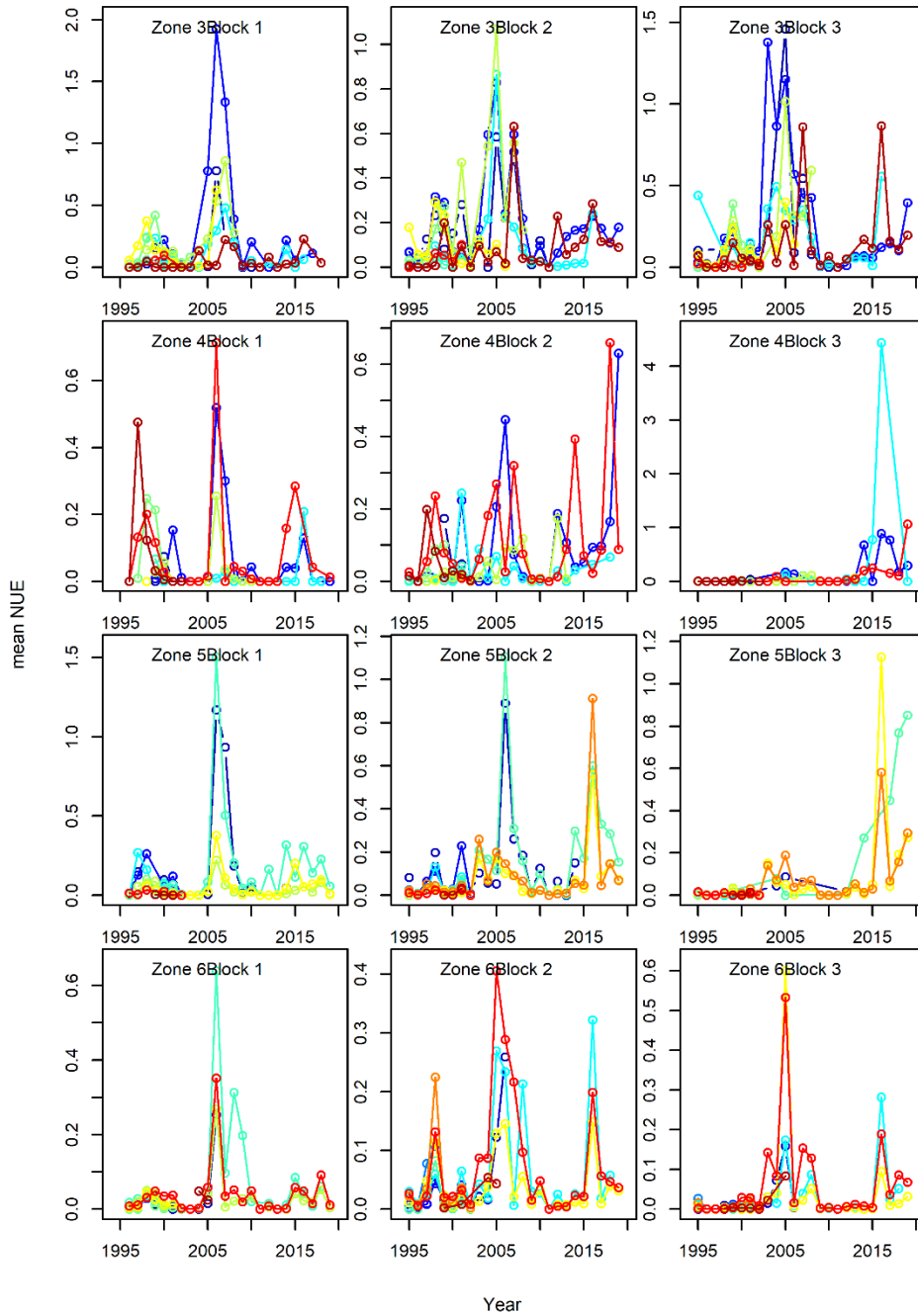


Figure A27. Site-specific annual mean numbers per unit effort (NUE) by zone and seasonal block for cod age 12 in the Sentinel gillnet program. Values for individual sites are distinguished by colour in each zone and block.

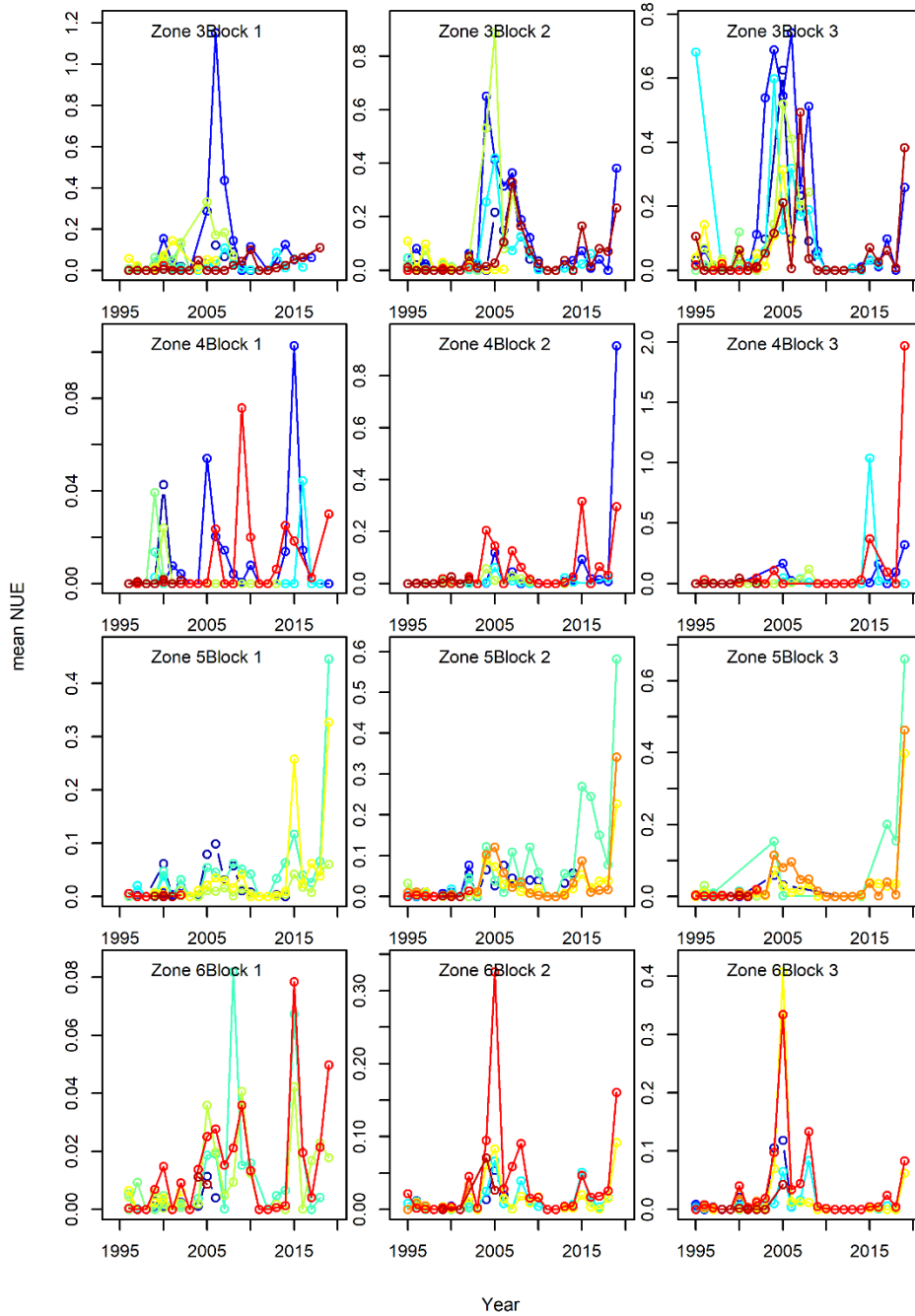


Figure A28. Site-specific annual mean numbers per unit effort (NUE) by zone and seasonal block for cod age 13+ in the Sentinel gillnet program. Values for individual sites are distinguished by colour in each zone and block.

14. APPENDIX II

14.1. CATCH AT AGE FOR FIXED SENTINEL FISHERY DATA

Data from the fixed sentinel fishery program for the 1995-2019 period were used for this analysis. For each fishing activity, the proportions at age for each length found in the length frequency data were calculated. First, age-length keys (1 cm classes) were created for all year, month and gear type (gillnet or longline) combinations found within the length frequency data (> 22K unique combinations). Second, for each of these combinations, aged cod samples to use in the associated age-length key were identified using a modified version of the *get.samples()* function from the R package *catchR* (Ouellette-Plante et al. 2022). This modified version used a decision tree with five possible levels of aggregation:

Year, month, gear type

Year, month, all types of gear combined

Adjacent months (± 1), all types of gear combined

Adjacent months (± 2), all types of gear combined

All years, all types of gear combined.

Unlike the original version of this function that used a minimum number of samples as a threshold, the one used in the present analysis was set arbitrarily at a minimum of 100 aged cod. For example, the July 2003 longline survey catch-at-age numbers could not use aggregation level 1, as only 32 aged cod were available at that level. Moving on to the second level, 134 additional aged cod were available from the July 2003 gillnet fishery, which stopped the function in its search. In the event that the age-length key created did not fully cover the lengths found in the associated length frequencies, the *multinom* function from the *nnet* R package (Venables et Ripley 2002) was used to construct multinomial logistic regressions to infer ages to missing lengths (Ouellette-Plante et al. 2022).

More than half of fishing activities had enough aged cod to use only those extracted from aggregation level 1. Less than 20% required using samples based on aggregation levels 3-5. 41% of fishing activities used an age-length key comprising < 150 cod. Age imputations using multinomial logistic regressions were used in < 5% of all fishing activity – length class combinations.

Numbers at age were then calculated by fishing activity by first calculating the numbers at age for a specific length j ($j = 1, 2, \dots, J$) as:

$$n_{aj} = FL_j \cdot p_{aj} \cdot frac \tag{1}$$

where FL_j is the number of cod of length j measured in the length frequency sample from that specific fishing activity, p_{aj} is the proportion at age a for length j cod and $frac$ is the sample fraction for the entire catch (sample weight / catch weight). Then, numbers at ages from all lengths were combined as

$$n_a = \sum_j n_{aj} \tag{2}$$

Cited references:

Ouellette-Plante, J., van Beveren, E., Benoît, H.P. and Brassard, C. 2022. [Details of catchR, an R package to estimate the age and length composition of fishery catches, with an application to 3Pn4RS Atlantic cod](#). DFO Can. Sci. Advis. Sec. Res. Doc. 2022/015. iv + 69 p.

Venables, W.N., and Ripley, B.D. 2002. Modern Applied Statistics with S. Dans Fourth. Springer, New York.